Characterization Of Human Syndecan-3

And Its Influence On The Actin Cytoskeleton

Dissertation

zur Erlangung des Doktorgrades

des Fachbereichs Biologie der Universität Hamburg

vorgelegt von

Christine Charlotte Berndt

aus Laupheim, Deutschland

Hamburg

Juli 2002

Genehmigt vom
Fachbereich Biologie der
Universität Hamburg
auf Antrag von Herrn Professor Dr. H.-P. MÜHLBACH

Weitere Gutachter der Dissertation:
Herr Professor Dr. S. Vilaro´

Tag der Disputation: 12. Juli 2002

Hamburg, den 28. Juni 2002

Professor Dr. U. Wienand
Dekan

UNIVERSITAT DE BARCELONA

Avda. Diagonal 645
Facultat de Biologia
08028 Barcelona
Tel/Fax (93) 402 10 00
e-mail robin@porthos.bio.ub.es

Escola d'Idiomes Moderns
Servei d'Assessorament Lingüístic

I **Robin Rycroft**, Head of the Language Advisory Service at the Escola d'Idiomes Moderns at the University of Barcelona, hereby CERTIFY:

That I have personally revised and corrected the PhD Thesis presented by CHRISTINE BERNDT, entitled ***"Characterization of human syndecan-3 and its influence on the actin cytoskeleton"***.

Signed

Barcelona,
24 May. 2002

Acknowledgements

I would like to thank everybody who helped and supported me during this thesis.

First my Spanish (Prof. Senén Vilaró, Prof. Manuel Reina and Dr. Myriam Fabre) and German supervisors (Prof. Hans-Peter Mühlbach and Prof. Ulrike Beisiegel) and all of my Spanish and Catalan colleagues: postdocs, predocs and technicians.

I especially want to thank Dr. Ricardo Casaroli and Dr. Joan Villena, with whom I shared some projects and Dr. Mercè Martín for all her good advice. ¡Moltes gracias a tothom! ¡Muchas gracias a todos! I am also particularly grateful to Robin Rycroft who is responsible for the correct English version of this thesis. Thanks a lot!

In Germany, I thank all those who were kind enough to act as a referee for my thesis even when the topic was far from their field, and I want to mention Pia Kuss, who was my first student during the preparation of my thesis. Vielen herzlichen Dank an alle!

Finally, I thank J. Collard (Amsterdam) and M. Bernfield (Boston) for their collaboration by endowing us with antibodies and plasmids. This thesis was supported by grants from the European Commission, the Deutsche Studienstiftung and Biomed.

Further I want to thank my friends in Germany and in Barcelona who helped me to feel at home in another country. My heartily thanks go to

Anna for listing
Bea for being so important to me
David for his constancy
Inga for never forgetting me
Ingo for the way he is
Israel for discussing
Ivonne for being marvelously different
Jörg for our great friendship
Laia for forming part of my life
Lars for his fidelity
AND
Eloi for his affection and for being on my mind

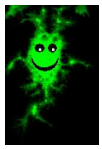

My whole family, who has always been a big support in all my decisions
Above all, my parents to whom I dedicate this thesis

“Ein Weg ist ein Weg, auch im Nebel”
“A road is a road, even in fog”
“Un camino es un camino aunque haya niebla”
Max Frisch (1979)

Index

Introduction

1. Introduction

Cell motility and communication are essential throughout life, particularly during development but also in pathological processes such as wound healing or tumor progression among others.

Communication is achieved over long distances by diffusible factors that often form concentration gradients of attracting and repulsive cues (for example, guiding the axonal growth cone), and in the short range by cell-cell and cell-matrix interactions (Mueller, 1999).

1.1. Cell adhesion molecules

For these special functions cells are endowed with cell adhesion proteins, which allow them to detect their extracellular milieu. Cadherins, selectins and cell adhesion molecules (CAMs) of the Immunoglobulin- (Ig-) superfamily mediate cell-cell contact while integrins and proteoglycans are the main binding partners to the extracellular matrix (ECM) (Aplin et al., 1999; Juliano, 2002), ***see fig. 1.1***.

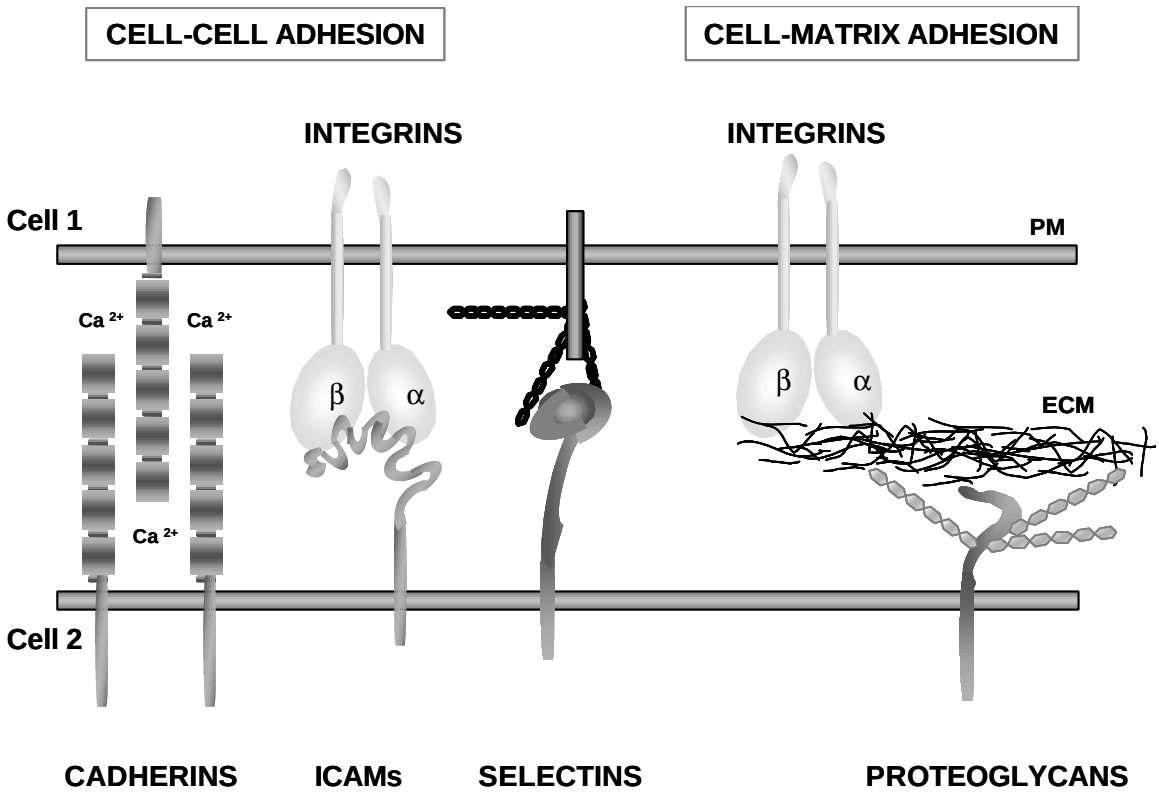

Figure 1.1: ***Schematic representation of cell-cell and cell-matrix interactions*****. Cadherins form Ca^{2+}-dependent homophilic interactions. ICAMs can perform either homophilic or heterophilic interactions (with integrins, for example). Selectins bind to carbohydrate structures on the cell surface. Integrins and proteoglycans are involved in cell-matrix interactions. ECM = Extracellular matrix, ICAMs = Intercellular cell adhesion molecules, PM = Plasma membrane.**

1.1.1. Cadherins

Cadherins form Ca^{2+}-dependent homophilic interactions and play an important role in the selective adhesion of embryonic cells and in the establishment of stable junctions between cells in tissues. The first cadherin described in the literature was E-cadherin, which together with VE-, N- and P-cadherin are known as the “classical” cadherins. VE-cadherin leads to selective adhesion of endothelial cells, while N-cadherin (neural cadherin) and P-cadherin (placenta cadherin) mediate adhesion of other cell types (Angst et al., 2001; Juliano, 2002; Takeichi, 1991).

1.1.2. ICAMs

The intercellular cell adhesion molecules (ICAMs) belong to the Ig superfamily due to structural similarities with other members and are also implicated in cell-cell adhesion mechanisms. ICAMs can perform heterophilic interactions, e.g. with integrins, but other members of the Ig superfamily also perform homophilic interactions. This leads to the establishment of adhesion between two cells of the same type. One example is the neuronal expressed N-CAM, which in this way establishes association of nerve cells (Juliano, 2002).

1.1.3. Selectins

The selectins are important molecules in cell-cell recognition during the inflammatory response in injured tissues. Leukocytes express L-selectin, which recognizes oligosaccharide (OG) structures on the cell surface. The endothelial cells on the other hand, have E- and P-selectin, which recognize OGs expressed on the leukocyte (Juliano, 2002; Zak et al., 2000).

1.1.4. Integrins

The integrins are the CAMs on which most research has been done. They form heterodimers composed of an α- and a β-subunit. More than 17 α- and 8 β-chains have been described, which can combine with each other and are expressed in a cell-type specific manner (Plow et al., 2000). They are involved in both cell-cell and cell-matrix interactions. Although they posses no integral kinase activity, clustering leads to the binding of intracellular adaptor domains, which in turn activates downstream signaling pathways. ***Fig. 1.2*** shows, as one example, ligand binding which finally ends in the formation of focal adhesion (FA) sites. This process will be discussed later on (Calderwood et al., 2000; Giancotti and Ruoslahti, 1999; Howe et al., 1998; Hynes, 1992; Schwartz, 2001).

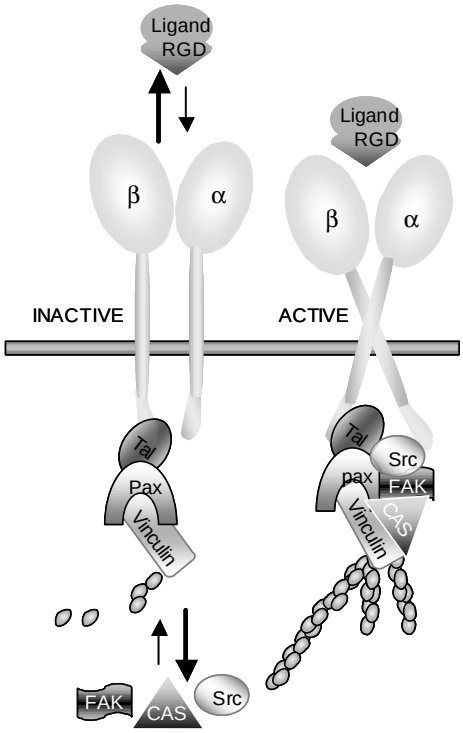

Figure 1.2: ***Integrin function in the formation of focal adhesions*****. Integrins are composed of an a- and b-chain. After ligand binding, chains undergo conformational changes, which results in binding of intracellular proteins and finally to the formation of focal adhesions. The activation of other downstream signaling pathways is not shown (outside-inside signaling). Integrins can also transmit cytoskeletal changes to the exterior (inside-outside signaling). Pax = Paxilin, FAK = Focal adhesion kinase, Tal = Talin, Vin = Vinculin, CAS = Crk-associated substrate. Modified after Schwartz, 2001 and Giancotti, 1999.**

1.1.5. Proteoglycans

Although the most important members of the above mentioned families are the integrins and cadherins, many groups have recently focused on the proteoglycans (PGs; Delehedde et al., 2001; Gahmberg and Tolvanen, 1996; Lander, 1993; Lander, 1998; Ruoslahti, 1989; Ruoslahti and Yamaguchi, 1991).

PGs consist of a core protein and an attached glycosaminoglycan (GAG) chain that can account for up to 95% of their molecular weight. GAGs are repetitive disaccharide sequences of N-acetylglucosamine (GlcNAc) and N-acetylgalactosmine (GalNAc), which vary in their type of linkage and number and location of sulfate groups and can be classified into the following groups: Chondroitin sulfate (CS), dermatan sulfate (DS), heparan sulfate (HS) and its secreted counterpart heparin, keratan sulfate (KS) and hyaluronic acid which is neither sulfated nor attached to a core protein (Ruoslahti and Yamaguchi, 1991). The following chapter will focus on one subfamily of the PG, on the HSPGs (heparan sulfate proteoglycans).

1.2. HSPGs

HSPGs can be found as cell surface PGs or in soluble form (Park et al., 2000b; Rapraeger, 1993; Rapraeger, 2000; Rapraeger, 2001), ***see fig. 1.3***.

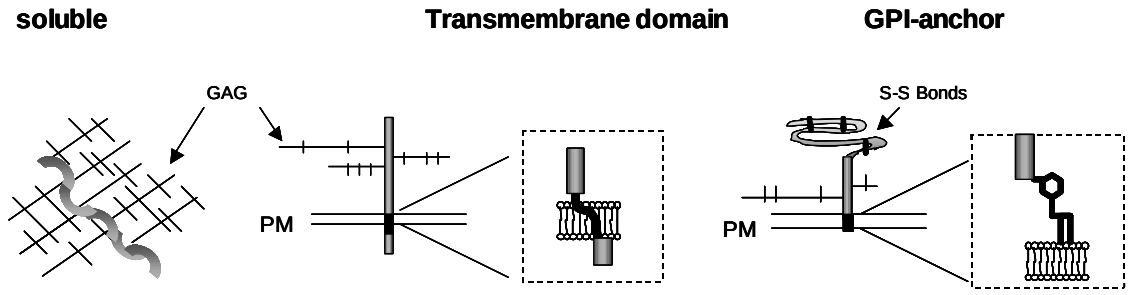

Figure 1.3: ***Modes of membrane anchoring*****: "soluble" HSPGs without any anchoring (e.g. heparin), anchoring by transmembrane domain (syndecans, CD 44, betaglycan) and by GPI-anchor (glypicans). GAG = Glycosaminoglycan, GPI = Glycosyl phosphatidylinositol, PM = Plasma membrane.**

1.2.1. Soluble HSPGs

Most of these "soluble" (without any anchoring) HSPGs are large modular proteins, which contribute to the structure, permeability, hydration and elasticity of the ECM (Ruoslahti and Yamaguchi, 1991). Prominent examples are aggrecan, versican, decorin, and fibromodulin. Perlecan, agrin and type–XVIII collagen form part of the basement membranes. Heparin, which is used in clinics as an anticoagulant is an HSPG secreted by mast cells (Bernfield et al., 1999; Blackhall et al., 2001; David, 1993; Perrimon and Bernfield, 2000).

1.2.2. Cell surface HSPGs

The cell surface HSPGs can be divided into two subfamilies owing to their different mode of membrane anchoring: ***see fig. 1.3*** (David, 1993). The family of the glypicans is attached by a glycosyl phosphatidylinositol (GPI) anchor while the syndecans are type I transmembrane proteins. CD 44 and betaglycan (= transforming growth factor (TGF) β type III receptor), which also possess a transmembrane region, are called "part-time" HSPGs, since they only contain GAG chains under special conditions and will not be further discussed here. Apart from the different membrane anchor the most obvious differences between syndecans and glypicans can be found in their three-dimensional structure: the extracellular domains of glypicans are more globular due to the possible formation of disulfide bonds (Bernfield et al., 1999), while those of the syndecans have a more extended 3-dimensional structure. Additionally, the GAG attachment sites of glypicans are located more proximal to the plasma membrane (PM) than in syndecans (David, 1993).
Glypicans will be introduced briefly before discussing the syndecans, since they share some common features with the syndecans and are therefore used in many studies as control proteins to determine syndecan-specific functions.

1.2.2.1. Glypicans

Different genes in mammals express six glypicans. Based on similarities in their gene structures, glypican 1/2, 3/5 and 4/6 form subfamilies (Bernfield et al., 1999; Veugelers et al., 1998). All glypicans share an N-terminal signal sequence, a region about 50 kDa containing a characteristic pattern of 14 highly conserved cysteines, a region near the plasma membrane with 2-3 GAG attachment sites and a C-terminal region, which is involved in formation of the GPI anchor. Glypicans are predominantly expressed in neural tissues with the exception of glypican-2. The latter is expressed more ubiquitously and localizes to the basolateral membrane. However, when its HS chains were deleted, glypican-2 was also found apically (Bernfield et al., 1999 and references therein).

1.3. Syndecans

1.3.1. Syndecan family members

The syndecan family of HSPGs comprises four members, which are expressed by different genes on four different chromosomes in mammals (Spring et al., 1994a). Their gene structures indicate that they arose by gene duplication (Carey, 1997). Their expression is strongly regulated in a tissue-specific and developmentally dependent manner (David, 1993; Kim et al., 1994).

Syndecan-1 (CD 138) is most abundant in epithelial cells (Hayashi et al., 1987; Mali et al., 1990; Saunders et al., 1989), syndecan-2 (fibroglycan) is the predominant syndecan in fibroblasts, syndecan-3 is also called N-syndecan due to its high expression in the central nervous system (CNS) and syndecan-4 (amphiglycan, ryudocan) is more ubiquitously expressed by multiple cell types (Bernfield et al., 1992; Carey, 1997; David, 1993; Rapraeger, 1993; Woods and Couchman, 1998; Zimmermann and David, 1999). In Drosophila, a unique syndecan has been described called D-syndecan (Spring et al., 1994b). In mammals, syndecan-1 and -3 and syndecan-2 and -4 share stronger sequence homologies and therefore represent two subfamilies.

1.3.2. Structure

1.3.2.1. Gene structure and regulation

The genes of the syndecans are divided into five exons: Exon 1 contains the 5'-untranslated region and the signal peptide, exon-2 contains the N-terminal cluster of GAG attachment sites, exon 3 codes for the ectodomain spacer region, exon 4 for the proximal GAG attachment clusters and 10 bp of the transmembrane region and exon 5 for the rest of the transmembrane, the cytoplasmatic tail and the 3'-terminal untranslated region (Carey, 1997), ***see fig. 1.4***.

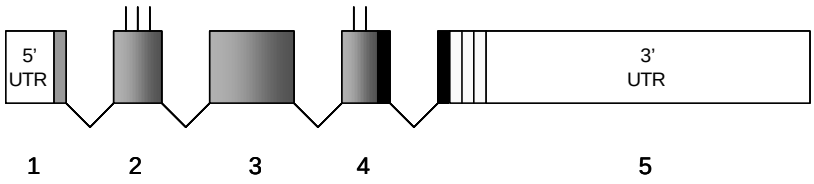

Figure 1.4: *Syndecan gene structure*. Hatched bar represents the signal peptide, grey boxes the extracellular domain with GAG attachment sites (vertical bars). Transmembrane domain is shown in black, cytoplasmic domain is labeled by dots. Introns are represented as lines between exons (1-5). UTR = Untranslated region.

For the promoter region of syndecan-1 and -4, several binding sites for transcription factors (NF-κB, MyoD, Antennapedia- and multiple Sp-1 among others) and repressors (WT-1) have been identified (Bernfield et al., 1999; Carey et al., 1997; Hinkes et al., 1993; Takagi et al., 1996; Tsuzuki et al., 1997; Vihinen et al., 1993; Vihinen et al., 1996; Baciu et al., 1994).

Besides FIRE (FGF-Inducible Response Element), a far upstream enhancer has been shown to mediate syndecan-1 induction in fibroblasts by fibroblast growth factor (FGF) (Jaakkola et al., 1997; Jaakkola et al., 1998; Jaakkola and Jalkanen, 1999). In keratinocytes, this induction could be performed by epidermal GF (EGF) but not by FGFs. Keratinocyte GF (KGF) activation of FIRE is modulated by ECM. On collagen, no induction of syndecan-1 was obtained, while on fibronectin (FN) and laminin FIRE was activated without affecting proliferation induced by KGF (Maatta et al., 1999).

1.3.2.2. Protein structure

All syndecans share a common structure, ***see fig. 1.5***. They possess a large extracellular domain with a signal peptide and varying amounts of GAG attachment sites, a single transmembrane domain and a very short (28-34 amino acids) cytoplasmic domain. They differ in their extracellular domains, but show high homology (>50%) in the transmembrane and C-terminal domains. The latter contains four tyrosine residues that are 100% conserved in all known syndecans and might serve as putative phosphorylation sites. The last four amino acids of the cytoplasmic tail (EFYA), also identical in all syndecans, represent the binding sequence for PDZ (PSD-95/Disc-large/ZO-1) domain-containing proteins; ***see also fig. 1.6***.

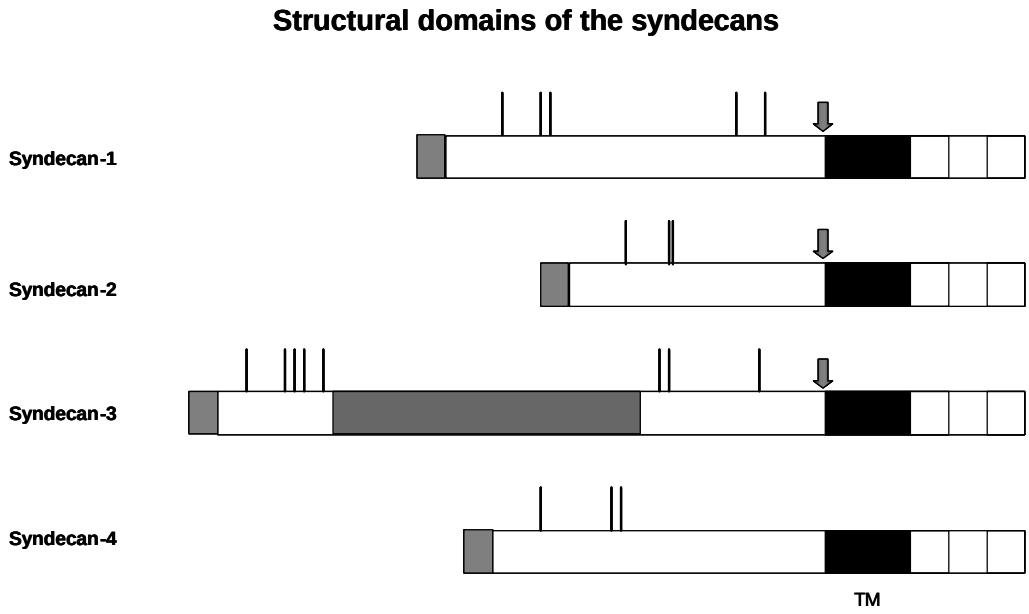

Figure 1.5: *Structure of the different members of the syndecan family*. Hatched box represents the signal peptide. Putative GAG attachment sites (vertical bars) are located in the extracellular domain. The transmembrane (TM) domain is shown in black. The cytoplasmic domain can be divided into three regions (see also fig. 1.6). The mucin-like domain of syndecan-3 is indicated by bubbles; the dibasic repeats which represent the predicted cleavage site of a protease (absent in syndecan-4) are indicated by an arrow. Modified after David, 1993.

1.3.2.2.1. Extracellular domain

The extracellular domain differs among the syndecans in number of putative GAG attachment sites (between 3-8), defined by serine-glycine sequences flanked by hydrophobic and acidic

residues. In syndecan-2 and -4, these attachment sites are found as clusters distal to the PM, while in syndecan-1 and -3 a PM proximal cluster can also be found. Besides, syndecan-1 and occasionally syndecan-3, also contain CS chains attached proximally to PM. Various specific functions of the syndecans depend on the presence of sugar chains. This will be discussed later (***see 1.4***) as well as the biosynthesis of the GAG chains (***see 1.3.2.2.4***).
Near to the plasma membrane, a dibasic repeat is found (except for syndecan-4, which has only a single basic residue). This site is understood to be the recognition site for ectodomain cleavage. Nevertheless, D-syndecan can also be released from the cell surface despite of the lack of this potential cleavage site predicted for mammalian syndecans (Spring et al., 1994b). The mechanisms and function of this so-called “shedding” will be explained further on (***see 1.4.5***). Moreover, the extracellular domain contains a cell interaction domain and parts of the oligomerization motif (Bernfield et al., 1999).
Syndecan-3 is the only member of the syndecan family to have a mucin-like domain in the extracellular spacer domain, for which no specific function has been found. It has been reported that syndecans can self-associate but the involvement of HS chains remains to be established. Oligomerization will be explained in more detail in the following paragraph.

1.3.2.2.2. Transmembrane domain

The transmembrane domain is highly conserved among the syndecans. The first 13 amino acids of this region have an extended secondary structure with rare and highly conserved glycine residues alternating with bulky residues. The subsequent 11 residues of the transmembrane membrane region adopt a helical structure.

Oligomerization seems to be common in the syndecan family. For syndecan-3 and -4, this was further investigated. Recombinant syndecan-3 forms tight, non-covalent dimers, tetramers and higher-ordered SDS-resistant oligomers, as shown by SDS gel electrophoresis, gel permeation chromatography and covalent cross-linking (Asundi and Carey, 1995). This was independent of disulfide bonds and of the cytoplasmic domain, but part of the ectodomain (ERKE) and the transmembrane (TM) domain were essential for oligomerization. Therefore, it was proposed that not only simple hydrophobic interactions, but perhaps also interdigitations of small and bulky side chains of adjacent core proteins (Asundi and Carey, 1995) were responsible for these homophilic interactions in syndecan-3 (Carey, 1997). Replacement of the conserved glycine abolished dimerization. Surprisinlgy, the phosphorylation of the cytoplasmatic domain had the same effect, which the authors showed not to be involved in oligomerization (Asundi and Carey, 1995; Carey, 1997) For syndecan-4, it was shown that oligomerization was necessary for its activation of protein kinase C (PKC) and that phosphorylation of its cytoplasmic tail abolished this activation by impeding oligomerization (***see also 1.4.6.2***). The TM domain is also considered to contain motifs for interaction with other TM proteins (Carey, 1997).

1.3.2.2.3. The cytoplasmic tail and its binding partners

The cytoplasmic domain of syndecans can be divided into three domains: two constant regions (C1 and C2), which are highly conserved among the syndecans, separated by a variable (V) region that is specific for each family member (***see fig. 1.6***).

Syndecan-1 with -3 and syndecan-2 with -4 form two subfamilies among the syndecans due to their similarity in the cytoplasmic tail and in the ectodomain. The last four amino acids of the cytoplasmic tail (EFYA) are 100% conserved in all syndecans and form an interacting motif with PDZ proteins. To date, several binding partners have been described for each of these regions, which can be specific for one syndecan although lying in a region of great homology with other family members. They will be mentioned briefly here but discussed in ***1.7***. The cytoplasmic tail also contains four tyrosine residues, which may serve as putative phosphorylation sites (bold “Y”).

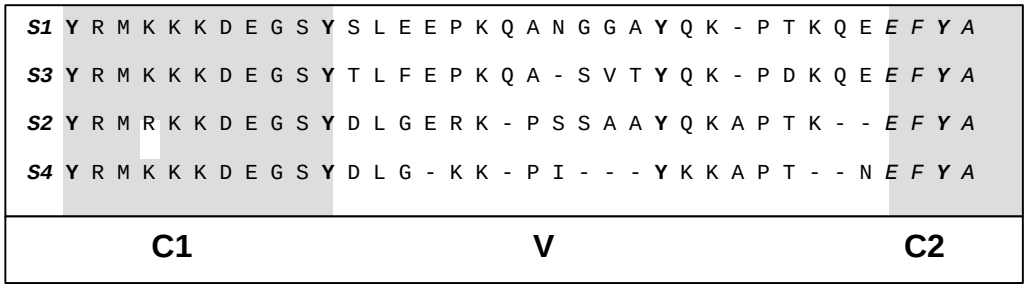

Syndecan			
-1		Microfilaments[4]	
-2	Ezrin[1]		Synbindin[7] CASK/LIN-2[9] Syntenin[8]
-3	Fyn, src, cortactin, tubulin[2]		CASK/LIN-2[9]
-4		PIP_2, PKC[5] Syndesmos[6]	Synectin[10]
All	Neurofibromin[3]		

Figure 1.6: ***Sequences of cytoplasmic domain of syndecan family members and their binding partners*****. All syndecans show high homology in the C1 and C2 regions (for constant region) separated by the V-region (for variable region), which is sequence specific for each syndecan. PIP_2 = Phosphatidyl inositol phosphate 2, PKC = Protein kinase C, CASK = calcium/calmodulin-dependent serine protein kinase, [1](Granes et al., 2000), [2](Kinnunen et al., 1998b), [3](Hsueh et al., 2001), [4](Carey et al., 1994b), [5](Oh et al., 1998), [6](Baciu et al., 2000), [7](Ethell et al., 2000), [8](Grootjans et al., 1997), [9](Cohen et al., 1998; Hsueh et al., 1998), [10](Gao et al., 2000).**

Serine phosphorylation

Two groups (Prasthofer et al., 1995) showed that PKC only phosphorylated syndecan-2 (ser 197) and -3 (ser 339), but not syndecan-1 or -4. Oh (Oh et al., 1997a) demonstrated that both serines in syndecan-2 can be phosphorylated and that syndecan-4 was not a substrate of PKC$\alpha\beta\chi$. Syndecan-4 phosphorylation in a single serine was controlled by a novel PKC isoenzyme, possibly PKCδ (Murakami et al., 2002), and a bFGF- (basic FGF)-dependent serine-threonine phosphatase (Horowitz and Simons, 1998a; Horowitz and Simons, 1998b).

Tyrosine phosphorylation

Following treatment with the phosphatase inhibitors sodium orthovanadate or pervanadate NmuMG cells accumulated tyrosine phosphorylation and ectodomain shedding of syndecan-1 (Reiland et al., 1996). In similar experiments, pervanadate treatment led to high tyrosine phosphorylation of syndecan-1 and -4 while the basal percentage was about 1.5% (Ott and Rapraeger, 1998). The authors concluded that src kinases were involved. By the use of a bacterial elk-kinase it was shown that all four tyrosine residues of recombinant syndecan-3 could also be phosphorylated (Asundi and Carey, 1997).

As protein phosphorylation is one of the most common mechanism to reversibly activate a wide range of cell responses to environmental signals, it is assumed and in some cases demonstrated, that syndecan phosphorylation similarly contributes to modulation of their functions.

1.3.2.2.4. Biosynthesis of GAG chains

Although the core protein is responsible for some functions of the syndecans, the sugar chains are necessary for optimal function, e.g. as co-receptors of FGF-2. Changes in HS composition are found during development and aging and also associated with some diseases (Lindahl et al., 1998; Salmivirta et al., 1996).

The HS biosynthesis is tightly controlled and can be divided into three steps: (I) formation of a region linking HS to the protein, (II) generation of a polysaccharide chain and (III) enzymatic modification of the chain to yield specific saccharide sequence and structural organization (Bernfield et al., 1999; Lindahl et al., 1998).

First, a common tetrasaccharide linkage region (**2**) starting with xylose is produced by addition of sugar nucleotides to serine (**1**). This process takes place in the Golgi. A single GlcNac is added to the linker (**3**) and then alternating GlcA (glucuronic acid) and GlcNac (**4**) are added, catalyzed by the action of HS polymerase or GlcNAc/GlcA polymerase (**5**) producing a 1,4-link between the sugar residues (**4**). The conversion of UDP-glucose to UDP-glucuronic acid is catalyzed by UDP-glucose dehydrogenase (**6**). Once assembled, (50-150 disaccharides) enzymatic modifications by the action of Golgi enzymes take place: Epimerization from glucuronic acid to iduronic acid (IdoA) by the action of GlcA C5-epimerase (**7**) and addition of sulfate groups by N-deacetylase/N-sulfotransferase (NSDT) and 2-, 3- and 6-O-sulfotransferases (OSTs) (**8**) (Perrimon and Bernfield, 2000; Selleck, 2000), ***see fig. 1.7***.

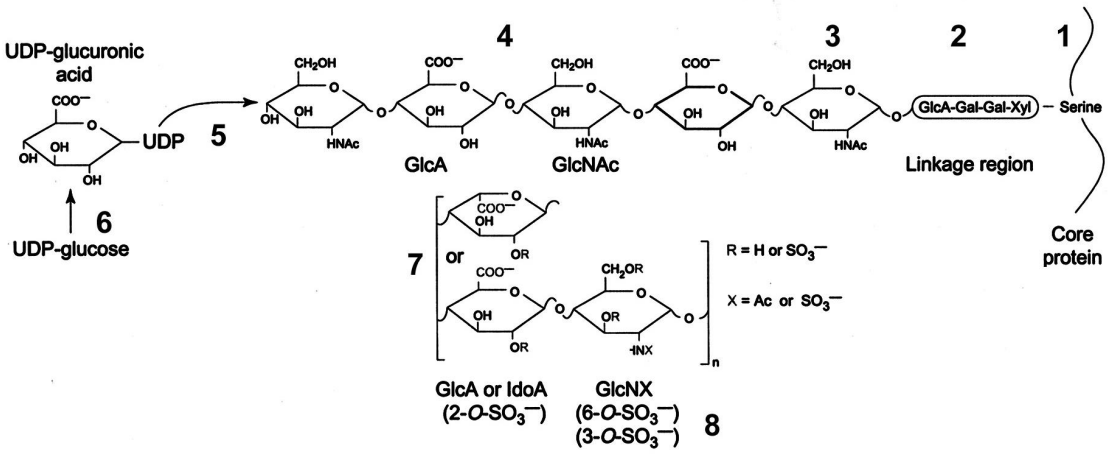

Figure 1.7: *Scheme of HS biosynthesis*: Individual steps are explained in the text. Modified after Perrimon and Bernfield, 2000 and Selleck, 2000. GlcA = Glucuronic acid, GlcNac = N-acetyl glucosamine, Gal = Galactose, Xyl = Xylose, IdoA = Iduronic acid.

1.3.2.2.5. Diseases associated with defective HS biosynthesis or defect core protein

Until recently, the importance of proteoglycans was neglected as they were only considered as “multipurpose glue” (Ruoslahti, 1989). In the last decade, it has been shown that they are involved in many severe developmental defects, in cancer and in neurodegenerative disorders such as Alzheimer’s disease (AD).
In Drosophila, developmental abnormalities were associated with mutations in the enzymes that are necessary for the biosynthesis of HS. Some of the genes described so far are *sugarless* (coding for UDP-glucose dehydrogenase), *tout velu* (coding for HS polymerase), *sulfateless* (coding for NSDT) and *pipe* (coding for 2-OST). When these genes were defective due to mutations, HSPG/GF interactions were inhibited. For many of these genes, the mouse

homologues have been cloned and the corresponding developmental aberrations have also been found. Even in human, a very rare disease hereditary multiple exostoses (HME) (incidence 1:50 000) has now been related to a mutation in the gene for HS polymerase (coded by the gene *EXT 1*). It is manifested by benign tumors of bones, which in 2% of the cases become malignant (Blackhall et al., 2001; Selleck, 2000).

Another disease, related with HSPGs, is Simpson-Golabi-Behmel-Syndrome (SGBS), an X-linked syndrome characterized by prenatal and postnatal overgrowth and high risks for tumors. It is provoked by a mutation in the glypican-3 gene (Blackhall et al., 2001; Selleck, 2000; Veugelers et al., 1998). Its Drosophila homologue, the gene product of *dally* (*division abnormally delayed*) has been shown to have a differential influence on two developmental pathways: Wg/Wnt (wingless) and Dpp (Decapentaplegic) pathways (Tsuda et al., 1999). This again confirms the importance of HSPG in developmental processes.

1.4. Functions of syndecans

Until now, the “main” function of syndecans has not been discovered. It seems that these proteoglycans have a “side-role” in a variety of biological processes, for some of which they are indispensable (Bernfield et al., 1992; Bernfield et al., 1999; Carey, 1997; Park et al., 2000b; Rapraeger, 2000; Rapraeger, 2001; Yanagishita and Hascall, 1992; Zimmermann and David, 1999).

They can act as co-receptors for GFs, mediate cell-cell and cell-matrix adhesion, modulate the activation of proteases and their inhibitors, be low affinity-receptors of enzymes, and serve as attachment sites for viruses. They can release their ectodomain by a process called “shedding” and thereby modulate various biological processes. For a brief overview, ***see fig. 1.8***. Besides, specific functions of each syndecan in development and diseases have been described. In the following chapter, the functions of syndecans will be discussed in detail.

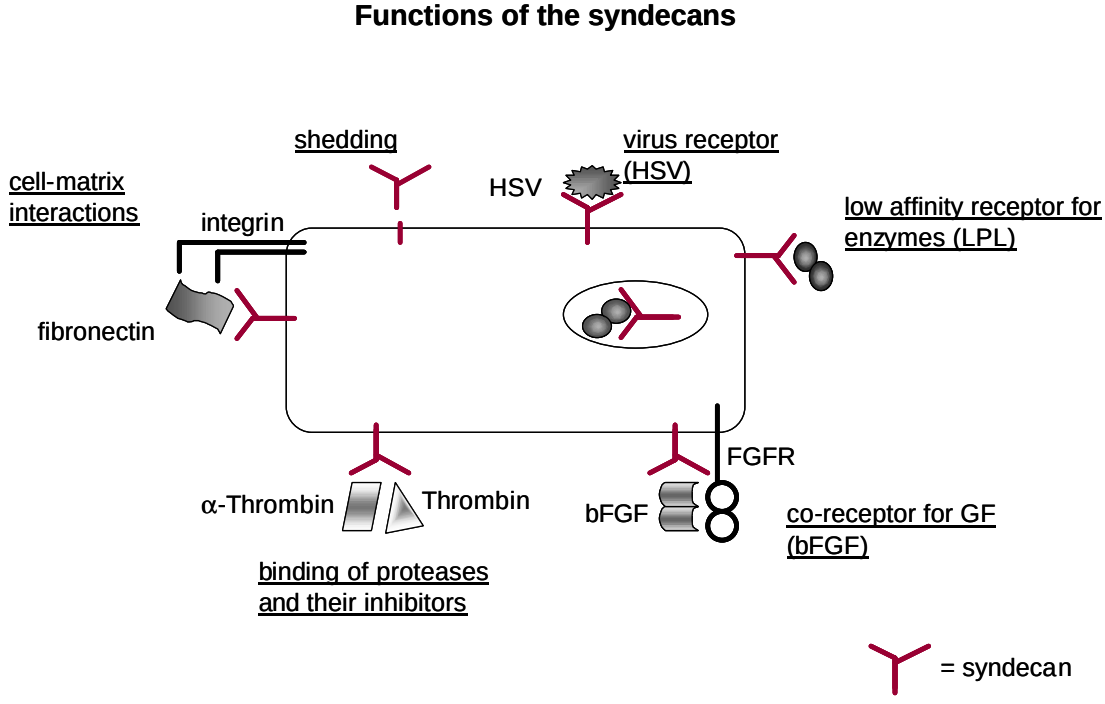

Figure 1.8: ***Summary of major functions described for syndecans*****. LPL = Lipoprotein lipase, HSV = Human simplex virus, GF = Growth factor, bFGF = basic fibroblast GF. Modified after Bernfield et al., 1992.**

1.4.1. Syndecans as co-receptors of GFs

Syndecans can serve as co-receptors for GFs such as FGF-1, FGF-2 (Filla et al., 1998), TGF-β, platelet factor 4 and others (Bernfield et al., 1999; Ruoslahti and Yamaguchi, 1991; Schlessinger et al., 1995). The contribution of syndecans (and glypicans) varies with the cell-type, GF and culture conditions.

The mechanisms by which syndecans and other HSPGs might perform this co-receptor role involve several strategies: they limit the diffusion of soluble ligands from three to two dimensions, thereby concentrating the specific GF; they can immobilize the ligand and present it to its specific receptor or prevent its degradation. Additionally, they can contribute to the dimerization of GFs (Zioncheck et al., 1995) and/or modify their interaction with their receptor (Bernfield et al., 1999 and references therein).

Nevertheless, the situation can be more complex (Schlessinger et al., 1995). With increasing HS/heparin concentrations, a hyperbolic potentiation of GF activation was often observed: at low concentrations there is a stimulating effect of HS on GF activation as mentioned above, while at high concentrations activity decreases (Zioncheck et al., 1995). This might be due to an excess of surface binding sites for the GF. Since inhibitory effects were often associated with soluble forms of HS/HSPG, it was proposed that cell association of HSPG might be crucial for GF receptor activation. This was confirmed (Steinfeld et al., 1996) in K562 cells, where syndecans and glypicans supported bFGF- FGFR1 (FGF Receptor 1) interactions and signaling, and cell surface association increased their efficiency.

Further clarifying experiments came from Zhang (Zhang et al., 2001), who determined auto-phosphorylation of the FGFR1 as a criterion of activation by FGF comparing membrane-bound and soluble HSPGs (obtained by trypsinization). They found that all membrane-bound HSPGs stimulated FGF2-induced FGFR1 activation independent of the nature of their core protein (syndecan or glypican). Heparitinase first stimulated and then inhibited activity of the HSPG-carrying cells. Soluble HSPGs (obtained by by trypsinization) did not induce FGFR phosphorylation but digestion of those fragments transformed them into potent activators. Therefore, two different situations were defined: “*proteolytic shedding*”, diluting the GF and thereby down-regulating GF receptor activation and “*heparanolytic* shedding”, which has an up-regulating role.

Accordingly, Kato et al. (Kato et al., 1998) showed that the ectodomain of syndecan-1 inhibits heparin-mediated FGF-2 mitogenicity, while degradation with platelet heparinase transformed the ectodomains into heparin-like molecules, which could then activate FGF-2 mitogenicity.
Nevertheless, one possible explanation for the discrepancies seen in the abundant studies of growth factor activation could be the different end-point measurements of GF activation (receptor phosphorylation, cell proliferation, etc.) and the diversity of HS compositions.

As mentioned above, it seemed that syndecans as well as glypicans could support FGF-FGFR1 interactions (Steinfeld et al., 1996). Somehow contradictory results to those of Steinfeld were obtained by testing syndecan-1, -4 and glypican-1 and chimeric constructs for their ability to mediate bFGF effects on migration and proliferation in immortalized human cells. In these experiments, only syndecan-4 transfected cells were influenced by the GF that depended on the cytoplasmic tail of syndecan-4 (Volk et al., 1999). However, in another approach, Richardson (Richardson et al., 1999) showed that syndecan-4 was down regulated at higher cell density, thus impeding activation of FGFR1. This further indicates that cell density can also regulate HSPG expression and thus the activity of bFGF.

Interestingly, GFs themselves can induce the expression of syndecans on the cell surface. This produces a positive loop of GF stimulation that can be inhibited by increased shedding. In this context, bFGF and TGF-β have been described to induce syndecan-1 expression and shedding in 3T3 cells but not in NmuMG cells (Elenius et al., 1992), further demonstrating the cell-specificity of this induction. Similar results have been reported for syndecan-2 and FGF-2

(Clasper et al., 1999). In this context, the importance of the discovery of GF-inducible elements in the syndecan promoters becomes more evident, ***see also 1.3.2.1***.

1.4.2. Syndecans may serve as low-affinity receptors for enzymes

HSPGs are implicated in the lipoprotein metabolism in many aspects (Kolset and Salmivirta, 1999). Most importantly, they bind lipoproteins and their lipases, which strongly depends on the apoprotein composition of the lipoprotein particles. HSPGs cooperate with lipoprotein receptors and lipases in the uptake, lysosomal delivery and degradation of the lipoproteins (Fuki et al., 1997). Besides, HSPGs present and stabilize LPL and hepatic lipase (HL) on cell surfaces. Furthermore, they carry out important functions in the pathology of arteriosclerosis. Unfortunately, many experiments were performed without distinguishing between the nature of cell surface HSPGs (syndecan or glypican). For further information, the following reviews are recommended: Lookene et al., 1997; Williams and Fuki, 1997; Kolset and Salmivirta, 1999.

1.4.3. Syndecans supply attachment sites for virus

Some viruses take advantage of syndecans to attach to cells. Thus, HSV (= herpex simplex virus) and pseudorabies virus glycoprotein C bind to HSPG (Feyzi et al., 1997; Rue and Ryan, 2002). HSPGs initiate dengue virus infection of hepatocytes (Hilgard and Stockert, 2000). A specific implication of syndecans could only be shown when used as attachment receptors for HIV-1 (human immunodeficiency virus) on macrophages (Saphire et al., 2001).

1.4.4. Syndecans act as regulators of protease/protease inhibitor interactions: Implication in wound healing

It is well known that wound healing is regulated by a fine balance between proteases and their inhibitors, which might be disturbed in some diseases (Kainulainen et al., 1998). One of the first protease inhibitors reported was antithrombin III, which bound to all kinds of membrane-bound HSPGs (Mertens et al., 1992). Based on these findings and the properties of the syndecans mentioned above (***see 1.4.1***), the interest in their role in wound-healing processes has grown in the last few years.

After incision wounding, syndecan-1 and -4 were induced (Elenius et al., 1991; Gallo et al., 1996) and found as soluble, shed forms in wound fluids (Baciu et al., 1994) participating in the maintenance of the proteolytic balance of the wound (Kainulainen et al., 1998). More sophisticated studies revealed that after skin injury, syndecan-1 and syndecan-4 expression was transiently decreased in keratinocytes migrating into the wound, but increased in proliferating keratinocytes at the margin (Elenius et al., 1991). Syndecan-1 and/or -4 induction was also observed in different situations such as platelet derived GF- (PDGF)-induction or balloon catheter dilatation (Bernfield et al., 1999; Cizmeci-Smith et al., 1997). When syndecan-1 and -4 knockout mice were generated, surprisingly, both mice were viable, without morphogenetic defects and fertile. However, in both mice, deficits in skin repair (syndecan-1; Bernfield et al., 1999 and unpublished data), and defects in wound-healing and angiogenesis (syndecan-4) were observed (Echtermeyer et al., 2001). Syndecan-4 $^{-/-}$ mice also presented a higher susceptibility to kappa-carrageen-induced renal damage (Ishiguro et al., 2001b) and to septic shock by lipopolysaccharides (LPS) (Ishiguro et al., 2001a). Unexpectedly, transgenic mice over-expressing syndecan-1 in skin also delayed wound healing (Bernfield et al., 1999).

1.4.5. Shedding of syndecans and functional implications

As mentioned above, syndecans shed from the cell-surface as do 1% of the membrane-anchored proteins. As already mentioned, the potential cleavage site (***see fig. 1.5, arrow***) is a dibasic (syndecan-1, -2, -3) and basic repeat (syndecan-4) located immediately next to the TM domain (Bernfield et al., 1992). Nevertheless, D-syndecan is also shed, although no similar sequence was found (Spring et al., 1994b). The shedding process releases a soluble fragment corresponding to the ectodomain, which can act as a dominant negative form competing for binding partners with the membrane-bound syndecan. Shed syndecan-1 and -4 have been found in body fluids during wound healing indicating that shedding is a physiological process (Subramanian et al., 1997).

Shedding is cell-specific and highly regulated. Syndecan-1 and -4 shedding can be accelerated by activation of PKC and by EGF (tyrosine kinase) family members (but not by other GFs) and thrombin receptor (G-coupled receptor) activation (Subramanian et al., 1997). This increase in shedding was due to a greater turnover, since mRNA and cell surface levels stayed the same.

As responsible enzyme (sheddase, secretase, convertase), Fitzgerald (Fitzgerald et al., 2000) identified a tissue-inhibitor of metalloproteinases-3 (TIMP-3) sensitive metalloproteinase (MP). They also demonstrated that several mechanisms and pathways might lead to accelerated shedding: inhibition of PKC prevents shedding induced by phorbol myristate acetate (PMA) and cellular stress but not by receptor activation, which, in contrast was abolished by mitogen activated protein (MAP) kinase inhibition. Accelerated shedding was inhibited by TIMP-3 treatment while hydroxamate prevented constitutive shedding. These results led to the model represented in ***fig. 1.9***. The membrane-associated MP might be ADAM-12 (a disintegrin and metalloproteinase; Iba et al., 2000). This was propsed as the sheddase.

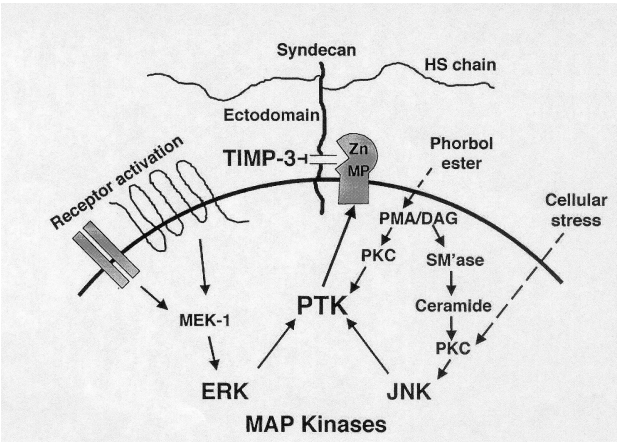

Figure 1.9: *Schematic presentation of the pathways involved in accelerated shedding*. Receptor activation leads to the activation of the MAP kinase pathway, while cellular stress activates JNK. Both pathways lead to the stimulation of a PTK, which also can be activated directly by PKC. This PTK activates a TIMP-3-sensitive metallo-proteinase. PTK = Protein tyrosine kinase, TIMP-3 = Tissue inhibitor of metalloproteinases-3, MEK-1 = Mitogen-activated protein kinase kinase, ERK = Extracellular signal-regulated kinase, JNK = C-jun NH_2-terminal kinase, PKC = Protein kinase C, DAG = Diacylglycerol, HS = Heparan sulfate, PMA = Phorbol myristate acetate; SM'ase = Sphingomyelinase, MAP kinase= Mitogen-activated protein kinase; (Fitzgerald et al., 2000).

The shedding function is most evident in wound healing processes, but it might modulate any interaction that a syndecan undergoes with other proteins.

Recently, a very interesting role of syndecan shedding was demonstrated: it was known that the virulence factor Las A enhanced shedding of syndecan-1 (Park et al., 2000a). $S1^{-/-}$ mice were resistant to infection of *Pseudomonas aeruginosa* by nasal application (Park et al., 2001). Suppression of shedding in normal mice also suppressed infection. This implied that some pathogens exploit the physiological shedding mechanisms of syndecans. The increased concentration of shed molecules may lead to binding of poly-anionic substances, which normally prevent infection.

1.4.6. Syndecans in cell adhesion

1.4.6.1. Syndecans contribute to cell-cell adhesion: Implication in cancer?

Syndecan-1 localizes to adherens junctions (Hayashi et al., 1987; Jalkanen et al., 1987; Kato et al., 1995; Leppa et al., 1992), thereby strengthening cell-cell adhesion.

Recently, many studies have examined the role of syndecans, in particular syndecan-1, in cell adhesion processes. It has been demonstrated that loss of syndecan-1 affects the organization of actin cytoskeleton and E-cadherin expression (Kato et al., 1995): mouse mammary epithelial cells became fusiform, lost anchorage-dependence of growth and invaded collagen gels (Kato et al., 1995) resembling mesenchymal cells. Experiments with transfected lymphoid cells confirmed that syndecan-1 led to the formation of cell-cell contacts, which stained strongly for syndecan-1 (Sebestyen et al., 2000; Stanley et al., 1995).

Similar results were obtained for syndecan-4 (Stanley et al., 1995). Other studies showed that the recombinant extracellular domain of syndecan-4 serves as a substrate for the attachment of mammalian cells (McFall and Rapraeger, 1997; McFall and Rapraeger, 1998). It has also been shown that syndecan interacts with a heterophilic counterpart, since the transfected cells also adhered to non-transfected ones. To date, no direct interactions of cell-cell adhesion molecules and syndecans have been demonstrated, but among the possible candidates are CAMs from the Ig-superfamily such as platelet endothelial cell adhesion molecule 1 (PECAM-1) or N-CAM or selectins (Stanley et al., 1995).

In other studies, experiments were performed with the epithelial-derived cell line S 115, which becomes tumorgenic (colony-forming) when exposed to steroids. This was suppressed by syndecan-1 transfection, which restored the phenotype and inhibited the colony-forming capacity of the wild type (Leppa et al., 1992). In deletion experiments, it could be shown that the syndecan-1 ectodomain was sufficient for the restoration of the epithelial phenotype and for the inhibition of proliferation of S115 and other carcinoma cell lines but not of normal cells (Mali et al., 1994).

Opposite results were obtained for syndecan-2. Its ectopic expression in HT-29 M6 epithelial cells induced their transformation into a migratory phenotype with concomitant decrease of E-cadherin expression (Contreras et al., 2001).

All these data indicate that loss of syndecan-1 (and perhaps other syndecans) might be implicated in cancer progression in a tumor-suppressing way. Nevertheless, no tumor-associated gene inactivation of syndecans has been described so far and clinical studies have revealed an ambiguous contribution of syndecans (mainly syndecan-1) to cancer development. First, it was thought that the loss of syndecan-1 correlates with a negative outcome of cancer and therefore syndecan-1 was proposed to have a "tumor-suppressor" function. This matched with the fact that its expression was associated with the maintenance of epithelial morphology, anchorage-dependent growth and inhibition of invasiveness (Blackhall et al., 2001 and references therein; Inki et al., 1992; Inki et al., 1994; Inki and Jalkanen, 1996). Nevertheless, it has now become clear that syndecan-1 has a “tumor-suppressor” as well as a “tumor-promoter” function depending on the tissue affected. Due to lack of evidence for any genetic changes in the syndecan-1 genes and given that the syndecan-1 $^{-/-}$ mice develop normally, the implication of syndecan-1 in neoplastic progression is epigenetic. ***Tab. 1.1*** shows an incomplete list of publications emphasizing the implication of syndecan-1 in cancer.

“Tumor suppressor”

Low S1 expression: unfavorable overall survival in head and neck carcinoma (Anttonen et al., 1999)
Shed S1 inhibited growth and induced apoptosis of myeloma cells (Dhodapkar et al., 1998)
S1 positive mesotheliomas showed longer survival (Kumar-Singh et al., 1998)
Reduced S1 expression correlated with human hepatocellular carcinoma with high metastasic potential (Matsumoto et al., 1997)
Tumorigenity of chemically transformed keratinocytes was higher with lower S1 expression (Inki et al., 1992)

“Tumor promoter”

$S1^{-/-}$ mice showed a significant lower susceptibility of Wnt1 induced tumorgenesis (Alexander et al., 2000)
Enhanced S1 expression in pancreatic cancer (Conejo et al., 2000)
S1 as a functional co-receptor promotes hepatocyte GF (HGF) signaling in multiple myeloma cells stimulating survival and proliferation of tumor cells (Derksen et al., 2002)
Higher survival in the S1 low group in multiple myeloma (Seidel et al., 2000)
High S1 expression is related with metastatic potential in infiltrating ductal carcinomas: a role in angiogenesis via FGF (Stanley et al., 1999)

Table 1.1: ***Possible functions of syndecan-1 as” tumor suppressor” or” promoter”.*** **S1 = syndecan-1.**

1.4.6.2. Syndecans are implicated in cell-matrix adhesion and in the re-organization of the actin cytoskeleton

Syndecans cooperate with integrins by providing secondary binding sites thereby strengthening adhesive force (Couchman and Woods, 1999; Schwartz, 2001; Woods et al., 1993; Woods and Couchman, 1998).

Binding to the ECM is specific to each syndecan: syndecan-1 binds to type I collagen and FN but not to laminin or vitronectin (Elenius et al., 1990; Sanderson et al., 1992). In early mouse embryo, it colocalizes with the initial site of ECM accumulation and syndecan-1 and -3 colocalize with tenascin during tooth (Koyama et al., 1996a) and limb development respectively. Syndecan-3 interacts specifically with the heparin-binding growth associated molecule (HB-GAM) (Raulo et al., 1994) and syndecan-3 binding to a novel HS binding site in type V collagen has been described. Type V collagen is synthesized by Schwann cells, where it inhibits outgrowth of dorsal root ganglions (DRGs) and promotes Schwann-cell migration (Chernousov et al., 2001; Erdman et al., 2002). Laminin-5, a component of skin basement membrane, presents a heparin-binding domain and promotes cell adhesion via syndecan-2 and -4 (Utani et al., 2001).

It has also been shown that spreading of fibroblasts on FN depends on syndecan-4 (Saoncella et al., 1999; Woods et al., 1993). $FN^{-/-}$ mouse fibroblasts did not spread on the cell-binding domain (CBD) of FN (which binds to integrins) or on antibodies against β-integrin alone. The addition of anti-syndecan-4 antibodies initiated spreading in a C3-transferase inhibitable manner, which suggested an implication of the small GTPase Rho A in this process (***see tab. 1.2***). Activation of Rho A bypassed the necessity for syndecan-4 antibodies and also allowed cells to spread on the CBD of FN (Saoncella et al., 1999; Woods et al., 2000). From these experiments the heparin-binding fragment of FN (HepII) was identified as syndecan-4 binding domain.

Syndecan-4 has a special role among the syndecans concerning cell-matrix adhesion, since it has been found to localize to FAs (Woods and Couchman, 1994). Stable transfection of syndecan-4 cells increased size and number of FAs and stress fibers (SFs). This resulted in a stronger anchorage to the ECM and decreased migratory ability. When the cytoplasmic region was deleted or antisense syndecan-4 was introduced into cells, a decreased spreading and less FA formation, independent of integrin, was observed (Couchman and Woods, 1999; Longley et al., 1999; Saoncella et al., 1999). Syndecan-4 core protein was sufficient for the assembly of FA (Echtermeyer et al., 1999), while deletion of the V-region (***see fig. 1.6***) of the cytoplasmic domain yielded a dominant negative form of syndecan-4 (Couchman and Woods, 1999; Oh et al., 1997b).
In summary, all these results generated an increased interest in investigating the underlying signal mechanisms and over the last few years great advances have been made in the understanding of the role of syndecan-4 in focal adhesion formation (***see fig. 1.10***).

When syndecan-4 binds to ECM, e.g. via the HepII of FN (Woods et al., 2000), it is immobilized and oligomerizes. This leads to the binding of phosphatidyl inositol phosphate 2 (PIP_2) and the catalytic domain of PKCα to the syndecan-4 cytoplasmic tail, thus recruiting them to form FAs. Through this recruitment, syndecan-4 potentiates synergistically with PIP_2 the activity of PKCα which becomes independent of Ca^{2+} (Lee et al., 1998; Oh et al., 1997c; Oh et al., 1997b; Oh et al., 1998). PKCα activation leads to the formation of FAs (Woods and Couchman, 1992). For full activation dimerization of syndecan-4 is not sufficient; oligomerization is necessary (Oh et al., 1997b). PIP_2 levels increase after integrin ligation and control cytoskeletal rearrangement via Rho family, which connects the syndecan-4 and the integrin pathway in the formation of FAs (Couchman and Woods, 1999; Rapraeger, 2000) and PIP_2 can also activate various actin-binding proteins and activate and translocate PKC (Couchman and Woods, 1996). Interestingly, it was found that syndecan-4 was phosphorylated at a single serine in growth-arrested cells. Activation with PMA augmented phosphorylation. Phosphorylation of syndecan-4 cytoplasmic domain, which reduced binding to PIP_2, impeded oligomerization and further decreased activation of PKCα.

The phosphorylation state of syndecan-4 depends on the activity of a novel PKC isoenzyme and a bFGF dependent serine-threonine phosphatase (Horowitz and Simons, 1998b; Horowitz and Simons, 1998a) which might be PKCδ (Murakami et al., 2002). This means that syndecan-4 might be implicated in the formation of FA under control of bFGF. ***Fig. 1.10*** summarizes the results of these experiments.
Activation by PMA leads on one hand to the activation of PKC and thereby to an augment of FA formation, but Horowitz et al. showed that syndecan-4 phosphorylation is also augmented by PMA-induced PKC activation, which leads to an decrease in FA adhesion (Horowitz and Simons, 1998a). In the same way, Baciu (Baciu and Goetinck, 1995) showed that PKC activation was necessary to recruit syndecan-4 into focal contacts. These discrepancies might be due to the different cellular systems analyzed or due to the variety of PKC isoforms.

The outstanding role of syndecan-4 in the formation of focal adhesion has been questioned due to new findings: analysis of fibroblasts from syndecan-$4^{-/-}$ mice showed that they formed normal FAs when plated on CBD and HepII domain of FN. They only showed impaired FA formation when plated on the CBD of FN and when the HepII fragment was added in a soluble form to cells. Anti-syndecan-4 antibodies did not induce the generation of FAs in syndecan-$4^{-/-}$ fibroblasts seeded on the CBD of FN in a soluble nor in a substrate-bound state (Ishiguro et al., 2000). This unexpected finding was explained by possible compensatory effects of other syndecans. According to this hypothesis, recently, syndecan-2 has been proposed to participate in the formation of stress fibers in cooperation with integrin $\alpha_5\beta_1$ since it also binds to the HepII domain of FN (Kusano et al., 2000). Moreover, the over-expression of syndecan-2 led to stress fiber formation (Munesue et al., 2002).

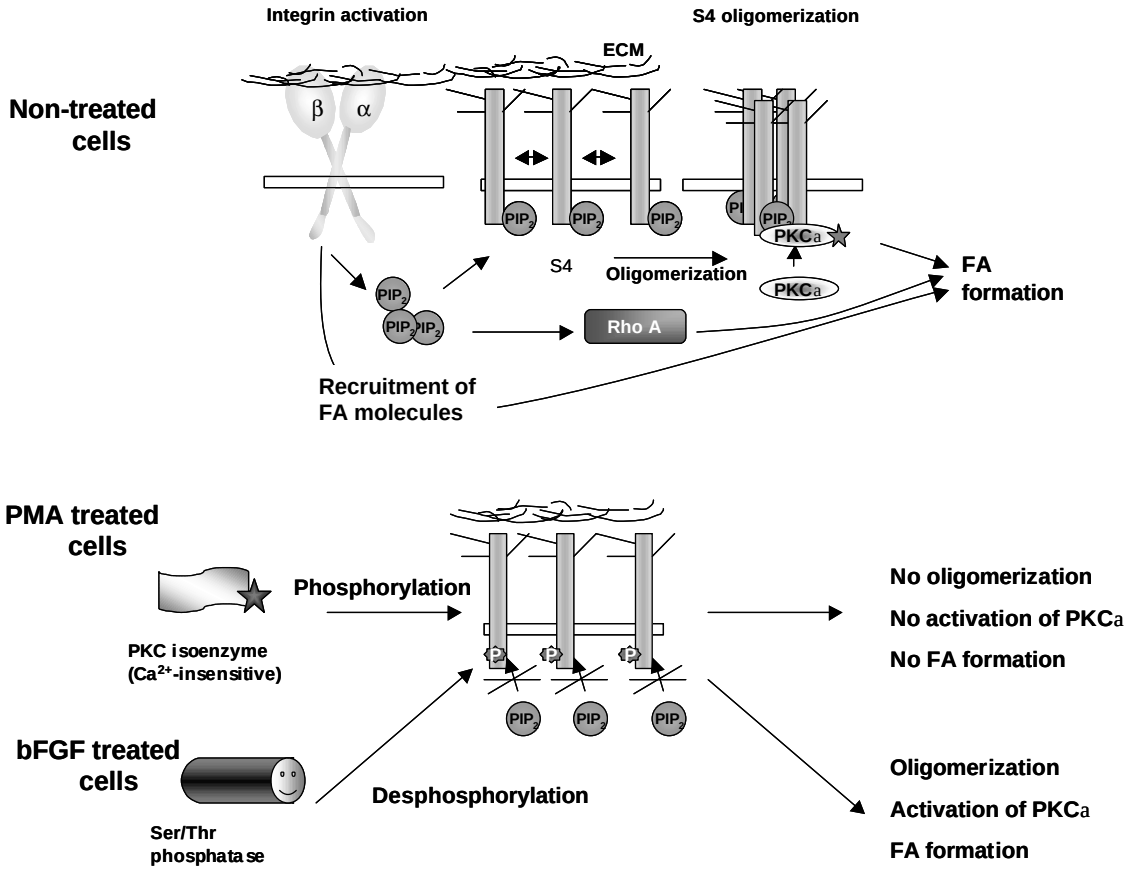

Figure 1.10: ***Proposed simplified mechanisms by which syndecan-4 contributes to FA assembly.*** **See also text. bFGF = basic fibroblast growth factor, ECM = Extracellular matrix, FA = Focal adhesion, PMA = Phorbol myristate acetate, S4 = Syndecan-4, PKC = Protein kinase C, PIP_2 = Phosphatidyl inositol phosphate 2.**

The contribution of other syndecans in the interaction with the cytoskeleton is not so well established. For syndecan-1, it has been demonstrated that aggregating anti-syndecan-1 antibodies led to its association with microfilaments (Carey et al., 1994b) depending on the presence of the cytoplasmic domain. Finally, syndecan-2 over-expression in COS-1 cells led to formation of filopodia and concomitant rearrangement of the actin cytoskeleton and to strong co-localization between syndecan-2 and actin (Granes et al., 1999).

1.5. Syndecans in development

As syndecans are expressed in a developmentally and cell-specific manner (Bernfield et al., 1993), many papers report the role of syndecans in development of different species (Rapraeger, 2001). Their implication has been described in early embryo development in mouse (David, 1993), where syndecan-1 expression was first detected, followed by syndecan-3 and –2 expression. They are also implicated in chick limb (Gould et al., 1992; Koyama et al., 1996a; Koyama et al., 1996b; Gould et al., 1995) and bone development (Modrowski et al., 2000). To simplify, here only two well-described systems are discussed: syndecans in muscle differentiation and in the development of the nervous system.

1.5.1. Syndecans in muscle differentiation

Syndecan-1, -3 and –4 are expressed in developing muscle. Syndecan-3 and -4 expression in muscle tissue was restricted to quiescent satellite cells, the myogenic stem cells. This suggests a role in maintenance or activation of regeneration processes. Both syndecans are co-expressed with FGFR1 and HGFR (c-met) during development (Cornelison et al., 2001). This study is somewhat contradictory to that of Larrain (Larrain et al., 1998), who demonstrated that syndecan-1 was necessary for myogenic differentiation of C2 cell line. On the other hand, it confirms studies in cultured limb buds (Olguin and Brandan, 2001; Fuentealba et al., 1999), which showed that syndecan-3 was transiently expressed in developing muscle but absent in adult muscle and that antisense expression of syndecan-3 in myoblasts led to accelerated myogenesis.

1.5.2. Syndecans in the development of the nervous system

In the nervous system, syndecan-3 is mainly found in axons from the developing brain while syndecan-2 is concentrated in synapse and appears later in development, in the mature brain. Both proteins can interact with the calcium/calmodulin-dependent serine protein kinase (CASK) the expression of which changes during development correlating spatial-temporally with expression of both syndecans (Hsueh et al., 1998; Hsueh and Sheng, 1999). The role of CASK in the regulation of gene expression will be discussed later (***see 1.7.1.3***). The selective localization of syndecan-2 in synapses suggested a role in spine development. Indeed, when hippocampal cultures were transfected with syndecan-2, accelerated spine formation was observed, which depended on the PDZ domain interacting motif (Ethell and Yamaguchi, 1999). Deleting this motif did not affect targeting or clustering of syndecan-2. On the other hand, it was suggested that the deletion of this motif could impede interactions with synbindin, a protein co-localizing with syndecan-2 in postsynaptic membranes (Ethell et al., 2000; Ethell and Yamaguchi, 1999). Recently, it has also been shown that syndecan-2 is phosphorylated by EphB2 (Ephrin B2) receptor tyrosine kinase, which is crucial for the clustering- and spine-formation activity of syndecan-2 (Ethell et al., 2001; Henkemeyer and Frisen, 2001). Interestingly, syndecan-3 was phosphorylated by EphB1 *in vitro* (Asundi et al., 1997).
Syndecan-3 has also been associated with neurite outgrowth by interacting with HB-GAM and thereby activating a pathway in which src, cortactin and microtubules are involved. This will be discussed more in detail below (***see 1.6.1).*** A summary of syndecan-2 and -3 functions in the CNS can be found in ***fig. 1.11***. Syndecan-1 is expressed earlier, around day 10, but it does not seem to be implicated in the development of the CNS (Nakanishi et al., 1997).

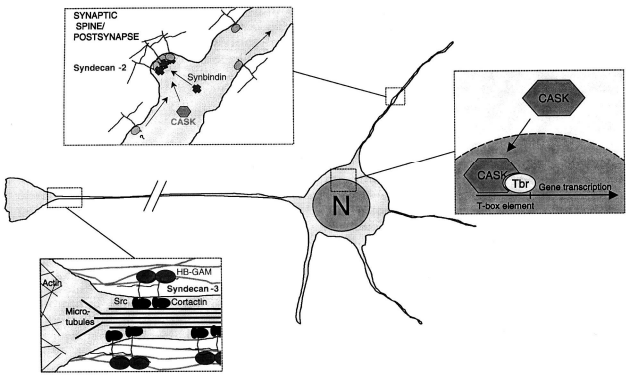

Figure 1.11: ***Syndecan function in the CNS;*** **Rapraeger, 2001; see also text.**

In some aspects, HSPGs are implicated in AD: Amyloid-β may be an HSPG core protein (Schubert et al., 1988), HSPGs were found in neurotic plaques in AD in early stages of development and also in Amyloid-β deposits (Fukuchi et al., 1998). Specifically, syndecan-2 has been associated with AD (van Horssen et al., 2001).

1.6. Syndecan-3

Syndecan-3, also called N-syndecan due to its abundance in the nervous system, was first cloned in rat from a Schwann cell library (Carey et al., 1992). It is the largest of the syndecan family members.

Since the structure and general functions of the syndecans have been explained already, in this chapter only the specific properties of syndecan-3 will be discussed.

1.6.1. Syndecan-3 in the nervous system

Syndecan-3 has important functions in the development (***see also 1.5.2***) of chicken limbs and in cartilage differentiation (Gould et al., 1992). It is only expressed in immature chondrocytes and it regulates their maturation (Shimazu et al., 1996) and antibodies against syndecan-3 inhibit cartilage differentiation (Seghatoleslami and Kosher, 1996). Its implication in muscle differentiation (Fuentealba et al., 1999; Koyama et al., 1996b) has already been mentioned above.
Although some of the aspects of the function of syndecan-3 in the nervous system have also been discussed earlier, this special function will be examined here in further detail due to the abundance of literature that has been published recently.

Syndecan-3 expression strongly correlates with the differentiation of oligodendrocytes and Schwann cells as well as myelination in the CNS and peripheral nervous systems (PNS) respectively. Despite of its proposed function in myelin formation, it is not a structural component of it. In the PNS, Schwann cells are the main or only source of N-syndecan (Carey, 1996).

The role of syndecan-3 in oligodendrocyte differentiation could be related to its ability to bind bFGF during nervous tissue development. Syndecan-3 binds bFGF with high affinity (Kd = 0.5 nM) in a saturable manner (Chernousov and Carey, 1993). Oligodendrocyte precursors, which express syndecan-3, also have bFGF receptors and are stimulated by bFGF to proliferate (Gard and Pfeiffer, 1993). This could be blocked by the inhibitor of HSPG synthesis, sodium chlorate (Bansal and Pfeiffer, 1994; Carey, 1996).

Syndecan-3 also promotes attachment and spreading of Schwann cells (Chernousov et al., 1996) by binding to p200, a heparin-binding glycoprotein secreted by Schwann cells. Syndecan-3 is up regulated in differentiated neural stem cells after retinoic acid-induced differentiation (Inatani et al., 2001).

Syndecan-3 also functions as a receptor for the cell-surface and ECM-associated molecule HB-GAM (pleiotropin, midkine) (Raulo et al., 1992; Raulo et al., 1994). Nolo et al. (Nolo et al., 1995) showed that syndecan-3 and HB-GAM (18 kDa) were co-expressed in the developing rat brain when neural connections develop rapidly (Kinnunen et al., 1999; Rauvala et al., 1994). HB-GAM lines developing axons and promotes neurite outgrowth in brain neurons (Kinnunen et al., 1998a). Interaction of syndecan-3 with HB-GAM was implicated in axon guidance and neurite outgrowth. This depended on the presence of sugar chains and a minimum of 10

monosaccharides was necessary for binding of HB-GAM to syndecan-3 (Kinnunen et al., 1996; Rauvala and Peng, 1997). Axon outgrowth was mediated by the cortactin-src kinase-signaling pathway (Kinnunen et al., 1998b). The C1 domain of the cytoplasmic region of syndecan-3 was shown to interact with c-src and c-fyn, both of which were phosphorylated. In the immunoprecipitated complex further cortactin and microtubules were found, suggesting the model presented in ***fig. 1.11*** (Kinnunen et al., 1998b).

The finding that HB-GAM injected into dendritic area inhibited tetanus-induced long term potentiation (LTP) without affecting baseline synaptic transmission, also suggested a role of syndecan-3 in synaptic plasticity (Lauri et al., 1996; Lauri et al., 1998). Indeed, it was shown that src, fyn and cortactin co-purified with syndecan-3 from the CA1 region of the hippocampus and that this association was increased after LTP (Lauri et al., 1999). Accordingly, the first results published on the syndecan-3 knock-out mice showed that although apparently normal, they have deficits in LTP and spatial memory (Reizes et al., 2001; Rapraeger, 2001).

Syndecan-3 participates in the regulation of β-actin mRNA localization by interactions with HB-GAM (Fages et al., 1998). This was demonstrated using microbeads loaded with HB-GAM. The binding to HB-GAM was mimicked by anti-syndecan-3 antibodies-coated beads. Src-kinase inhibitor blocked β-actin mRNA localization. Using colcemid and cytochalasin-D as inhibitors, the authors demonstrated that this process also depended on microtubules and actin, respectively (Fages et al., 1998).

1.6.2. Syndecan-3 and appetite

Finally, a role of syndecan-3 in the control of feeding behavior has been described. Transgenic expression of syndecan-1 in the hypothalamus led to hyperphagia and obesity in mice (Reizes et al., 2001; Strauss, 2001). This phenotype was reminiscent of mice with reduced α-melanocyte stimulating hormone (α-MSH; satiety peptide). Syndecan-1 potentiated, via its HS chains, the action of the α-MSH inhibitor agrp (agouti-related protein, antisatiety peptide) and inhibited the binding of α-MSH to its receptor. Since in normal mice, the main syndecan expressed in the hypothalamus (where the control of energy balance is located) is syndecan-3, food-deprivation experiments with normal mice were performed. This led to an induction of syndecan-3 and binding and potentiation of the antisatiety peptide, which was shed in the fed state. Now the satiety peptide bound to its receptor, which reduced food intake. Accordingly, in syndecan-3 knockout-mice, food deprivation reduced hyperphagia. The results of this study are summarized in ***fig. 1.12***.

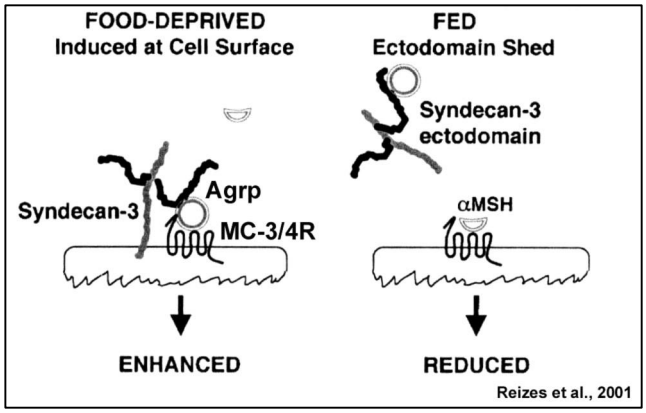

Figure 1.12: ***Putative mechanisms for the involvement of syndecan-3 in the regulation of feeding behavior*****. Syndecan-3 is induced in response to food deprivation, possibly potentiating the action of the antisatiety peptide agrp with its receptor MC-3/4R, and enhances feeding. Shedding would remove the stimulus and reduce feeding, thus allowing the binding of the satiety peptide a-melanocyte-stimulating hormone (a-MSH). agrp = agouti-related protein; MC-3/4R melanocortin-3/4 receptor.**

1.7. Intracellular binding partner of syndecans

As already mentioned, a variety of proteins have been described to bind to syndecan extra- and intracellular domains. The abundance of extracellular ligands makes it impossible to mention all of them here. Besides, the intracellular binding partners are of special interest as they might be involved in signal transduction pathways and their analysis might reveal common mechanisms. Therefore these proteins or protein families will be presented in the following chapter.

1.7.1. PDZ proteins

These proteins take their name from three proteins: PSD-95 (Postsynaptic Density-95), Discs-large (Dlg) and Zonula Occludens-1 (ZO-1). PSD-95 is a 95 kDa protein of the postsynaptic density; Dlg is the product of Drosophila discs large-1 tumor suppressor gene, and ZO-1 is a vertebrate tight-junction protein (Cohen et al., 1998). These proteins bind specifically to C-terminal sequences at the inner surface and are thought to link membrane components to the underlying actin-containing cytoskeleton (Bernfield et al., 1999).
The common feature of these proteins is the PDZ-domains, which are domains (with about 80 amino acids) composed of compact α- and β-modules, containing 5-6 β-strands and two α-helices. The binding peptide fits into a hydrophobic pocket. PDZ domains are selective (Grootjans et al., 2000). There are two classes of PDZ domains: Type I binds to peptides with a terminal (S/T)XV consensus motif and Type II selects peptides with hydrophobic or aromatic side chains at position –2 relative to the C-terminal (Cohen et al., 1998; Grootjans et al., 2000). Among the syndecan-binding proteins, many are members of the PDZ-family such as syntenin, synectin and MAGUKs (membrane-associated guanylate kinases), which can bind to the last four amino acids (EFYA) of the syndecan cytoplasmic tail.

1.7.1.1. Syntenin

Syntenin (33 kDa) presents two (tandem) class II PDZ domains. It was shown to interact with syndecan-2 by co-localization, two-hybrid system and surface resonance experiments, as well as overlay assays. Although these results were obtained for syndecan-2, it seems that syntenin does not discriminate between syndecans, as it binds to the motif EFYA that is identical in all syndecans. Syntenin is highly expressed in cell surface projections, cell adhesion sites, FAs, SFs and in the nucleus. Over-expression provokes flattened cell morphology and enhances plasma extensions, which can be reverted by active Rho A. Its function might be that of an adaptor, coupling syndecan to the cytoskeleton (Grootjans et al., 1997). In detail, both PDZ domains can interact with syndecan by cooperative binding and the stoichiometry between syndecan: syntenin is 2:1. Syntenin also binds to neurexins, B-class ephrins, and ephrin receptors (Grootjans et al., 2000; Zimmermann et al., 2001). The PDZ domains are also required for PM localization of syntenin.

1.7.1.2. Synectin

Synectin also belongs to the Type II class of PDZ proteins and its over-expression inhibits migration in ECV304 cells in a dose-dependent manner without affecting adhesion or growth rate of cells. Its molecular mass is 36.1 kDa and it is highly expressed in brain and spleen. It forms homodimers and heterodimers with syntenin and might be involved in the assembly of signaling complexes by serving as a scaffold. Synectin binds exclusively to syndecan-4. This

binding requires additional sequences to the PDZ domain. This does not rule out the possibility that other similar proteins might also bind to the other syndecans (Gao et al., 2000).

1.7.1.3. MAGUKs

MAGUKs are important kinases in the organization of membrane signaling. They possess an src homology 3 (SH3) domain, a domain with homology to guanylate kinase (GUK) without enzymatic activity, a PDZ domain and an N-terminal Ca^{2+}-calmodulin dependent protein kinase-(CAMK-) like domain. They might operate as scaffolding proteins that recruit or organize other proteins at the PM to coordinate signal transduction within the cortical cytoskeleton.

h-CASK is the human homologue of LIN-2A, a *Caenorhabditis elegans* scaffolding protein. Mutations in the *lin-2* gene inactivate the LET-23 receptor tyrosine kinase/Ras/Map kinase pathway necessary for vulval cell differentiation in *C. elegans*. h-CASK is ubiquitously expressed, localizes to the PM of epithelial cells and was found to bind to syndecan-2 and protein 4.1 by two-hybrid experiments (Cohen et al., 1998; Craven and Bredt, 1998; Hsueh et al., 1998). This led to the theory that h-CASK might mediate a link between ECM, syndecans and actin via protein 4.1 (Cohen et al., 1998). Protein 4.1 belongs to the ERM (Ezrin/Radixin/Moesin) family, which will be discussed later (***see 1.7.4***).
hCASK binds to all four syndecans, although with higher affinity to -2 and -4, and to neurexins, TM proteins that are localized near synapses and thought to play role in axon guidance or adhesion (Cohen et al., 1998; Hsueh et al., 1998; Hsueh and Sheng, 1999).

The interactions of syndecans with CASK gained importance when it was discovered, that CASK could translocate to the nucleus. It was shown to regulate gene transcription by interacting with Tbr-1, a T-box transcription factor and to induce for example the expression of reelin, which is essential for cerebrocortical development (Bredt, 2000; Hsueh et al., 2000). By co-expressing syndecan-3 with CASK, CASK translocation to the nucleus was inhibited. This offers an exciting possible explanation of how syndecans might regulate gene expression.

1.7.2. Synbindin

Synbindin is a 24-kDa protein that presents homology to yeast proteins participating in vesicle transport. It was isolated by two-hybrid system assays using the cytoplasmic domains of syndecan-2 as bait. Although it binds to the EFYA motif of syndecan-2, it has no classical PDZ domains. It is mainly found in dendritic cells, especially in the post-synaptic density, co-localizing with syndecan-2 (Ethell et al., 2000). These authors suggest that synbindin clustering induced by syndecan-2 might facilitate local synthesis and transport of neurotransmitter receptors (***see 1.5.2 and fig. 1.11).*** No association of synbindin to other syndecans has been described.

1.7.3. Syndesmos

This protein specifically interacts with parts of the C1- and the V-region of syndecan-4. This 40-kDa protein is ubiquitously expressed and can be myristylated. It co-localizes with syndecan-4 in cells plated on FN and its over-expression leads to cell spreading and FA contact formation in a serum-dependent manner. At mRNA level, syndecan-4 and syndesmos are expressed in the same tissues (Baciu et al., 2000). These authors suggest an involvement of syndesmos in FA formation, in cooperation with syndecan-4. This theory was supported by recent findings that syndesmos also binds to the focal adhesion adaptor protein, paxilin, and to the paxilin homologue hic-5 (Denhez et al., 2002).

1.7.4. The ERM family

The ERM family is named after the first three members to be isolated. Ezrin was first discovered as a structural component of microvilli, radixin as an F-actin capping protein from adherens junctions, and moesin as heparin-binding molecule. They belong to the superfamily of the 4.1 proteins, which also comprises the protein 4.1 and merlin/schwannomin (among others).

Suppression of ezrin, radixin and moesin proteins led to the destruction of microvilli, cell-cell and cell-substrate adhesion, suggesting a role of Erm family members in these processes. They have been proposed as cross-linkers between transmembrane proteins and the actin cytoskeleton (Bretscher, 1999; Bretscher et al., 2000; Mangeat et al., 1999; Tsukita and Yonemura, 1997; Tsukita and Yonemura, 1999; Vaheri et al., 1997). In cells, they are present in an inactive form, with the N-terminal domain interacting with the C-terminal domain. They can be activated by Rho A and PIP_2, see ***fig. 1.13***.

Granes (Granes et al., 2000) showed that ezrin interacts with syndecan-2 *in vivo* by co-localization and co-immunoprecipitation from COS-1 cells. This interaction was resistant to 0.2% Triton X-100, indicating that ezrin interacted with the cytoskeleton. Rho A or lysophosphatidic acid (LPA) treatment increased both syndecan-2 insolubility and syndecan-2/ezrin interactions. This indicated that the ERM protein was implicated in the signal transduction from syndecan-2.

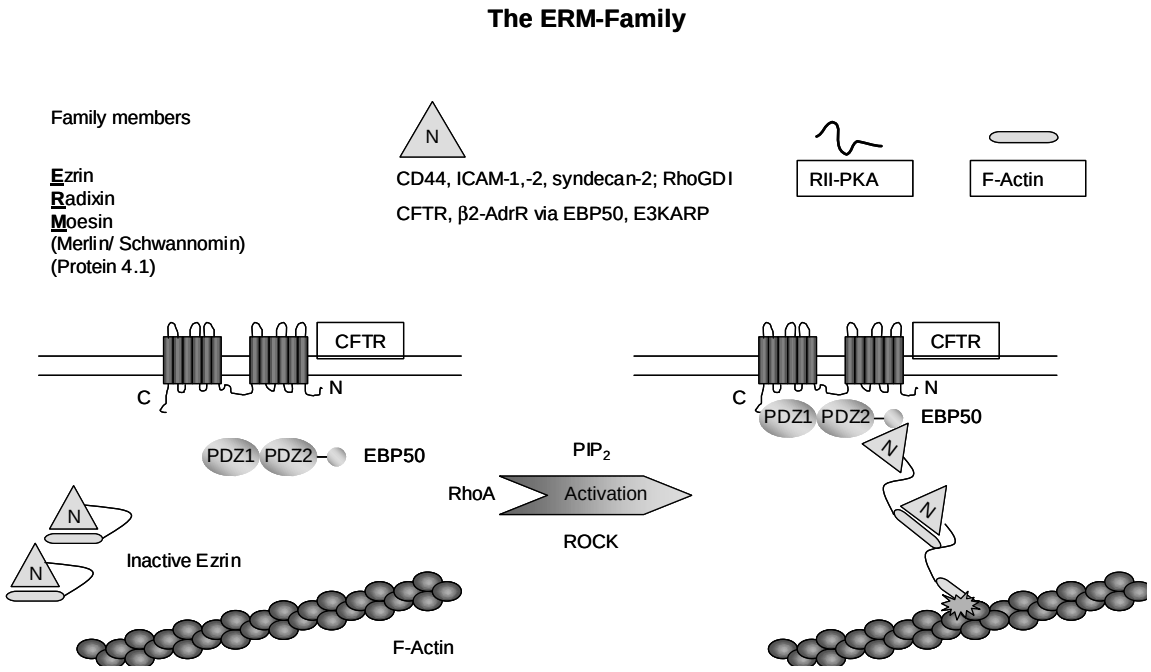

Figure 1.13: ***Scheme of ERM family activation*****. ERM proteins (here represented by ezrin), are present in an inactive form due to intramolecular interactions. Rho A activates ERMs by increasing PIP_2 via PIP4K and by activating ROCK thereby unfolding the protein, enabling it to bind directly or indirectly via adaptor proteins to transmembrane receptor. By head-to-tail binding, they can convey signal from those receptors to the actin cytoskeleton. PIP_2 = Phosphatidyl inositol phosphate 2, CFTR = Cystic fibrosis transmembrane conductance regulator, ICAM = Intercellular adhesion molecule-1, ROCK = Rho-associated kinase, EBP 50 = (ERM)-binding phosphoprotein-50, ERM = Ezrin-Radixin-Moesin, b2-AdrR = b2-Adrenalin-R, NHE-3 = Na^+/H^+-exchanger-3, E3KARP = NHE3 kinase A regulatory protein, PKA = Protein kinase A, RhoGDI = Rho GDP dissociation inhibitor.**

1.7.5. Neurofibromin

Neurofibromin is a large tumor-suppressor protein expressed from the neurofibromatosis type 1 (*NFT1*) gene. Its mutation leads to benign or malignant tumors of the nervous system. It binds to all syndecans shown by two-hybrid experiments. For interaction, the TM and the TM proximal sequences of syndecans are necessary. Neurofibromin, syndecan-2 and CASK have overlapping distribution, as shown by co-IP from rat brain and immunostaining (Hsueh et al., 2001).

1.7.6. Others

The binding of PKC and PIP_2, specific for syndecan-4, as well as the specific binding of src, fyn, cortactin and tubulin for syndecan-3, have already been discussed earlier. The association with microfilament has also been mentioned briefly in the text and will not be discussed further.

1.8. GTPases

As observed, many of the processes in which syndecans are involved are paralleled by changes in the actin cytoskeleton. The family of small GTPases (***see fig. 1.14***) has been described to be key components for the regulation of the actin cytoskeleton. This last chapter is therefore dedicated to a short introduction of these molecules.

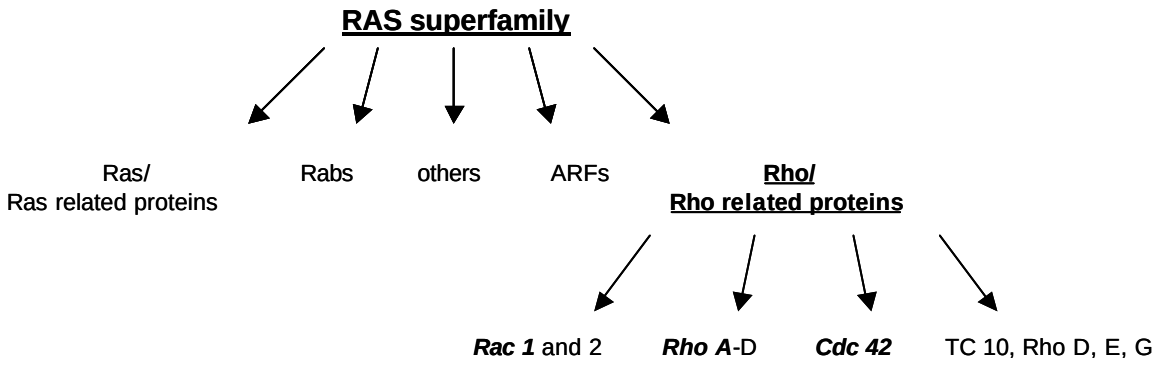

Figure 1.14: *The Ras superfamily*. The Rho (= Ras homologue) family of small GTPases belong to the superfamily of Ras GTPases (Ras/Ras related proteins, Rho/Rho related proteins, ARFs, Rabs) and comprises (in mammals): Rho A – C, Rac 1 and 2, cdc 42 and others (TC10, RhoD, E, G) (Bar-Sagi and Hall, 2000; Kaibuchi et al., 1999; Schmidt and Hall, 1998). Rab = Ras from brain, ARF= ADP ribosylation factor.

1.8.1. Activation cycle

GTPases cycle between an inactive (GDP-bound) and an active (GTP-bound) state (***see fig. 1.15***). The GDP-GTP exchange can be catalyzed or accelerated by guanine nucleotide-exchange factors (GEFs), which are often oncogenes, or inhibited by guanine nucleotide dissociation inhibitors (GDIs). In the same way GTPases accelerating proteins (GAPs) can increase the rate of GTP hydrolysis. Among the effectors of the GTPases are kinases, phosphatases and adaptor proteins (Bar-Sagi and Hall, 2000; Bobak, 1999; Kaibuchi et al., 1999).

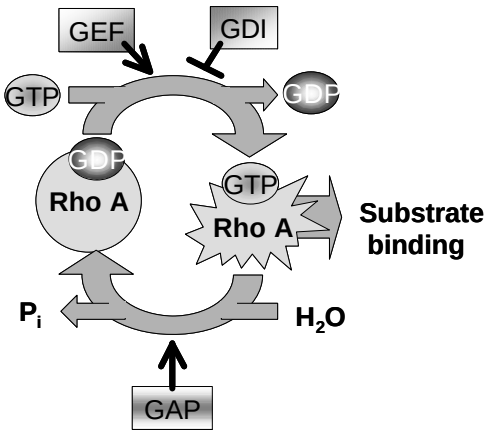

Figure 1.15: ***GTPases cycle between an active (GTP-bound) and inactive (GDP-bound) state*****. Activation can be influenced by different factors: GEFs (Guanine nucleotide-exchange factors), GDIs (Guanine nucleotide dissociation inhibitors) and GAPs (GTPases accelerating proteins)**.

1.8.2. Inhibition by toxins

The clostridial toxins and exoenzymes covalently modify and inactivate Rho family members (Bobak, 1999; Lerm et al., 2000). Two classes of transferase-reactions are catalyzed: ADP-ribosylation and UDP-glycosylation/UDP-glucosaminylation. C3-transferase (exoenzyme of *C. botulinum*) belongs to the first class and modifies Rho A, B and C specifically (Bobak, 1999; Aktories, 1997), while glycosylation affects all Rho GTPase family members. By the use of these and other toxins, as well as dominant positive and negative mutants of each GTPase, it was possible to study the implication of the GTPases in the regulation of the actin cytoskeleton and further control in cell-adhesion (Fukata et al., 1999), see ***tab. 1.2***.

GTPase	Cdc 42	Rac 1	Rho A
Dominant Positive	Cdc V12	Rac V12	Rho V14
Dominant Negative	Cdc N17	Rac V12N17	Rho N19
Activator	Bradykinin or sphingosine-1 phosphate (S1P)	Platelet derived GF (PDGF)	Lysophosphatidic Acid (LPA)
Inhibitor (General)	e.g. Toxin A, B (*Clostridium difficile)*	e.g. Toxin A, B (*Clostridium difficile*)	e.g. Toxin A, B (*Clostridium difficile*)
Inhibitor (Specific)	-	-	C3-transferase (*Clostridium botulinum*)

Table 1.2: ***Small GTPases activators and inhibitors*** **(Bobak, 1999; Kozma et al., 1995; Ridley, 2001; Ridley and Hall, 1992)**

1.8.3. Functions

1.8.3.1. Control of the actin cytoskeleton

The best-studied GTPases are cdc 42, which is responsible for the outgrowth of filopodia (Nobes et al., 1995; Nobes and Hall, 1995) , Rho A which is implicated in the establishment and maintenance of SFs and FAs (Ridley and Hall, 1992; Ridley, 2001) and Rac 1 which is necessary for lamellipodia formation (Allen et al., 1997; Bar-Sagi and Hall, 2000; Hall, 1998; Kaibuchi et al., 1999; Sander et al., 1999; Small et al., 1999; Nobes and Hall, 1999), ***see fig. 1.16***.

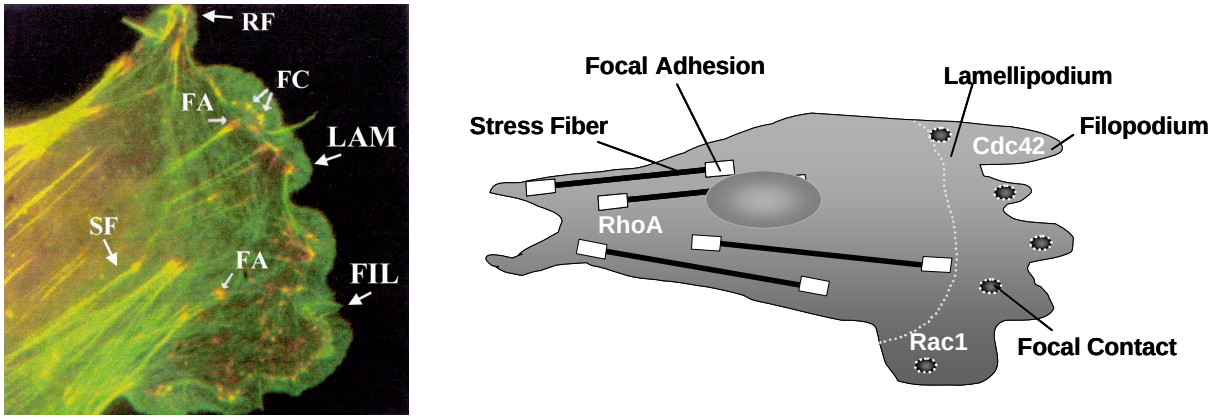

Figure 1.16. ***The actin cytoskeleton*****. Actin cytoskeleton and substrate adhesion complexes shown by vinculin (red) and actin (green) labeling of a fibroblast. FC = Focal contact, RF = Ruffle, FA = Focal adhesion, LAM = Lamellipodium, FIL = Filopodium, SF = Stress fiber. (B) In a cartoon the implication of each GTPase is demonstrated.**

Lamellipodia are thin (5 μm wide and 0,5 μm thick) structures, composed of a loose network of unipolar actin bundles. They are fast-growing structures, which are always directed outwards. Filopodium like microspikes are composed of actin bundles, have a diameter of about 0.15 μm and extend from lamellipodia. Both structures are protrusive (Small et al., 1999). FAs are structures with an extension of 10-15 nm, where the cell attaches to the substrate, and are composed of 50 proteins (vinculin, among others). Rac 1-induced focal contacts (FCs) can be converted into FAs by active Rho A, which supports the theory that FCs are precursors of FAs. Depending on cell type, several other actin-containing structures are found in cells containing antiparallel arrays of actin and myosin and therefore have contractile potential. These are: SFs, concave bundles, convex bundles (which seem to be characteristic of epithelial cells), polygonal networks and dorsal arcs. These structures will not be discussed further. ***For review see*** (Hu and Reichardt, 1999; Kaverina et al., 2002; Small et al., 1999).

Rho might recruit PIP_5-kinase to the PM and increased PIP_2 might interact with vinculin in such a way that binding sites of talin and actin are uncovered. This would also link the implication of syndecan-4 in this process, which is oligomerized depending on PIP_2 (***see 1.4.6.2***). Another connection between syndecans and the GTPases was shown by Granés (Granes et al., 1999) by co-transfection experiments. The expression of syndecan-2 led to the induction of filopodia by activating cdc 42. This provides a link between syndecan-2, cdc 42 and the actin cytoskeleton. Moreover, there exists a connection between GTPases and ERM proteins via the activating effect of Rho A on Ezrin, ***see also 1.7.4***.

Until some years ago, it was thought that there was a hierarchical model of activation among the GTPases, but it is now accepted that the situation is more complex. In general, the activation of Rho A leads to cell adhesion and contractility, while the pathways via cdc 42 and Rac 1 lead to more spreading and ruffling (Sander et al., 1999), ***see fig. 1.17***. This is also important for cell migration (Kaverina et al., 2002).

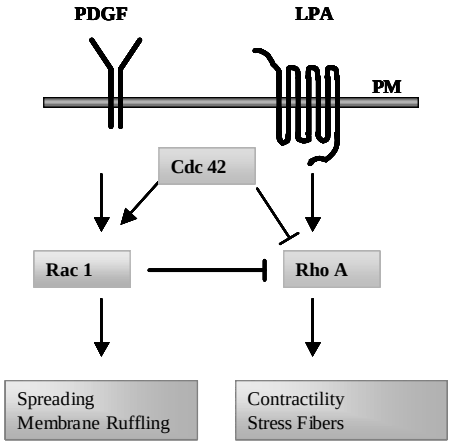

Figure 1.17: ***Simplified model of the implications of the small GTPases in the control of cell motility*****. Activation of cdc 42 leads to the inhibition of Rho A and the activation of Rac 1. Rac 1 can also be activated directly by PDGF (platelet derived GF) binding to its receptor. This pathway increases membrane ruffling and spreading, while the activation of Rho A leads to contractility, the formation of SFs and FAs, which means greater adhesion. (Sander et al., 1999), LPA = Lysophosphatidic acid, PM = Plasma membrane.**

1.8.3.2. Other functions

The activation of small GTPases is implicated in other signaling pathways apart from regulating the actin cytoskeleton.

They can activate gene expression: Rho A mediates signal transduction that links lysophosphatidic acid (LPA) to activation of transcription factors, while cdc 42 and Rac 1 affect gene expression by activating the JNK/SAPK (stress activated protein kinase) and p38 MAP kinase pathways (Coso et al., 1995; Minden et al., 1995; Tapon and Hall, 1997) and are implicated in cell cycle progression independent from their actin cytoskeleton controlling mechanisms (Lamarche et al., 1996). Rho A has also been described to be involved in cell cycle progression (Olson et al., 1995). Rac 1 and Rho A may also be engaged in endo- and exocytic processes. Finally, Rho family member Rac 1 might bind to MT and thereby link them to the actin cytoskeleton via β-catenin (Small et al., 1999 and references therein).

Aims

Over the last few years, proteoglycans have gained importance in our understanding in many physiological and pathological processes. Many authors have focused their interest on syndecans, which are Type I transmembrane proteins belonging to the family of heparan sulfate proteoglycans.

In this context, four syndecans have been cloned and characterized from various species. In human, only syndecan-1, -2 and -4 cDNA sequences have been described. Thus, the ***first aim*** of this thesis was the cloning and characterization of human syndecan-3 cDNA.

Syndecans have been shown to play a role in cell-cell and cell-matrix adhesion, mostly by reorganizing the actin cytoskeleton. The ***second aim*** of this thesis was to establish the effects of human syndecan-3 protein on the actin cytoskeleton through transfection experiments and further immunocytochemical, biochemical and functional analyses.

Cell surface receptors modify intracellular levels of signalling molecules. This has been demonstrated for syndecan-4. The ***third aim*** of this thesis was to study the underlying mechanisms induced by human syndecan-3 responsible for the effects observed.

Materials and Methods

2. Materials and Methods

2.1. Bacteria

2.1.1. Bacterial culture

LB–Medium (Luria Broth): 10 g/l tryptone, 5 g/l yeast extract, 5 g/l sodium chloride
Bacterial growth plates: LB-medium with 1.5% bacterial agar was autoclaved, cooled to 50°C, and after addition of antibiotics, poured into bacterial culture dishes. Bacterial strains were seeded and incubated overnight at 37°C.
Antibiotic solutions: Antibiotics were dissolved in MilliQ water, filtered (0.22 µm) and stored at -20°C.

Antibiotic	Final solution in medium
Ampicillin (Amp)	100 µg/ml
Kanamycin (Kan)	50 µg/ml
Tetracycline (Tet)	12.5 µg/ml

Table 2.1: ***Antibiotic concentrations***

Strain	Resistance	Use
XL_1 Blue	Tet	Host of λZAPII
SORL	Kan	Recombination with XL_1 Blue
JM109	-	Transformation
DHα5	-	Transformation

Table 2.2: ***Bacterial strains***

2.1.2. Preparation of glycerol stocks

To store bacteria for long periods, glycerol stocks were prepared: 500 µl of glycerol was poured into cryotubes and autoclaved. To each tube, 1.5 ml bacteria in LB was added and rapidly frozen at -80°C.

2.1.3. Production of competent bacteria

Transformation solution: 60 mM $CaCl_2$, 15% glycerol, 10 mM PIPES, pH 7.0. PIPES=Piperazine-N,N´-bis[2-ethanesulfonic acid]
A single colony was chosen, grown overnight in 4 ml LB/Amp, diluted in 150 ml LB and grown in an orbital shaker at 250 rounds per minute (rpm) and 37ºC until optical density $(OD)_{600nm}$ was ≈0.35-0.4 (1 OD_{600nm} ≈$0.8x10^9$ bacteria). Culture was placed for 10 min on ice and centrifuged (7 min, 1600x*g*, 4°C, without brake). Supernatant (SN) was discarded and the pellet was carefully resuspended in 10 ml transformation solution and centrifuged (5 min, 1100x*g*, 4°C, without brake). Pellet was resuspended in 10 ml transformation solution and kept on ice for 30 min, then centrifuged as before. Pellet was resuspended in 2 ml of transformation solution for each 50 ml of culture volume. 250 µl of competent cells was distributed into 1.5 ml Eppendorf tubes on EtOH/dry ice and stored at -80°C.

2.1.4. Transformation

Bacteria were thawed, placed on ice for 5 min, 5 µl of ligation mix (corresponding to approx. 25 ng of vector or 2 ng if purified vector was used), was added and incubated on ice for 30 min. Heat-shock was performed at 42°C for 45 sec. Bacteria were incubated on ice for 2 min. 1 ml of LB medium was added followed by incubation for 1 h at 250 rpm and 37°C. Three distinct volumes of bacterial solution were plated on selective dishes (50, 100 µl and the remaining volume), and incubated overnight at 37°C.
Transformation efficiency: Number of colonies/volume of plated bacteria x volume of bacteria total/ng of DNA used for transformation x 1000 ng/µg. Bacteria had a transformation efficiency of about 10^6 colonies/µg DNA.

2.2. Phages

2.2.1. Phage culture

Escherichia coli (*E.coli*) XL_1Blue is the host of λZAPII (both from Stratagene). To ensure a satisfactory infection rate, bacteria were grown in the presence of 10 mM maltose (which leads to the expression of the λ-receptor, and 10 mM $MgSO_4$ (to stabilize the λ-phages)
SM-Buffer: 50 mM TrisHCl pH 7.5*, 100 mM NaCl, 8 mM $MgSO_4$, 0.01% gelatin. *Tris=Trizma=Tris (hidroxymethyl)aminotethane
Soft Agar: LB Medium, 0.75% agar or agarose respectively
Phage library: Human fetal brain (HFB) library in λZAPII, host XL_1Blue
E.coli XL_1Blue was seeded on LB/Agar/Tet dishes (∅10 cm), and incubated overnight at 37°C. A colony was picked and grown overnight at 37°C. Next day, 2 ml of the overnight culture were mixed with 4 ml LB/Amp. Maltose and $MgSO_4$ were added to final concentrations (*see above*). Bacteria were allowed to grow in these conditions for 1 h, and then centrifuged (3 min, 400x*g*, room temperature (RT)). The pellet was resuspended in 3 ml $MgSO_4$. 10 µl of phage solution diluted in $MgSO_4$ was mixed with 100 or 150 µl of bacterial solution and incubated for 30 min at 37°C (when phages bind to the bacteria). 3 ml soft agar was added to the bacteria/phages mixture and rapidly poured onto previously prepared LB/Amp plates. Plates were incubated overnight at 37°C to allow bacterial growth and lysis.
For the first steps of library screening, ∅15 cm culture dishes were used. 300 µl of bacteria was mixed with λ-solution and incubated for 30 min, and 10 ml soft agarose was then added and plated.

2.2.2. Titulation of library

A range of dilutions of the library were prepared and incubated with their host bacteria as described above. Next day, plaques were counted and the concentration of plaque forming Units (pfUs) was calculated.

2.2.3. Phage extraction

To each (semi-) confluent bacterial dish (∅15 cm) with plaques, 5 ml of SM-medium was added and incubated for 4 h at RT. SN was transferred to sterile glass tubes, 200 µl of chloroform was added to kill bacteria and phages were stored at 4°C until further processing.

2.2.4. Preparation of hybridization filters

10x SSC: 1.5 M NaCl, 0.15 M sodium citrate
Sol A (denaturalization solution): 0.5 N NaOH, 1.5 N NaCl
Sol B (neutralization solution): 1.5 N NaCl, 0.5 N TrisHCl, pH 8.0
Sol C (washing solution): 2x SSC, 0.2 N TrisHCl, pH 8.0
For cDNA-positive phage screening, culture dishes (containing 10 000 or 50 000 pfUs for ∅10 or 15 cm dish) were placed for ≥ 30 min at 4°C. Filters (0.45 µm, Schleicher and Schull) were placed for 60 sec on each culture dish. As parts of the phages stuck to the membrane, filters were an identical copy of the plaques on the culture dish. In this step, filters and dishes were labeled by piercing with an ink-filled needle through the filter into the agar, thereby allowing phages to be located later on. Filters were incubated on 3 mm Whatman paper moistened with the respective solutions: 2 min Sol A, 5 min Sol B and 30 sec Sol C, then dried. DNA was then cross-linked for 2-3 h at 80°C. DNA was now accessible for the screening with a radioactive labeled probe (obtained by random priming: ***see 2.3.12.1***). After several washing steps, films were exposed to filters. Every spot on the film corresponded to a phage containing specific sequences. These phages were localized on the culture dishes, picked and plated again. This procedure was repeated until culture dishes contained only positive phages.

2.2.5. Recombination of phages (Obtention of phage DNA from λZAPII)

To recover DNA from phages, λZAPII phage was recombined with a helper phage (Ex Assist, Stratagene), which contains pBluescript as plasmid. Both phages were incubated with XL_1Blue bacteria, where they recombined. Then SOLR bacteria were transfected with the rescued phagemid in the presence of Amp. λZAPII phage does not infect SOLR bacteria, while the helper phage alone might infect bacteria but does not survive Amp selection. Therefore all the bacterial colonies obtained had the recombined plasmid.

2x YT medium: 10 g/l tryptone, 10 g/l yeast extract, 5 g/l sodium chloride
SM-Buffer: 50 mM TrisHCl pH 7.5, 100 mM NaCl, 8 mM $MgSO_4$, 0.01% gelatin
200 µl of *E.coli* XL_1Blue ($OD_{600\ nm}$≈1.0) was mixed in a glass tube with 100 µl (10^5 pfUs) phage solution in SM buffer and 1 µl helper phage (>1x10^6 pfUs/µl) and incubated for 15 min at 37°C. 5 ml 2x YT was added and incubated for 2 h at 37°C with agitation. The tube was heated to 70°C for 20 min, centrifuged (15 min, 4000x*g*) and SN was transferred to a sterile tube. 200 µl of *E.coli* strain SOLR (OD_{600nm}≈1.0) was mixed with 1, 50 or 200 µl phage stock and incubated for 15 min at 37°C. 100 µl of bacteria was plated onto LB/Amp plates and grown overnight at 37°C.

2.3. Molecular biology

2.3.1. DNA electrophoresis

TAE buffer: 40 mM TrisHCl, 20 mM CH_3COOH, 5 mM EDTA (Ethylenediaminetetraacetic acid)
DNA loading buffer 6x: 50% glycerol, 1 mM EDTA, 0.1% Bromphenol Blue
Commercial markers used*:* λ *Eco*RI/*Hind*III (Promega)*;* 100 base pair (bp) ladder (Pharmacia), KiloBase DNA marker (Pharmacia)

Agarose (0.75-3%) was dissolved in 1x TAE-buffer, heated briefly in microwaves and cooled to 50°C. 2-7 diamino-10-ethyl-9 phenyl phenanthridinium bromide (ethidium bromide) was added

to a final dilution of 0.5 µg/ml; DNA loading buffer 6x was added to samples. Samples were run in 1x TAE-buffer.

2.3.2. Determination of DNA concentration

2.3.2.1. By OD measurement

DNA concentration was estimated by measuring OD_{260nm} in a Quartz precision cell (Hellma). **ss** (single-strand) DNA (Primer, etc) ≈ 20 µg/ml and **ds** (double-strand) DNA (plasmids, etc) ≈ 50 µg/ml

2.3.2.2. By comparison with DNA marker

It was also estimated by comparison with the intensity of marker bands.

bp	µg in 6 µl*
21000	0.218
5184	0.053
4973	0.0512
4298	0.0443
3530	0.0363
2027	0.02089
1904	0.0196
1584	0.0163
1375	0.0141
947	0.0097
831	0.0058
564	0.0012
(125)	(-)

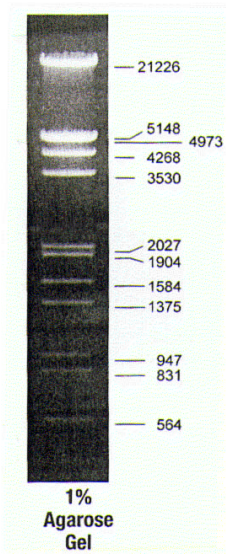

Table 2.3: λ ***Hind*III/*Eco*RI marker bands in 1% agarose gel***. * Volume loaded per gel

2.3.3. DNA digest

Enzymes used (purchased from: Promega, Amersham, Pharmacia, Biolabs, Boehringer): *Acc*II, *Asc*I, *Ava*I, *Bam*HI, *Eag*I, *ECO47*III, *Eco*RI, *Eco*RV, *HAE*III, *Hind*III, *Nco*I, *Nde*I, *Nhe*I, *Not*I, *Pst*I, *Pvu*II, *Sac*I, *Sac*II, *Sal*I, *Sau*3A, *Sma*I (30ºC), *Srf*I, *Xba*I, *Xho*I.

Restriction enzymes isolated from bacteria cut DNA by recognizing specific palindrome sequences. 3 units (U) of each enzyme was used for every µg DNA, and the amount of enzyme solution did not exceed more than 10% of the total reaction volume. Digests were performed for 1 or 2 h at 37°C. Enzymes were used together in double digests if their buffer conditions were compatible (e.g. in one-for-all-buffer (OPA)). For some selected clones, restrictions maps were produced before sequencing.

2.3.4. Polymerase Chain Reaction (PCR)

The PCR technique permits the amplification of minimal amounts of any DNA using sequence-specific primers and a heat-stable polymerase named Taq polymerase (Perkin Elmer). In an

initial denaturalization step (95°C), the two strands of the DNA are melted. Then primer annealing is allowed by cooling-down the reaction mix to a temperature that is specific for each primer pair (annealing temperature = T_m). In the elongation phase (72°C), the polymerase elongates the primers by incorporating deoxynucleotides from the reaction mix, thereby producing an exact copy of the sequence of the mother strand. This cycle is repeated 25-35 times, which yields an exponential amplification of DNA. Optimized conditions for each PCR performed during this thesis can be found in ***tab. 2.4***.

Aim	DNA template/	Primer	Cycle
S3 with deletion of C2 of C-terminal domain (ΔEFYA)	FL-S3 in pcDNA3	42d S3004	95°C for 4 min, (92°C for 1 min, 32°C for 1 min, 72°C for 2 min) x35 cycles, 72°C for 5 min.
S3 with deletion of V-region of C-terminal domain (ΔV)	FL-S3 in pcDNA3	42d S3003	95°C for 4 min, (92°C for 1 min, 32°C for 1 min, 72°C for 2 min) x35 cycles, 72°C for 5 min.
S3 with deletion of C-terminal domain (ΔC)	FL-S3 in pcDNA3	42d S3002bis	95°C for 4 min, (92°C for 1 min, 46°C for 1 min, 72°C for 2 min) x35 cycles, 72°C for 5 min.

Table 2.4: *PCR conditions*. FL-S3 = full-length syndecan-3.

2.3.5. Plasmids

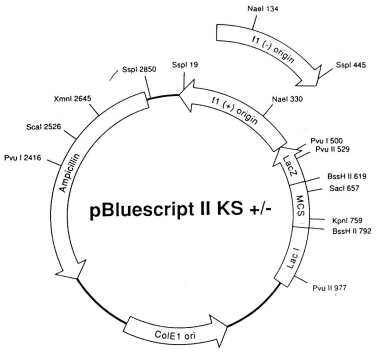

2.3.5.1. pBluescript

Figure 2.1: The pBluescript vector is used for single strand DNA rescue. It contains the lacZ promoter, which allows selection by blue/white-screening (Stratagene).

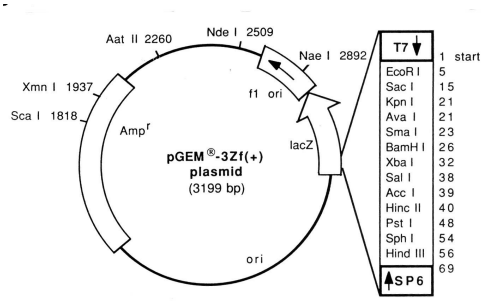

2.3.5.2. pGEM3Z

Figure 2.2: pGEM3Z is used for subcloning and amplification of DNA in bacteria and also contains a lacZ promoter (Promega).

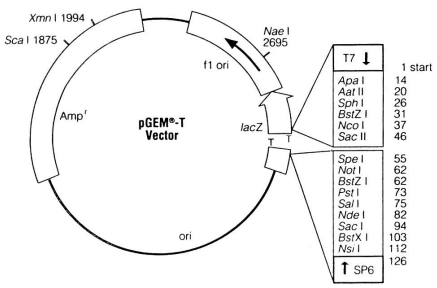

2.3.5.3. pGEMT

Figure 2.3: The pGEMT vector is specially designed for the ligation of PCR fragments. During PCR, Taq polymerase adds an additional A at the end of the amplification products, which can specifically anneal to "sticky T-ends" of the pGEMT vector (Promega).

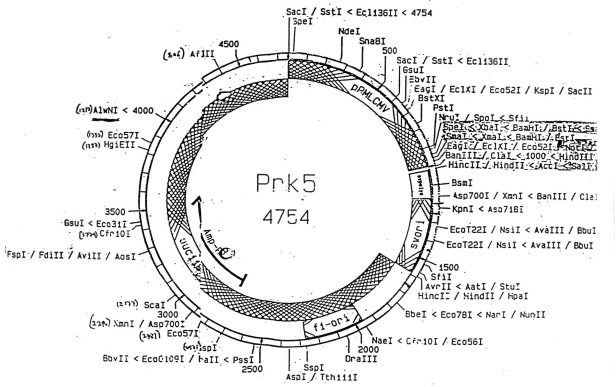

2.3.5.4. Prk5

Figure 2.4: Prk5 is a high-copy eukaryotic vector, which is used for transient transfection experiments (gift from J. Ureña).

2.3.5.5. pcDNA3

Figure 2.5: pcDNA3 carries a G418 resistance that permits selections of transfected eukaryotic cells after transfection and is therefore used for the generation of stable cells lines (Invitrogen).

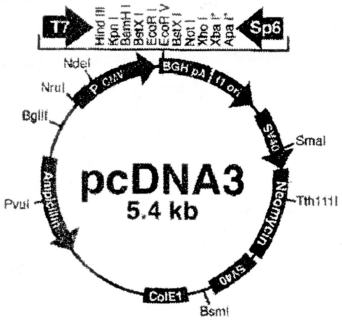

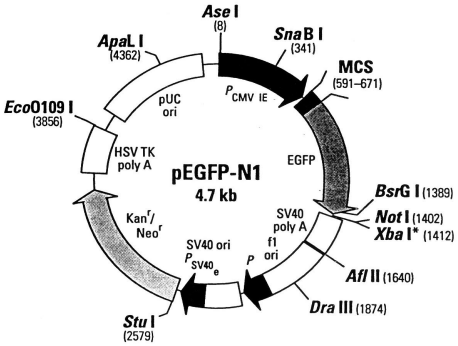

2.3.5.6. pEGFP

Figure 2.6: By the use of pEGFP vectors it is possible to generate fusion protein with the Green Fluorescent Protein (GFP). The GFP-molecules can be attached to the C- or N-terminal of the fusion protein. Plasmids are available for all reading frames (Clontech).

2.3.5.7. pGEX

Figure 2.7: The pGEX vector is used to produce glutathione-S-transferase- (GST-) fusion protein in bacteria (Pharmacia).

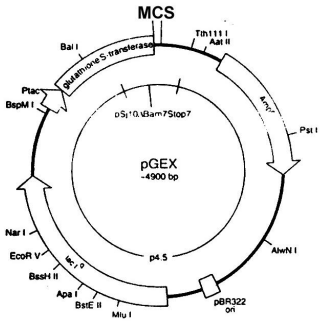

2.3.6. Dephosphorylation of a vector

To avoid self-ligation of a one-cut or blunt-end vector, the vector was dephosphorylated. For each 2 µg of linearized DNA, 1 U Alkaline Phosphatase (AP, Boehringer) was added and incubated in 60 µl total volume of 1x desphosphorylation buffer (Boehringer) for 1 h at 37°C. The enzyme was inactivated in the presence of 5 mM EDTA for 10 min at 75°C.

2.3.7. Klenow reaction

Non-compatible sticky ends were converted into blunt ends by enzymatic action of the Klenow fragment of DNA polymerase I. The reaction mix contained deoxynucleosintriphosphates (= dNTPs), which were incorporated until the whole gap of the sticky end had been filled in. The composition of the dNTPs was adjusted to specific palindrome of the enzyme.
200-500 ng digested DNA was incubated with 1mM dNTPs in the presence of 5 mM Mg^{2+} in 20 µl. For each µg of DNA 1 U Klenow fragment (Boehringer) was added and incubated for 15 min at RT. The mixture was heated to 75°C for 10 min to inactivate enzyme.

2.3.8. Ligation and transformation

DNA fragments can be incorporated into different cloning vectors if cut by the same enzymes or present compatible ends. Some restriction enzymes such as *Eco*RI produce overhanging ("sticky"), others produce smooth ("blunt") ends. Compatible ends can anneal to each other and be connected by ligase. For each ligation reaction, 50 ng vector was used. The amount of insert to be ligated was calculated according to the following formula.

Sticky ends: 50 ng vector x (bp insert/bp vector) x 3 x (1/[insert]) = ml of insert
Blunt ends: 50 ng vector x (bp insert/bp vector) x 6 x (1/[insert]) = ml of insert

Control ligations without insert were performed. By counting colonies growing with and without insert, the minimum number of colonies to be analyzed can be evaluated. It should be taken into account that in the case of blunt/blunt ligation or ligation after a single enzyme digest, the insert can be incorporated in two orientations.
Ligation reactions were performed in a total volume of 10-30 µl containing the appropriate amounts of vector and insert and 1 U of ligase. 10x ligation buffer was added to a final concentration of 1x. Ligation mix was incubated for 1 h at RT for sticky and overnight at 15°C for blunt ends. Conditions for each ligation and transformation can be found in ***Annex IV: Constructs***.
For transformation, competent bacteria were used (DHα5 or JM109, ***see tab 2.2***). Briefly, the bacterial wall was made permeable for DNA by the presence of $CaCl_2$ and heat-shock (***see 2.1.4***).

Blue/White screening:
IPTG/Xgal plates: LB/Agar/Amp plates as described above with 20 µg/ml Xgal and 8 µg/ml IPTG.
Some vectors contain the gene for β-galactosidase within which the multi-cloning site (MCS) is located (see pGEMT for example). In the presence of an inductor IPTG (= Isopropyl-β-D-thiogalactopyranoside), this enzyme converts a colorless substrate Xgal into a blue derivative. Colonies transformed with an intact vector (without insert) will express intact β-galactosidase and produce blue colonies, while those with insert will not produce the enzyme and generate white colonies, thus allowing rapid screening by color.

2.3.9. DNA isolation from bacteria (MINI-, MIDI- and MAXI-preparations)

From one bacterial colony, an overnight culture was grown. For plasmid DNA isolation, different protocols were used depending on the degree of purity needed. For restriction analysis, rapid DNA purification (Zhou et al., 1990) was used. DNA destined for sequencing or complex restriction digests was prepared with Qiaprep Spin Miniprep Kit Protocol (Qiagen). If larger amounts of DNA were needed, DNA MIDI and MAXI preparation Kits were used (Qiagen).

2.3.9.1. Qiaprep Spin Protocol, MINI/MIDI/MAXI (Qiagen)

MINI, MIDI and MAXI DNA preparations were performed according to the manufacturer's instructions.

2.3.9.2. Rapid DNA Mini-Preparation (Zhou et al., 1990)

TE-buffer: 10 mM TrisHCl, pH 8.0, 1 mM EDTA
TENS-buffer: TE and 0.1 N NaOH and 0.5% SDS (sodium dodecyl sulfate)
NaAc: 3 M, pH 5.2
1.5 ml of bacterial overnight culture was spun (10 sec, 14 000 rpm), SN was decanted with 50-100 µl left in the tube. Bacteria were resuspended by vortexing, 300 µl TENS was added. After short vortexing (3-5 sec), 150 µl NaAc was added and mixed by pipeting up and down 3 times. Centrifugation (2 min, 14000 rpm) removed cell debris. SN was centrifuged again and transferred to fresh tube. 0.9 ml EtOH 100% was added to precipitate DNA. After 2 min spin, SN was discarded and pellet was washed in 70% EtOH, dried and resuspended in 20-50 µl TE buffer containing 50 µg/ml DNAse-free RNAse A.

2.3.9.3. Phenol/Chloroform extraction

To 100 µl sample volume, 100 µl of Phenol (Tris-equilibrated, pH 8.0) was added, and mixed, and the phases were separated by centrifugation (5 sec, 14 000 rpm). 100 µl chloroform was added to the aqueous phase and the process was repeated. The aqueous phase was transferred to a fresh tube; 50 µl 3 M NaAc, pH 5.2 was added and mixed with 450 µl 100% EtOH. Precipitation was allowed for at least 30 min at -20°C. After centrifugation (15 min, 14 000 rpm, 4°C), SN was discarded, and the pellet was rapidly washed in 70% EtOH (-20°C), centrifuged and dried. Pellet was dissolved in TE-buffer. (A variant of this protocol was also applied using 1:1 phenol/CIA (= Chloroform: Isoamylalcohol, 49:1) for the first and chloroform for next three extraction steps).

2.3.9.4. Purification of DNA fragment from a gel

When necessary DNA fragments were cut out from an agarose gel and extracted by QIAquick (Qiagen) gel extraction kit according to the manufacturer’s instructions.

2.3.10. Primers

Primers employed for first sequencing steps annealed in the vector sequence and allowed reading approx. 400 bp from both ends. To obtain information about the rest of the sequence, new primers were designed to have a length of about 17 bp and lie inside the fragment already sequenced. Additionally, primers were checked if they had any sequences that allow them to anneal to each other or to themselves and if they anneal only to a unique sequence in the DNA fragment to avoid manifold annealing. Primers for sequencing and further subcloning procedures are listed ***in tab. 2.5;*** alignment on the syndecan-3 cDNA is shown in ***fig. 2.8.***

S3001	GTT **GAA TTC** CAC AAA GGC GC
S3003	CTA A**GA ATT C***CT* *A*CG CCT GCT TGG G
S3004	GAG A**GA ATT C***CT* *A*CT CCT GCT TGT C
S3002(bis)	CGG C**GA ATT C***CT* *A*AC GAT AGA TGA GCA GTG
CMV-P	GGT AGG CGT GTA CGG TGG GAG G
Ks	CGA GGT CGA CGG TAT CG
M13-20	GTA AAA CGA CGG CCA GT
S339a	CCA GGC AGC TGG GAG CTT TG
S339b	CCA CTA CCC CCG AGG CG
$S339b_3$	CTG AGC AGC TGA GCT GCC C
$S339b_2$	GGG CGG GGT GGT GGG CGC
S37a	CGG GCA AAT TGC TTG AGC CC
S37b	CCC AGC ACT TTG GGA GGC
S38a	GTG GGC AAT GGT GTC TGT GC
S38b	CTA CTC CGG GTC GGG CTC GG
S42a	GCT CAT CTC AAC CCC CAC CC
S42c	GTG GGA GGG GCT GCG GCC
S42d	CCT GGA CCC ACA GAG GTG
S42e	AAG GGA CAC CCT CTC ACC
S42f	AGA GAG GGC AGA GAA GAA CT
S42g	TCC GAC CTA CAA GCA CCA CCC
S42h	GGG GCT CAT CTC CAG TAG GTC
S46a	TGG TGT GCC CAC AGG CTG G
Sk	TCT AGA ACT AGT GGA TC
Sp6	TAT TTA GGT GAC ACT ATA G
T3	ATT AAC CCT CAC TAA AG
T7	AAT ACG ACT CAC TAT AG
Tini-1	GTG CTG GGG GTG GCG GTG GCC

Table 2.5: *Primer sequences*. Sequences used to introduce a new enzyme restriction site are represented in bold, STOP codon in italic letters. The localization of al primers annealing to syndecan-3 cDNA can be found in fig. 2.8.

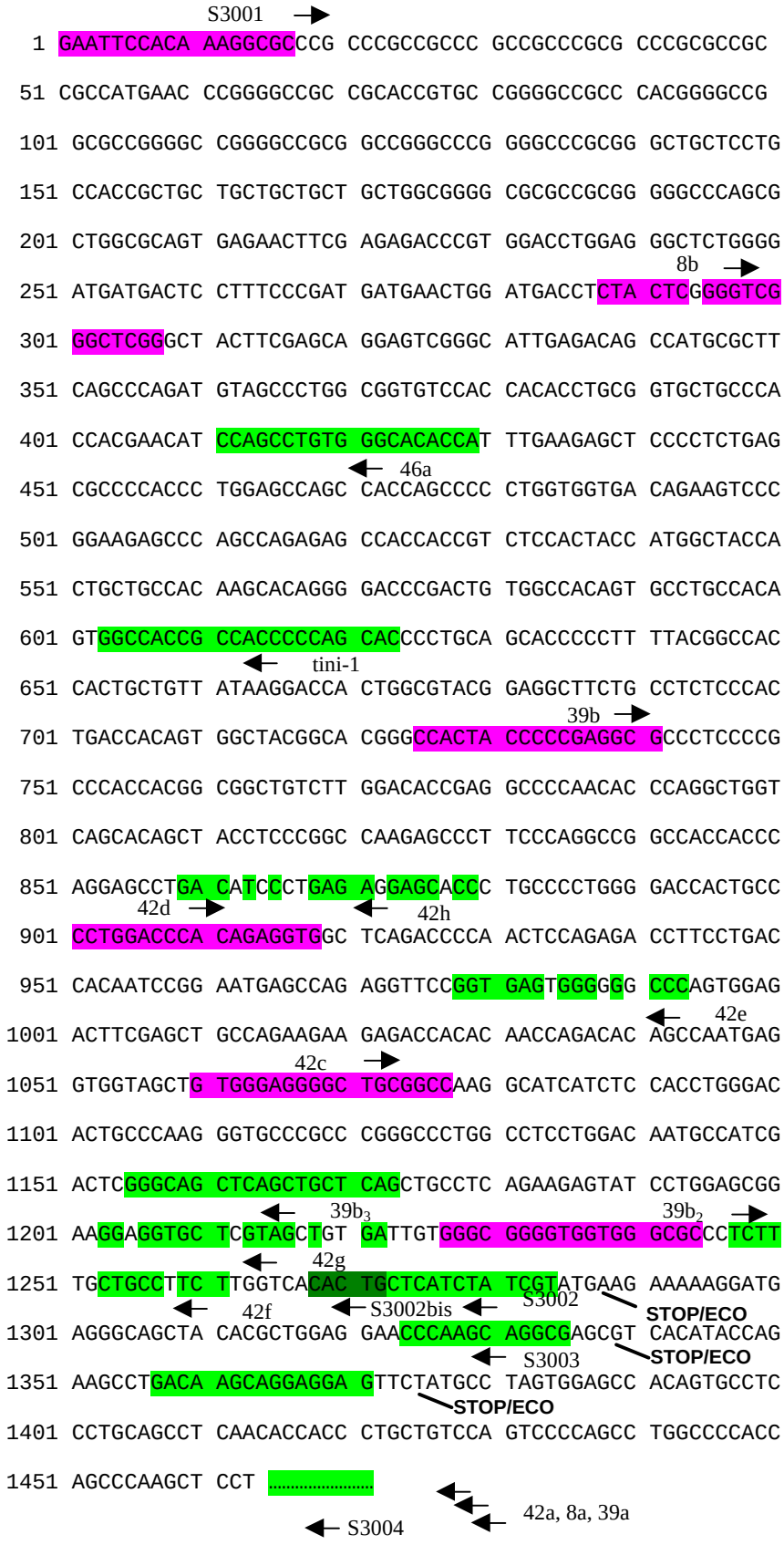

Figure 2.8: ***Alignment of primers on subcloned syndecan-3 cDNA. Arrows indicate orientation; green and pink color annealing sequence of forward and reverse primers respectively.***

2.3.11. Sequencing

2.3.11.1. Sequencing kits

Sequencing reactions are based on the method of Sanger (Sanger et al., 1977). DNA polymerase catalyzes the template-directed replication of DNA sequences after annealing of a specific primer. The incorporation of fluorescent-labeled dideoxyynucleotides (ddNTPs) leads to the termination of chain elongation. As the incorporation occurs accidentally, chains differ in length. These are separated by capillary elelectrophoresis.
Various PCR-based sequencing kits with distinct protocols were used. Protocols are explained briefly.

Thermo Sequenase TM dye terminator cycle sequencing premix kit (a; Amersham)
Sequencing reaction: Sequencing reagent pre-mix: 4.0 µl, Primer (5 µM): 0.5 µl, DNA template (0.1-1.0 µg): 5.5 µl
Cycling program: 96°C (1 min); [96°C (30 sec); 45°C (15 sec); 60°C (4 min)] x25; 4°C: ∞
Precipitation: To the sequence solution 1 µl 3 M NaAc pH 5.2 and 27.5 µl 100% EtOH were added, placed 10 min on ice and centrifuged (15 min, 4°C, 14000 rpm). Pellet was dried by speed-vac, resuspended with formamide loading dye and loaded on a sequencing gel.

Thermo Sequenase TM dye terminator cycle sequencing premix kit (b; Amersham)
The reaction mix was the same, but cycling and precipitation was different.
Cycling program: 96°C (1 min); [96°C (30 sec); 50°C (15 sec); 60°C (1 min)] x25; 4°C: ∞
Precipitation was performed with 1 µl 1.5 M NaAc pH>8/250 mM EDTA. 100% EtOH was cooled (-20°C), the incubation time on ice was 15 min and the pellet was washed before drying in 250 – 500 µl 70% EtOH (-20°C).

D Rhodamine Terminator Cycle Sequencing Ready Reaction (Perkin Elmer)
Instead of one sequence reagent pre-mix, two solutions A and B was mixed before use.
Sequencing reaction: Terminator Ready Reaction Mix: 4.0 µl, Primer (3.2 pmol): 0.5 µl, DNA template (0.5 – 0.75 µg): 5.5 µl
Cycling program: 96°C (5 min); [96°C (30 sec); 50°C (15 sec); 60°C (4 min)] x25; 4°C: ∞
Precipitation: As before. This precipitation protocol was changed again. 1 ml 70% EtOH was mixed with 1 µl 0.5 M $MgCl_2$ by vortex. 74 µl of mixture was added to PCR reaction mix. The incubation time was 15 min at RT, followed by 15 min centrifugation at RT and washes in 70% EtOH.

2.3.11.2. Sequence analysis

Capillary electrophoresis was analyzed by computer, which provided the sequence directly. In the case of overlapping peaks the sequence was read from the peak pattern, see ***fig. 2.9***.

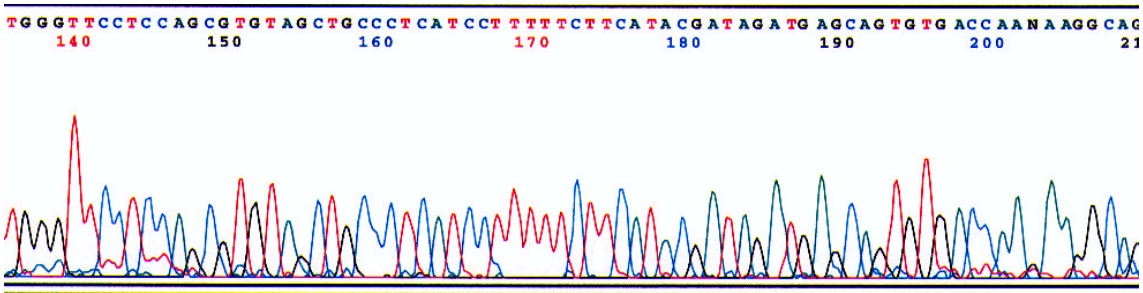

Figure 2.9: ***Example of sequence analysis by capillary electrophoresis*****. Sequence can be read directly from peak pattern. Each nucleotide is represented by a different color.**

2.3.11.3. Comparison of obtained sequences/data bank search

Various computer programs and data banks were used for alignment and comparison of the sequences obtained. The main program used was Assemble from GCG (Genetics Computer Group, University of Wisconsin, Package version 8 to 10.2, Madison, Wisconsin) run on a Unix computer on the Spanish EMBNET node (embnet.cnb.uam.es) or in UB-Genetics Computer (adam.ird.ub.es).
Comparison of data with data banks was performed by using public programs or services like SRS (Sequence Retrieval System) at European Bioinformatics Institute (www.abi.ac.uk) or GCG utilities like TFASTA or BLAST in Spanish EMBET node (embnet.cnb.uam.es).

2.3.12. Library screening

2.3.12.1. Random Primed DNA Labeling Kit

This method is based on the idea that in a mixture of random hexanucleotides it is always possible to anneal to a given DNA sequence. This "primer" is used by the DNA polymerase for template-directed elongation of the DNA sequence, incorporating three unlabeled (dATP=2'-deoxyadenosine-5'-triphosphate, dGTP=2'-deoxyguanosine-5'-triphosphate and dTTP=2'-deoxythymidine-5'-triphosphate) and one ^{32}P-labeled nucleotide (dCTP=2'-deoxycytidine-5'-triphosphate). Purified radioactive sample was used for phage library screening.
TE: 10 mM Tris-HCl pH 7.5, 1 mM EDTA
The Random Primed DNA Labeling Kit was used according to the manufacturer's instructions (Boehringer): Briefly, a pre-reaction mix was made, containing 20 µl of each dATP, dGTP and dTTP, all 0.5 mM, in Tris buffer and 40 µl hexanucleotide mix in 10x concentrated buffer, aliquoted in 5.5 µl and stored at - 20°C. About 25 ng of DNA corresponding to the ectodomain of syndecan-3 (fragment *Eco*RI-*Bam*HI of pMB284) in 10 µl volume was denaturalized for 10 min at 95 °C, placed on ice and centrifuged. 5 µl of the pre-reaction mix and 2 µl Klenow (2 U/µl) were added and placed on ice. 5 µl of dCTP-α^{32}P (3000 Ci/mmol) was added and the reaction proceeded for 45 min at 37ºC. Enzyme was inactivated by incubation for 10 min at 65ºC in the presence of 2 µl EDTA (0.2 M, pH 8.0) and placed on ice. After addition of 80 µl TE, 2 µl was taken for counting by Cerenkov.

2.3.12.2. Purification of radioactive labeled probe from nucleotides

Labeled DNA was separated from unincorporated nucleotides by gel filtration using spin columns (Roche). They were inverted to mix the matrix and collocated in a 15 ml tube, and centrifuged (4 min, 4000x*g*). Flow-through was discarded. Labeled probe was added (maximal 100 µl), the column was placed into a fresh tube and centrifuged (4 min, 1100x*g*). Sample was transferred to an Eppendorf tube and counted. Normal incorporation was between 15-40%.

2.3.12.3. Pre-hybridization and hybridization of filters

1x SSC: 0.15 M NaCl; 0.015 M sodium citrate, pH 7.2
50x Denhardt's solution: 0.5 g ficoll, 0.5 g of polyvinylpyrrolidone, 0.5 g Bovine Serum Albumin (BSA) in 50 ml MilliQ water
Pre-hybridization stock solution: 5x SSC, 20 mM PO_4^{3-} (PB), pH 7.4, 5x Denhardt's solution, 50% formamide

Sol A (Pre-hybridization solution): Pre-hybridizing stock solution, 0.5% SDS, 0.15 mg/ml ssDNA (heated for 10 min at 95°C and placed on ice)
Sol B (Hybridization solution): pre-hybridizing solution with 1.4% dextran sulfate and radioactive labeled probe (in 0.5 ml water and heated for 10 min at 95°C)
Washing Sol1: 0.5x SSC and 0.5% SDS
Washing Sol2: 0.2x SSC and 0.5% SDS
Filters were moistened with 6x SSC, incubated in pre-hybridization solution for 2 h at 42°C and then left overnight in hybridization solution at 42°C. Filters were then washed in: 500 ml Washing Sol1 (10 min, RT); in 500 ml Washing Sol1 (2x30 min, 65°C), in 500 ml Washing Sol2 (2x30 min, 65°C). Filters were dried on Whatman filters and a Kodak X-OMAT UV film was exposed to the filters at -80°C with intensifying screens for 6-18 h.

2.3.12.4. Localization of phages

By comparison between autoradiography and culture dishes, positive phages were localized and picked. To each agar piece, 1 ml SM-buffer and 100 µl chloroform were added to kill bacteria. After 1-2 h incubation at RT with occasional vortexing, phages were diluted 1:200 and plated as described above.

2.3.13. RNA dot blot

A commercial poly A RNA dot blot from human tissues and cell lines (Clontech) was incubated with α^{32}P-labeled probe corresponding to the ectodomain of syndecan-3 (fragment *Eco*RI-*Bam*HI of pMB284). The manufacture's instructions were followed. Densitometry measurements were performed by using a Phosphoimager (Biorad). Results were analyzed with Molecular Analyst software (Biorad).

2.4. Cell culture

2.4.1. Maintaining of cells

Cell line	Source
COS-1 (Kidney, SV 40 transformed, African Green Monkey	ATCC CRL 1650
CHO K1 (Ovary, Chinese Hamster)	ATCC CRL 9618
CHO 745 (xylosyl transferase deficient mutant of CHO K1)	Esko et al., 1985
3T3	ATCC CCL-92

Table 2.6: ***Cell lines used.*** **ATCC = American Type Culture Collection (Manassas, USA)**

COS-1 cells/ 3T3 cells
Medium: Dulbecco's Modified Eagle Medium (DMEM) with 4.5 g/l glucose, 10% FCS (fetal calf serum, Whittaker), penicillin G sodium (100 U/ml) and streptomycin sulfate (100 U/ml) and glutamine (2-3 mg/ml)
CHO K1 and CHO 745 cells
Medium: Ham's F10 medium, FCS, penicillin, streptomycin, glutamine as described above

2.4.2. Transient Transfection

Eukaryotic cells can express exogenous proteins after introduction of their corresponding cDNA sequence inserted in expression vectors. Depending on cell type and experiment, different transfection methods have been employed. In transient transfection experiments, vectors are employed (e.g. Prk5), which lead to a high protein expression but which are not integrated into the cell genome. Plasmids are lost during cell division, which leads to the “transient” character of the transfection. Therefore, in order to generate stable cell lines, other plasmids are employed to integrate into the genome, and which allow selection of transfected cells (e.g. pcDNA3).

2.4.2.1. DEAE-Dextran-Method

Only COS-1 cells and for transient transfection
1x TBS (Tris-buffered saline): 10 mM TrisHCl, pH 7.4, 150 mM NaCl
"DNA-solution": 1x TBS, 0.5 mg/ml DEAE-dextran (= Diethylaminoethyl-dextran), 0.3 µg/ml DNA (≈25 ng DNA/cm^2)
Chloroquine solution (freshly prepared, protected from light): 5 mg/ml in culture medium
Glycerol-solution: 20% in culture medium
Cells were seeded with or without coverslips and transfected at 30-50% density (∅ 10 cm dish). Cells were washed twice in 6 ml 1x TBS. 6.6 ml DNA solution was added and incubated for 30 min at 37°C. Solution was removed and 6 ml of chloroquine solution (which avoids DNA degradation by inhibiting lysosomal functions) was added and incubated for 3 h at 37°C. Cells were washed twice in 6 ml 1x TBS. 6 ml of glycerol solution (this opens pores in the cell membrane to let DNA enter the cell) were added and left exactly 4 min at 37°C. After two washing steps in 6 ml 1x TBS, medium was added. Cells were fixed or lysed 12-72 h after transfection for further experiments.

2.4.2.2. Superfect™ Transfection Agent (Qiagen)

3T3 cells: Cells were seeded with or without coverslips in a ∅3.5 cm dish in order to reach about 30-50% confluence the next day. To 1.7 µg DNA 50 µl medium without antibiotics and FCS were added (≈170 ng/cm^2). 7 µl of Superfect™ was added and mixed by pipeting up and down five times. The mixture was incubated for 10 min at RT; meanwhile cells were washed in phosphate buffered saline (PBS) 100 mM. 333 µl medium was added to mixture, pipetted up and down twice and added to cells that were incubated 2-3 hours in incubator. After washing once in PBS 100 mM, medium was added. Cells were fixed or lysed after 12-72 h post-transfection. For CHO K1/CHO 745 cells, the same protocol was used with the difference that cells were seeded into ∅6 cm dishes and 2 µg DNA was used (≈70 ng/cm^2).

2.4.2.3. Lipofectamine (Gibco)

The day before, 10^6 CHO K1/CHO 745 cells were seeded with or without coverslips in a ∅3.5 cm dish. 1.5 µg DNA (≈160 ng/cm^2) was mixed with 100 µl serum-free medium and, in a separate tube, 100 µl serum-free medium was mixed with 7 µl Lipofectamine. The contents of both tubes were mixed and incubated for 30 min at RT with occasional agitation. Meanwhile cells were washed twice in serum-free medium. 800 µl serum-free medium was added to the mixture and rapidly poured onto cells. After 2.5 hours serum-free was changed for serum-containing medium. Next day, medium was changed again. Cells were fixed or lysed 12-72 h after transfection. For larger dishes, volumes were proportional to area.

2.4.3. Stable transfection

In order to obtain cells that express the desired protein in a stable manner, cells were transfected with a vector that can be integrated into the genome of the cell (here pcDNA3) and makes transfected cells resistant against the antibiotic G418. As a result the expression is maintained in successive passes. All cells originating from one transfected cell (clone) will produce the desired protein but neither the integration site in the genome nor the integration mechanisms is clear. Once selected for G418 resistance, clones have to be characterized phenotypically and by biochemical and functional assays.

2.4.3.1. Determination of critical G418 concentration

The concentration of G418 at which CHO K1 cells die was determined by incubating them in different concentration of the antibiotic (200–1200 µg/ml) for 10 days in 6-well plates ($2.5x10^5$ cells/well). At a concentration of 600 µg/ml almost all cells were dead after this time period. Selection was therefore performed in presence of this concentration.

2.4.3.2. Obtention of stable transfected cell

Day 1: $1.2x10^5$ CHOK1 cells were seeded into each well of a 6-well plate.
Day 2: Cells were transfected as described above with the exception that DNA solution was filtered before being mixed with Lipofectamine. Constructs used: pcDNA3 (Control), S3-FL in pcDNA3 (syndecan-3 full-length) and ΔC (syndecan-3 without cytoplasmic tail).
Day 5: Trypsinization and distribution into two ∅150 cm dishes; until day 14 maintained with G418 (600 µg/ml)
Day 14/15: Isolation of resistant clones: FL (30), ΔC (30) and control (10), micro-trypsinization using cloning cylinders and seeding into 24-well plate.
In the following days, medium was changed every two days and clones were maintained in the presence of 600 µg/ml G418. When they reached confluence, clones were trypsinized and transferred to 25 cm^2 bottles. From each clone two vials were frozen and some cells were seeded onto coverslips for characterization.

2.5. Sample preparation for immunocytochemical and electro-microscopic analysis

2.5.1. Immunocytochemistry

Immunocytochemistry allows the detection of proteins on fixed cells by the use of specific primary antibodies and their detection by fluorescent-labeled secondary antibodies. Analysis was performed by (confocal) fluorescent microscopy.
PBS/Ca^{2+}/Mg^{2+}: 10 mM PBS, 1 mM $CaCl_2$, 0.5 mM $MgCl_2$
Fixing solution: 3% paraformaldehyde (Merck), 2% sucrose in 100 mM PB, pH 7.4
PBS/glycine: 10 mM PBS, 20 mM glycine
Blocking buffer: PBS/glycine, 1% BSA
Cells grown on coverslips were rinsed in PBS/Ca^{2+}/Mg^{2+} and fixed for 20-45 min at RT. Cells were washed three times in PBS. If necessary, cells were permeabilized for 7 min in PBS/glycine/0.1% Triton X-100 (TX-100) , followed by two washing steps in PBS/glycine.

Another possibility was to perform all steps in the presence of saponin 0.1%, which in contrast to TX-100, leads only to reversible permeabilization. Blocking was performed for 10-20 min with blocking buffer at RT. Primary antibody was incubated for 45-60 min at 37°C at appropriate dilution (***see tab. 2.7***) in blocking buffer. Coverslips were washed three times for 5 min in PBS/glycine. To visualize primary antibodies, FITC-conjugated swine anti-rabbit or TRITC-conjugated goat anti-mouse secondary antibodies were used (30-45 min at 37ºC, ***see tab. 2.8***). For actin labeling, coverslips were then further incubated with TRITC-conjugated phalloidin at 1:1000 – 1:2000 dilution in blocking buffer containing 0.1% TX-100 for 7 min. After several washing steps in PBS/glycine and PBS, coverslips were mounted in Mowiol.

2.5.2. Transmission electron microscopy (TEM)

PB (Phosphate Buffer): 0.1 M
PBS/Ca^{2+}/Mg^{2+}: ***see 2.5.1***
Fixing solution: 2% paraformaldehyde, 2.5% glutaraldehyde in PB
Cells were grown on gold grids. Cells were washed rapidly in PBS/Ca^{2+}/Mg^{2+} followed by overnight fixing at 4ºC. After extensive washing in 0.1 M PB, disks were cut into 2x2 mm squares. They were then post-fixed with 1% osmidium tetroxide (Merck) in 0.1 M PB for 1 h at 4ºC, dehydrated with gradient ethanol solutions and embedded in SPURR resin. Semithin (1 µm) and ultrathin (700 Å) sections were cut perpendicularly to the culture plane with an Ultracut-E ultramicrotome (Reichert-Jung). Ultrathin sections were stained with uranyl acetate and lead citrate.

2.5.3. Scanning electron microscopy (SEM)

PBS/Ca^{2+}/Mg^{2+}: ***see 2.5.1***
Cells were grown on ∅10 mm coverslips. Before fixing, cells were washed in PBS/Ca^{2+}/Mg^{2+}. Fixing was performed as described in ***2.5.2***. After washing in PBS, coverslips were dehydrated with increasing concentrations of ethanol, and dried by the CO_2 critical point method. They were then mounted on metal stubs for SEM, and covered by evaporation with a thin carbon layer.

2.6. Image analysis

2.6.1. Confocal laser scanning microscopy (CLSM)

CLSM is a special kind of fluorescent microscope, which permits the user to focus a selected plane of the sample without detecting light coming from zones others than the focus. Thereby it produces an optical section of the sample. Sections can be composed with the aid of a computer to give three-dimensional images. To obtain images, a Leica TCS 4D, adapted to an inverted microscope (Leitz DMIRB) and the 63X (NA 1.3, Ph3, oil) Leitz Plan-Apochromatic objective was used. FITC and TRITC were excited by sequential excitation at 488- and 568-nm lines of a krypton-argon laser. Three-dimensional projections were made from horizontal sections. Each image represents the average of eight line scans at the standard scan rate, but some structural details were collected at slow scan rate and zoom.

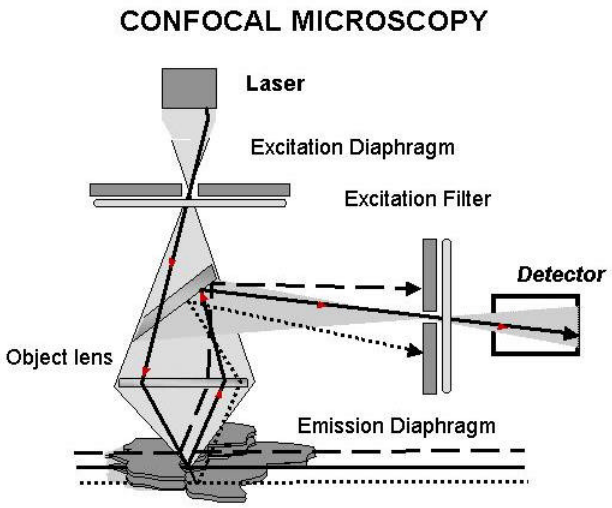

Figure 2.10: ***Model of confocal microscope.*** **A fluorescent sample is illuminated by a diaphragm-focused light point (laser). The fluorescent light point emitted by the sample is focused by a second diaphragm (emission diaphragm) and reaches the detector. Light coming from other sites of the sample is out of the focus of this diaphragm and therefore excluded from detection.**

2.6.2. Laser Scanning Cytometry (LSC)

With the LSC technique it is possible to count and analyze a population of cells grown on coverslips due to fluorescent labeling. The strength of the fluorescent signal of each cell can be plotted and so the distribution of labeling can be analyzed. Moreover, individual cells can be localized and their phenotype determined.
Immunocytochemistry was done as described above and cells were analyzed (WinCyte™ software). With the aid of the microscope (Olympus BX50 with 10x, 20X and 40X objectives, argon/helium laser) individual cells were localized and photographed.

2.6.3. TEM/SEM

Prepared samples were examined with a Hitachi 600AB electron microscope and a Hitachi S2300 microscope respectively.

2.7. Functional cell assays

2.7.1. Proliferation

PBS/Ca^{2+}/Mg^{2+}: ***see 2.5.1***
a) By counting: 10^4 cells were seeded into 24 well plates, trypsinized and counted after one, two and three days.
b) By Crystal violet: Cells were rinsed with PBS/Ca^{2+}/Mg^{2+} after different days of culture, stained for 20 min with crystal violet, washed twice in water and dried.150 µl of 0.1 M HCl was added and absorbance at 630 nm was determined. Graphs were plotted using Microsoft Excel. Experiments were performed in triplicate.

2.7.2. Adhesion

10^5 cells were seeded into 24 well plates and allowed to attach for 2 h, then washed briefly in PBS/Ca^{2+}/Mg^{2+} (***see 2.5.1***) and stained with crystal violet. The same experiment was performed in the absence and presence of 10 U/ml heparin and on different substrates (BSA, FN, collagen type I, all 10 μg/ml, coating overnight at 4ºC or for 2 h at 37ºC).

2.7.3. Wound healing

For wound-healing experiments cells were seeded into 24-well plates. At confluence, a small wound was performed by scratching the cell layer with a yellow tip and observed by phase microscopy. Closing of wound was documented by taking photos after different time points (up to 16 h). The area of wound was calculated with the aid of Leica QWin (2) software and wound area decrease per time was calculated by Excel. Some experiments were performed in the presence of C3 transferase (Sigma, 10 μg/ml).

2.7.4. Cell size

$3x10^5$ cells were seeded into ∅6 cm dishes, trypsinized after 2 days in culture and counted with a particle counter (Multisizer II). Exclusion size was 100 μm. Statistical analysis was performed by Coultermultisizer Accucomp running under Microsoft Windows.

2.8. Protein biochemistry

2.8.1. Antibody production

2.8.1.1. Animals

Four New Zealand White rabbits were purchased from Isoquimen, Spain.

2.8.1.2. Fusion protein production and purification

This technique is used to yield high amounts of a desired protein, produced by transformed bacteria. Purification of the protein takes advantage of the fact that the protein is fused to GST, which binds specifically to glutathione beads. The proteins obtained can be used for antibody production, overlay and pull-down experiments, etc. Protocols were adjusted to each protein.
Different fusion protein constructs and purification protocols were performed in order to obtain a high yield of syndecan-3 fusion proteins. Testing different protocols for purification, the following one using lysozyme for bacterial lysis presented highest efficiency, as indicated by Western blot analysis with an anti-mouse-syndecan-3 antibody (generous gift from M. Bernfield).

Buffer A: 50 mM TrisHCl pH 7.5, 2.3 M sucrose, 10 mM EDTA and PI (*see below*)
Buffer B: 50 mM TrisHCl pH 7.5, 10 mM KCl, 1 mM EDTA, 1 mM Dithiothreitol (DTT), 1.25 mg/ml lysozyme

Protease inhibitors (PI): 10 µg/ml Leupeptin, 2 mM PMSF (Phenylmethylsulfonylfluoride), 0.25 TIU (Trypsin Inhibiting Units) Aprotinin, *10 mM sodium pyrophosphate (NaPPi), *0.2 mM sodium ortho vanadate (Na_3VO_4), *10 mM sodium fluoride (NaF)
* Inhibitors of phosphatases were added in only some experiments.

Glutathione beads (Sigma): Beads (approx. 90 mg/ml) were hydrated two hours in distilled water and then washed twice in buffer C with 1 mM DTT and PI, or only hydrated for two hours, depending on the experiment.

First Day: Pre-culture from single clone was grown overnight in 50 ml LB/Amp at 250 rpm and 37ºC.
Second Day: Bacteria were diluted 1:20 in LB/Amp and grown until OD_{600nm}≈0.7 at 250 rpm and 37ºC. Protein production was induced by addition of 0.1 mM IPTG for 3 h at 30°C. Bacteria were harvested by centrifugation in 4 tubes (30 min, 3000 rpm, 4°C, GSA rotor, Sorvall). Pellets were frozen at -20°C until use.
Third Day: Pellet was thawed on ice and washed in ice-cold NaCl 0.9%. Bacteria were centrifuged (10 min, 4000 rpm, 4ºC, GSA rotor, Sorvall), SN was discarded and each pellet was resuspended in 625 µl Buffer A. Bacteria suspension was left 30 min on ice with vortexing every 5 min. Buffer B was added, mixture was vortexed and incubated 1 h on ice with vortexing every 5 min. After 1 h sodium deoxycholate (final concentration 0.1%), $MgCl_2$ (final concentration 10 mM) and DNAse (final concentration 15 µg/ml) were added. Mixture was incubated 15 min on ice with vortexing every 5 min and then centrifuged (15 min, 3600 rpm, 4ºC, GSA rotor, Sorvall). SN was recuperated and added to prehydrated glutathione beads and incubated overnight at 4°C.
Fourth Day: Beads were washed five times for 10 min in 10 mM HEPES* at 4°C. Fusion protein was eluted by addition of 10 mM reduced glutathione in 50 mM TrisHCl pH 8.0, incubation for 10 min at RT and 5 min centrifugation. This elution procedure was repeated several times. Different amounts of BSA were loaded on gel together with aliquots of eluted fractions in order to evaluate yield of protein purification. *HEPES=N-[2-Hydroxyethyl]piperazine-N´-[2-ethanesulfonic acid]

2.8.1.3. Injection protocol

Two animals (MAX and MORITZ) were inoculated with the eluted fusion protein while other two animals (CLEVER and SMART) were inoculated with the protein band corresponding to syndecan-3-GST fusion protein cut out of the gel and homogenized by freezing with liquid N_2. The eluted protein as well as the homogenized gel band were mixed with Freund's Adjuvant. The injection frequency was every three weeks except for a second injection after one month. Before first inoculation, between 2-10 ml blood was recovered representing the "pre-immune" serum. Ten days later, this procedure was repeated to monitor the immune response. Blood was incubated for 30 min at 37ºC, left several hours on ice and then centrifuged to eliminate blood cells and coagulated proteins. Serum was stored at -20ºC until use.

2.8.1.4. Antibody purification by Protein G affinity

In order to purify antibodies, they were incubated with Protein G-sepharose that specifically binds the IgG-fraction from the serum thereby eliminating serum proteins and other antibodies such as IgM.

Binding Buffer (BB): 50 mM TrisHCl, pH 7.0
Eluting Buffer (EB): 0.1 M citric acid, pH 3.0
Collecting Buffer (CB): 1M TrisHCl, pH 8.0
1 ml of Protein G-sepharose was used for each 2.5 ml of serum. Protein G-sepharose was washed in 3 volumes BB. Sepharose was incubated with serum in batch overnight at 4°C,

centrifuged (5 min, 500x*g*, Heraeus), washed three times in BB. Column was packed, antibody eluted by addition of 500 µl EB. Fractions were collected in Eppendorf tubes containing 50 µl CB to neutralize pH. Yield of antibody can be approximated by measuring absorbance with 1 OD_{280nm}≈0.8 mg/ml protein or by comparison with BSA standard in a Coomassie SDS gel, ***see fig. 2.11***. Gel electrophoresis shows two bands corresponding to the light (27 kDa) and heavy (55 kDa) chains of the antibodies. Fractions were pooled, dialyzed and aliquoted.

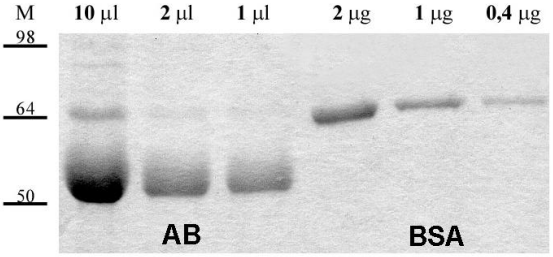

Figure 2.11: ***Concentration of antibody (Clever) after purification by affinity to Protein G-sepharose.*** **Comparison with BSA in Coomassie gel.**

2.8.1.5. Affinity-purification of antibody

Therefore 2.5 ml of Protein G-purified antibody (= 5 mg) was used. The total fusion protein amount used for cross-linking to GST-beads corresponds to 3.5 mg dialyzed protein. Concentration after purification: approx. 80 µg/ml (total 400 µg). This low yield may be attributed to poor binding of eluted fusion protein to beads and therefore a low supply of cross-linked protein. Antibodies were characterized by Western blot analysis, immunoprecipitation and immunocytochemistry.

2.8.2. Determination of small GTPases activation status through “pull-down” experiments

This technique takes advantage of the fact that only the active (GTP)-form of the small GTPases binds to their substrates (C21 or Rhotekin for Rho A and PAK for cdc 42 and Rac 1). Substrates are produced as bacterial fusion protein and bound to glutathione beads. Total cell extracts were incubated with the beads and only the active portion of the small GTPases bound to the bead-substrate complex (***see fig. 2.12***) (Sander et al., 1998). Amount of active GTPases which is “pulled-down” by the beads was compared to total amount of the GTPase in the cell lysates.

2.8.2.1. Protein production

Fusion proteins were generous gifts from J. Collard. For further details see Sander et al., 1998.
Bacterial lysis buffer: 20% sucrose, 10% glycerol, 50 mM TrisHCl pH 8.0, 0.2 mM $Na_2S_2O_5$, 2 mM $MgCl_2$, 2 mM DTT and PI (***see 2.8.1.2***).
GST fish buffer: 10% glycerol, 50 mM Tris pH 7.4, 100 mM NaCl, 1% NP-40, 2 mM $MgCl_2$ and PI.
50 µl of glycerol stock was grown overnight in LB/Amp, diluted 1:10 and grown for 1 h. Protein production was induced by addition of 0.1 M IPTG for 2 h. Bacteria were centrifuged (15 min, 4ºC, 5000 rpm, GSA Rotor, Sorvall). Pellet can be stored at –20ºC until use. Pellet was resuspended in 10 ml lysis buffer, sonicated 2-3 min and spin (20 min, 10 000 rpm, 4ºC, SS34 rotor, Sorvall). SN was incubated for >45 min with 1 ml glutathione slurry beads (50%). Beads were washed 3 times in lysis buffer and resuspended in GST-fish buffer.

2.8.2.2. Pull-down assay

4x10^6 cells were plated two days before experiment on ∅15 cm plates. For each experiment 2 plates were used. Cells were washed in ice-cold PBS and lysed in GST fish-buffer. Lysis was performed by incubating for 5 min on ice and centrifuging (5 min, 4ºC, 14 000 rpm). SN was transferred to a fresh tube and total volume was measured. 20 µl was stored for protein quantification. To each SN the same volume of substrate-bound beads was added. Incubation with beads was allowed at 4ºC for at least 1 h. After washing three times in GST fish buffer, beads were resuspended in 1x loading buffer (***see 2.8.8***), heated to 95ºC for 10 min and loaded on 12.5% gel.

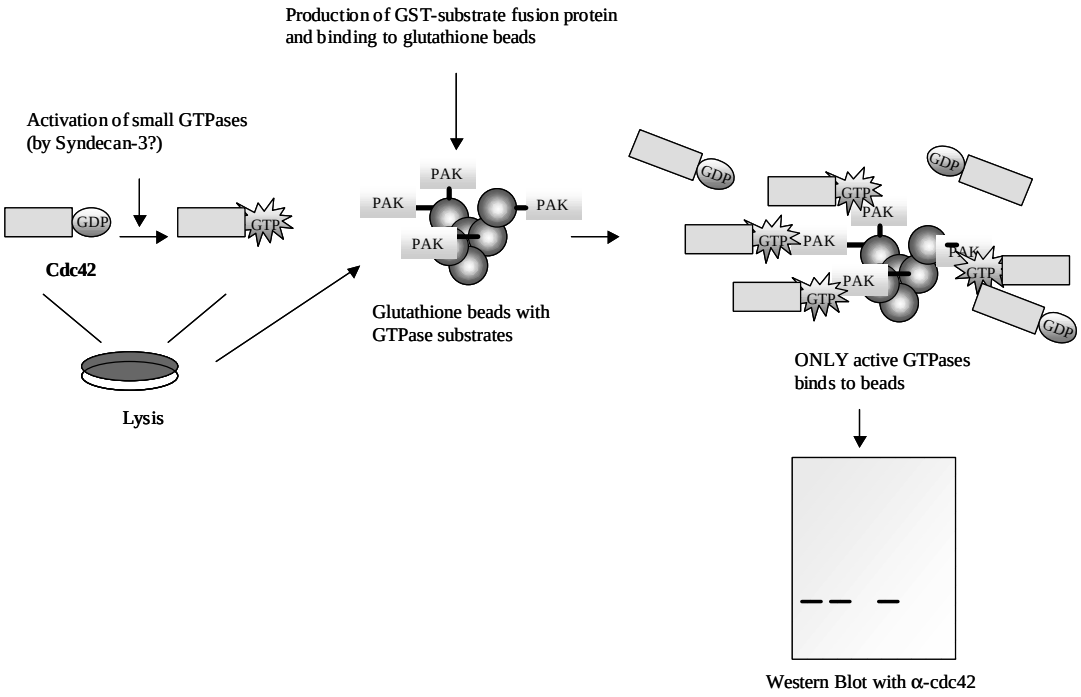

Figure 2.12: Scheme of *"Pull-down" experiment*. Active GTPases (here cdc 42) are "pulled-down" together with their substrate fusion proteins, which are bound to beads. Western blot analysis is performed using antibodies against the respective GTPase.

2.8.3. Total protein extraction

Extraction buffer: 50 mM TrisHCl pH 7.4; 150 mM NaCl, 1% TX-100, 1 mM EDTA and PI (***see 2.8.1.2***)

Cultures dishes were placed for 5 min on ice and washed in ice-cold 10 mM PBS. Then extraction buffer was added (1 ml for ∅15 cm, 0.5 ml for ∅10 cm, 0.2-0.3 ml for ∅6 cm) and cells were incubated for 5 min on ice. Then cells were harvested by scraping and homogenized by pipeting up and down. Centrifugation (20 min, 13 000 rpm, 4°C) removed TX-100 insoluble components. SN was transferred to fresh tubes and stored at –20°C.

2.8.4. Cellular fragmentation

This protocol was used to perform differential protein extraction according to solubility in non-ionic and ionic detergents. The following fractions were obtained:
- Soluble (containing proteins of the cytoplasm)
- TX-100 soluble fraction (containing membrane proteins)
- TX-100 insoluble fraction (containing proteins associated with the cytoskeleton)
- SDS insoluble fraction (containing cytoskeletal proteins)

Buffer A: 25 mM TrisHCl pH 7.5, 1 mM EDTA, 10 mM NaCl and PI/phosphatases inhibitors (***see 2.8.1.2***)
Buffer B: 25 mM TrisHCl pH 7.5, 1 mM EDTA, 1% SDS and PI/phosphatases inhibitors.

Cells were washed once in PBS, lysed in buffer A, homogenized with the aid of a 1 ml syringe, incubated for 30 min on ice and then centrifuged (30 min, 12 000 rpm, 4°C). SN contained the cytoplasmic proteins. The pellet was homogenized in buffer A with 1% of TX-100, incubated 30 min on ice and centrifuged 30 min at 4 °C and 12 000 rpm. The SN contained the membrane proteins. Pellet was homogenized in buffer B, incubated 10 min at 100°C and centrifuged (30 min, 12 000 rpm, 4°C). SN contained the proteins, which are associated with the cytoskeleton. The resulting pellet contained the cytoskeleton. Depending on the experiment, first extraction step was performed directly in presence of TX-100.

2.8.5. Determination of protein concentration

Protein concentration was determined with BCA kit (Pierce) according to the manufacturer's instructions.

2.8.6. Digest with Heparitinase/Chondroitinase ABC (ChABC)

Heparitinase buffer: 50 mM HEPES pH 7.0, 1 mM $CaCl_2$, 100 mM NaCl, 100 µg/ml BSA and PI
Heparitinase: (Seikagaku): 0.2 U/ml (Stock 1 U/ml in 1 mM $CaCl_2$ and 50 mM HEPES pH 7.0)
Chondroitinase ABC (ChABC): 0.2 U/ml (Stock 5 U/ml in PBS/Ca^{2+}/Mg^{2+}, ***see 2.5.1***) (600 units Sigma = 1 U).

Lysates (no more than 3 µl) were adjusted with $CaCl_2$ to a final concentration of 2 mM to avoid inhibitory effect of EDTA from lysis buffer on enzyme activity. To these 3 µl, 27 µl Heparitinase buffer with enzymes were added and incubated overnight shaking at 37ºC.

Since only little protein could be digested and high amounts of enzyme were needed with this protocol, the protocol was changed.
10x Heparitinase buffer: 250 mM Tris-HCl, pH 7.5, 1.5 M NaCl, 2 mM $CaCl_2$
To samples, 10x Heparitinase buffer with Heparitinase (0.01 U/ml) and ChABC (0.05 U/ml) was added to a final concentration of 1x.

2.8.7. (Co)-Immunoprecipitation (IP)

Using a specific antibody, the corresponding protein can be precipitated from a total lysate and pulled down with protein A or G sepharose beads. This technique can be used to prove interactions between different proteins (A+B). If they are bound to each other in the lysate, the antibody specific for protein A will co-IP the whole "complex". The association between both proteins can be visualized through Western blot analysis (***see 2.8.10***) using specific antibodies against B.

A pre-clearing step, incubating the lysate (1 mg of total protein) for 30 min at 4 °C in the presence of 10 µl protein G beads was performed. This serves to eliminate unspecific binding of total lysate proteins to the beads. The pre-cleared lysate was incubated with antibody for 4 h at 4°C, rotating. Then, lysate was centrifuged and 20 µl pre-blocked (1 h, 4°C, 5 mg/ml BSA) protein G or A beads were added to SN and incubated for 1 h at 4°C rotating. Beads were washed six times in extraction buffer (***see 2.8.3***), 30 µl 1x loading buffer (***see 2.8.9***) were added and incubated for 10 min at 100°C. Alternatively, IP was digested by Heparitinase/ChABC as described in ***2.8.6***. This digest was performed in a big volume to assure good accessibility of enzymes to beads.

2.8.8. SDS polyacrylamide gel electrophoresis (PAGE)

5x Loading buffer: 50% glycerol, 5% SDS, 250 mM TrisHCl, pH 6.8, 25% ß-mercaptoethanol, 0.25% bromophenol blue
Electrophoresis buffer (10x): 250 mM TrisHCl, 1.92 M Glycine, 1% SDS
Protein separation was performed by SDS PAGE as first described by Cleveland (Cleveland et al., 1977). According to resolution needed, running gel had 10, 12.5 or 15% and stacking gel 4% acrylamide. Loading buffer was added and samples were heated to 100ºC for 5-10 min to denaturalize proteins. Molecular weight of analyzed protein was determined by comparison with a commercial protein marker (SeeBlueTM Pre-Stained Standards, Invitrogen, ***see fig. 2.13***).

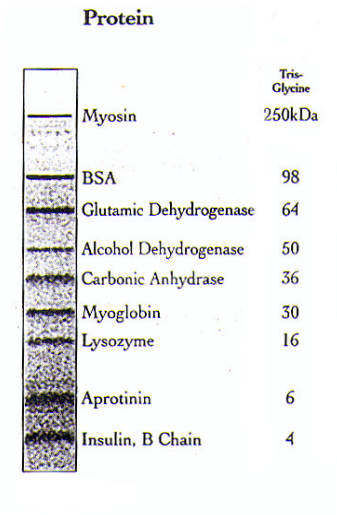

Figure 2.13: ***SeeBlueTM Pre-Stained Standards***

2.8.9. Coomassie staining:

De-staining solution: 40% MeOH, 10% AcOH, 50% distilled water
To visualize proteins, gels were incubated for at least 30 min in de-staining solution containing 0.1% Coomassie Blue and then de-stained with de-staining solution for several hours. Gels were dried by Gel Dryer (Biorad).

2.8.10. Western blotting

Proteins were transferred to a nitrocellulose membrane (Schleicher and Schull) for detection by antibodies.
10x transfer stock: 250 mM Tris, 1.92 M glycine

Transfer buffer: 10% 10x transfer stock, 20% MeOH, 70% distilled water
Ponceau solution: 0.5% Ponceau S, 1% acetic acid
Blocking buffer: TBS, 5% milk powder or 5% BSA with phenol red
Washing buffer: TBS, 0.05% TX-100
Transfer voltage was selected according to the size of proteins and time of blotting. Ampere (A) limit was between 0.2 and 0.25. Blotting was always performed at 4°C with additional cooling.

Correct transfer was checked by Ponceau staining. De-stained membrane was blocked for 1.5 h at RT in blocking buffer and incubated with primary antibody diluted in blocking buffer in a sealed plastic bag at RT for 2 h or at 4°C overnight. Membrane was washed three times for 10 min in washing buffer and briefly once in TBS. Secondary antibody conjugated to HRP (Horse Radish Peroxidase (1:2000)) was incubated 1.5 h at RT in blocking buffer. This enzyme transforms a non-emitting (luminol) into an emitting substrate that can be detected by autography (***see 2.8.11***). Membrane was washed three times for 10 min in washing buffer and twice for 10 min in TBS.

Antibodies	Origin	Specie	WB	IC
α-β_1-Integrin	Merck	Rabbit	1:500 (NR!)	1:25
α-β_3-Integrin	Merck	Rabbit	1:500 (NR!)	1:25
α-β_5-Integrin	Merck	Rabbit	1:500 (NR!)	1:50
α-(Mouse-) S3	M. Bernfield	Rabbit	1:500	1:200
α-Actin	Sigma	Mouse	1:500	-
α-Cdc 42	Santa Cruz	Rabbit	1:500	-
α-Delta-heparansulfate (3G10)	Seikagaku	Mouse	1:500–1:1000	-
α-Ezrin	P. Mangeat	Rabbit	1:2-5000	1:500
α-FAK	Transduction Lab	Mouse	1:1000	1:50
α-FAK	Ferran Burgaya	Rabbit	-	1:300
α-GST	Santa Cruz	Mouse	1:1000	-
α-Moesin	P. Mangeat	Rabbit	1:1000-2000	1:500
α-Paxilin	Transduction Lab.	Mouse	-	1:50
α-Rac 1	Santa Cruz	Rabbit	1:100	-
α-Radixin	P. Mangeat	Rabbit	1:1000-2000	1:500
α-Rho A	Santa Cruz	Mouse	1:500	-
α-S3 (Clever), PG-purified	Antibody production	Rabbit	In test	1:1-5000
α-S3: (Max), PG-purified	Antibody-production	Rabbit	In test	1:1-5000
α-S3: (Smart), PG-purified	Antibody-production	Rabbit	In test	1:1-5000
α-Src	Santa Cruz	Mouse	1:500	1:50
α-Talin	Transduction Lab.	Mouse	-	1:50
α-Vinculin	Transduction Lab.	Mouse	-	1:20

Table 2.7: Primary antibodies. **NR = non-reducing conditions (= loading buffer without b-mercaptoethanol), S3 = syndecan-3.**

Antibody	WB	IC
HRP-goat-α-mouse	1:2-5000	-
HRP-Swine-α-rabbit	1:2-5000	-
FITC-Rabbit-α-mouse	-	1:50
FITC-Swine-α-rabbit	-	1:50
TRITC-Swine-α-rabbit	-	1:50

Tab. 2.8: Secondary Antibodies **(DAKO, Denmark), IC = immuno cytochemistry; WB = Western blotting.**

2.8.11. Enhanced chemiluminescence (ECL)

Solution A: 5 ml 100 mM TrisHCl, pH 8.5, 90 mM coumaric acid, 250 mM luminol
Solution B: 5 ml 100 mM TrisHCl, pH 8.5, 30 % H_2O_2 3 µl
Solution A and B were mixed in the dark and membrane was incubated for 1-2 min with mixture. A Kodak X Omat film was exposed to membrane.

2.8.12. Stripping

Membranes can be reused after stripping to remove primary and secondary antibodies, but not the proteins on the membrane.
Stripping solution: 62.5 mM TrisHCl, pH 6.7, 100 mM 2-mercaptoethanol, 2% SDS
Membranes were incubated for 30 min at 50°C with agitation in stripping solution, extensively washed in PBS/TX-100 0.05% and finally in TBS. Successful stripping was tested by ECL incubation.

2.8.13. Dialysis

To get rid of salts or small molecules which are present in buffers of protein solutions, proteins can be dialyzed, using a membrane which is only permeable for salts but not for the proteins, ***see fig. 2.14***.
Membrane was microwaved in distilled water, then washed ≥ five hours in distilled water, then microwaved for 10 min in 10 mM EDTA, pH 8.0 to inactivate proteases. Small volumes (1-5 ml) of protein solutions were dialyzed against large volumes (1-2 l) of buffer. Dialysis was performed overnight at 4°C in PBS or TBS depending on experiment.

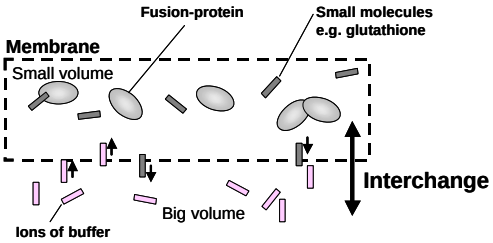

Figure 2.14: ***Scheme of dialysis***

2.8.14. Concentrating of proteins

A YM-30 tube (Centricon) was used to concentrate diluted eluates from protein purification. Centricon tubes were washed by addition of 2 ml distilled water and centrifugation (20 min, 1000xg). The tube was turned upside down and centrifuged (5 min, 1000x*g*) to dry column. 2 ml sample was added and centrifuged (35 min, 1000x*g*). The tube then was turned upside down and 75–150 µl concentrated protein solution was recovered, ***see fig. 2.15***.

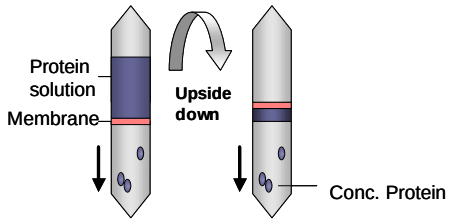

Figure 2.15: ***Concentrating mechanisms by Centricon YM-30***

All chemicals were purchased from Sigma or Gibco if not indicated otherwise.

Results

3. Results

3.1. Cloning of Human Syndecan-3

3.1.1. Library screening

A human fetal brain λZAPII library (10^4 pfUs/ml) was screened with a radioactively labeled probe corresponding to 702 bp of the ectodomain of human syndecan-3 cut out plasmid *pMB284* (a generous gift from Merton Bernfield, ***see fig. 3.1***).

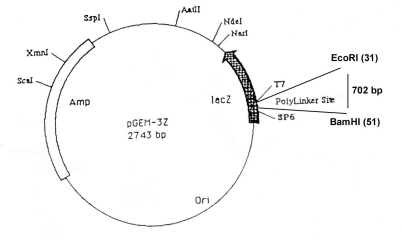

Figure 3.1: *Plasmid pMB284*. A 702-bp sequence of human syndecan-3 ectodomain sub-cloned in pGEM3Z was cut out with *Eco*RI and *Bam*HI, radioactively labeled and used for library screening.

Screening: **10** positive phages were isolated from the first screening round, but only **4** positive phages were left after the third round. Therefore, screening was repeated. **32** positive phages were obtained after the first round. Finally, the yield of this second screening was **24** positive phages, which, together with the **4** positive phages from the first screening gave a total **28** positive clones for human syndecan-3.
Recombination of phages: Phages were recombined with an ExAssist™ helper phage to integrate the different clones into double-strand pBluescript phagemid. *E. coli* SORL cells were transfected with the phagemids. From **27** phagemids, colonies were obtained.

3.1.2. Analysis of positive clones

Overnight cultures were grown, glycerol stocks were prepared and plasmid DNA was isolated and digested with *Eco*RI to isolate inserts, ***see fig. 3.2***. Inserts of varying size (1.1 – 4.4 kb) were subjected to restriction analysis (*not shown*).

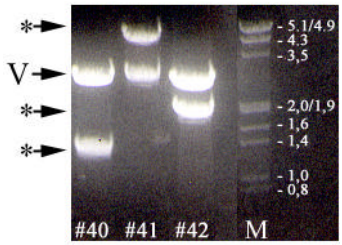

Figure 3.2: *Excision of insert by EcoRI digestion of clones*. Inserts differed in size: clone #40 about 1.5 kb, clone # 41 about 4 kb and clone #42 about 2 kb. V = vector, asterisks indicate inserts.

Certain clones overlapped or contained fragments that were too short for further analysis. Only 19 clones out of 27 were sequenced. The alignment of all clones sequenced is depicted in ***fig. 3.3***.

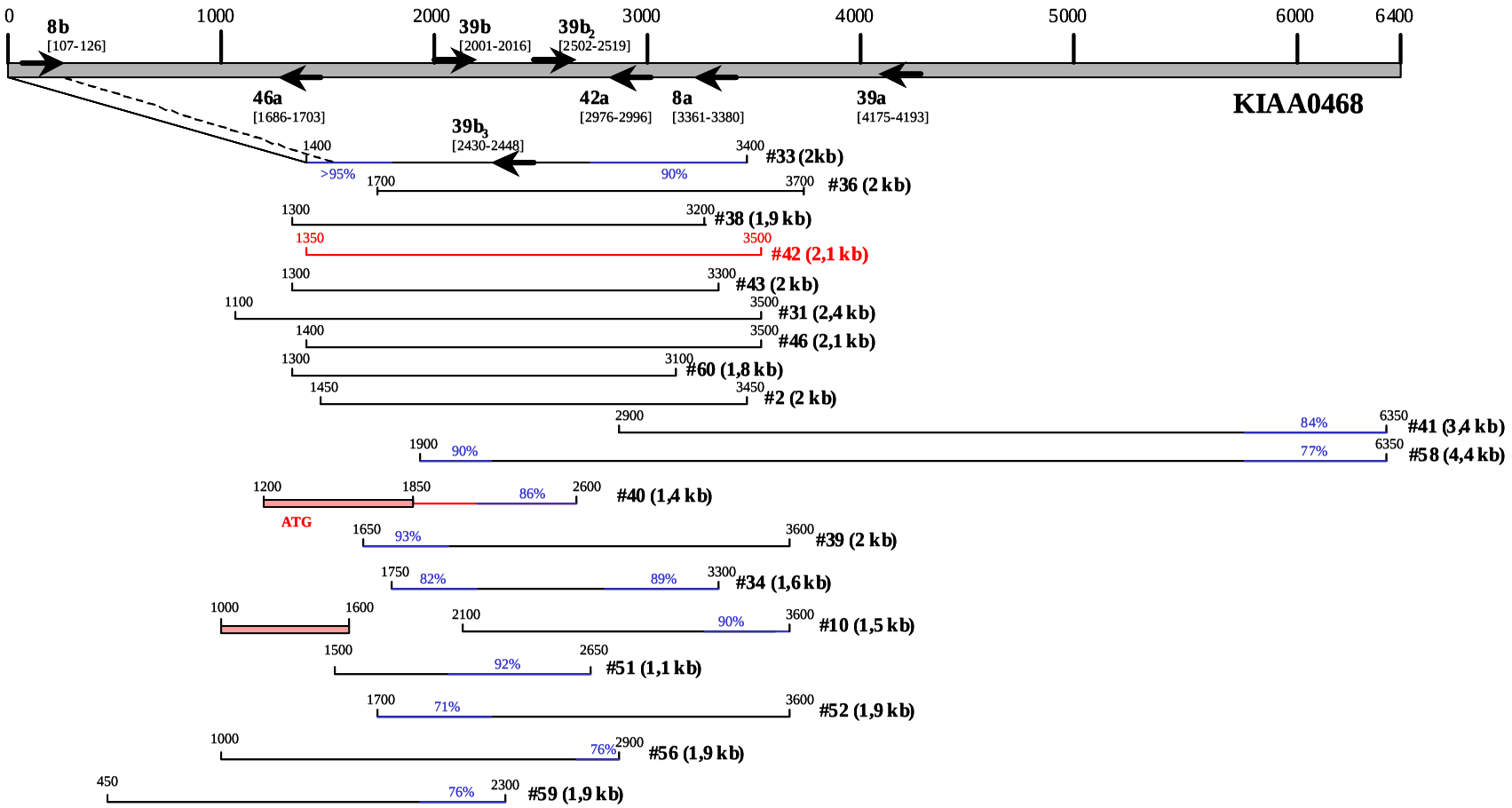

Figure 3.3: ***Alignment of positive clones with unidentified sequence found by databank search.*** **Arrows indicate localization and orientation of primers used in the first sequencing steps (for exact localization of primers: see 2.3.10). Approximate size of each clone is given in brackets. Alignment on bp 1-6400 from KIAA0468 (EMBL ACC. #AB007937) was performed using Gel Assemble from GCG (Genetics Computer Group) as basis for comparison with the clones obtained. Regions of high homology are shown in blue (percentage is indicated above bars); red bars: the clones that were combined to obtain the FL cDNA. Hatched bars indicate regions containing the ATG start codon.**

3.1.3. Yield of syndecan-3 FL cDNA from clone #40 and #42

The sequences obtained were compared by database research (***see 2.3.11.3***). Homology with chicken syndecan-3 was high, although higher homology was found with an uncharacterized DNA sequence of 6400 bp called KIAA0468 (EMBL ACC. #AB007937), which was therefore used to align clones (Seki et al., 1997).

None of the clones analyzed corresponded to FL human syndecan-3 cDNA. Nevertheless, this was obtained by cutting two clones (#40 and #42) with restriction enzymes and ligating them. The resulting plasmid was called "*Ce5*" and was sequenced, ***see fig. 3.4***.

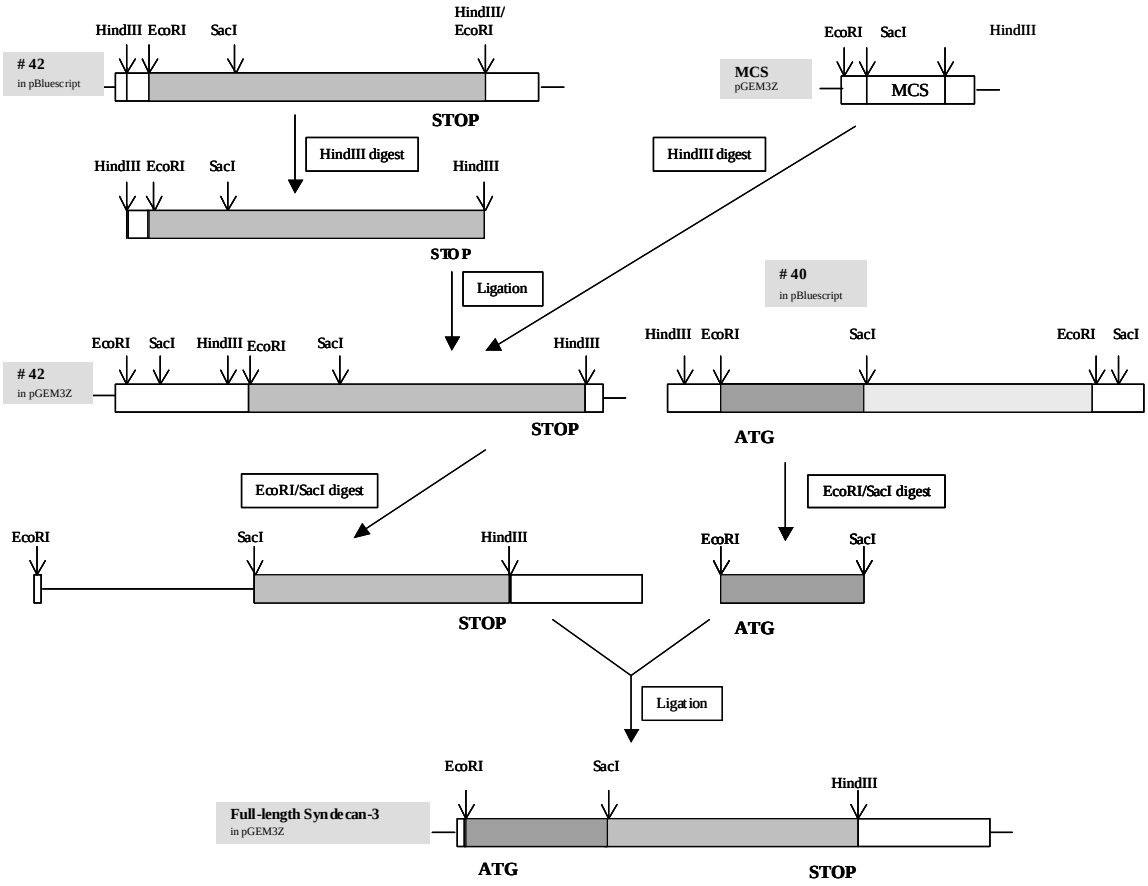

Figure 3.4: *Strategy to obtain FL syndecan-3 from clones #40 and #42*: The complete sequence of #42 was subcloned into pGEM3Z, then the sequence between the recognition sites of *Eco*RI and *Sac*I was cut out and replaced by the corresponding sequence of clone #40, which contained the entire 5'-domain including the ATG start signal.

Sequencing revealed that we had cloned the complete cDNA sequence of human syndecan-3. The nucleotide sequence reported in this thesis has been submitted to the Genbank ^{TM}/EMBL Data Bank with registration number **AF248634**.

3.1.4. Full-length cDNA and protein sequences of human syndecan-3

By using various data banks and computer programs (***see 2.3.11.3***) to align and compare cDNA and protein sequences of human syndecan-3, we obtained the following results.

The cDNA sequence has an open reading frame (ORF) of 1329 bp, predicting a polypeptide of 443 amino acids (***see fig. 3.5, Panel A***). The protein sequence was divided into 3 different structural regions (***see fig. 3.5, Panel B***): A large extracellular domain, followed by a single glycine-rich transmembrane domain and a short cytoplasmic tail (34 amino acids). The extracellular domain bears a proline-rich spacer and eight putative GAG attachment sites (consisting of the dipeptide repeat serine and glycine). These attachment sites are arranged in two clusters, located distal (five dipeptide repeats) and proximal (three dipeptide repeats) to the plasma membrane. Next to the transmembrane region, a dibasic repeat is found. The cytoplasmic tail contains three characteristic regions of syndecans: two constant (C1- and C2-) regions, separated by a variable (V-) region. Four conserved tyrosine residues are located in these regions. The C2 region consists of four amino acids (EFYA), the motif reported to interact with PDZ domain-containing proteins for all syndecans (Carey et al., 1997; Carey, 1997).

The amino acid sequence of human syndecan-3 shows high homology with other published sequences (62% with chicken, 84% with rat), reaching 100% in the transmembrane and cytoplasmic domain of rodents. In all the clones we analyzed, the only differences were found in amino acids 7-23, ***see fig. 3.6***. This stretch, which lies in the region of the hypothetical signal peptide, is characterized by an accumulation of small, neutral amino acids (82%). Thus, 9/17 and 5/17 are glycine and alanine residues, respectively. No identical sequence was found in a database search.

A

```
   1 GAATTCCACAAAGGCGCCCGCCCGCCGCCCGCCGCCCGCGCCCGCGCCGCCGCCATGAAG  60
                                                           M  K   2
  61 CCGGGGCCGCCGCACCGTGCCGGGGCCGCCCACGGGGCCGGCGCCGGGGCCGGGGCCGCG 120
     P  G  P  P  H  R  A  G  A  A  H  G  A  G  A  G  A  G  A  A   22
 121 GCCGGGCCCGGGGCCCGCGGGCTGCTCCTGCCACCGCTGCTGCTGCTGCTGCTGGCGGGG 180
     A  G  P  G  A  R  G  L  L  L  P  P  L  L  L  L  L  L  A  G   42
 181 CGCGCCGCGGGGGCCCAGCGCTGGCGCAGTGAGAACTTCGAGAGACCCGTGGACCTGGAG 240
     R  A  A  G  A  Q  R  W  R  S  E  N  F  E  R  P  V  D  L  E   62
 241 GGCTCTGGGGATGATGACTCCTTTCCCGATGATGAACTGGATGACCTCTACTCGGGGTCG 300
     G  S  G  D  D  D  S  F  P  D  D  E  L  D  D  L  Y  S  G  S   82
 301 GGCTCGGGCTACTTCGAGCAGGAGTCGGGCATTGAGACAGCCATGCGCTTCAGCCCAGAT 360
     G  S  G  Y  F  E  Q  E  S  G  I  E  T  A  M  R  F  S  P  D   102
 361 GTAGCCCTGGCGGTGTCCACCACACCTGCGGTGCTGCCCACCACGAACATCCAGCCTGTG 420
     V  A  L  A  V  S  T  T  P  A  V  L  P  T  T  N  I  Q  P  V   122
 421 GGCACACCATTTGAAGAGCTCCCCTCTGAGCGCCCCACCCTGGAGCCAGCCACCAGCCCC 480
     G  T  P  F  E  E  L  P  S  E  R  P  T  L  E  P  A  T  S  P   142
 481 CTGGTGGTGACAGAAGTCCCGGAAGAGCCCAGCCAGAGAGCCACCACCGTCTCCACTACC 540
     L  V  V  T  E  V  P  E  E  P  S  Q  R  A  T  T  V  S  T  T   162
 541 ATGGCTACCACTGCTGCCACAAGCACAGGGGACCCGACTGTGGCCACAGTGCCTGCCACA 600
     M  A  T  T  A  A  T  S  T  G  D  P  T  V  A  T  V  P  A  T   182
 601 GTGGCCACCGCCACCCCCAGCACCCCTGCAGCACCCCCTTTTACGGCCACCACTGCTGTT 660
     V  A  T  A  T  P  S  T  P  A  A  P  P  F  T  A  T  T  A  V   202
 661 ATAAGGACCACTGGCGTACGGAGGCTTCTGCCTCTCCCACTGACCACAGTGGCTACGGCA 720
     I  R  T  T  G  V  R  R  L  L  P  L  P  L  T  T  V  A  T  A   222
 721 CGGGCCACTACCCCCGAGGCGCCCTCCCCGCCCACCACGGCGGCTGTCTTGGACACCGAG 780
     R  A  T  T  P  E  A  P  S  P  P  T  T  A  A  V  L  D  T  E   242
 781 GCCCCAACACCCAGGCTGGTCAGCACAGCTACCTCCCGGCCAAGAGCCCTTCCCAGGCCG 840
     A  P  T  P  R  L  V  S  T  A  T  S  R  P  P  R  A  L  P  R  P   262
 841 GCCACCACCCAGGAGCCTGACATCCCTGAGAGGAGCACCCTGCCCCTGGGGACCACTGCC 900
     A  T  T  Q  E  P  D  I  P  E  R  S  T  L  P  L  G  T  T  A   282
 901 CCTGGACCCACAGAGGTGGCTCAGACCCCAACTCCAGAGACCTTCCTGACCACAATCCGG 960
     P  G  P  T  E  V  A  Q  T  P  T  P  E  T  F  L  T  T  I  R   302
 961 AATGAGCCAGAGGTTCCGGTGAGTGGGGGGCCCAGTGGAGACTTCGAGCTGCCAGAAGAA 1020
     N  E  P  E  V  P  V  S  G  G  P  S  G  D  F  E  L  P  E  E   322
1021 GAGACCACACAACCAGACACAGCCAATGAGGTGGTAGCTGTGGGAGGGGCTGCGGCCAAG 1080
     E  T  T  Q  P  D  T  A  N  E  V  V  A  V  G  G  A  A  A  K   342
1081 GCATCATCTCCACCTGGGACACTGCCCAAGGGTGCCCGCCCGGGCCCTGGCCTCCTGGAC 1140
     A  S  S  P  P  G  T  L  P  K  G  A  R  P  G  P  G  L  L  D   362
1141 AATGCCATCGACTCGGGCAGCTCAGCTGCTCAGCTGCCTCAGAAGAGTATCCTGGAGCGG 1200
     N  A  I  D  S  G  S  S  A  A  Q  L  P  Q  K  S  I  L  E  R   382
1201 AAGGAGGTGCTCGTAGCTGTGATTGTGGGCGGGGTGGTGGGCGCCCTCTTTGCTGCCTTC 1260
     K  E  V  L  V  A  V  I  V  G  G  V  V  G  A  L  F  A  A  F   402
1261 TTGGTCACACTGCTCATCTATCGTATGAAGAAAAAGGATGAGGGCAGCTACACGCTGGAG 1320
     L  V  T  L  L  I  Y  R  M  K  K  K  D  E  G  S  Y  T  L  E   422
1321 GAACCCAAGCAGGCGAGCGTCACATACCAGAAGCCTGACAAGCAGGAGGAGTTCTATGCC 1380
     E  P  K  Q  A  S  V  T  Y  Q  K  P  D  K  Q  E  E  F  Y  A   442
1381 TAGTGGAGCCACAGTGCCTCCCTGCAGCCTCAACACCACCCTGCTGTCCAGTCCCCAGCC 1140
     *
1441 TGGCCCCACCAGCCCAAGCTT                                        1461
```

B

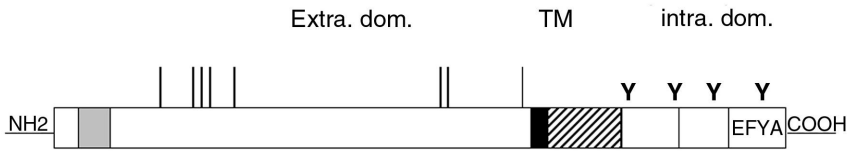

Figure 3.5: ***Organization of human syndecan-3.*** **(*A*) cDNA and aligned protein sequence of human syndecan-3. Putative GAG attachment sites (serine and glycine) are underlined once. The transmembrane sequence is double underlined; the stop codon is indicated by an asterisk. (*B*) Schematic representation of human syndecan-3 protein structure. The grey box represents the human syndecan-3 specific sequence, vertical lines indicate the putative GAG attachment sites, the black box marks the dibasic repeat and the hatched box the transmembrane region. Bold "Y's" symbolize the tyrosine residues in the C-terminal. The final amino acid sequence EFYA is the motif that interacts with intracellular PDZ proteins.**

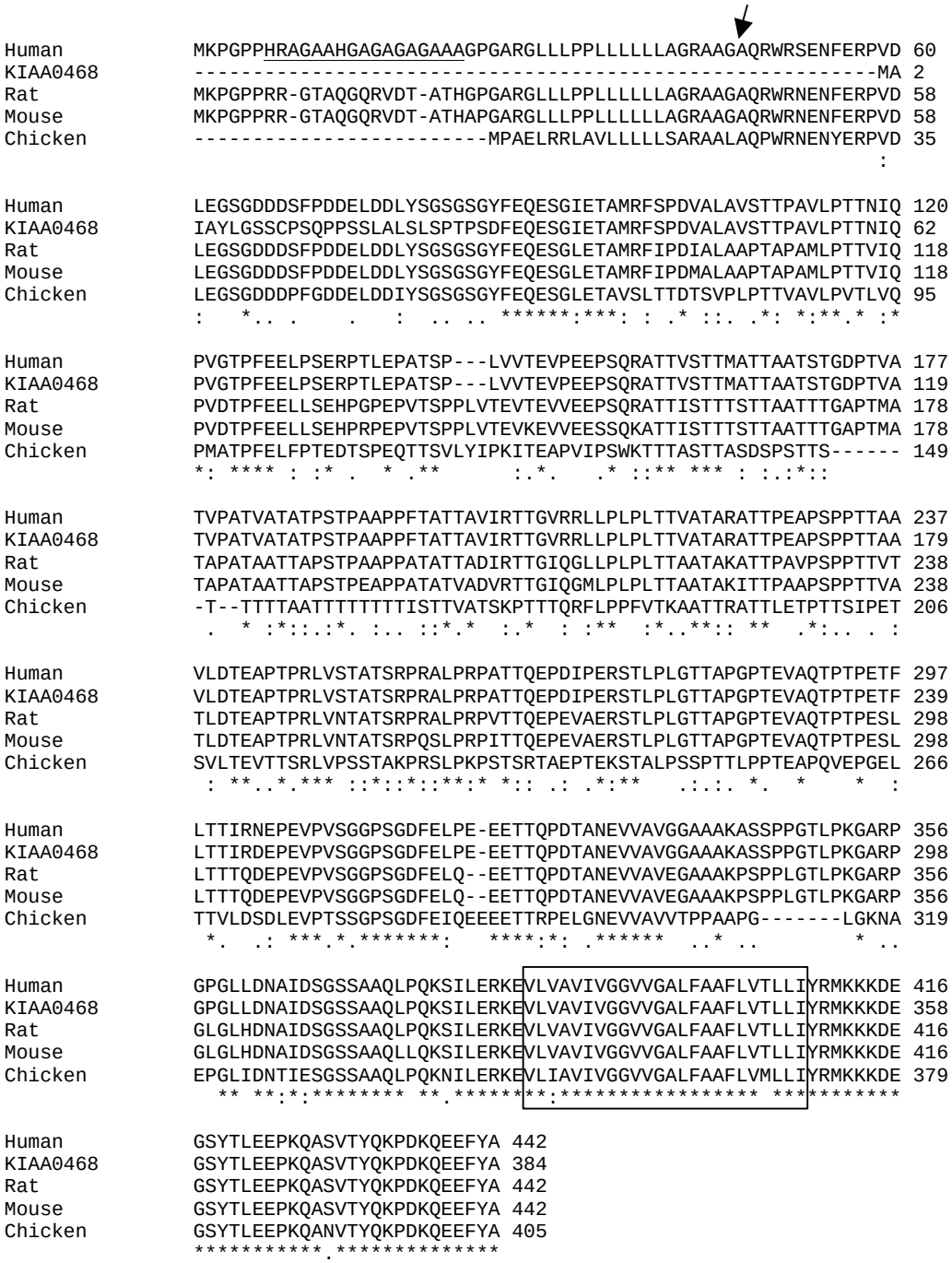

Figure 3.6: ***Alignment of the human syndecan-3 protein with its rat, mouse and chicken homologues*****. Although almost the whole human syndecan-3 sequence is very similar to that of mouse and rat, amino acids 7-23 (underlined) corresponding to a region lying within the hypothetical signal peptide, are strikingly different. "*" = Identical or conserved residues in all sequences in the alignment; ":" = conserved substitutions; "." = semi-conserved substitutions. Transmembrane region is marked by a box, the end of the hypothetical signal peptide of human syndecan-3 by an arrow. KIAA0468 (Seki et al., 1997) is the sequence of a human clone from the database, which was not further characterized.**

3.2. Expression of syndecan-3 mRNA in human tissues and cell lines

To examine the expression of human syndecan-3 mRNA, the oligonucleotide probe used in the screening process was labeled with dCTPα^{32}P and used to perform a RNA dot blot analysis of 76 human poly A^+ RNA's (from various tissues and cell lines) and 8 control RNA's. As shown in ***fig. 3.7, A*****,** syndecan-3 was mostly expressed in the brain (adult and fetal), the adrenal gland and the spleen. In the nervous system strong expression was found in almost all regions examined, except for the pituitary gland. Very strong labeling was detected in the temporal lobe (highest levels), in the corpus callosum and the spinal cord, ***see fig. 3.7, B***. In the gastrointestinal system, syndecan-3 mRNA was mainly found in the stomach, transverse and descending colon, duodenum and rectum (***see fig. 3.7, C***), while in the heart expression was predominantly found in the aorta (***see fig. 3.7, D***)***.*** In fetal tissues, strong signals were obtained with mRNA from fetal brain and spleen (***see fig. 3.7, E***). The only cell line from three leukemia, two lymphoma, one lung carcinoma, one adenocarcinoma cell lines and HeLa cells, that showed syndecan-3 expression, was the colorectal adenocarcinoma cell line SW480 (***see fig. 3.7, F***).

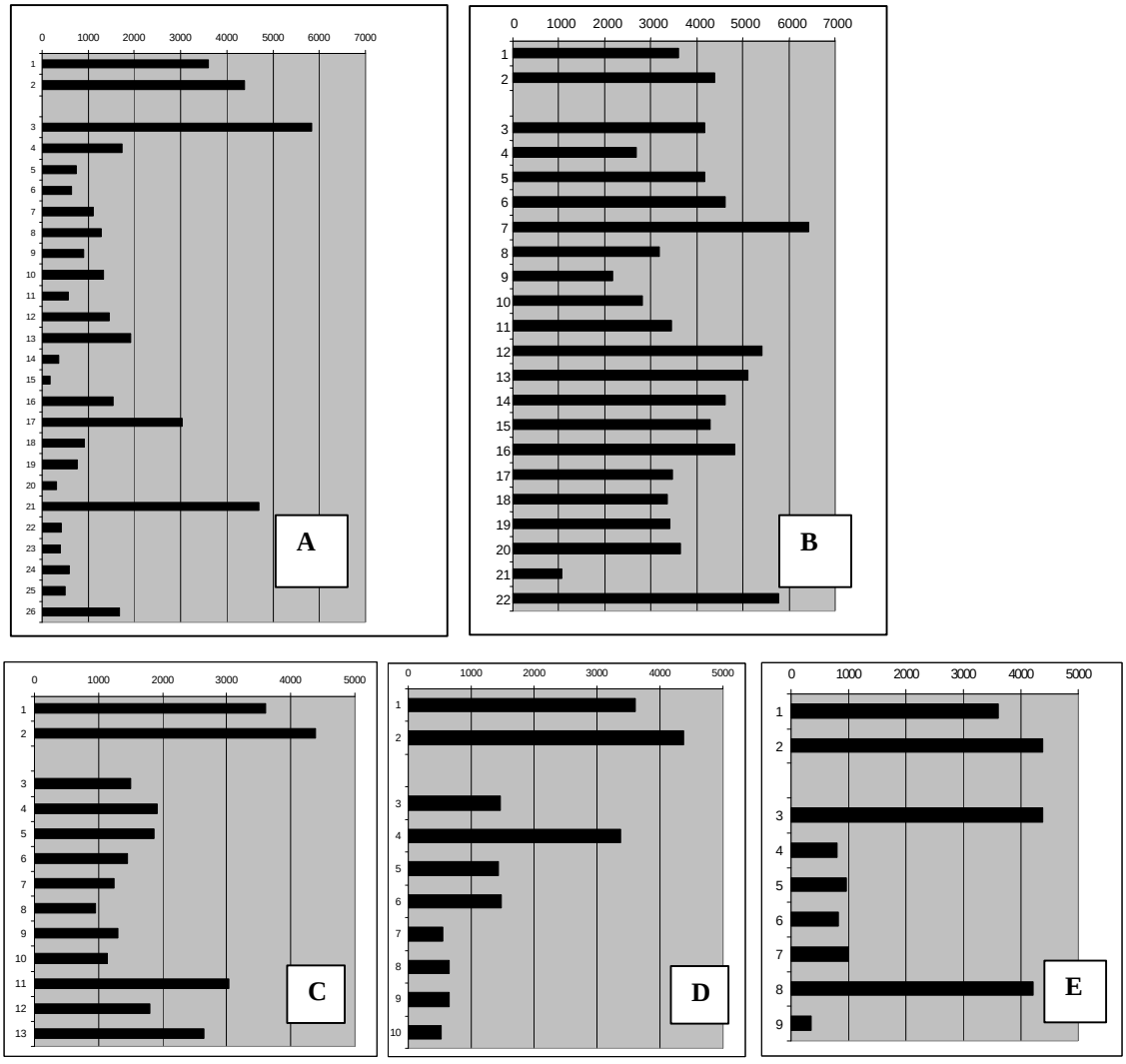

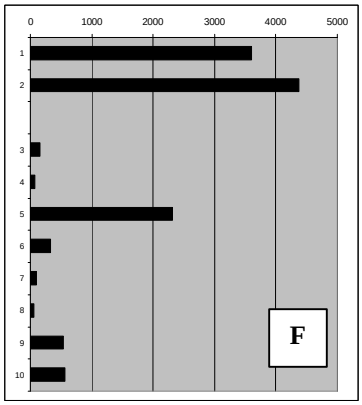

Figure 3.7: *Analysis of human syndecan-3 mRNA expression*. For dot blot analysis, 76 human poly A^+ RNA's and 8 control RNA's arranged on a nylon membrane (Clontech) were incubated with a radioactively labeled (^{32}P) syndecan-3 DNA oligonucleotide. The amount of radioactivity was determined using a Phosphoimager. The expression in whole (1) and fetal brain (2) is shown in every graph as control for expression levels.

(A): In human tissues. 1: Whole brain; 2: Fetal brain; 3: Adrenal gland; 4: Bladder; 5: Bone marrow; 6: Kidney; 7: Liver; 8: Lung; 9: Lymph node; 10: Mammary gland; 11: Ovary; 12: Heart; 13: Stomach; 14: Pancreas; 15: Peripheral blood leukocyte; 16: Placenta; 17: Colon, transverse; 18: Prostate; 19: Salivary gland; 20: Skeletal muscle; 21: Spleen; 22: Testis; 23: Thymus; 24: Thyroid gland; 25: Trachea; 26: Uterus.

(B): In regions from human brain. 1: Whole brain; 2: Fetal brain; 3: Cerebral cortex; 4: Frontal lobe; 5: Parietal lobe; 6: Occipital lobe; 7: Temporal lobe; 8: Paracentral gyrus of cerebral cortex; 9: Pons; 10: Cerebellum left; 11: Cerebellum right; 12: Corpus callosum; 13: Amygdala; 14: Caudate nucleus; 15 Hippocampus; 16: Medulla oblongata; 17: Putamen; 18: Substantia nigra; 19: Nucleus accumbens; 20: Thalamus; 21: Pituitary gland; 22: Spinal cord.

(C): In the gastrointestinal system: 1: Whole brain; 2: Fetal brain; 3: Esophagus; 4: Stomach; 5: Duodenum; 6: Jejunum; 7: Ileum; 8: Ilocecum; 9: Appendix; 10: Ascending colon; 11: Transverse colon; 12: Descending colon; 13: Rectum.

(D): In the heart: 1: Whole brain; 2: Fetal brain; 3: Heart; 4: Aorta; 5: Left atrium; 6: Right atrium; 7: Left ventricle; 8: Right ventricle; 9: Interventricular septum; 10: Apex of the heart.

E): In fetal tissues: 1: Whole brain; 2: Fetal brain; 3: Fetal brain; 4: Fetal heart; 5: Fetal kidney; 6: Fetal liver; 7: Fetal lung; 8: Fetal spleen; 9: Fetal thymus.

(F): In human cell lines: 1: Whole brain; 2: Fetal brain; 3:Burkitt's lymphoma Daudi; 4: Burkitt's lymphoma Raji; 5: Colorectal adenocarcinoma SW480; 6: HeLa S3; 7: Leukemia - MOLT4; 8: Leukemia HL-60; 9: Leukemia K-562; 10: Lung carcinoma A549.

3.3. Generation of anti-human syndecan-3 ectodomain antibody in rabbit

3.3.1. Production and purification of GST-syndecan-3 fusion protein for immunization of rabbits

When a range of constructs was tested, the best induction of fusion protein expression was obtained using a pGEX vector, which contained a large part of the ectodomain of human syndecan-3 but not the transmembrane and cytoplasmic domains ("*pGEX little*", ***see also Annex IV: Constructs***).
Fig. 3.8 shows the results of the corresponding fusion protein purification (***Panel A***). Coomassie staining revealed two strong bands at about 100 and 65 kDa. High protein amounts were found in the bacterial lysis but most was lost during centrifugation. Protein purification was greatly improved by using a protocol, based on the use of lysozyme (***see fig. 3.8, Panel B***) instead of TX-100 (***see fig. 3.8, Panel A***) for bacterial lysis.

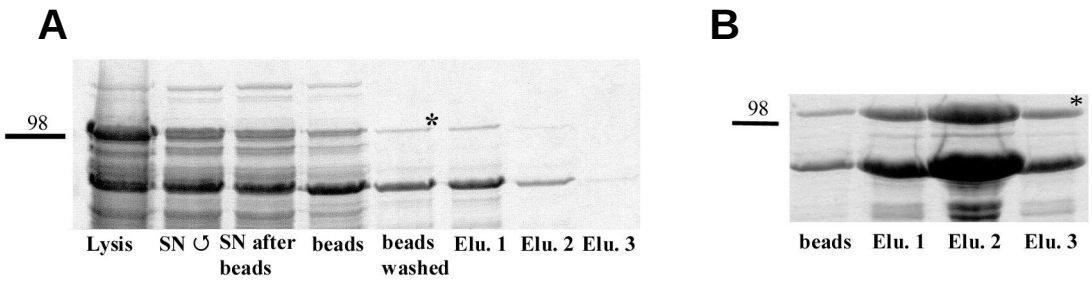

Figure 3.8: ***GST-syndecan-3 fusion protein purification.*** **Coomassie staining of the individual steps of protein purification with TX-100 (A) and lysozyme (B). 10 µl of each fraction was loaded on each lane, except for beads: 5µl. SN = supernatant, Elu = Eluate; arrow indicates centrifugation; asterisks mark the syndecan-3-GST fusion protein.**

The calculated molecular mass of the fusion protein was about 75 kDa, but both syndecans produced in bacteria and syndecans digested from cell lysates show abnormal migratory behavior (Bernfield et al., 1992; Carey, 1996), so the fusion protein could correspond to the 100-kDa band. In order to confirm that this band was the syndecan-3 fusion protein, Western blot analysis was performed with anti-GST and anti-mouse syndecan-3 (923) antibodies (the latter directed against the syndecan-3 ectodomain, was a generous gift from Dr. Merton Bernfield). Since the individual syndecans are highly homologous in human and rodent, ***see also fig. 3.6*** (Bernfield et al., 1992; Bernfield et al., 1999; Carey, 1997), the mouse antibody was expected to recognize the human protein.

The antibody raised against the mouse syndecan-3 also recognized the human protein specifically. This experiment also showed that the band corresponding to the human GST-syndecan-3 fusion protein was indeed the band with a molecular mass of about 100 kDa, ***see fig. 3.9***.

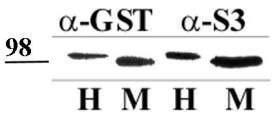

Figure 3.9: ***The antibody raised against the mouse syndecan-3 ectodomain recognized the human protein.*** **100 ng/each lane. Western blot of mouse (M) and human (H) GST-syndecan-3 fusion proteins with anti-GST (α-GST) and anti- (mouse)-syndecan-3 antibody (α-S3; M. Bernfield).**

The purified GST-syndecan-3 fusion proteins were used for the immunization of white New Zealand rabbits as described in Materials and Methods. Two rabbits were injected with the eluted protein (Max and Moritz) and the other pair (Clever and Smart) were injected with the homogenized protein band at 100-kDa cut out from a polyacrylamide gel.

3.3.2. Characterization of antibodies

In order to evaluate the specificity of the antibodies, Western blot analysis was performed with the unpurified pre- and post-immune serum. In this first analysis, all antibodies recognized the GST-syndecan-3 fusion protein even when highly diluted (*not shown*).
This indicated a high specificity of all antibodies. Nevertheless, one antibody (Clever) was purified on Protein G sepharose in order to eliminate Igs other than IgG. When the experiment was repeated, some gain in specificity was observed compared to the results obtained with the unpurified serum. At the same concentrations, no labeling by the pre-immune serum was found, ***see fig. 3.10***.

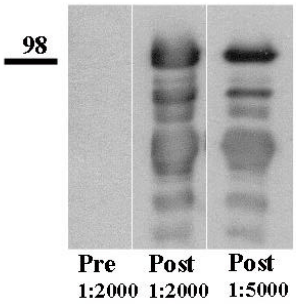

Figure 3.10: ***Anti-syndecan-3 antibodies (here Clever) recognized the GST-syndecan-3 fusion protein at high dilutions*****. Representative Western blot analysis for all antibodies: Approx. 3 µg eluted GST-syndecan fusion protein per lane. Western blot was performed with pre-immune (Pre) and Protein G purified post-immune serum (Post) at the indicated dilutions.**

In the next step, the ability of antibodies to recognize the eukaryotic protein was further studied. Therefore, total lysates of cells transfected with syndecan-3 were analyzed by Western blot, ***see fig. 3.11***.

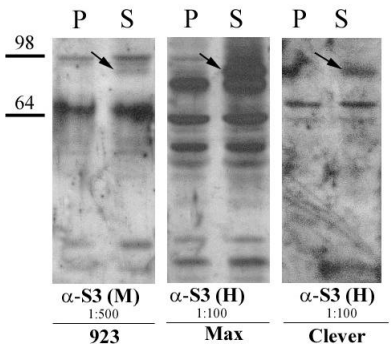

Figure 3.11: ***Antibodies recognize a specific band in syndecan-3 transfected cells.*** **Western blot analysis was performed with total lysates from cell transfected with control vector (P) or syndecan-3 (S). Arrows indicate the band corresponding to syndecan-3 in the syndecan-3-transfected cells. Protein amount per lane: 10 µg. M = Mouse, H = Human. 923 = anti-syndecan-3 (mouse) antibody (M. Bernfield). Primary antibodies were used at indicated dilutions, unpurified (Max, 923) or purified by Protein G (Clever).**

As can be seen in ***fig. 3.11***, the Max antibody (unpurified) and the Clever antibody (Protein G purified) specifically recognized a band that was only present in the lysates of syndecan-3 but not in the mock-transfected cells. The Max antibody showed more intensive but also more unspecific staining while the Clever antibody presented a fainter but more specific stain. The anti-syndecan-3 (mouse) antibody (923; M. Bernfield) labeled the same band as the antibodies raised against the human protein, although with very low intensity. Possible reasons will are discussed below (***see 4.1.2.2.1***).

To further characterize antibodies, IP experiments were performed, ***see fig. 3.12***.

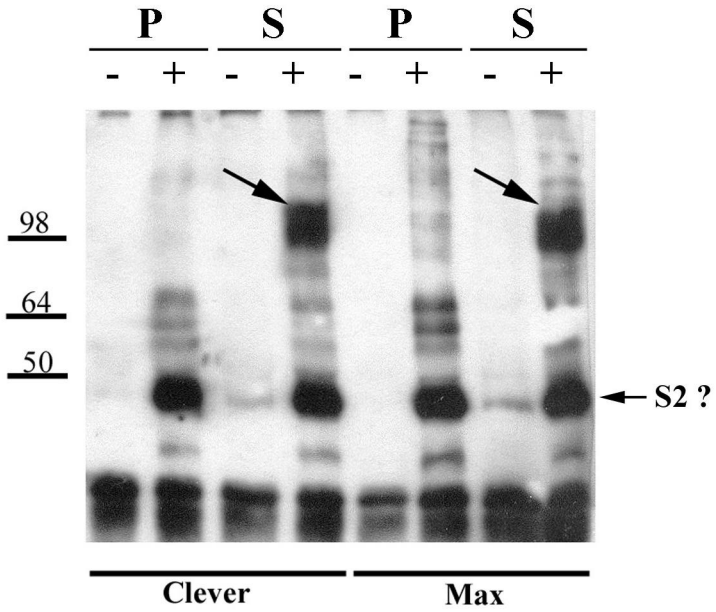

Figure 3.12: *Antibodies immunoprecipitated syndecan-3 and -2.* Western blot analysis of IP with Protein G purified antibodies Clever and Max. 10 µl of each antibody were incubated with 50 µg of lysis from CHO K1 cells transfected with control vector (P) or syndecan-3 (S). After IP, samples were digested with Heparitinase/ChABC (+). Undigested (-) samples were used as control for first antibody (3G10). Arrows indicate syndecan-3 band, the protein at about 50 kDa might be syndecan-2.

Fig. 3.12 shows that antibodies immunoprecipitated a protein with a molecular mass of about 100-120 kDa, which corresponds to syndecan-3 and another protein, which is present in transfected and untransfected cells, which might be syndecan-2.

Finally, antibodies were checked for their specificity in immunocytochemistry. In parallel, the most promising antibody of all previous results (Clever) was affinity-purified by incubation with GST-syndecan-3 fusion protein linked to beads. The results are summarized in ***fig. 3.13***.

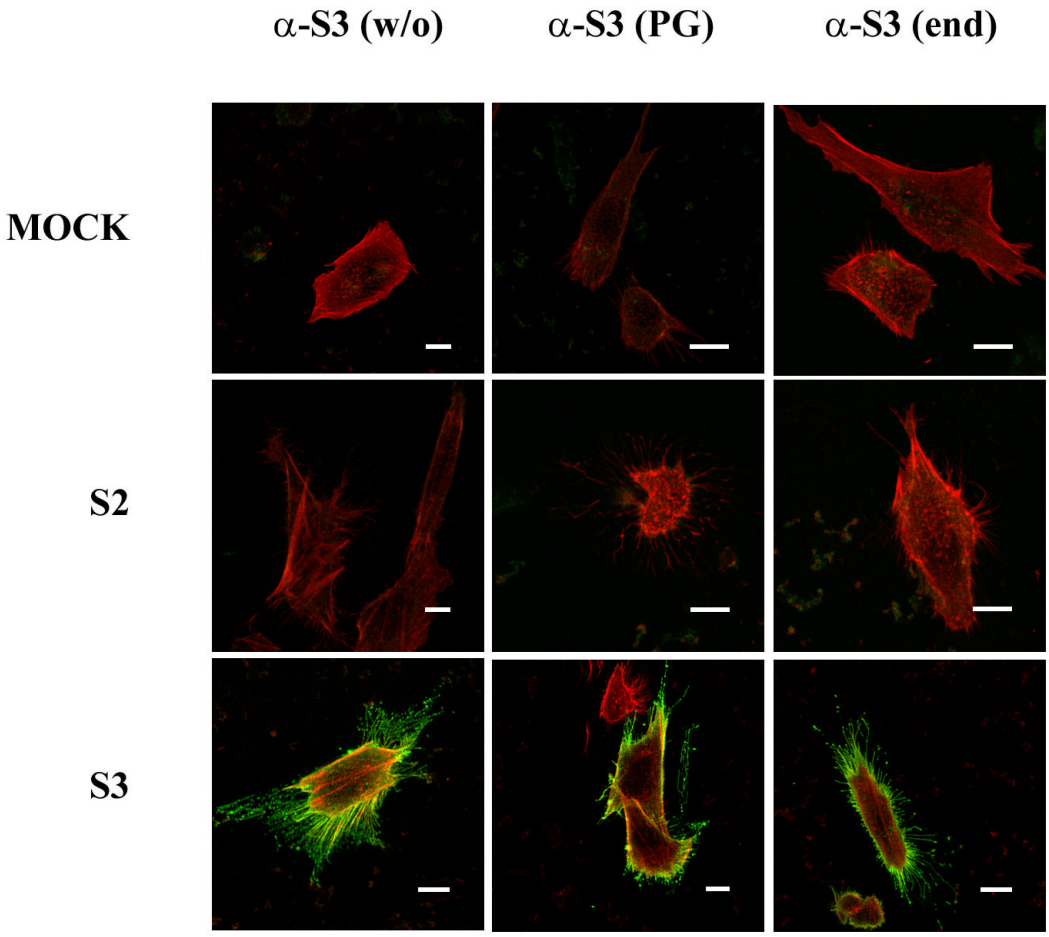

Figure 3.13: ***All antibodies (here Clever) specifically recognized syndecan-3 in transfected cells.*** **Confocal microscopy analysis of CHO K1 cells transfected with control vector (MOCK), syndecan-2 (S2) or syndecan-3 (S3). Antibody concentrations: unpurified (w/o; 1:2000), purified by Protein G (PG; 1:1000) or affinity purified (end; 1:100). Cells were labeled with TRITC-conjugated phalloidin (red) for actin and anti-syndecan-3 and FITC-conjugated anti-rabbit IgG secondary antibody (green) for human syndecan-3.**

Fig. 3.13 shows that the Clever antibody specifically recognized syndecan-3 in transient transfected cells independently of its degree of purification. No background labeling was seen either in control- or in syndecan-2-transfected cells. The expression of the syndecan-2 protein was checked by staining cells in another coverslip with anti-syndecan-2 antibody (*not shown*).

In summary, the antibodies raised are suitable for Western blot analysis of GST-syndecan-3 fusion proteins and for immunocytochemistry experiments. As to the Western blot and IP analysis of cell lysates, no conclusive results were obtained which might be due to experimental problems (***see 4.1.2.2.1***). For these reasons, in Western blot experiments, syndecan-3 detection was performed with 3G10 antibody after Heparitinase/ChABC digest.

3.4. Transient transfection of full-length syndecan-3 led to the induction of filopodia-like structures, microspikes and varicosities

3.4.1. Phenotype of transient transfected cells

In order to study the function of the syndecan-3 protein, transient transfection experiments were performed in COS-1 cells (***see fig. 3.14, Panel A***). Cells were transfected with the control vector (***see fig. 3.14, A***) or with the FL syndecan-3 cDNA sequence (***see fig. 3.14, B,C***), fixed 48 hours post transfection and immunolabeled with polyclonal anti-mouse-syndecan-3 antibody (***see fig. 3.14, A-C***)**.**
At the confocal microscopy, strong membrane staining was observed in the syndecan-3 transfected cells (***see fig. 3.14, B,C***), while in control cells only a diffuse background stain across the whole cell surface was seen. This result indicates that syndecan-3 was located at the membrane, since the antibody is directed against the ectodomain of the protein and the immunocytochemistry was performed in non-permeabilized cells. The expression of the FL protein in COS-1 cells led to the induction of a large number of filopodia-like structures (***arrows***), some of which had varicosities at their tip (***see fig. 3.14, B, arrowheads***). These effects were not seen in the control (***see fig. 3.14, A***).

Surprisingly, COS-1 cells transfected with a construct in which GFP was fused to the C-terminal domain of syndecan-3 (*S3GFP*) also showed an altered phenotype (***see fig. 3.14, E,F***), similar to syndecan-3 transfection without tag, bearing filopodia (***arrows****)* and varicosities (***arrowheads****)*. This was not expected, since GFP is a large molecule, which could hinder interactions of the short syndecan-3 cytoplasmic tail with intracellular proteins. This indicates that the induction of this phenotype does not depend on the interaction of the C-terminal part of the cytoplasmic tail (***see 3.4.4***). Cells transfected with the vector bearing the GFP in the N-terminal domain of syndecan-3 (*GFPS3*; ***fig. 3.14, D***) or with GFP alone showed the typical green color. However, as GFP is a cytoplasmic protein, the fusion protein was not delivered to the membrane and also did not induce the syndecan-3 phenotype. This indicates that the export of syndecan-3 to the membrane is a prerequisite for the formation of the filopodia-like structures, further implicating the extracellular domain (***see 3.4.3***). However, the induction of the phenotype was not seen in all COS-1 cells after transfection with *S3GFP*. One possible explanation is that the fusion protein had not reached the plasma membrane although GFP staining was already seen. There was also evidence of cell degeneration in GFP-transfected cells (these cells often presented many vacuoles), which might also explain why these transfected cells do not produce long filopodia.

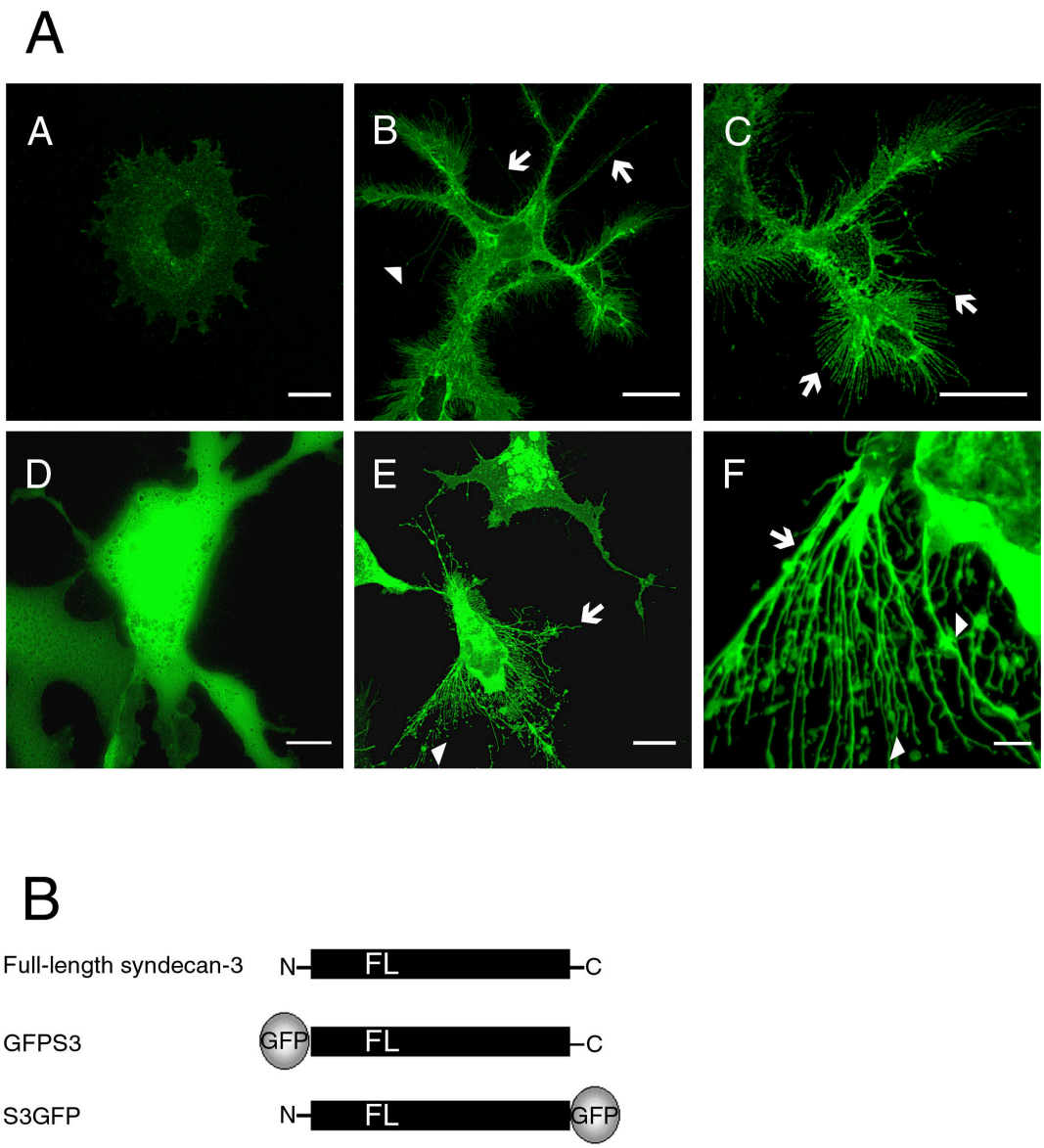

Figure 3.14: ***Syndecan-3 expression induced the generation of filopodia-like structures, microspikes and varicosities in COS-1 cells.*** **(Panel A): COS-1 cells were transiently transfected with control vector Prk5 (A) and FL syndecan-3 cDNA (B,C). 24 or 48 h after transfection, immunostaining with rabbit polyclonal anti-mouse-syndecan-3, revealed by FITC-conjugated anti-rabbit IgGs antibody, was performed. Cells were analyzed by confocal microscopy. GFP fluorescence of COS-1 cells transfected with GFPS3 (control, D) and S3GFP (E,F). Transient expression of syndecan-3 led to the induction of long filopodia (*arrows*) and varicosities (*arrowheads*). Results are representative of at least four independent experiments. Bars represent 20 µm (A-E) and 3.3 µm (F). (Panel B): Schematic representation of the constructs used in the transfection experiments. FL = full-length; GFP = green fluorescent protein.**

3.4.2. Syndecan-3 co-localizes with re-organized actin cytoskeleton

To verify that the effect observed was not unique to COS-1 cells, 3T3 (***see fig. 3.15, A-C***) and CHO K1 (***see fig. 3.15, D-F***) cells were transfected with the FL construct and immunocytochemistry experiments were performed. Among the transfected cells from each cell line, slightly different phenotypes were found. For every "phenotype" one representative example is shown. Some cells had an "ice-crystal"-like structure, often combined with a multitude of varicosities (***see fig. 3.15, C; arrowheads***). The most dramatic effect was seen in CHO K1 cells, some of which had several hundreds of long projections (up to 50 μm) from the cell body, sometimes without any ramifications (***see fig. 3.15, D***) or they showed an abundance of varicosities (***see fig. 3.15, F; arrowheads***).
The syndecan-3 protein co-localizes strongly with actin in all cell lines tested. The main sites of co-localization were the filopodia-like structures, the microspikes and the cortical actin. 3T3 (***see fig. 3.15, A,B; arrows***) and CHO K1 cells (***see fig. 3.15, D,E; arrows***) are shown as examples. The distribution of syndecan-3 was homogeneous inside the whole prolongation, while actin staining decreased with the distance from the cell body. Compared with the untransfected cells (***see fig. 3.15, B,E, asterisks***) in transfected cells the whole cytoskeleton was remodeled. Actin was re-distributed to the cell periphery, near the base and inside the filopodia-like structures, or re-organized into thick bundles. Scanning electron microscopy confirmed the immunocytochemical results in CHO K1 cells (***see fig. 3.15, G-I***). As a result of transitory transfection, both the smooth, untransfected (***asterisks***) and the hairy, transfected phenotype with filopodia and microspikes were seen in the same cell preparations (***see fig. 3.15, G***). ***Fig. H-I*** show the detailed fine structure of filopodia tips and varicosities (***see fig. 3.15, H,I; arrowheads***).

As the experiment of syndecan-3 transfection was performed by using a high expression vector, one possible explanation of the observed phenotype would be over-expression of the protein. Therefore Laser Scanning Cytometry (LSC) was performed in order to demonstrate that the "typical" syndecan-3 effect was not due to over-expression but rather to the specific properties of syndecan-3. The advantage of LSC over FACS (Fluorescence Activated Cell Sorting) lies in the fact, that the analysis of transfected cells can be performed on coverslips. It is then possible to correlate phenotype with amount of fluorescence labeling.
Therefore, CHO K1 cells were transfected with syndecan-2 or -3 or control vector (***see fig. 3.16*****),** labeled with polyclonal anti-syndecan-2 and -3 antibodies respectively (1:1000) and secondary antibody (FITC-swine-anti-rabbit-IgG), and analyzed by LSC.

These experiments showed that the expression level of syndecan-3 was comparable to that of syndecan-2, which produces similar cellular protrusions after transfection (Granes et al., 1999). This means that the amount of syndecan that induces the phenotype was comparable in both experiments. Cells marked by the window were checked visually and showed the phenotype at high percentage (> 85%; *not shown*).

To further confirm that the effect observed after syndecan-3 transfection is not an artifact due to over-expression of the protein, transfection experiments were performed with syndecan-3 and its control vector. Cells were labeled by anti-syndecan-3 antibody and secondary antibody (FITC-swine-anti-rabbit-IgG) and various coverslips were analyzed (***see fig. 3.17***)**.** The upper cytofluorograms contain the same red window as in the former experiment as a reference. Then, new windows were defined in the cytofluorogram, corresponding to cells that do not express syndecan-3 (which corresponds to the window in which the mock transfected cells lie, (***blue box***), which express low (***yellow box***), middle (***pink box***) and high (***green box***) amounts of syndecan-3 protein. Cells were then checked visually and representative photos were taken from cells corresponding to each window (***see fig. 3.17***)**.** Since the image quality obtained by LSC was poor, brightness and contrast were increased in the low and middle syndecan-3 expressers to improve prints. As the "typical" syndecan-3 phenotype was also induced in low and middle expressers, we conclude that the observed phenotype is not caused by over-expression of the protein.

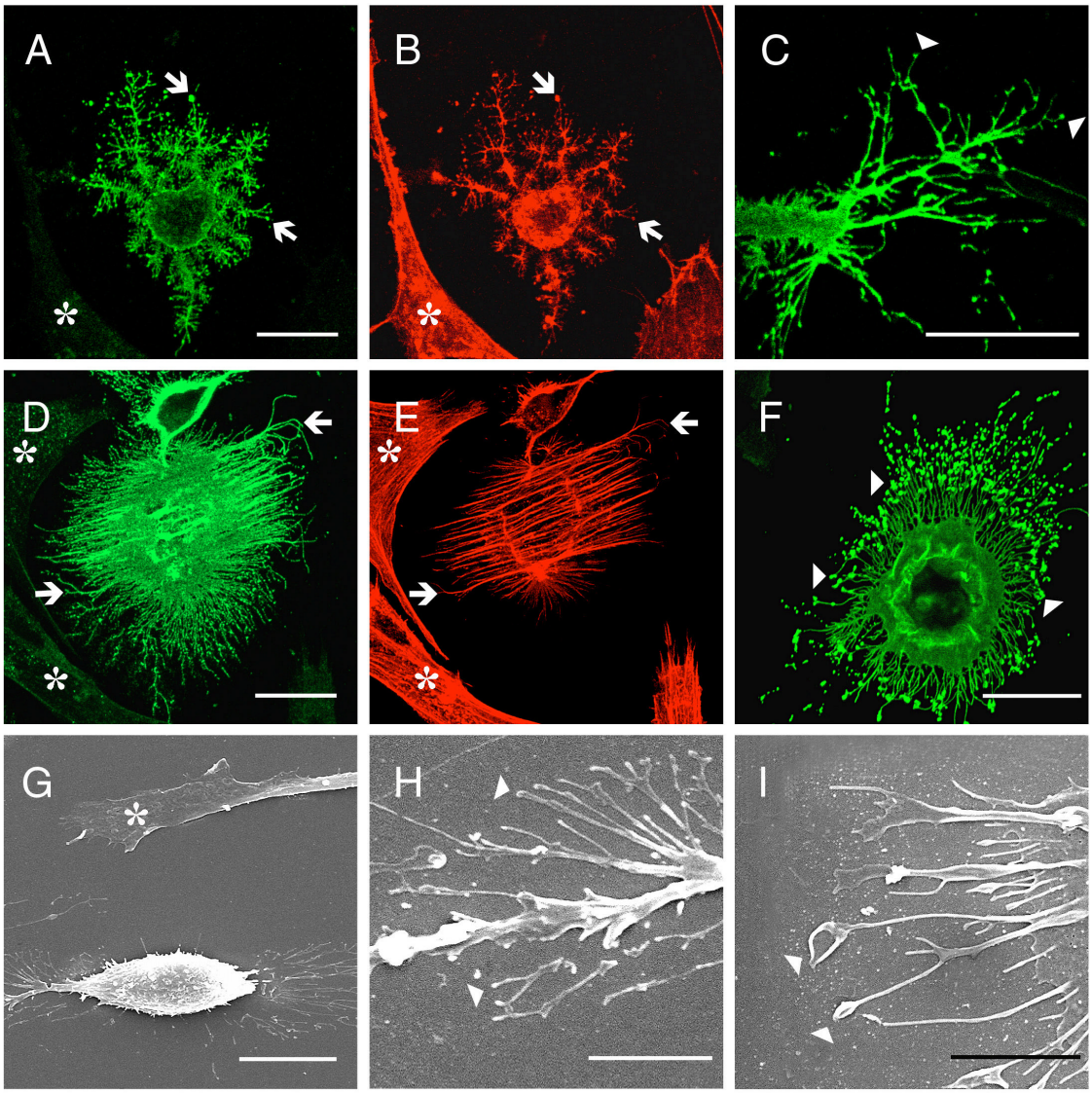

Figure 3.15: ***Transient expression of syndecan-3 reorganized the actin cytoskeleton in 3T3 and CHO K1 cells*****. Liposome-mediated transfection of 3T3 SA (A,B,C) and CHO K1 (D,E,F) cells with the FL syndecan-3. Immunocytochemistry with anti-syndecan-3 (A,C,D,F) antibody was performed as described in *fig. 3.14*. Actin was stained with TRITC-conjugated phalloidin (B,E). Arrowheads indicate varicosities. Syndecan-3 co-localizes with the actin cytoskeleton, especially in the cell periphery and the cell protrusions (arrows). Scanning electron microscopy was performed with syndecan-3-expressing CHO K1 cells (G,H,I), confirming the structural differences between transfected "hairy" and non-transfected cells (G, asterisk). Detailed analysis (H,I) shows the fine structure of filopodia tips and varicosities (arrowheads). Results are representative of more than four (A-I) or two (G-I) independent experiments. Bars represent 20 µm (A-F), 10 µm (G) and 4 µm (H,I). Asterisks label untransfected cells.**

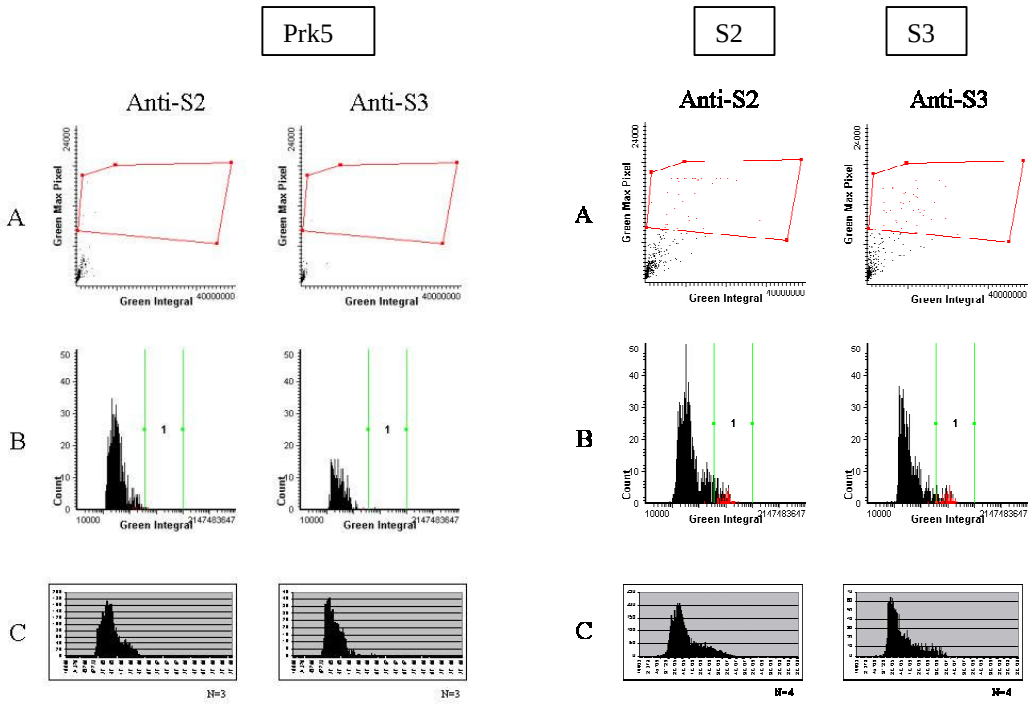

Figure 3.16: ***The amounts of transient expressed syndecan-3 are similar to that of syndecan-2*****. LSC analysis of CHO K1 cells, transiently transfected with a control vector (Prk5) or syndecan-2 or -3 FL and labeled by rabbit anti-syndecan-2 and –3 (Clever) antibodies respectively. Panel A shows the distribution of cells corresponding to absolute value of fluorescence (Green Integral) and to the maximum intensity of green pixels (Green Max Pixel). Values obtained by Prk5 transfection were considered as background. All cells with higher intensities (here symbolized by a red window) were considered as transfected. These cells appear in Panel B inside the green frame as a new peak in the cytofluorogram.**
A **and** ***B*** **show one representative experiment, while in Panel C all experiments are summarized. The higher staining of Prk5 transfected cells by syndecan-2 antibody is due to the endogenous syndecan-2 of CHO K1 cells. (N = number of coverslips analyzed in two independent experiments).**

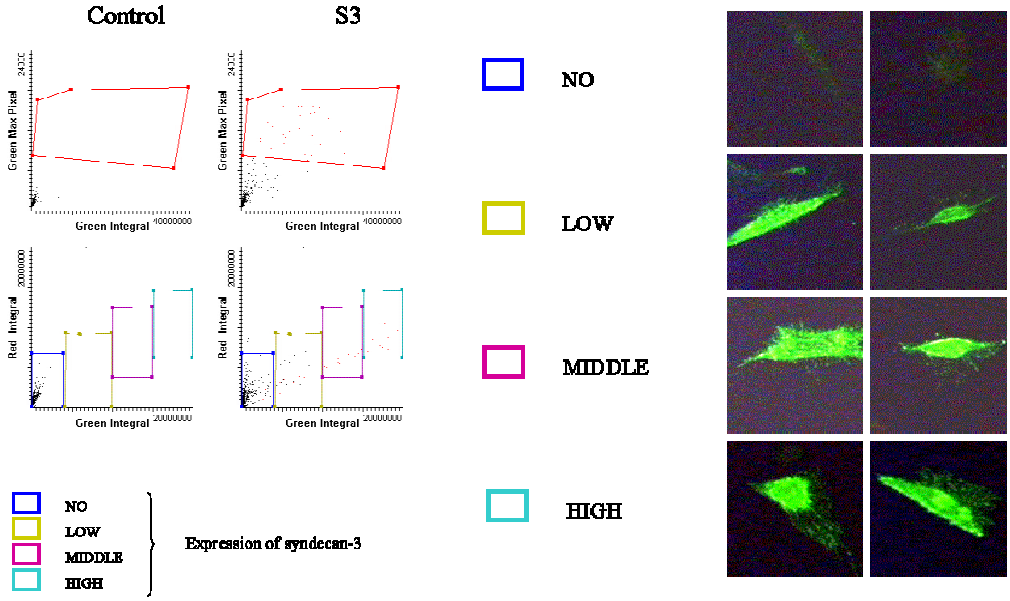

Figure 3.17: ***The filopodia-inducing effect of syndecan-3 is not due to over-expression of the protein*****. LSC analysis of CHO K1 cells transiently transfected with a control vector (Prk5) and FL syndecan-3. As described in fig. 3.16, fluorescence of Prk5 transfected cells was considered as background, all with higher intensity as transfected cells. Then, among the syndecan-3-transfected cells, four pools were arbitrarily determined: No, low, middle and high expressers corresponding to the blue, yellow, pink and green windows respectively. From each pool representative pictures were taken. In low- and middle expressers contrast and brightness was increased in order to improve poor print quality. It can be seen that the generation of filopodia in CHO K1 cells was also observed in low expressers.**

3.4.3. Implication of syndecan-3 extracellular domain: Importance of GAG chains

In order to find out whether the over-expression of the syndecan-3 core protein was sufficient to provoke the phenotypes observed, or if the protein had to be glycosylated, we performed transfection experiments on cell lines with abnormal glycosylation (CHO 745; ***see fig. 3.18, Panel A, C,D***) and compared them with wild type cells (CHO K1; ***fig. 3.18, Panel A, A,B***). The CHO 745 cell line does not synthesize GAG chains due to defect in xylosyltransferase (Esko et al., 1985). Transfected cells were classified into two distinct phenotypes: Cell manifesting the “typical” syndecan-3 phenotype, or not. Cells that were difficult to classify were omitted from the calculations. Values are expressed as percentage of phenotype-presenting of all transfected cells.

Most of the transfected CHO 745 cells showed membrane-staining and some microspikes on the cell-surface (***see fig. 3.18, Panel A, C,D***), but very few showed the phenotype seen with CHO K1 cells (***see fig. 3.18, Panel A, A,B***). Only 8.7 % of the transfected CHO 745 cells manifested a typical syndecan-3 phenotype, while 64.5 % did not (***see fig. 3.18, Panel B***). In contrast, in the CHO-K1 cell line, 69.4% showed the typical syndecan-3 effects, while 12.7% were not different from the wild type. The remaining 17.9% of the CHO K1 cells and 26.8% of the CHO 745 cells were omitted since they were difficult to classify.

To further determine the importance of the sugar chains CHO K1 cells were transfected as before, then grown for 48 h in the absence or presence of 10 U/ml heparin. No cells bearing the “typical” syndecan-3 phenotype were seen among the heparin-treated cells in three independent experiments, while in control the number of syndecan-3 phenotype-presenting cells was the same as in former experiments (*not shown*). In the transfected CHO 745 and in the heparin-treated CHO K1 cells, a large number of cells (more than 30%) had a round form and retracted cell extensions as if they were in the process of collapsing and detaching (*not shown*). The reason for this is not known.

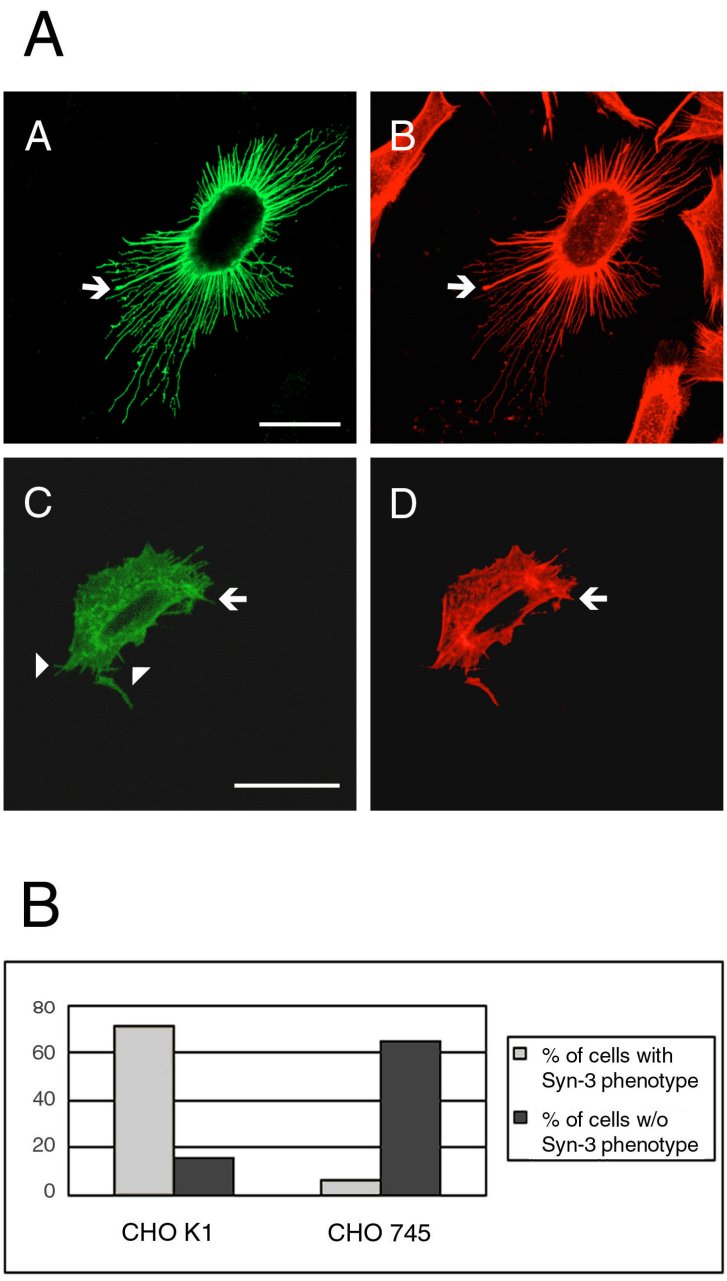

Figure 3.18: ***The lack of sugar chains inhibits the formation of filopodia-like structures*****. (Panel A) Transfection and immunocytochemistry with anti-syndecan-3 (A,C) antibody was performed as described in fig. 3.14. Actin was stained with TRITC-conjugated phalloidin (B,D). In CHO K1 cells, the effect of FL syndecan-3 was clearly seen (A) in the rearrangement of the actin cytoskeleton (B), which co-localized with the syndecan-3 protein (arrows). Most of transfected CHO 745 cells (C,D) only developed microspikes (arrowheads). Very few cells showed a typical syndecan-3 phenotype, although co-localization with actin was also observed (D; arrows). Results are representative of three independent experiments. Bars: 20 mm. (Panel B) Transfected cells expressing the described phenotype were quantified. About 700 CHO K1 cells and 150 CHO 745 cells were counted in three independent experiments. Results are expressed as percentage of cells showing an effect after transfection with FL syndecan-3 DNA, in respect to the total number of transfected, syndecan-3 positive cells. The quantitative analysis demonstrates the importance of sugar chains for the induction of the syndecan-3 phenotype.**

3.4.4. Implication of the intracellular domain in the induction of the phenotype

3.4.4.1. Production of different cytoplasmic deletion mutants of syndecan-3

In order to study the implication of the C-terminal domain in the induction of filopodia, different deletion constructs were generated (***see fig. 3.19, Panel A and B***). These will be further used for transient transfection studies and the generation of stable cell lines.

A

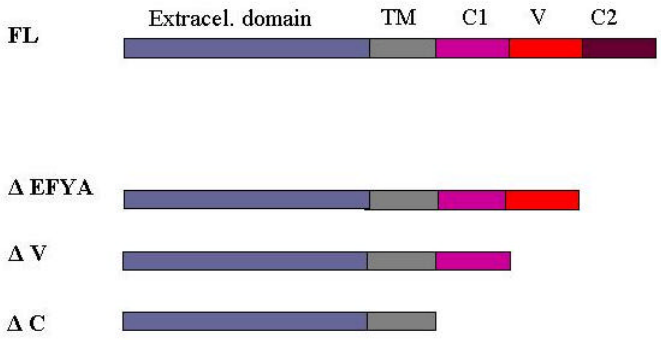

B

```
1201  AAGGAGGTGCTCGTAGCTGTGATTGTGGGCGGGGTGGTGGGCGCCCTCTT
        K  E  V  L  V  A  V  I  V  G  G  V  V  G  A  L  F
1251  TGCTGCCTTCTTGGTCACACTGCTCATCTATCGTATGAAGAAAAAGGATG
        A  A  F  L  V  T  L  L  I  Y  R  M  K  K  K  D
1301  AGGGCAGCTACACGCTGGAGGAACCCAAGCAGGCGAGCGTCACATACCAG
      E  G  S  Y  T  L  E  E  P  K  Q  A  S  V  T  Y  Q
1351  AAGCCTGACAAGCAGGAGGAGTTCTATGCCTAG
       K  P  D  K  Q  E  E  F  Y  A  *
```

Figure 3.19: ***Cytoplasmic deletion variants of syndecan-3.*** **(A) Cartoon of constructs; (B) Corresponding sequences of deleted cytoplasmic tail of syndecan-3. Deleted sequences are represented in bold for DC = deletion of entire cytoplasmic domain, single underlined for DV = missing V- and C2-region and double underlined for DEFYA = missing EFYA motif which interacts with PDZ proteins. Transmembrane domain is shown in italic. Asterisk labels STOP codon.**

A PCR-based strategy (***see fig. 3.20***) using internal primers was performed, producing C-terminal fragments, which contained cytoplasmic deletions further used to substitute the corresponding sequence of the FL-syndecan-3. The corresponding sequence of the FL-syndecan-3 in pcDNA3 was cut out and substituted with the three different fragments respectively. Selection for positive clones was performed by enzymatic digest with *Sma*I. The enzyme cut twice in negative clones while in those clones that contained the fragment in right orientation, an additional *Sma*I recognition site was restored. Therefore all digests that generated three fragments were checked by sequencing.

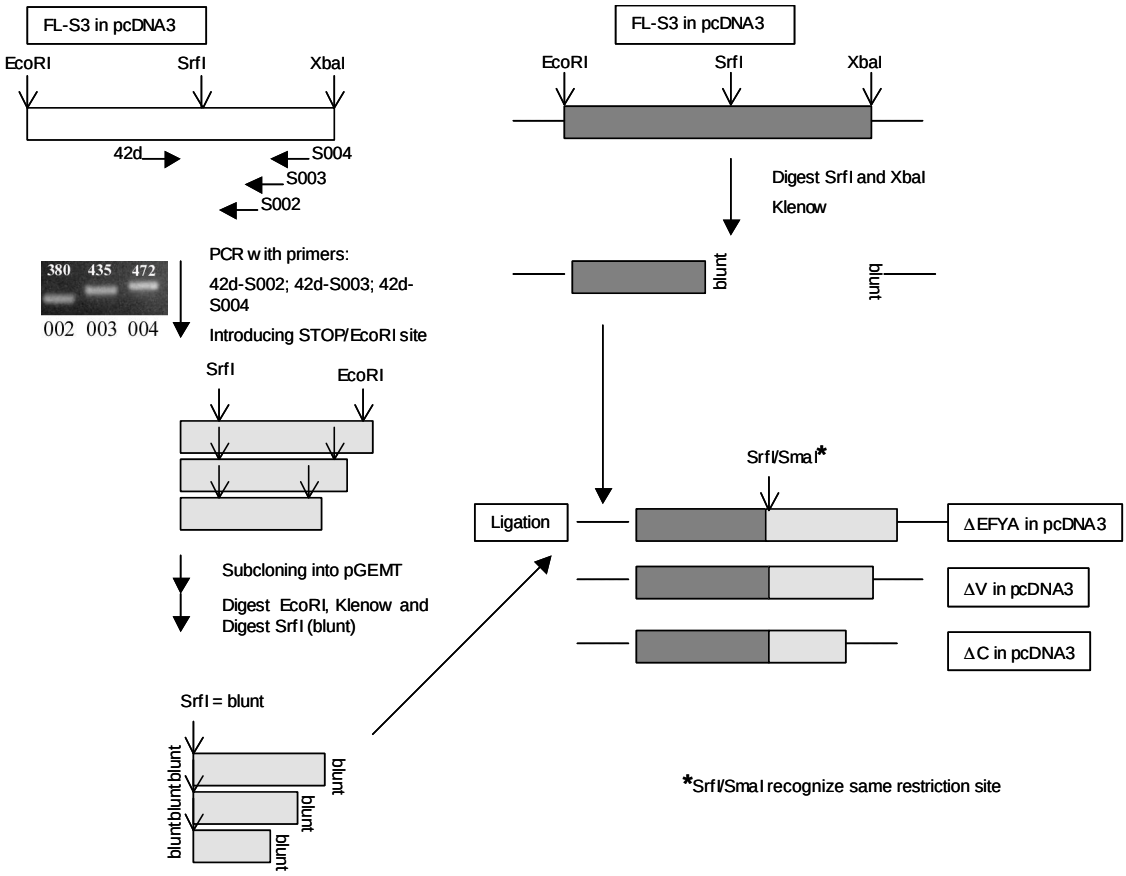

Figure 3.20: ***Strategy to obtain different cytoplasmic deleted variants of syndecan-3.*** **First, a PCR was performed with a common forward primer (42d) and the three primers (S002, S003, S004), which produced shorter cytoplasmic fragments. Primers introduced a stop-codon and an *Eco*RI restriction site for further sub-cloning. These PCR fragments were sub-cloned into pGEMT, cut out with *Eco*RI/*Srf*I and treated with Klenow polymerase to obtain blunt ends. Finally these blunt end fragments were used to substitute the corresponding sequence of FL-syndecan-3 in pcDNA3 (FL-S3).**

Positive clones obtained for each construct are shown in ***fig. 3.21 (Panel A-C)***. From 24 distinct plasmid DNA minipreparations, 4, 1 and 2 positive clones were obtained for ΔC, ΔV and ΔEFYA respectively. All positive clones were sequenced. Sequence analysis revealed that Δ**C #15,** Δ**V #17** and Δ**EFYA #1** had correct sequences and were therefore used for further experiments.

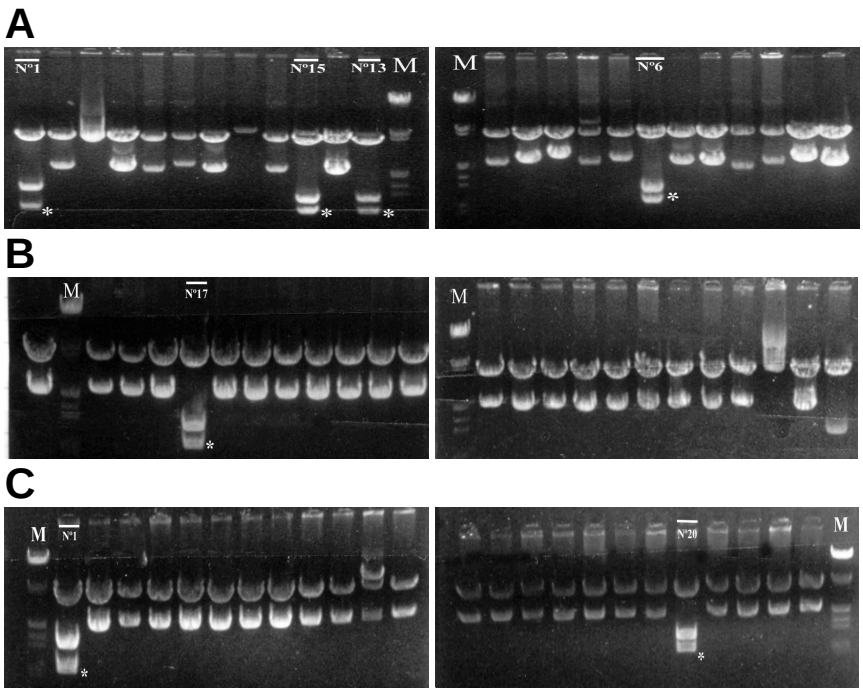

Figure 3.21: ***Digest detects positive clones*****. Plasmids were digested with *Sma*I. Positive clones presented three *Sma*I restriction sites. 4, 1 and 2 positive clones (indicated by asterisks) were obtained for Δ**C **(Panel A),** Δ**V (Panel B) and Δ**EFYA (Panel C) respectively.**

3.4.4.2. Characterization of CHO K1 cells transiently transfected with cytoplasmic deleted syndecan-3 constructs

To obtain further insight into the functions of the different microdomains of the cytoplasmic tail of syndecan-3, the above-described C-terminal deletion constructs of syndecan-3 were transiently transfected into CHO K1 cells. The phenotype generated by the different constructs was analyzed by immunocytochemistry and confocal microscopy (***see fig. 3.22***) and SEM (***see fig. 3.23***).

As shown in ***fig. 3.22***, all protein variants were properly expressed and delivered to the cell membrane since the syndecan-3 protein could be detected without permeabilizing cells. This suggested that the cytoplasmic region of syndecan-3 was not necessary for delivery to the PM.

Further analysis revealed that the transient transfection of ΔV or ΔEFYA constructs led to the generation of long filopodia similar to those already described for FL transfection. In contrast, only very few cells made long filopodia after ΔC transfection. Indeed, among these cells only an increase of microspikes on the cell surface was seen in comparison with the control-transfected cells. Furthermore, in some of the ΔV and many of the ΔEFYA transfected cells, another morphological change was observed: the generation of bubble- or mushroom-like structures covering the cell surface, strongly labeled by the syndecan-3 antibody and for actin. The function and composition of these structures is unknown but they are reminiscent of “blebs” (***see 4.2.3.4***).

SEM analysis revealed in more details the fine structure of transfected cells. ***Fig. 3.23*** shows that cells transfected by the control vector contained surface structures such as short microspikes, as did the cells transfected with the ΔC variant. The FL, ΔV and the ΔEFYA transfected cells presented very long and/or abundant filopodia, additionally to microspikes. ***Fig. 3.24*** shows the specific phenotype obtained by ΔEFYA transfection in more details: ΔEFYA transfection led to the generation of “bubble”- or “mushroom-like” structures (***white arrowheads***), emerging from the cell surface. These structures do not represent intracellular vesicles or vacuoles but rather membrane extrusions (***black arrows***).

Taken together, these results indicate that syndecan-3 induced the re-organization of the actin cytoskeleton and that the cytoplasmic tail was involved in this effect. As the removal of neither the C2 region (EFYA) nor the V-region prevented the generation of filopodia, we conclude that the interaction with intracellular partners occurs through the C1-region.

These data exclude some and favor other proteins to be implicated in the filopodia-outgrowing process (***see 4.2.3***). The “mushroom-like” structures found in ΔEFYA-transfected cells indicate that a process other than the filopodium-generating effect of syndecan-3 was induced (***see 4.2.3.4***).

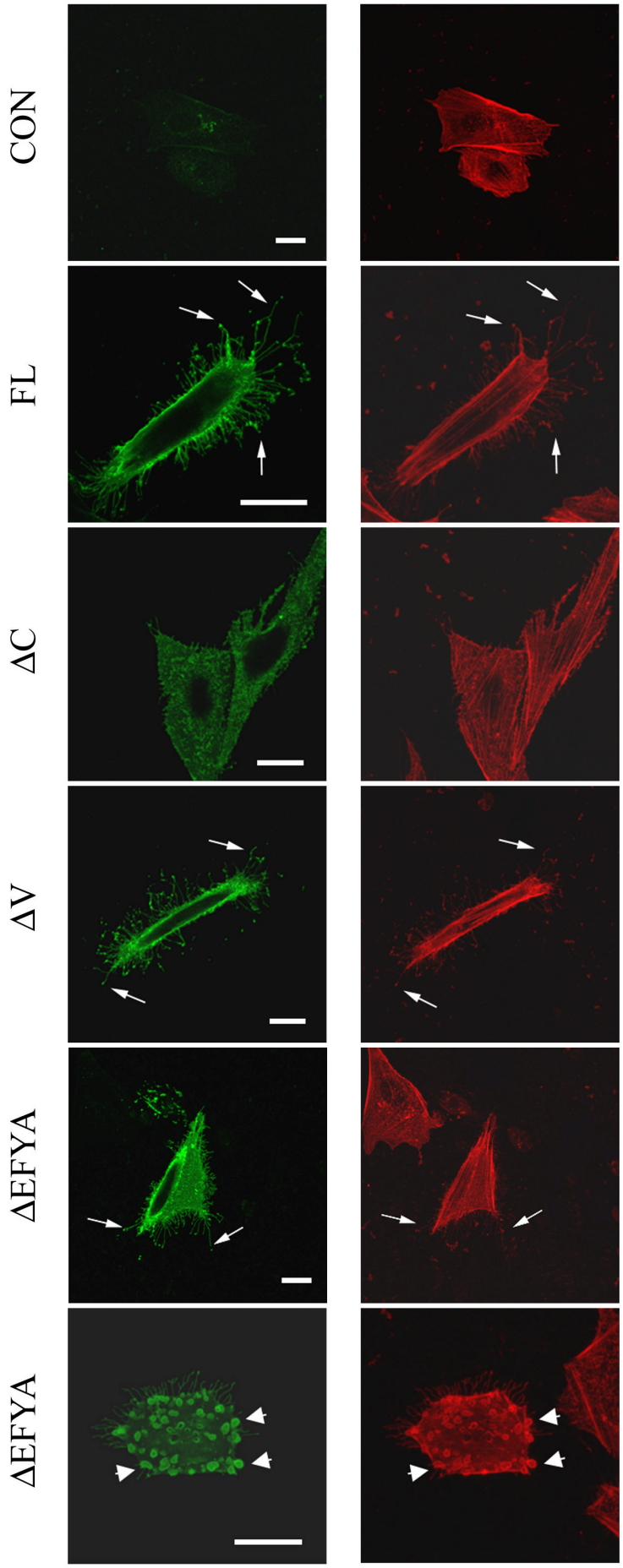

Figure 3.22: ***Transfection of cytoplasmic deleted syndecan-3 generates different phenotypes*****. Analysis of CHO K1 cells transiently transfected with C-terminal deletions of syndecan-3 by immunocytochemistry and confocal microscopy. Upper panel (green) shows anti-syndecan-3 staining (Clever, 1:2000) and lower panel actin labeling by TRITC-conjugated phalloidin (red). CON = control, FL = full-length syndecan-3, ΔC = syndecan-3 w/o cytoplasmic domain, ΔV = syndecan-3 missing V- and C2-region of cytoplasmic domain, ΔEFYA = syndecan-3 missing motif EFYA of cytoplasmic region. Arrows mark filopodia, arrowheads "bubble-like" structures. Bars = 20 µm.**

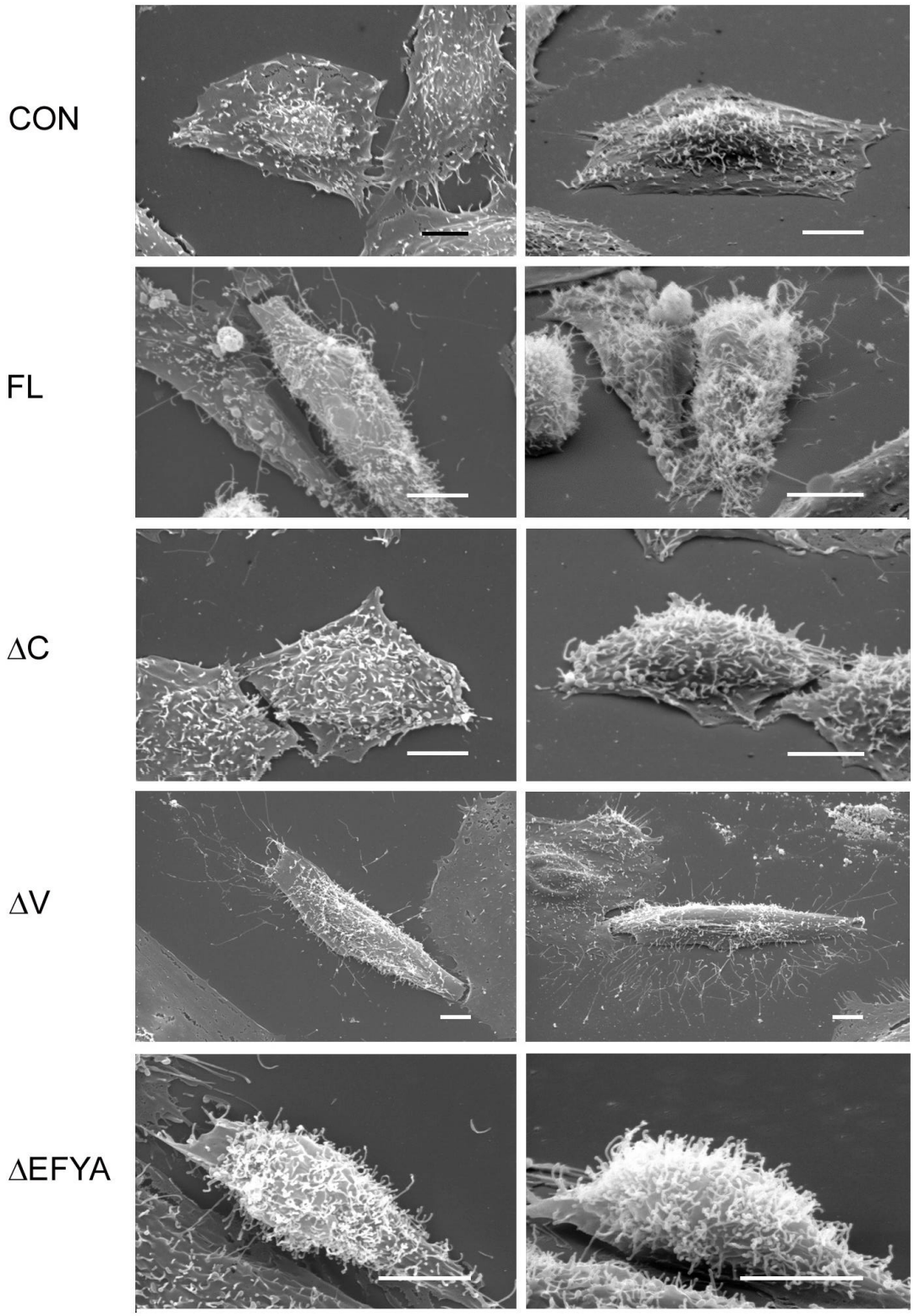

Figure 3.23: ***Transfection of cytoplasmic deleted syndecan-3 generates different phenotypes.*** **Analysis of CHO K1 cells transiently transfected with C-terminal deletions of syndecan-3 by SEM. CON = control, FL = full-length syndecan-3, ΔC = syndecan-3 w/o cytoplasmic domain, ΔV = syndecan-3 missing V- and C2-region of cytoplasmic domain, ΔEFYA = syndecan-3 missing motif EFYA of cytoplasmic region. Bars = 5 µm.**

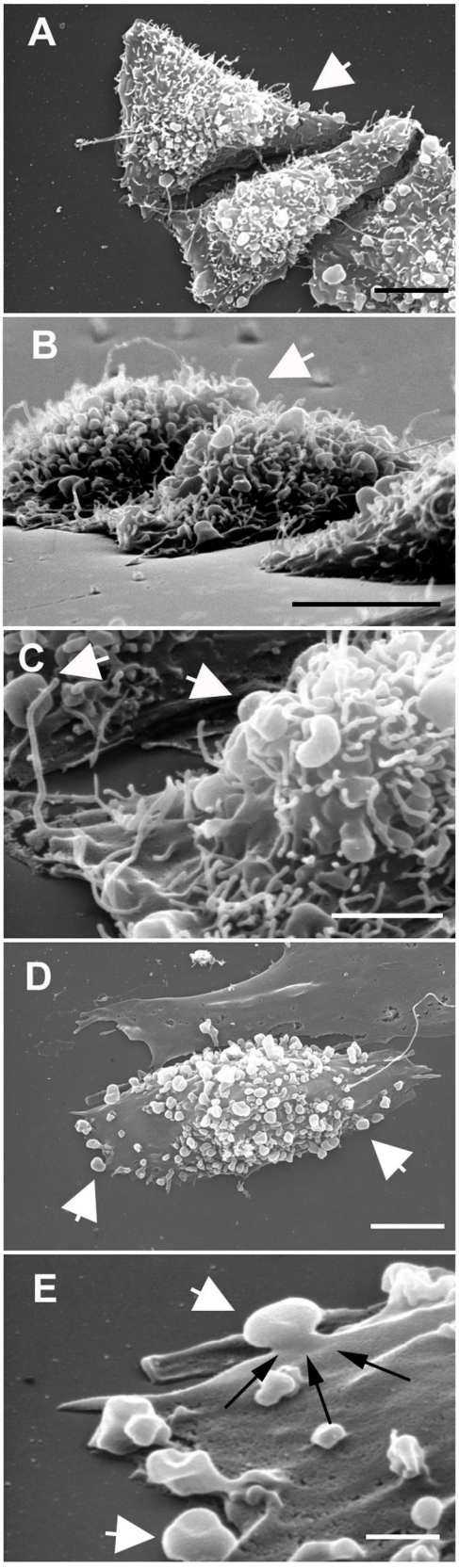

Figure 3.24: ***The transfection of the DEFYA generates an additional distinct phenotype*****: SEM-analysis of CHO K1 cells transiently transfected with EFYA-deleted syndecan-3. Bars = 5 µm (A,B,D), 2 µm (C) and 1 µm (E). White arrowheads indicate membrane exvaginations. Black arrows show the connection between these structures and the plasma membrane.**

3.5. Study of the involvement of syndecan-3 in the regulation of the actin cytoskeleton

3.5.1. Generation and selection of syndecan-3-stable transfectants

To examine the role of the cytoplasmic domain in the action of syndecan-3, stable cells lines were produced. Therefore we selected CHO K1 cells, which do not express endogenous syndecan-3. We generated clones containing the pcDNA3 vector without insert (CON), with the FL human syndecan-3 cDNA (S3) and with syndecan-3 without cytoplasmic tail (DC).

We obtained 24 (S3), 27 (DC) and 12 (CON) clones, which were further screened for syndecan-3 expression by immunofluorescence and Western blot analysis.

Western blot analysis of the immunofluorescence-syndecan-3 positive clones revealed that all FL and cytoplasmic-deleted clones (except one) expressed syndecan-3 (***see fig. 3.25***). After Heparitinase/ChABC digest, syndecan-3 was detected with 3G10 antibody as a clear band at approx. 120 kDa that was absent in control transfected cells (***see fig. 3.26***).

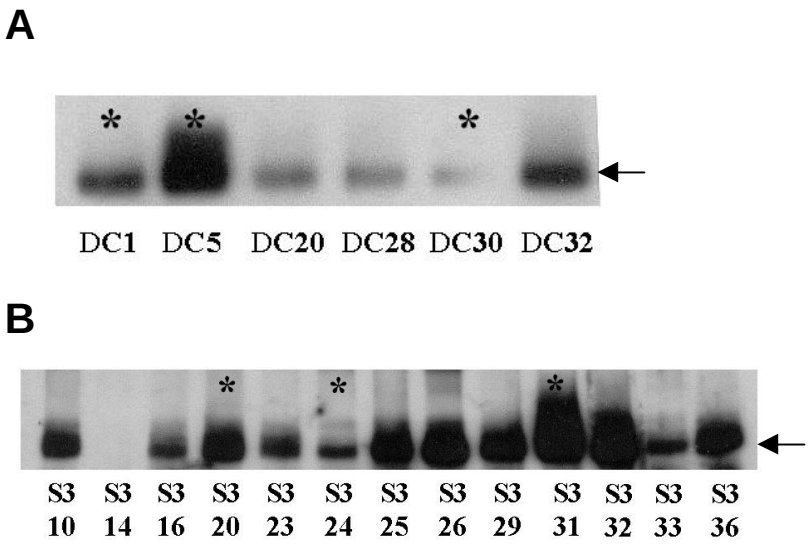

Figure 3.25: ***Clones express varying amounts of syndecan-3*****. Western blot analysis of six C-terminal deleted (Panel A) and thirteen S3 FL (Panel B) clones. 10 mg protein was digested with Heparitinase/ChABC. 3G10 antibody detects digested HSPGs. All clones expressed S3 (except for S3 14), indicated by an arrow. Three clones of both constructs with distinct expression levels were selected for further characterization (see asterisks). Note that expression levels cannot be compared between those two Westerns blots due to different film exposure times.**

As observed, expression levels varied among clones. Three clones, corresponding to low, middle and high levels of expression, were selected for each construct for further characterization (***see fig. 3.25, asterisks***).
Clones CON 10 and 13 (***see fig. 3.26***), DC 1, 5 and 30 (***see fig. 3.25, Panel A***) and S3 20, 24 and 31 (***see fig. 3.25, Panel B***) were selected from control, cyto-deleted and FL-syndecan-3 transfectants respectively.

3.5.2. Phenotypic characterization of stable transfectants

After selection, clones were first analyzed for their morphological and biochemical characteristics.

3.5.2.1. Morphology

Phase contrast microscopy was performed to study possible morphological differences among the clones (***see fig. 3.26, Panel A***). ***Fig. 3.26*** shows also the results of the immunocytochemistry performed with anti-syndecan-3 antibody (***Panel A***) and the Western blot analysis with 3G10 (***see fig. 3.26, Panel B***).

In phase contrast microscopy, differences were observed in transfectants presenting highest expression levels. Indeed, DC 5 cells were bigger and flatter and S3 31 cells showed a slightly elongated form. In immunocytochemistry experiments, all selected clones showed slightly (S3 20 and S3 24) or considerably higher (DC 1, DC 5, DC 30 and S3 31) labeling. The level of labeling was correlated to the intensity of the bands detected by Western blot analysis.
Highest expression levels and best membrane staining were detected for DC 5 and S3 31, which were selected for further experiments. As control, two mock-transfected clones (CON 10 and 13) were pooled (= CON MIX) and used as control for further characterization.

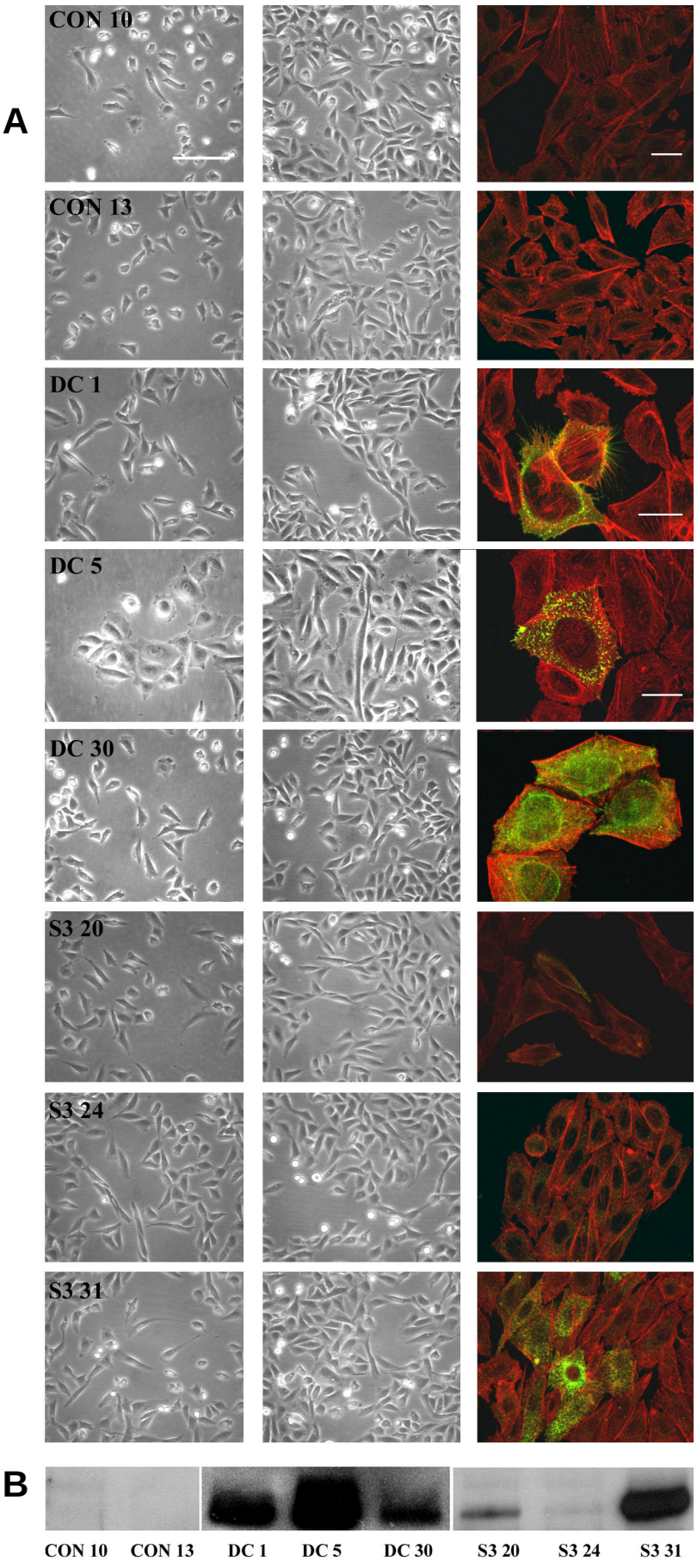

Figure 3.26: ***Characterization of clones by phase contrast microscopy, confocal microscopy and Western blot.*** **(Panel A) First two vertical panels show phase-contrast microscopy images of clones at low and high density. The DC clones, especially DC 5, were flatter and larger than control cells. Some cells among the FL-clones had a more elongated form, but bore greater resemblance to the control cells. Right panel shows confocal microscopy analysis of immunocytochemistry with anti-syndecan-3 antibody (Clever, 1:300, green) and FITC-labeled swine anti-rabbit IgG. Actin was labeled by TRITC-conjugated phalloidin (red). (Panel B) Levels of syndecan-3 expression in immunocytochemistry reflects levels of protein expression detected by Western blot with 3G10 after Heparitinase/ChABC digest. 10 µg protein was loaded per lane. Bars, 100 ㎜ for phase contrast microscopy and 20 ㎜ in confocal images. All fluorescent images have the same scale as the first image, if not indicated by another bar.**

Figure 3.27: *DC 5 cells form multi-layers at confluence*. Phase contrast microscopy of semi-thin sections from cells grown on gold grids until confluence, fixed and stained with methylene blue. DC 5 cells are larger and flatter than CON MIX and S3 31 cells.

Phase contrast microscopy analysis was performed on methylene blue-stained semi-thin sections from confluent cultures of each transfectants, ***see fig. 3.27***. As observed, DC 5 cells form a multi-layer while CON MIX and S3 31 do not.

3.5.2.2. Cellular distribution of syndecan-3

Immunocytochemical analysis performed without permeabilization on DC 5 and S3 31 clones (***see fig. 3.26***) revealed membrane staining, thus demonstrating that FL- as well as cytoplasmic deleted syndecan-3 reached the plasma membrane. This confirms results obtained from the transient transfection experiments described in ***3.4.4.2***. To obtain further evidence of the cellular distribution of syndecan-3 in our transfectants, cellular fractionation by using a differential extraction method was performed. Based on TX-100 detergent differential solubility, different cellular protein fractions are obtained, corresponding to the cytoplasmic proteins, the membrane-associated but not cytoskeleton-associated proteins (TX-100 soluble) and the cytoskeleton-associated proteins (TX-100 insoluble, but SDS soluble).

As observed in ***fig. 3.28***, the syndecan-3 band was exclusively detected in the membrane (TX-100-soluble) fraction. The absence of syndecan-3 in the fraction of proteins associated with the cytoskeleton (***see fig. 3.28, Panel A***) (TX-100-insoluble fraction) remained questionable. Indeed, tests with Heparitinase/ChABC revealed that the activity of this enzyme was totally inhibited by the presence of as low as 0.02% SDS (***see fig. 3.28, Panel B***). Therefore we cannot rule out that syndecan-3 was also present in the TX-100 insoluble fraction of the cytoskeleton-associated proteins.

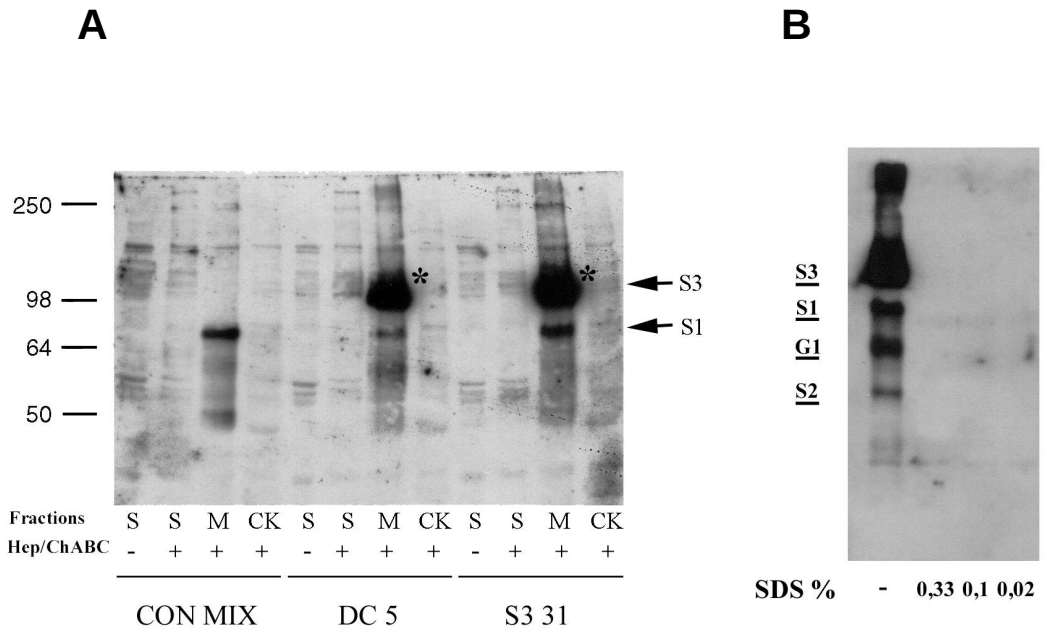

Figure 3.28: (A) ***Syndecan-3 was detected in the TX-100 soluble fraction*** **in cell fractionating experiments, which corresponds to the membrane-associated (but not cytoskeleton-associated) proteins (M). It was not found in the cytoplasmic fraction (S) nor in the TX-100 insoluble fraction containing proteins associated with the cytoskeleton (CK). Western blot was performed with 3G10 antibody after Heparitinase/ChABC digest (+/-). 20 mg was loaded per lane. One of two identical experiments is shown.**
(B) ***SDS inhibits Heparitinase/ChABC digest*****. 20 mg of the TX-100-soluble fraction of clone DC 5 was digested in the absence (-) or presence of SDS at indicated concentrations. 0.33% mimics the concentration of SDS present in the TX-100-insoluble fraction of the experiment shown in A. Western blot was performed with 3G10 antibody. The experiment shows that even at low concentrations SDS inhibits the action of the enzymes. S1 = syndecan-1, S2 = syndecan-2, S3 = syndecan-3, G1 = glypican-1.**

3.5.2.3. Cell diameter and volume

To quantify phenotypic differences observed in phase contrast microscopy, flow cytometer analysis was performed (***see fig. 3.29***). Our aim was to examine whether cells from the DC 5 clone were significantly larger than CON MIX and S3 31 cells. Consistently, the mean volume of clone DC 5 cells was about 20% larger than cells of the other two clones. Cells from the CON MIX and S3 31 clones had the same volume (***see fig. 3.29, Panel C***).

A

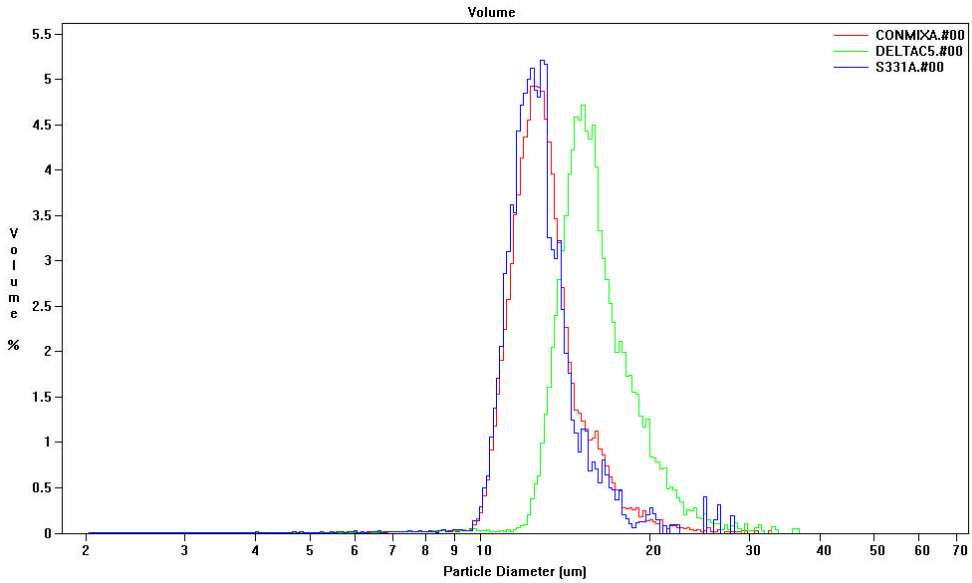

B

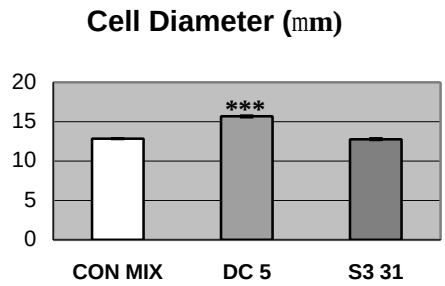

C

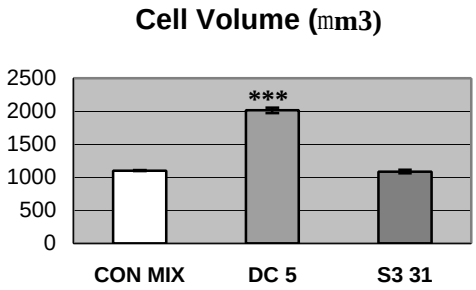

Figure 3.29: ***Cells from clone DC 5 are significantly larger than CON MIX and S3 31 cells*****. Determination of cell size (A,B) and volume (C) by flow cytometer analysis. At least 1.5x10^5 cells were counted each time (n=3). The counts of two experiments were pooled and analyzed comparing the means of each experiment (***p<0.05).**

3.5.2.4. Electron microscopy studies

Further enlargement of TEM pictures also demonstrates that DC 5 cells are flatter and larger than control cells. However, the S3 31 cells were also larger, but not to the extent of DC 5, ***see fig. 3.30***.

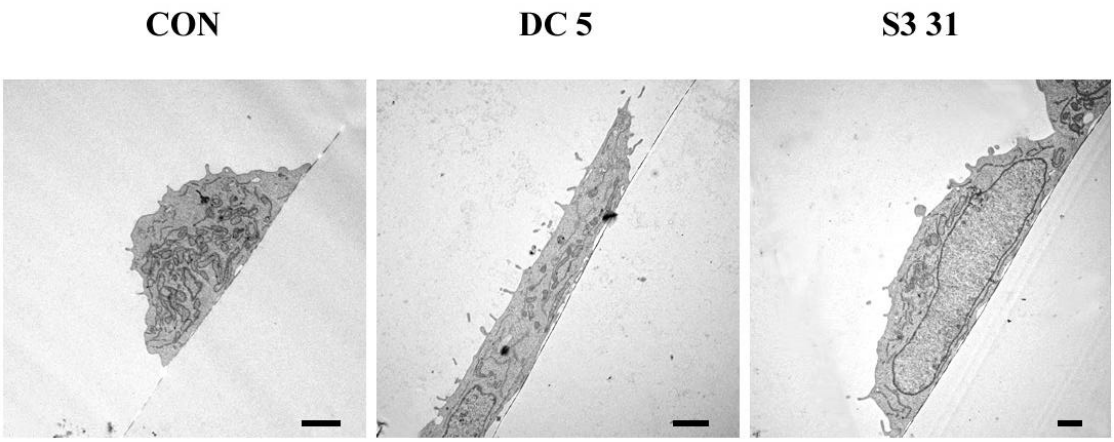

Figure 3.30: ***DC 5 cells are flatter and larger than control cells*****. TEM of sub-confluent cultures from transfectants. Bars: 1 mm (CON and S3 31) and 2 mm (DC 5).**

3.5.3. Functional characterization

The larger and flatter cells found in the DC 5 clone suggested that this clone might show stronger adhesion, while the slightly elongated morphology of the S3 31 clone rather suggested a more migratory phenotype. Therefore, in order to obtain further insight into the effect of syndecan-3 expression on cell behavior, proliferation, adhesion and migration assays were performed.

3.5.3.1. Proliferation

Cells were counted or stained with crystal violet (*not shown*) and by counting. In the crystal violet assay, the absorbency obtained at 12 h in culture was set as 1. Thereby seeding errors were minimized. This was also necessary, since cells of clone DC 5 showed higher absorbance value because of their size, which masked their decreased proliferation rate at short periods. When transfectants were analyzed for their ability to proliferate (***see fig. 3.31***), no significant difference was found between the CON and the S3 31 cells, although S3 31 grew slightly more slowly. In contrast, DC 5 cells showed a significantly lower proliferation rate.

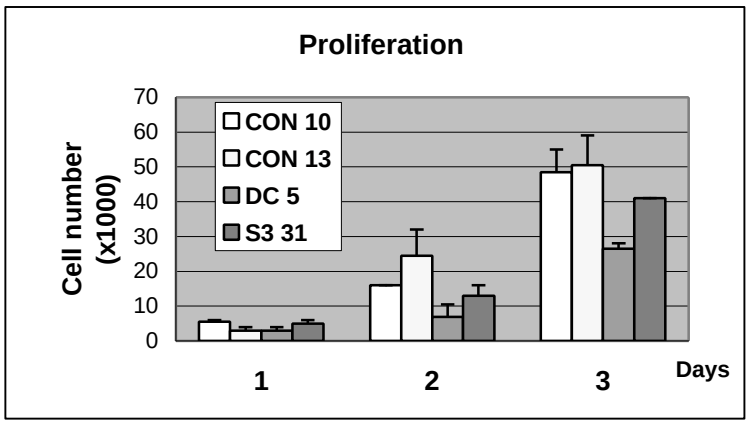

Figure 3.31: *DC 5 cells proliferated more slowly*. Proliferation measured by cell counting. 10^4 cells were seeded in 24-well plates, trypsinized and counted after 1, 2 and 3 days in culture, n=3. One of two representative experiments is shown.

3.5.3.2. Adhesion

In order to study the function of syndecan-3 in cell-substrate attachment, transfectants were seeded and allowed to attach for two hours. Cells were then stained with crystal violet and absorbance at 630 nm was measured (***see fig. 3.32***). Cells from the DC 5 and from the S3 31 clone adhered significantly more strongly to the substrate than control cells. On the other hand, significantly higher absorbance values were obtained for DC 5 than for S3 31 cells. This is consistent with the findings that cells are bigger and therefore cover a larger area.

To assess whether the adhesion properties of the transfectants depended on sugar chains or on the substrate, adhesion experiments in the presence of heparin and on different matrices respectively were performed (*not shown*). On different coatings (BSA/collagen/FN at 10 µg/ml), no significant differences were obtained compared with adhesion to BSA or plastic, which suggested that adhesion was not substrate-specific. Heparin did not inhibit the adhesion of the DC 5 clone to collagen at the concentrations used (up to 10 U/ml), which suggests that the increase in adhesion in the transfectants does not (merely) depend on the GAG chains.

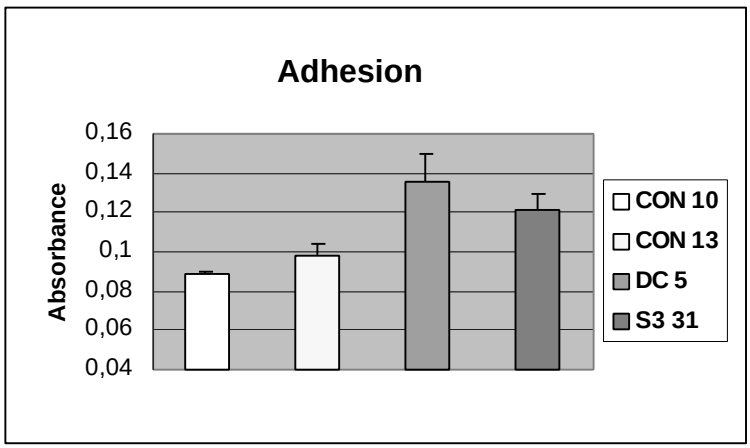

Figure 3.32: *Both syndecan-3 expressing clones showed stronger adhesion*. 10^6 cells were seeded into 24-well plates and stained with crystal violet after 2 h (n=3). One representative of three independent experiments is shown.

3.5.3.3. Migration

In order to establish the role of syndecan-3 in migration, wound–healing experiments were performed, ***see fig. 3.33, Panel A***. With the help of a tip, a small wound was scratched into a confluent cell layer of each clone. Images were taken after various time points to monitor the closing of the wound. The decrease in wound surface area per time was calculated. Quantification is shown in ***fig. 3.33, Panel B***.

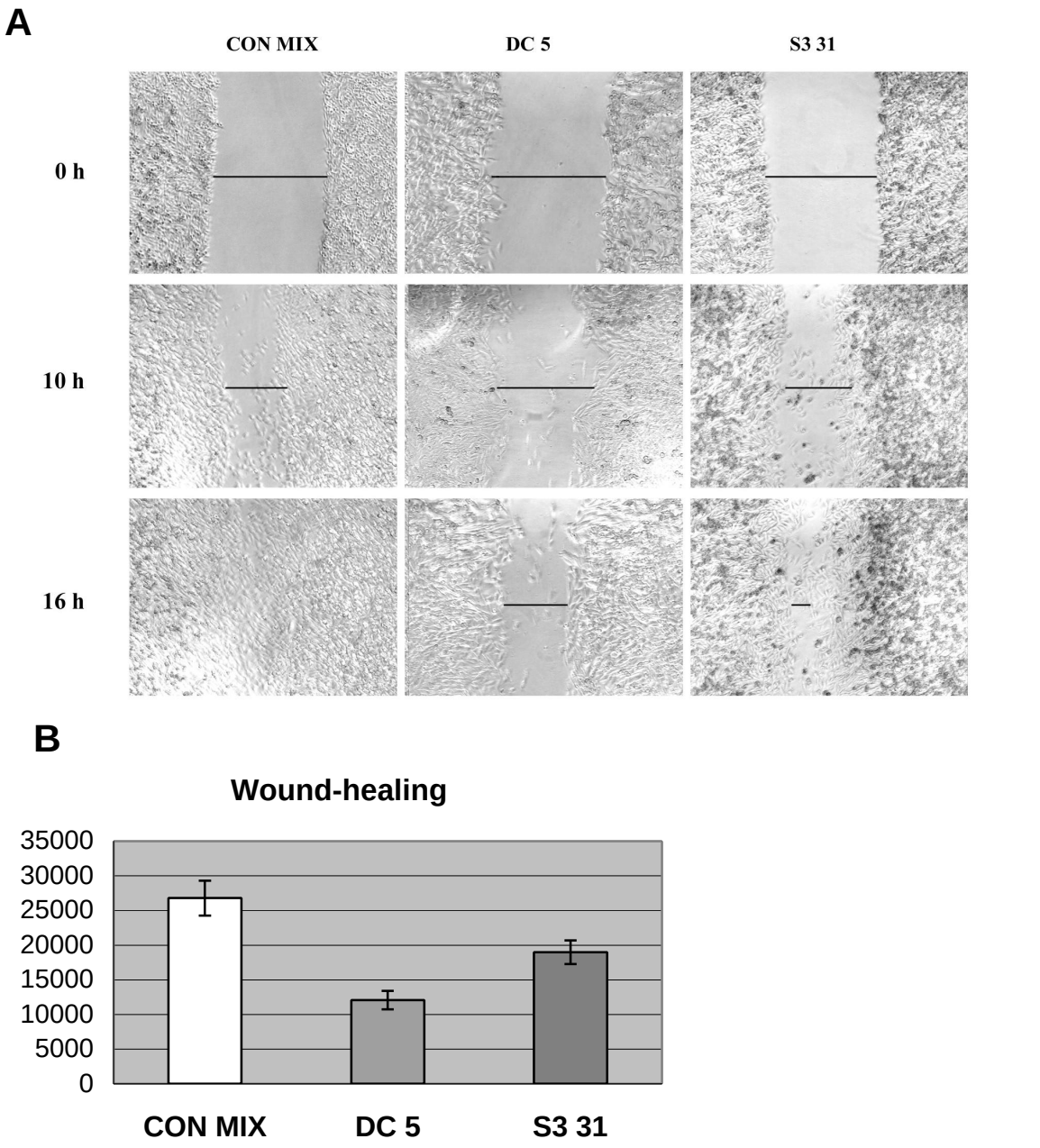

Figure 3.33: ***DC 5 cells were significantly slower in wound-healing assays*****. (A) The CON MIX and the S3 31 cells closed the wound more rapidly (approx. 16 h) than the DC 5 cells. (B) To quantify the effect, the decrease in wound surface area per time was calculated (x-axis: Decrease of pixels/time). One of three experiments is shown: n=3 for each experiment.**

Wound-healing assays (***see fig. 3.33, Panel A*** and ***B***) revealed that the S3 31 cells closed the wound slightly more slowly than the CON MIX, although the difference was not significant among all experiments. In contrast, the DC 5 cells were significantly slower in closing the wound than the CON MIX cells.

The results of the functional studies are consistent with observations in the morphology analysis. The cells from the S3 31 clone behaved like the CON cells in proliferation and migration and adhered slightly more strongly to the substrate. In contrast, DC 5 cells showed strong morphological and functional differences in all experiments: DC 5 cells are bigger, adhere more strongly to the substrate and migrate more slowly. This suggests that the deletion of syndecan-3 cytoplasmic tail affects the cytoskeleton, thus changing the functional properties of stably transfected cells.

3.5.4. Molecular mechanisms of syndecan-3 induced re-organization of the cytoskeleton

To obtain further information about the possible molecular mechanisms linking between phenotypic effects observed and the actin cytoskeleton in stable transfectants, we examined cell-matrix adhesion structures, the small GTPases, the kinases FAK and src and the ERM family.

3.5.4.1. Study of cell-adhesion structures

Phenotypic differences the cells from the DC 5 and the S3 31 and CON MIX clones related to their cell-substrate adhesion properties prompted us to look at FAs and SFs.

By analyzing the images obtained by confocal microscopy from immunocytochemistry experiments with antibodies against the FA proteins vinculin, paxilin, talin and TRITC-conjugated phalloidin (labeling actin cytoskeleton), it can be observed that DC 5 cells formed more FAs and thicker and more abundant SFs (***see fig. 3.34***). This was in accordance with the results obtained by phase contrast microscopy and functional adhesion assays, where DC 5 cells seemed to adhere mores strongly than the CON MIX and the S3 31 clone.

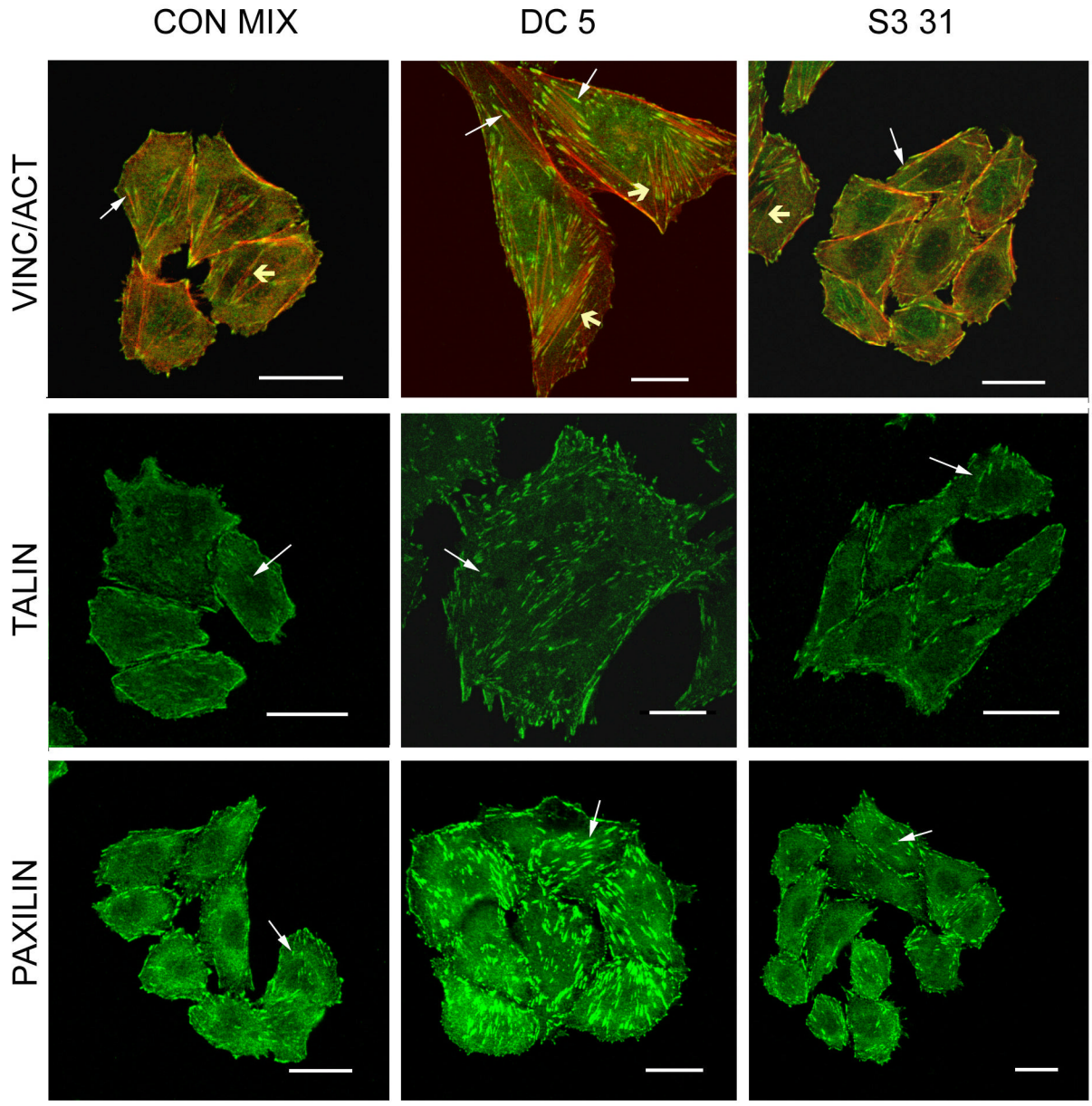

Figure 3.34: ***DC 5 cells present more focal adhesions correlated with the presence of thicker and more abundant stress fibers.*** **Immunocytochemical analysis of transfectants by confocal microscopy. Figure shows staining of FAs and actin SFs by labeling with anti-vinculin (Vinc), anti-talin and anti-paxilin (green) and corresponding FITC-conjugated secondary antibodies. Actin was labeled by TRITC-conjugated phalloidin (Act, red). Bars = 20 ㎛.**

3.5.4.2. Role of small GTPases

The small GTPases have been implicated in the organization of the actin cytoskeleton (***see 1.8***). Since transient transfection of syndecan-3 provoked the outgrowth of long filopodia, as previously described for syndecan-2 (Granes et al., 1999) an implication of cdc 42 GTPase in this process was suggested.

Therefore “pull-down” experiments were performed with lysates of CHO K1 syndecan-3 transiently transfected cells as described in ***2.8.2***.

As positive control, COS-1 cells were transfected with dominant positive cdc 42 V12and lysed. The lysate was incubated with beads bound to the substrate of active cdc 42, the binding domain of PAK (p21-activated kinase). Western blot analysis was performed using α-cdc 42 antibodies.

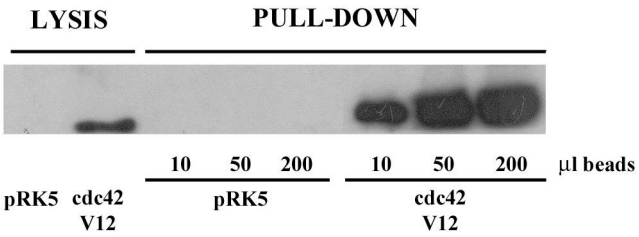

Figure 3.35: ***Positive control of the GTPases “pull-down” assay for cdc 42.*** **1.5 x 10^6 COS-1 cells were plated and transiently transfected with dominant positive cdc 42 V12 or control vector Prk5 by the DEAE-method. “Pull-down”-assay was performed as described in 2.8.2. Western blot was performed with anti-cdc 42 antibody (1:500). Different bead volumes were used in order to “pull-down” active cdc 42 of the lysate.**

In ***fig. 3.35*** anti-cdc 42 antibody specifically recognized cdc 42 in the dominant positive transfectants while in the mock-transfected cells the endogenous amount of cdc 42 was under detection limit. Cells transfected with cdc 42 V12 showed strong bands in the pull-down experiments, which were not seen in control cells. 10 µl of beads already pulled-down a high percentage of the active cdc 42. Nevertheless 50 µl of beads was necessary to pull-down the whole amount. Between 50 µl and 100 µl of beads there was no difference.

Nevertheless, when we performed the experiment with transiently transfected CHO K1 cells, activation of cdc 42 was hardly detected (*not shown*). These experiments might be repeated with another cell line, which can be transfected easily in high scale (COS-1) or by increasing activation in CHO K1 transient transfectants.

To further study the effect of syndecan-3 on cdc 42 activation, we performed the same experiments with cells from the clones CON MIX, DC 5 and S3 31 although they did not present the same morphological changes as the transient transfectants. Therefore, semi-confluents cultures were lysed after two days in culture. The whole volume of lysis was determined and, except for 20 µl, incubated with substrate-loaded beads. Western blot analysis against anti-cdc 42 was performed with the 20 µl of total lysate and the beads. Bands were scanned (Scan Wise and Quantity One, both under Microsoft Windows) and their intensity was measured. The percentage of active cdc 42 was calculated as follows:
% of active GTPase = Value of band corresponding to active cdc 42/(Volume of total lysis of cdc 42 incubated with beads x intensity of 20 µl total lysis/ 20 µl).

Surprisingly, as shown in ***fig. 3.36***, cdc 42 was more active in lysates of the DC 5 clone than of the control (8%) and of the S3 31 clone (17%). These results were unexpected, since this GTPase has been implicated in the generation of filopodia and, in general, it contributes to a more migratory phenotype (***see 1.8***). Nor did we see more filopodia nor an increase in migration for cells from the DC 5 clone. It might be possible, that in stable cells, active cdc 42 contributes to the generation of lamellipodia via Rac-activation (***see 1.8***). This would be consistent with observations made in experiments with ERM protein, where DC 5 cells presented stronger

labeling in lamellipodia than CON MIX and S3 31 cells (***see fig. 3.39***). Nevertheless, the experiments shown above have to be repeated and to be performed under different conditions, which will be discussed later (***see 4.3.3.5***).

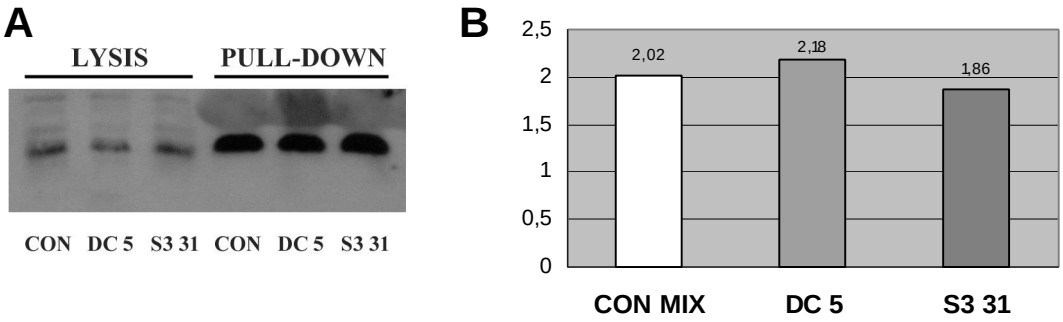

Figure 3.36: ***Cdc 42 activity is increased in DC 5 cells*****. Semi-confluent cells were lysed after two days in culture and lysates were incubated with PAK-loaded beads as described in 2.8.2. (A) Western blot analysis was performed with 20 µl of total lysates and SN of the beads from the pull-down assay. (B) Graph shows activated cdc 42 (pull-down) versus total GTPase (lysis) in percent corrected for volume differences obtained for each transfectant.**

Cells from the DC 5 clone presented stronger adhesion to the substrate and a higher number of FAs and SFs. Rho A activation has been associated with SF formation and regulation (Ridley and Hall, 1992), ***see also 1.8***. For this reason we studied in parallel by “pull-down” experiments on the corresponding lysates the possible activation of Rho A among our transfectants.

Experiments were performed with confluent cells and analyzed the same way as described above for the assays with cdc 42 with the only differences that the substrate bound to the beads was the binding domain of Rho A substrate C21/Rhotekin, ***see fig. 3.37***.

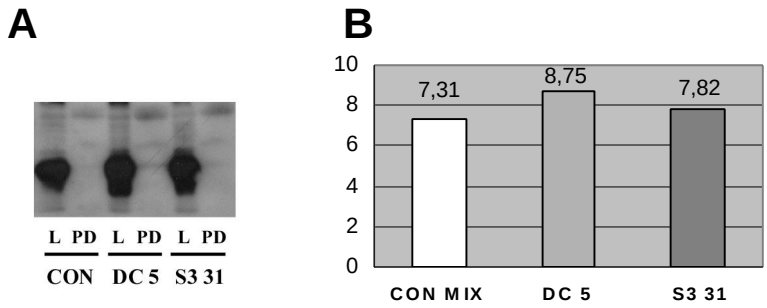

Figure 3.37: ***Rho A activity is increased in syndecan-3 expressing clones.*** **Experiment was performed as described above, but with confluent cells, C21-loaded beads and 400 µl lysates per assay. Due to very low levels of Rho A activity, the lysates and the pull-down bands were scanned independently. Therefore the values do not directly represent the percentage of activated Rho A.**

As shown in ***fig. 3.37*** the small GTPases Rho A was more active in lysates of the DC 5 (20%) and of the S3 31 (7%) than the CON MIX clone. The higher Rho A activity of clone DC 5 is consistent with the stronger adhesion and more abundant FAs and SFs.

3.5.4.3. Role of kinases

This part will focus on another class of molecules implicated in the regulation of the actin cytoskeleton: the src and FAK kinases. Syndecan-3 cytoplasmic tail associates specifically with src (Kinnunen et al., 1998). On the other hand, the focal adhesion kinase (FAK) has been directly implicated in the generation of FA. After integrin clustering, it is autophosphorylated at Y397 (Kornberg et al., 1992), which offers a binding site for the SH2-domain of src (Thomas et al., 1998). Therefore we examined whether these kinases could be differentially activated in the clones. Therefore co-IP experiments were performed, which take advantage of the exclusive binding of src to the activated form of FAK, ***see fig. 3.38***.

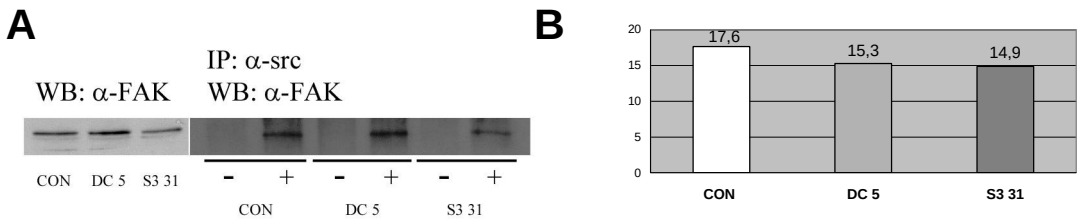

Figure 3.38: ***Syndecan-3 expression decreases FAK activity and consequently inhibits FAK-src interaction.*** **(A) Western blot analysis performed with anti-FAK antibody (1:1000). First three lanes show the signal obtained from 30 µg total protein, the following lanes represent the co-IP of src and FAK: 600 µg protein were immunoprecipitated with 7 µg anti-src antibody (+) or incubated without antibody (-). Only activated FAK bound to src. (B) Quantification of Co-IP shown in A. Density measured in the Co-IP was divided by the obtained for FAK in the total lysis. One representative experiment of two is shown. CON corresponds to the CON MIX clone.**

As ***fig. 3.38*** shows, the interaction of src with FAK decreased in both clone, irrespective of the presence of the cytoplasmic tail of syndecan-3. In a second experiment, a similar result was obtained concerning the difference between the CON MIX and the S3 31 clone, but the DC 5 behaved more like the CON MIX clone. These two experiments indicate that the presence of syndecan-3 lowered the interaction of src and FAK, but the implication of the cytoplasmic domain remains to be addressed.

3.5.4.4. Interaction with ERM proteins

As no direct interaction between syndecan-3 and either small GTPases, or kinases has been described, we hypothesized that intracellular adaptor molecules are involved in the signal transduction from syndecan-3 towards the actin cytoskeleton, which would explain observed phenotypes. The ERM proteins are cross-linker between membrane protein and the actin cytoskeleton (Mangeat et al., 1999; Tsukita and Yonemura, 1999). Since previous data from our laboratory had demonstrated the interaction between syndecan-2 and ezrin (Granes et al., 2000), we decided to further investigate the putative association of syndecan-3 with members of the ERM family in our transfectants.
It was not possible to perform co-IP assays since the anti-syndecan-3 antibody only worked in immunocytochemistry (***see 3.3***). Direct co-localization experiments could not be performed either since antibodies against syndecan-3 and the ERM proteins were raised in rabbit. We therefore studied the distribution of ERM in the three clones by immunocytochemistry (***see fig. 3.39***) and Western blot in order to determine possible changes in ERM cellular distribution induced by syndecan-3 expression.

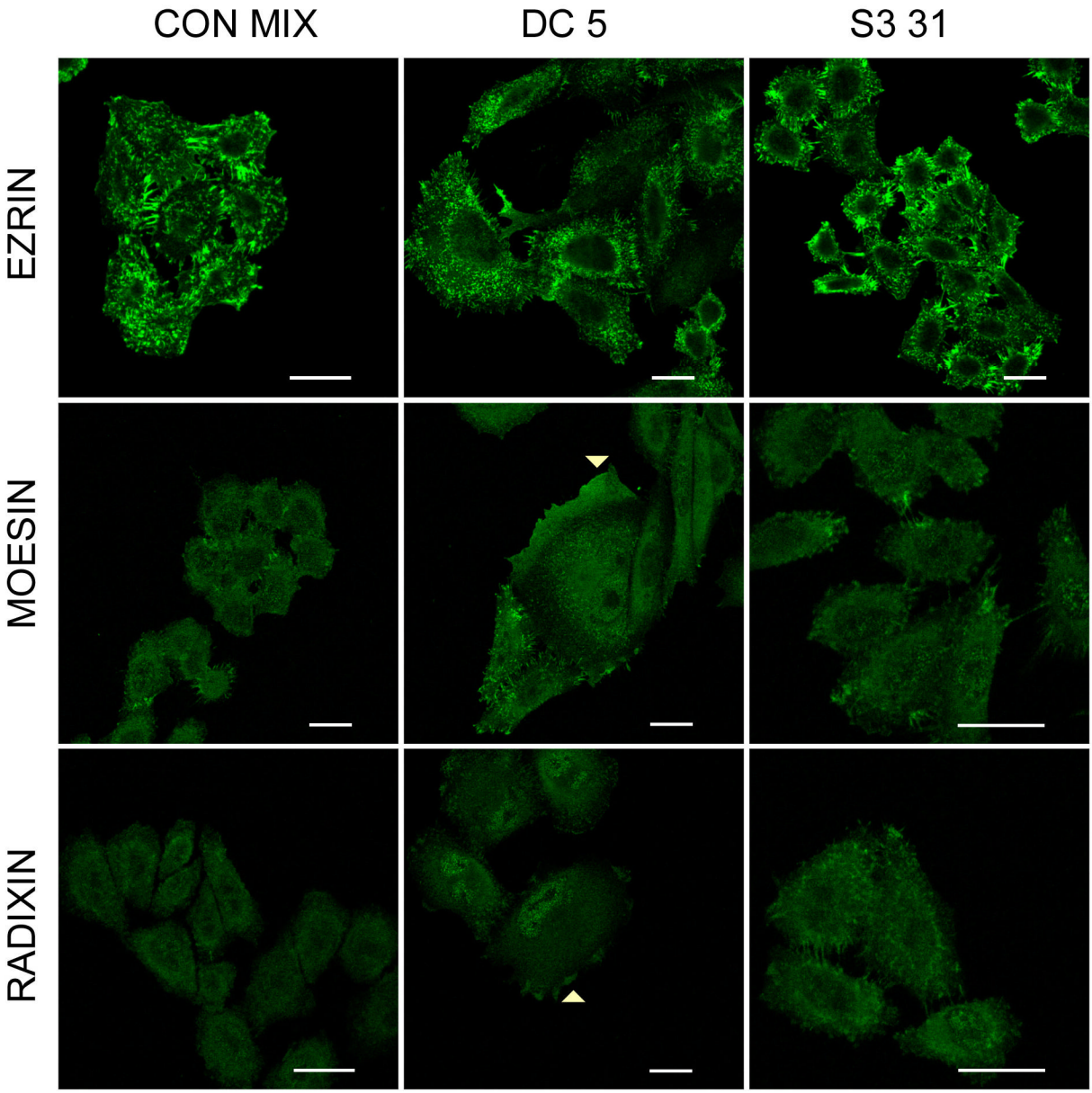

Figure 3.39: ***Staining with antibodies against the various ERM-proteins revealed slightly stronger staining in membrane ruffles and lamellipodia of clone DC 5 with the radixin and moesin antibodies*****. For Ezrin, no clear differences among the clones were seen. Bars = 20 µm. Arrowheads indicate lamellipodia.**

As shown, ezrin was localized at sites of cell-cell contacts and microspikes. No significant difference was found for ezrin. Staining for moesin and radixin was fainter. The experiments performed with anti-radixin and anti-moesin antibodies revealed a slightly stronger staining of cell membrane ruffles and lamellipodia for the DC 5 clone, ***see fig. 3.39, arrowheads***.
By Western blot analysis, no difference in ERM protein expression levels were detected among the clones (*not shown*).

In order to examine possible changes in their cellular distribution, we prepared TX-100 soluble and insoluble protein fractions from cells of the three clones. The TX-100 soluble fraction contains the cytoplasmic and membrane-associated proteins, while the TX-100 insoluble fraction contains proteins, which are associated with the cytoskeleton. The distribution of the different ERM proteins was then analyzed in those both fractions. Bands were scanned, quantified and normalized for actin and the percentage of ERMs present in the TX-100 insoluble fractions versus total ERM (sol. + insol.) was determined, ***see fig. 3.40***.

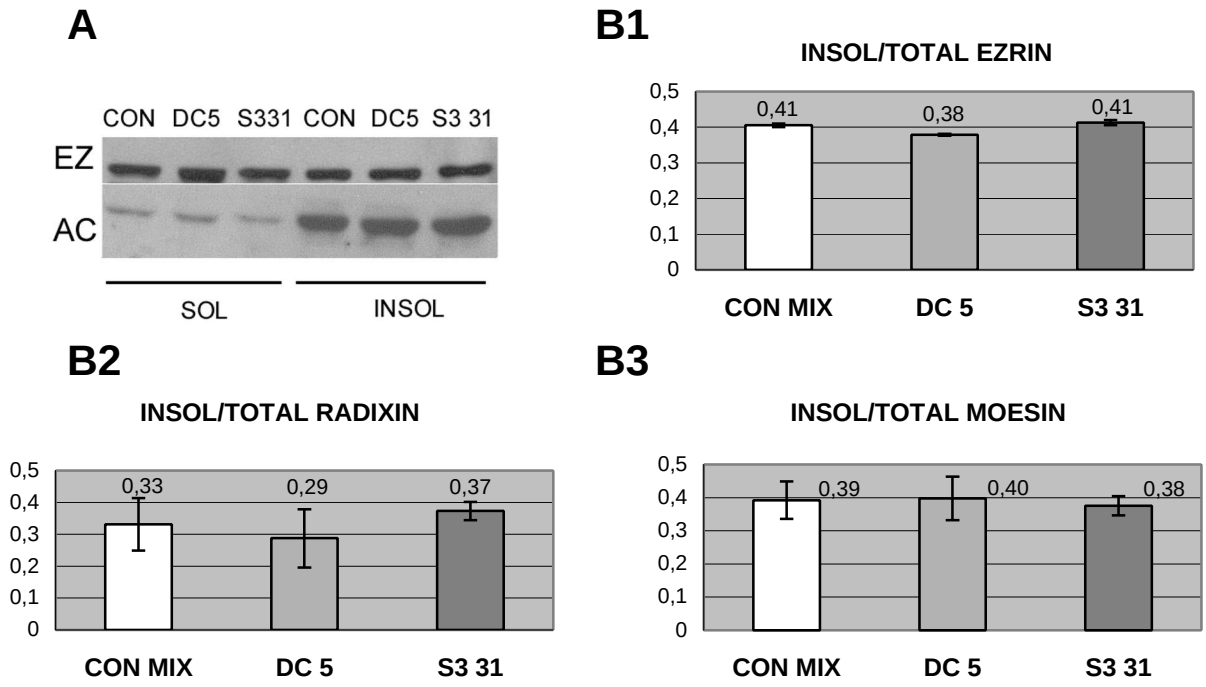

Figure 3.40: ***DC 5 cells presented lower levels ezrin in the insoluble fraction.*** **(A) Western blot analysis of distribution of ERM proteins in transfectants by comparison of TX-100 soluble and insoluble fractions. 20 µg protein per lane were loaded, here shown as example for ezrin. (B1-3) Quantification of ERM levels associated with the actin cytoskeleton. Western blot autoradiographs were scanned; ERM bands were quantified and normalized for actin in each fraction. For each clone, the percentage of ERM present in the TX-100 insoluble fraction versus total ERM levels was calculated. Graphs show the comparison between percentages of each individual ERM protein (B1: ezrin; B2: radixin; B3: moesin) associated with actin in the transfectants.**

As shown in ***fig. 3.40, Panel A, B1***, in the DC 5 clone, the proportion of TX-insoluble, which means cytoskeleton-associated ezrin was significantly decreased (7%), while the among the S3 31 cells an identical distribution of ezrin was found. A similar tendency was observed for radixin, ***see fig. 3.40, Panel B2***. The percentage of insoluble radixin was 12% and 21% lower in DC 5 cells compared with the CON MIX and S3 31 cells respectively. For cells from the S3 31, a slight shift of radixin to the insoluble fraction was observed (12% compared with the CON MIX cells). Nevertheless, in this case, the decrease was not significant. The analysis for moesin did not reveal any significant changes in the distribution of the protein, ***see fig. 3.40, Panel B3***.

As a summary, in the S3 31 clone a small shift of radixin to the insoluble pool can be observed. Further, the deletion of the syndecan-3 cytoplasmic tail seems to “prevent” the association of the ezrin and radixin with the cytoskeleton.

Discussion

4. Discussion

4.1. Sequence analysis and expression studies of human syndecan-3

4.1.1. Sequence analysis of human syndecan-3

Human syndecan-3 cDNA was isolated by screening a HFB library, as the highest expression is found in rat early in the development of the nervous system (Carey, 1996; Carey et al., 1997; Hsueh et al., 1998; Hsueh and Sheng, 1999)

The sequence of the human syndecan-3 cDNA revealed an ORF of 1329 bp, predicting a polypeptide of 443 amino acids. High cDNA sequence and protein homology was found between the human syndecan-3 and that of other species like mouse, rat and chicken. This high conservation of the syndecan-3 protein might reflect its biological importance in these organisms. Because of 100% homology in the transmembrane and cytoplasmic domain with the rodent protein, the human syndecan is assumed to have similar biochemical features, which are characteristic for these regions such as self-association (Asundi and Carey, 1995), tyrosine (Asundi and Carey, 1995) and serine phosphorylation by PKCβ (Prasthofer et al., 1995) or interaction with PDZ proteins such as syntenin (Zimmermann and David, 1999) and CASK/LIN-2 (Hsueh and Sheng, 1999).

Although we found high homology over almost the entire sequence, surprisingly amino acids 7-23 were unique to the human protein. This region, present in all clones screened, was characterized by an accumulation of small, neutral amino acids (82%), comprising 9 alanine and 5 glycine residues. Data bank comparison revealed that an identical motif has not been described in other proteins so far. The highest similarity (72%) was found with the signal peptide from the fibroin protein (Tsujimoto and Suzuki, 1979). The specific region lies in the putative signal peptide of the human syndecan-3 protein (amino acids 1-46), as deduced from a hydrophobicity plot (Nielsen et al., 1997). Although the syndecan-3 signal peptides from the various species have different lengths (chicken: 22 amino acids (Gould et al., 1995) and rat: 45 amino acids (Carey et al., 1997)) and vary in their amino acid composition, the beginning (except for chicken) and the end are conserved. Therefore it was concluded that the human syndecan-3 signal peptide contains a human-specific sequence, which has no influence on the delivery of the protein to the plasma membrane.

4.1.2. Expression studies

4.1.2.1. Syndecan-3 m RNA

The highest expression of human syndecan-3 was found in the brain, adrenal gland and spleen. The high expression detected in the whole nervous system (except for the pituitary gland) confirms the results of studies with rat N-syndecan (Carey et al., 1992; Carey, 1996). Strong labeling was detected in the temporal lobe (highest signal), the corpus callosum and the spinal cord. Accordingly, Hsueh and Sheng (Hsueh and Sheng, 1999) found high expression of rat syndecan-3 in the early post-embryonic brain, particularly in the cortex, corpus callosum, cerebellum and thalamus. The high expression detected in the spinal cord and adrenal gland

corroborates results from Nakanishi et al. (Nakanishi et al., 1997), while high expression of syndecan-3 in the spleen has not been described. In the gastrointestinal system (Nakanishi et al., 1997), syndecan-3 mRNA is mainly found in the stomach, transverse colon, descending colon, duodenum and rectum, while in the heart expression was predominantly seen in the aorta. As the syndecans are highly regulated, the expression pattern may depend on the stage of development. Nevertheless, in agreement with the results from adult tissues, strong signals were also obtained in fetal brain and spleen, asserting the relevance of syndecan-3 function in these tissues. The only tumor cell line presenting detectable syndecan-3 expression was SW480. This is consistent with the fact that the colon is one of the organs that expresses high levels of syndecan-3 RNA. The lack of syndecan-3 RNA detected in the other cell lines could mean either that they do not express detectable levels of syndecan-3, or that this expression was lost during transformation.

Syndecan expression is mainly regulated at transcription level. Nevertheless, there are also some reports of post-transcriptional control (Bernfield et al., 1999 and references therein). Thus, the high number of syndecan-3 transcripts in heart did not correlate with the amount of protein detected (Asundi et al., 1997). This may indicate that the detection of mRNA expression in the above-mentioned tissues does not always mean that the protein is also expressed.

4.1.2.2. Human syndecan-3 protein

4.1.2.2.1. Specificity of anti-human syndecan-3 antibody

The anti-syndecan-3 antibodies produced in rabbits recognized at high dilutions the bacterial GST-syndecan-3 fusion protein against which they had been raised. This recognition was specific since the pre-immune serum at same concentrations did not stain any protein bands. Since the labeling obtained by unpurified antibodies was already very strong, purification of the antibodies did not greatly improve the specificity of antibody recognition.
Although we obtained specific labeling of a band corresponding to syndecan-3 in FL-transfected cells the results were not always reproducible. One of the reasons therefore might be that the amount of syndecan-3 in lysates was beneath the detection limit of the method.
For IP experiments a similar situation was found as for the Western blot analysis: the experiment was successful only once. An additional problem of IPs is that samples have to be digested when bound on beads. This might prevent free access of Heparitinase/ChABC to the GAG chains. We also tried to digest samples before IP without improving the results.
In immuno cytochemistry experiments, very strong staining of transient transfected cells was obtained even at very high dilution (>1:5000). At these concentrations, background staining of un-transfected cells was not observed. Nevertheless, when the same experiments were performed with stably transfected cells, label was only seen at lower dilutions (between 1:100 – 1:300), which also led to an increase in background staining.

Method	Evaluation
WB of GST-syndecan-3 fusion protein	+++
WB of lysates from S3-transfected cells	+
IP with lysates from S3-transfected cells	+
IC with S3-transiently transfected cells	+++
IC with S3-stably-transfected cells	++

Table 4.1: *Evaluation of antibodies.* WB = Western blot, IP = immunoprecipitation, IC = immuno-cytochemistry.

In summary (***see tab. 4.1***), it was shown that antibodies had a high specificity and low affinity for syndecan-3. They only worked well in immunocytochemistry and, to some extent, in Western blot and IP experiments.
Nevertheless, the proteins used for the immunization represented bacterial fusion proteins, and they may not have been correctly folded. A large amount of GST-syndecan-3 fusion protein may have been collocated into the inclusion bodies during protein purification. Besides, bacterial produced proteins lack the sugar moieties of syndecans.
Alternatively, the digests with Heparitinase/ChABC might have interfered with the recognition by the antibody, the conditions of the IPs may have been too harsh or the sensitivity of the antibody too low.

4.1.2.2.2. Abnormal migratory behavior of human syndecan-3 protein

Digestion of HSPGs with Heparitinase/ChABC leaves a terminal unsaturated, uronic acid on the stub of the GAG chain remaining attached to the PG core proteins, which is specifically recognized by the 3G10 antibody.
When lysates from syndecan-3 transfected cells were submitted to Heparitinase/ChABC digestion and analyzed by Western blot, the 3G10 antibody detected a band at about 100-120 kDa which corresponded to about twice of the calculated molecular mass for syndecan-3. It should be noted that this difference was not due to the presence of sugar chains since 3G10 only recognizes Heparitinase/ChABC digested HSPG.

The aberrant migratory behavior is typical for all syndecans (***see tab. 4.2***). Two alternative explanations have been proposed: Carey (Carey, 1997) favors the theory that they form SDS-resistant dimers and reports that extracellular recombinant domains similarly migrate at twice the size (Carey, 1997) in up to 0.1 % SDS and up to 1% non-ionic detergent such as NP-40. Nevertheless, others blame the high prolin-content of the ectodomain for the migratory behavior observed (Bernfield et al., 1992). In the loading buffers used in the experiments of this thesis the final concentration was 1% SDS and samples were heated to 95ºC. No dimer formation was expected under these conditions considering that the interaction is based mainly on TM/TM interactions (***see also 1.3.2.2.2***).

Syndecan	Approx. calculated molecular mass (kDa)	Molecular mass deduced from SDS gel electrophoresis (kDa)
-1	30,6	69
-2	20,2	48
-3	50	100-120kDa
-4	19,5	30

Table 4.2: ***Syndecan core proteins show abnormal migratory behavior in SDS gels***

4.2. Phenotype of syndecan-3 transient transfected cells

4.2.1. Filopodia generation after FL-syndecan-3 transient transfection

Focusing our interest on the expression of human syndecan-3 in transfected COS-1 cells, syndecan-3 was detected at the plasma membrane, where it co-localized with the actin cytoskeleton. This was consistent with findings of Martinho (Martinho et al., 1996), who demonstrated that binding to HSPGs aligns LPL and FGF with the underlying actin cytoskeleton. While no morphological change was observed in control cells, the transfection of FL syndecan-3 induced abundant filopodia-like structures, microspikes and varicosities.

Microspikes cover the entire cell surface and are thought to be the "early" form of filopodia. Filopodia are sensors through which the cell receives and processes information about the environment, especially from the ECM and from surfaces of other neighboring cells. These structures, which are normally 5-35 µm, but occasionally up to 75 µm in length, are highly dynamic with an extension and retraction rate of about 10 µm/min. They can move the cell towards attracting signals, which in the case of the neuron growth cone contributes to the process of axon guidance (*for review see*: Mitchison and Cramer, 1996). Recently, they were implicated in the establishment of cell-cell contacts as shown in ***fig. 4.1*** (Wood and Martin, 2002; Vasioukhin et al., 2000). The molecular mechanisms underlying filopodium formation will be discussed later.

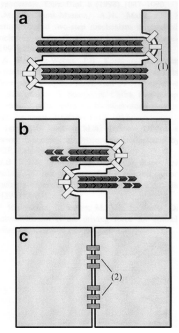

Figure 4.1: *Filopodia function during epithelial adhesion*. (a) Filopodia from two opposing cells contacts via filopodia and form weak adhesions at sites of membrane contact. (b) Filopodia then regress through actin depolymerization and (c) weak adhesions evolve into mature adherens junctions (Wood and Martin, 2002).

The induction of filopodia by transient syndecan-3 expression and its co-localization with the actin cytoskeleton clearly demonstrates that syndecan-3 is implicated in the re-organization of the actin-cytoskeleton. Since the observed effects were not specific for one cell-type, a common mechanism should underlie the filopodia generation induced by syndecan-3 expression.

In order to elucidate this mechanism, different strategies were followed (***see 3.4.3*** and ***3.4.4***) and the results will now be discussed in detail.

4.2.2. The implication of the extracellular domain in the filopodia-generating effect: Importance of sugar chains

As extensively demonstrated for other syndecans in previous studies, FL-syndecan-3 might function as a receptor or co-receptor for a soluble component of the cell medium or the ECM (***see 1.4.1*** and ***1.4.6***). After binding to this putative ligand, the syndecan-3 protein might transmit a signal inside the cell, which in turn would induce re-organization of the actin cytoskeleton promoting the outgrowth of the filopodia. The appearance of varicosities increases the surface area of the filopodia (comparable with the situation in growth cones), which augments the possibility of interactions between syndecan-3 and an assumed ligand. The nature of the ligand is unknown. However, it could be one of the GFs present in the medium such as bFGF, which has been shown to bind to syndecan-3 (Chernousov and Carey, 1993). Besides, interactions of syndecan-3 with ECM molecules might also have a function, like, for example, HB-GAM which has been shown to be important in axon outgrowth and guidance (Raulo et al., 1994).

As syndecans are highly glycosylated proteins we hypothesized that they might be involved in the filopodia-inducing effect by syndecan-3. Indeed, we demonstrate here that sugar chains are required on the cell surface for the filopodia-generating effect of syndecan-3, since neither GAG-deficient CHO 745 cells nor heparin-treated CHO K1 cells developed the typical syndecan-3 phenotype upon transfection. The small percentage of CHO 745 cells bearing the phenotype can be explained by residual enzymatic activity (1/15) that is always present in the CHO 745 cell line (Esko et al., 1985). According to our hypothesis, sugar-deficient syndecan-3 in CHO 745 cells would not bind cellular outgrowth-promoting factors. In heparin-treated CHO K1 cells, the latter would then compete with the sugar chains of expressed syndecan-3. These

findings firstly show the importance of sugar chains for the development of the typical syndecan-3 phenotype, and secondly suggest that the putative ligand would interact with syndecan-3 through its sugar residues. Another possibility could be, that oligomerization of syndecan-3 was responsible for the outgrowth of filopodia and that oligomerization depended on GAGs. Nevertheless, other groups have demonstrated that syndecan-3 is able to dimerize depending on the transmembrane domain and the ERKE motif of the extracellular domain located juxtamembrane but possibly not on sugar chains (Asundi and Carey, 1995; Bernfield et al., 1999), strongly supporting the ligand-binding theory. The two putative mechanisms are summarized in ***fig 4.2***, although it cannot be discarded that a combination of both mechanisms plays a role in the filopodia-inducing effect by syndecan-3.

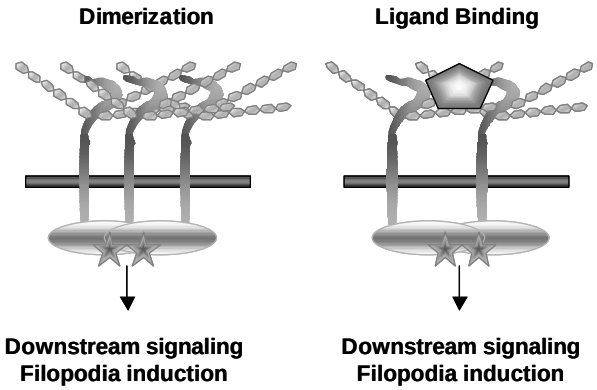

Figure 4.2: ***Possible mechanisms of activation by which syndecans might provoke changes in the actin cytoskeleton*** **to induce filopodia dependent on sugar chains: Dimerization or ligand binding.**

Heparin-treated transfected CHO K1 and transfected CHO 745 cells had a tendency to collapse. As heparin is supposed to compete for normal ligand, this observation further supports the ligand-binding theory.

4.2.3. The implication of the intracellular domain in the filopodia-generating effect: Possible pathways

In order to explore how syndecan-3 functions in the generation of filopodia, different cytoplasmic deletion mutants were performed (***see fig. 4.3*** and also ***3.4.4***).

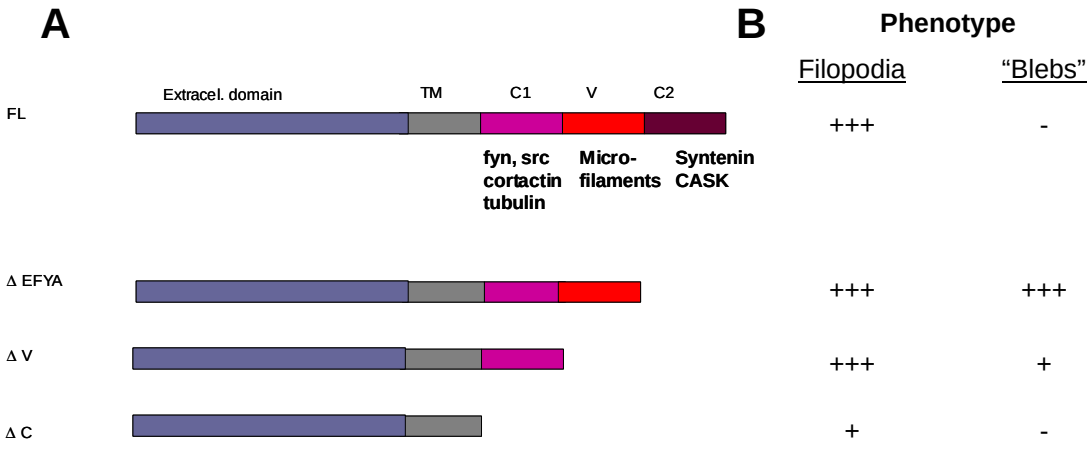

Figure 4.3: (A) ***Cytoplasmatic-deleted constructs used to study the implication of the cytoplasmic tail in the filopodia-inducing effect*****. Putative syndecan-3 binding partners are indicated below the corresponding regions. Note that, only for the C1-region, the binding partners have been experimentally demonstrated, while for the V- and C2 region binding was proposed due to high homology of these regions with other syndecans. (B)** ***Phenotypes*** **obtained after transient transfection with constructs shown in (A).**

As a functional requisite, we confirmed that all constructs reached the plasma membrane since they could be labeled by anti-syndecan-3 antibody without permeabilizing the cells. This is in agreement with results from Carey (Carey et al., 1994b; Carey et al., 1996), who demonstrated that deletion of almost the entire cytoplasmic domain of syndecan-1 did not influence its localization to the plasma membrane.

In the following chapter, the putative pathways that might be involved in the generation of filopodia will be discussed taking into account the results obtained from transient transfection experiments.

Transient expression of the constructs in CHO K1 cells (***see fig. 4.3, Panel A***) was compared with those of the control vector and FL-syndecan-3. Only the deletion of the entire cytoplasmic domain led to the abolition of the filopodia-generating effect of syndecan-3; and even among ΔC transfected cells, a small percentage also showed filopodia. Transfection with the FL, ΔV and ΔEFYA constructs led to similar phenotypes. Furthermore, some cells among the ΔV transfected and a high percentage among the ΔEFYA cells generated "blebs" (***see fig. 4.3, Panel B***) which will be discussed later (***see 4.2.3.4***). This indicates that the region of the cytoplasmic domain responsible for the filopodia-inducing effect can be mapped to the C1 region. To a lesser extent, however, oligomerization (independent of the cytoplasmic region) and ligand binding might also participate, as indicated by the small proportion of ΔC-transfected cells that generated filopodia.

4.2.3.1. The EFYA domain is not implicated in the generation of filopodia: No role for PDZ proteins

The EFYA domain of syndecans is an interacting motif for PDZ proteins (***see 1.7.1***). Indeed, one member of this protein family, syntenin (Grootjans et al., 1997; Grootjans et al., 2000; Zimmermann et al., 2001) is a good candidate for the generation of filopodia, since it has been reported to bind to the PDZ domain of all syndecans (***see 1.7.1.1***) and over-expression of its "dominant" positive form led to abundant cell protrusions, as seen in ***fig. 4.4***.

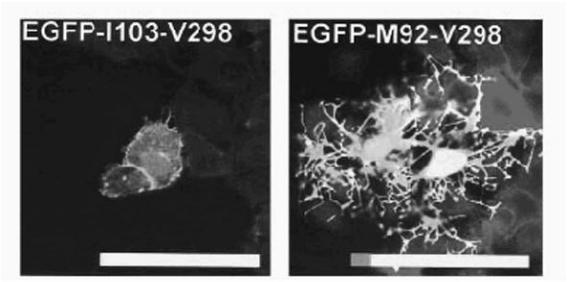

Figure 4.4: ***Effect of inactive (left) and "dominant positive" (right) syntenin by transfection into MCF-7 cells led to branching extensions*** **(Zimmermann et al., 2001).**

Similarly, another member of the PDZ protein family, CASK (Hsueh et al., 1998; Hsueh and Sheng, 1999) has been shown to bind to syndecan-2 and protein 4.1 thereby linking syndecans to the cytoskeleton (Cohen et al., 1998; Hsueh et al., 1998), and is therefore a potential mediator of syndecan-3 signals.

As ΔEFYA cells showed a similar phenotype to FL-transfected cells, this ruled out PDZ-proteins as direct transducers of syndecan-3 induced effects. However, they might bind to other regions of the cytoplasmic domain via an adaptor protein.

The results obtained with the transient transfection of the ΔEFYA construct confirmed the studies with GFP-tagged FL-syndecan-3. The attachment of a huge GFP tag was expected to

shield the neighboring amino acids. Since GFP was attached to the cytoplasmic domain and no induction of filopodia was observed, this further indicates that the first amino acids from the C-terminal end are not important for the filopodia-inducing effect.

4.2.3.2. The V-region is not necessary for the generation of filopodia: Is there a direct interaction of syndecan-3 with microfilaments?

The V-region is reported to associate directly with microfilaments for syndecan-1 and suggested for syndecan-3 (Carey et al., 1994b). As already mentioned, syndecan-1 and -3 form a subfamily among the syndecans due to similarities in their ectodomain and intracellular tail. Therefore, some of the results for syndecan-1 might be extrapolated to syndecan-3.

In agreement with Carey et al (Carey et al., 1994b; Carey et al., 1996), we observed the co-localization of FL-syndecan-3 with microfilaments, as they showed for syndecan-1 (Carey et al., 1996).

In transfection experiments these authors did not see any disruption of this co-localization when deleting 11 amino acids from the cytoplasmic tail (***see fig. 4.5, Syndecan-1: dark red***), which fits with our results obtained with the ΔEFYA transfectants. Nonetheless, in contrast to our results they observed abolition of the association of syndecan-1 with the actin cytoskeleton when deleting a further 12 amino acids. This deletion of a total of 23 amino acids corresponded to the deletion of the entire C2- and V- and small part of the C1-region (***see fig. 4.5, Syndecan-1: red***).

Figure 4.5: ***Comparison of deletion strategies of syndecan-1*** **(Carey et al., 1994b)** ***and syndecan-3*** **(present in this thesis). The different colors indicate the deleted regions. Green "Y" indicates tyrosine mutation analysis performed by Carey *et al*. in syndecan-1. Bold "Y" is the tyrosine which led to the abolition of microfilament association when deleted.**

As observed, the deleted sequences of the cytoplasmic tail of syndecan-1 and -3 differ notably, although some zones overlap. The sequence that might be responsible for the interaction with microfilaments might therefore lie in this small common region LEEPKQA.

Carey *et al*. also demonstrated, that the deletion of the third tyrosine (***see fig. 4.5, bold Y***) abolished the interaction with microfilaments, while we observed clear co-localization in the ΔV transfectants, which did not have this tyrosine. Possible explications are that tyrosine phosphorylation might not play an important role for syndecan-3, or that another tyrosine is implicated since it has been demonstrated that all tyrosines in syndecan-3 can be phosphorylated (Asundi and Carey, 1997). The implication of the first tyrosine in phosphorylation events seems to be likely since it is conserved in all, even in drosophila syndecan, and fits into the typical sequence for tyrosine kinases (Pierce et al., 1992). In syndecan-1 more than one tyrosine can be phosphorylated (Reiland et al., 1996). Interestingly, another group demonstrated that the cytoplasmic domain of syndecan-1 was not necessary for detergent insolubility (Carey et al., 1996; Carey et al., 1994a), a characteristic considered to be associated with TM protein interaction with cytoskeleton. Carey *et al.* attributed the insolubility of cytoplasmic-deleted syndecan-1 to interactions of the transmembrane domain.
The differences observed between syndecan-1 and –3 might be due to differences in sequences. It should be mentioned that Carey *et al.* did not discuss how syndecan's cytoplasmic tail might bind "directly" to actin, or whether binding is performed via adaptor or effector molecules.

4.2.3.3. The C1-region seems to be responsible for the filopodia-generating effect

The most important interactions described for the C-terminal region of syndecan-3 was that with a complex of src, fyn, cortactin and tubulin revealed by co-IP experiments in axons. Due to similarity between axons and filopodia, this pathway might also be implicated in the outgrowth of the latter (Kinnunen et al., 1998a). Src binding has been mapped to the C1-region (Kinnunen et al., 1998b). Cortactin, which is also present in the co-immunoprecipitated complex, activates and stabilizes the Arp 2/3 complex in parallel with N-WASP (Weaver et al., 2001). This might be a connection between this pathway and the pathway via cdc 42/N-WASP/Arp 2/3, which will be mentioned later (Higgs and Pollard, 2000).

Other candidate proteins to be implicated in the filopodia-inducing effect are the ERM proteins which are considered as cross-linkers between transmembrane and the actin cytoskeleton, ***see 1.7.4*** (Bretscher, 1999; Mangeat et al., 1999; Tsukita and Yonemura, 1997; Tsukita and Yonemura, 1999; Vaheri et al., 1997). Ezrin is found in microspikes and has been reported to bind directly to the cytoplasmic tail of syndecan-2 (Granes et al., 2000). There was also some evidence from previous work in our laboratory that the interaction sequence for ezrin with the cytoplasmic tail of syndecan-2 may lie in the C1 region (*Granes, personal communication*). Ezrin or other members of the ERM family (such as moesin, the most prominent ERM protein in neurons (Paglini et al., 1998)) may also bind specifically to syndecan-3. Moreover, the transfection of dominant positive ERM family members led to the outgrowth of filopodia (Amieva et al., 1999) (***see fig. 4.6***), while ERM distribution to cytoplasm led to microvilli breakdown (Kondo et al., 1997).

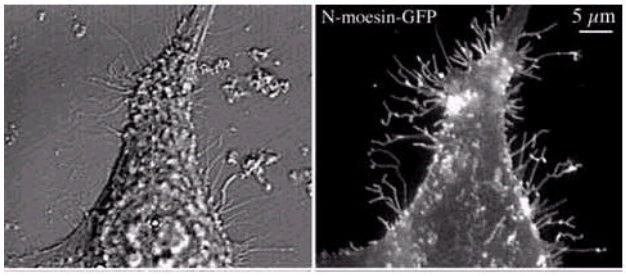

Figure 4.6: ***Transfection of dominant positive members of the ERM family also leads to the outgrowth of filopodia.*** **Here, transfection of N-moesin-GFP is shown in digitally enhanced differential interference contrast (DIC) and in immunofluorescence microscopy images (Amieva et al., 1999).**

Another interesting possibility to explain how syndecan-3 might be implicated in the organization of the actin cytoskeleton might be through localization of actin mRNA to sites of interaction with HB-GAM (***see 1.6.1***). This effect could be inhibited by src inhibitor PP1, which might indicate a connection with the pathway described above (Fages et al., 1998).

Independently of all pathways, which might be activated by syndecan-3, they seem finally to lead to the activation of the small GTPase cdc 42. Its direct implication had been demonstrated in syndecan-2 induced filopodia generation (Granes et al., 1999).

For a long time, cdc 42 activation has been associated with filopodia outgrowth (Hall, 1998; Sander et al., 1999; Tapon and Hall, 1997) since microinjection of cdc 42 led to microspike and filopodia formation in 3T3 cells (Kozma et al., 1995), ***see 1.8***. However, the underlying mechanisms have been unraveled only recently, ***see fig. 4.7***. Miki *et al* discovered in 1996 a new, ubiquitously expressed protein, N-WASP (N-Wiskott-Adrich syndrome protein), which transmits signals from tyrosine kinases, inducing polarized rearrangement of cortical actin filaments dependent on PIP_2 by actin polymerization (Miki et al., 1996; Miki et al., 1998). Mutation of N-WASP blocks cdc 42-induced filopodia formation. It was further evidenced that only the C-terminus dramatically stimulated nucleation, as did the FL protein after activation by cdc 42 and PIP_2.

All these data prompted the proposal of the model of a “dormant” molecule as a result of intramolecular interactions, which is unfolded upon activation (***see fig 4.7***). N-WASP binds to the Arp 2/3 complex thereby linking cdc 42 to the actin cytoskeleton (Carlier et al., 1999; Rohatgi et al., 1999). Arp 2/3 is a stable complex of seven subunits, two actin-related protein (Arp2 and Arp3) and five novel proteins (Mullins, 2000) that nucleates actin filaments and cross-links them into orthogonal networks. Finally, elongated free barbed ends induce protrusion of the membrane. As mentioned, N-WASP is also implicated in actin nucleation via profilin. Profilin is an actin monomer binding protein, which is also involved in microspike formation (Suetsugu et al., 1998). ***Fig. 4.7, Panel A*** and ***B***, shows a photograph of a co-transfection of cdc 42 and N-WASP which led to the outgrowth of long filopodia reminiscent of those seen after syndecan-3 transfection. Therefore syndecan-3 may activate N-WASP.

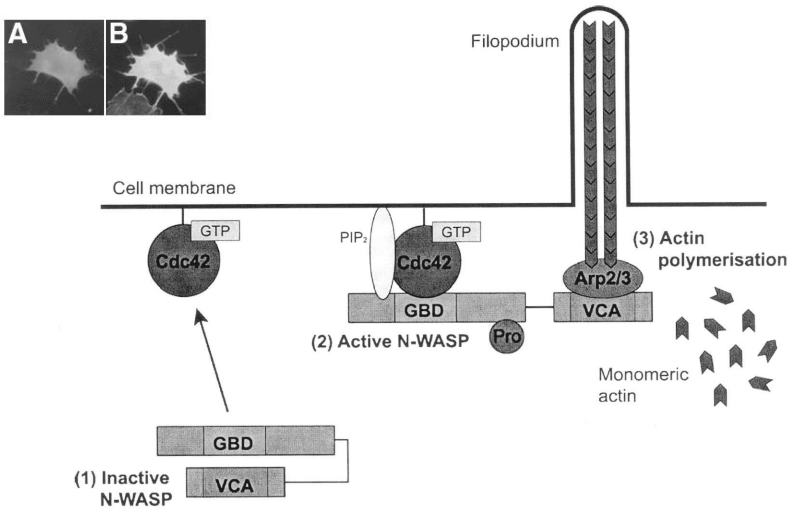

Figure 4.7: ***Mechanism of filopodia formation.*** **An activated Rho-family G protein recruits WASP-family protein to the membrane and leads to its activation synergically with PIP_2. N-WASP binds to the Arp 2/3 complex, which leads to actin polymerization and the outgrowth of filopodia (Mullins, 2000; Wood and Martin, 2002). (A and B)** ***Filopodia induction by transfection with dominant positive cdc 42 and N-WASP leads to the outgrowth of long filopodia in COS-7 cells*****. (A) Anti-myc staining of cdc 42 and (B) actin staining by TRITC-conjugated phalloidin (Miki et al., 1998). Arp = actin-related protein, N-WASP = Neural Wiskott-Aldrich Syndrome Protein, PIP_2 = Phosphatidyl Inositol Phosphate 2.**

Based on our results and data from the literature discussed above, ***fig. 4.8*** summarizes all proteins and pathways that might be implicated in the syndecan-3 induced filopodia outgrowth.

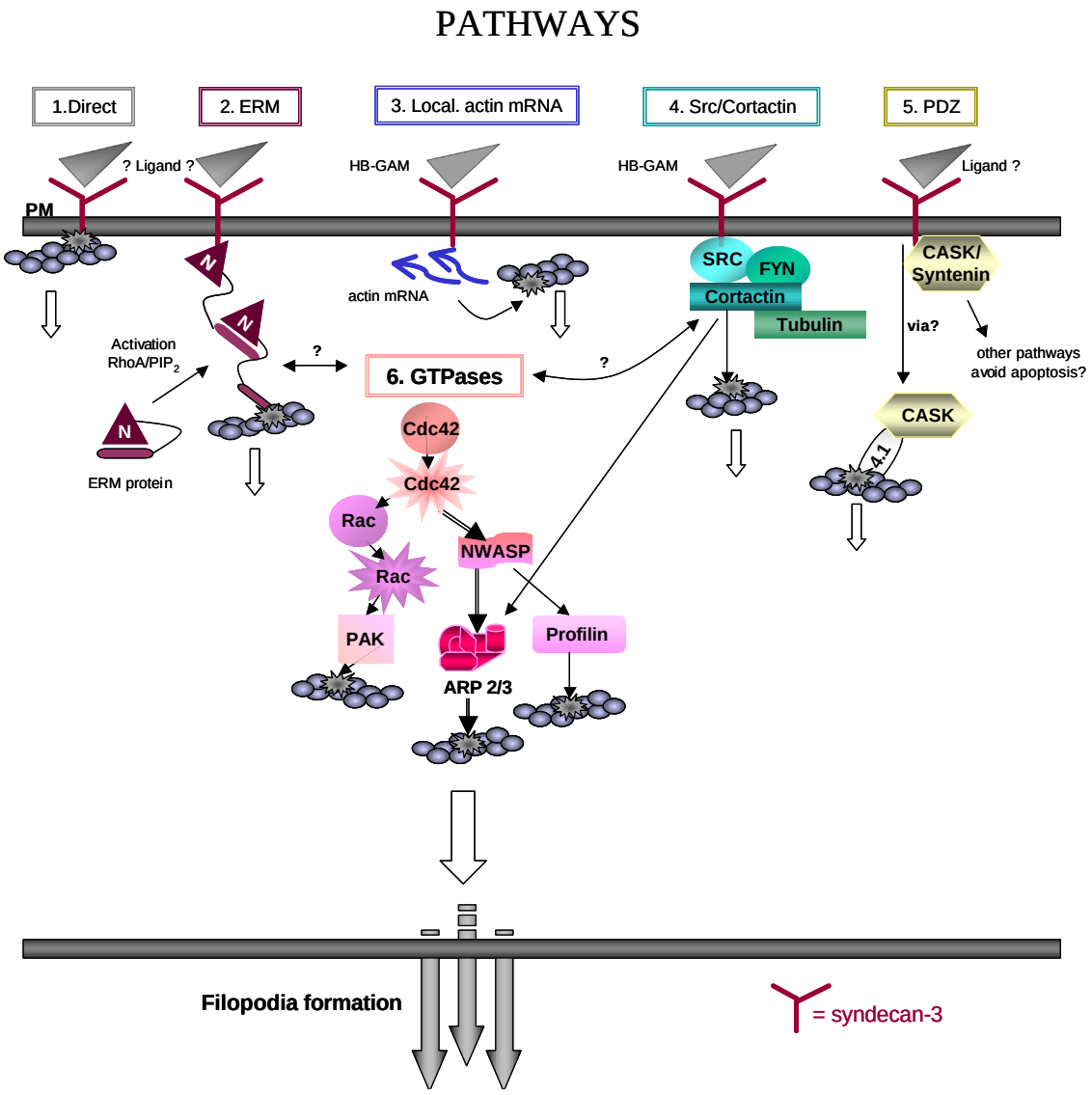

Figure 4.8: ***Schematic presentation of pathways which might be implicated in syndecan-3-induced filopodia outgrowth.*** **(1) Direct interaction with microfilaments, (2) interaction with ERM proteins, (3) localization of actin mRNA, (4) activation of the src/cortactin pathway and (5) indirect activation of PDZ proteins. The activation of the small GTPase cdc 42 (6) might lie downstream of all other pathways described above, especially (2) and (4). PM = Plasma membrane, ERM = Ezrin/Radixin/Moesin, HB-GAM = Heparin-binding growth-associated molecule, PAK = p21-activated kinase, Arp 2/3 = Actin-related protein 2/3, N-WASP = Neural Wiskott-Aldrich Syndrome protein, PDZ = PSD-95/Discs-large/ZO-1, CASK = Ca^{2+}-Calmodulin-dependent serine protein kinase, 4.1 = protein 4.1.**

The implication of the small GTPase cdc 42 is under current investigation. Therefore co-transfection and microinjection experiments in combination with time-lapse recording are planned. In these experiments, activators, inhibitors, dominant negative and positive forms of cdc 42 and also of Rho A and Rac 1 will be employed (***see tab. 1.2***). In the same manner, pull-down assays after transient transfection and stimulating with specific activators of each GTPase will be performed.

4.2.3.4. The deletion of the EFYA sequence leads to membrane blebbing

The final part of the discussion of the transient transfection experiments will be dedicated to the "bubble-like" structures which were seen in few of the ΔV transfected cells, but most abundant in the ΔEFYA transfection. Since these structures were rarely seen in the ΔC and FL-transfected cells, they might be specific for ΔV and ΔEFYA constructs. These structures are reminiscent of "blebs", which appear in early phases of apoptosis.

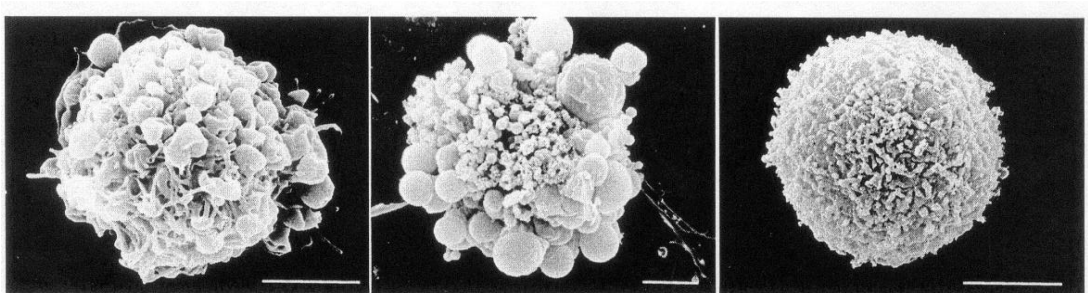

Figure 4.9: *"Blebbing", an early event of apoptosis*. NIH 3T3 cells treated with apoptosis-inducing TNF-α, TNF-α + C3-toxin (Rho A inhibitor) and TNF-α + Y-27632 (inhibitor of ROCK = Rho-associated kinase). TNF = Tumor necrosis factor, (Coleman et al., 2001).

Recently, in two independent publications, an association between the activation of Rho-associated kinase (ROCK) by Rho A and apoptosis was established for the first time (***see fig. 4.9***). It was known that blebbing was due to the phosphorylation of the myosin light chain (MLC) and that Rho A and myosin light chain kinase (MLCK) inhibition blocked membrane blebbing (Mills et al., 1998). Recent findings demonstrated that not Rho A itself but its substrate, ROCK, was activated by caspase-3 cleavage (Coleman et al., 2001; Leverrier and Ridley, 2001; Sebbagh et al., 2001) and in turn phosphorylates MLC (***see fig. 4.10***). It is not clear how in apoptotic cells ROCK-activation leads to blebbing while in other cells it leads to cell-contraction, but authors suggest that reduced attachment of cell to the ECM makes cells contract and round up.

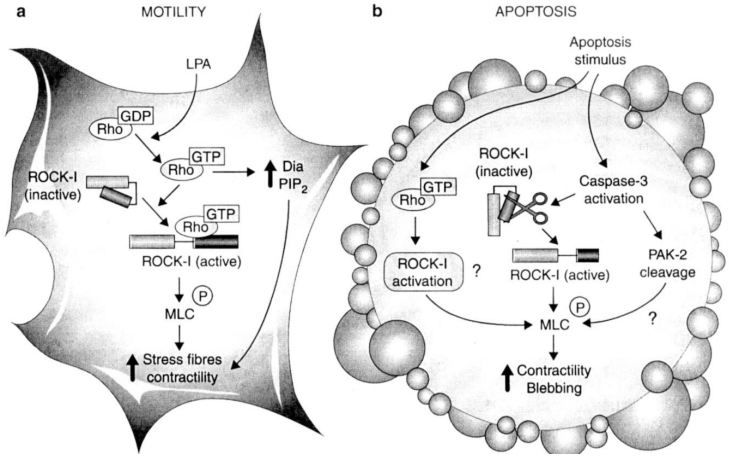

Figure 4.10: *Model of the implication of ROCK in cell contractility (a) and apoptosis (b).* LPA = Lysophosphatidic acid, MLC(K) = Myosin light chain (kinase), ROCK = Rho-associated kinase, PIP_2 = phosphatidyl inositol phosphate 2, PAK = p21-activated kinase (Leverrier and Ridley, 2001).

The aspect of cells, undergoing apoptosis, was highly reminiscent of the phenotype obtained after transfection with ΔEFYA. Therefore, we speculate that the EFYA region of syndecan-3 may bind to some PDZ domain containing protein (such as syntenin, CASK) which inhibits apoptosis provoked by syndecan-3. This mechanism seems to be independent of the filopodia-generating effect. To further examine this hypothesis, FACS analysis of ΔEFYA versus FL-syndecan-3-transfected cells after Hoechst (DNA) staining could be performed in order to measure the proportion of cells that undergo apoptosis, if any.

4.3. Phenotypic and functional changes observed in stably transfected CHO K1 cells

4.3.1. FL-syndecan-3 has only a slight effect on the phenotype of stably transfected cells and no role in proliferation or migration in the analyzed systems

On the basis of our results from transient transfectants, we assumed that stable expression of syndecan-3 in CHO K1 cells would influence the phenotype and migratory behavior of these cells. When we analyzed this, we found FL-syndecan-3 transfectants were slightly more elongated, but their phenotype did not bear a resemblance to the morphological changes caused by transient transfection. This might be due to the fact that the protein amount expressed in transient transfectants is much higher than in stably transfected ones. In functional experiment, S3 31 cells behaved similarly to the CON MIX clone. Indeed, there were no significant differences in proliferation or wound healing and only a slight increase in adhesion, probably, due to the increase in net negative surface charge due the higher syndecan-3 expression. We conclude that syndecan-3 has no role in proliferation or migration under our experimental conditions. Thus, no stimulus was applied to attract cells to migrate. S3 31 cells seeded on a specific ligand such as HB-GAM (Raulo et al., 1994) or bFGF as soluble factor (Chernousov and Carey, 1993) might migrate more rapidly than the CON MIX cells.

4.3.2. Stable transfection of cytoplasmic-deleted syndecan-3 induces morphological and functional changes in CHO K1 cells

Surprisingly, the clone, which behaved distinctly in all functional experiments, was DC 5 expressing a cytoplasmic-deleted variant of syndecan-3. This clone consisted of bigger cells, which adhered more strongly to the culture dish and migrated significantly more slowly. This matches the observations of the transient transfectants (ΔC), which also did not show a migratory phenotype (outgrowing filopodia), as did all the other transfectants (FL, ΔV and ΔEFYA). The stronger cell-substrate adhesion was further supported by the fact that DC 5 cells presented more FAs and thicker SFs than the CON MIX and the S3 31 cells. The higher adhesion may partly be explained by the increase of GAGs (as already discussed for the S3 31 clone, ***see 4.3.1***). Nevertheless this would explain neither the decrease in proliferation nor the increase in cell size and number of FAs and SFs.

The slower proliferation of the clone DC 5 might be related to its higher cell volume as cells need more time to grow and therefore divide more slowly. The reason for the higher cell volume could not be determined. There are very few reports in the literature about control of cell volume and they usually deal with phenomena such as osmotic regulation or hypertrophic responses especially in activated cardiomyocytes. In growth-arrested CHO K1cells (induced by a special medium) an impaired population growth, a delay in cell cycle progression through the S phase and an increase in cell size and increased adhesion to culture substrate was reported (Borman and Branda, 1989). Some interesting papers reported src as a volume-sensitive enzyme, which

phosphorylated cortactin upon shrinkage (Kapus et al., 1999). Nevertheless, the systems analyzed are too divergent to allow comparison.

The only study relating syndecans with proliferation referred to syndecan-4. Authors showed that syndecan-4 mRNA peaked in G_0 before reentering cell cycle (Landry et al., 2001). Since the small GTPases have been implicated in cell cycle progression and an influence of syndecans on the activation state of GTPases has been reported, these might be the connection between syndecans and proliferation.

4.3.3. Putative explanation for the distinct phenotype and functional properties of DC 5

In the following chapter, based on our results and knowledge from the literature, different pathways which might contribute to the stronger adhesion properties of DC 5 cells, will be discussed in detail. As a summary, ***see fig. 4.11***. The contribution of the GAG to the higher cell surface net charge will not be discussed again (***see 4.3.2***).

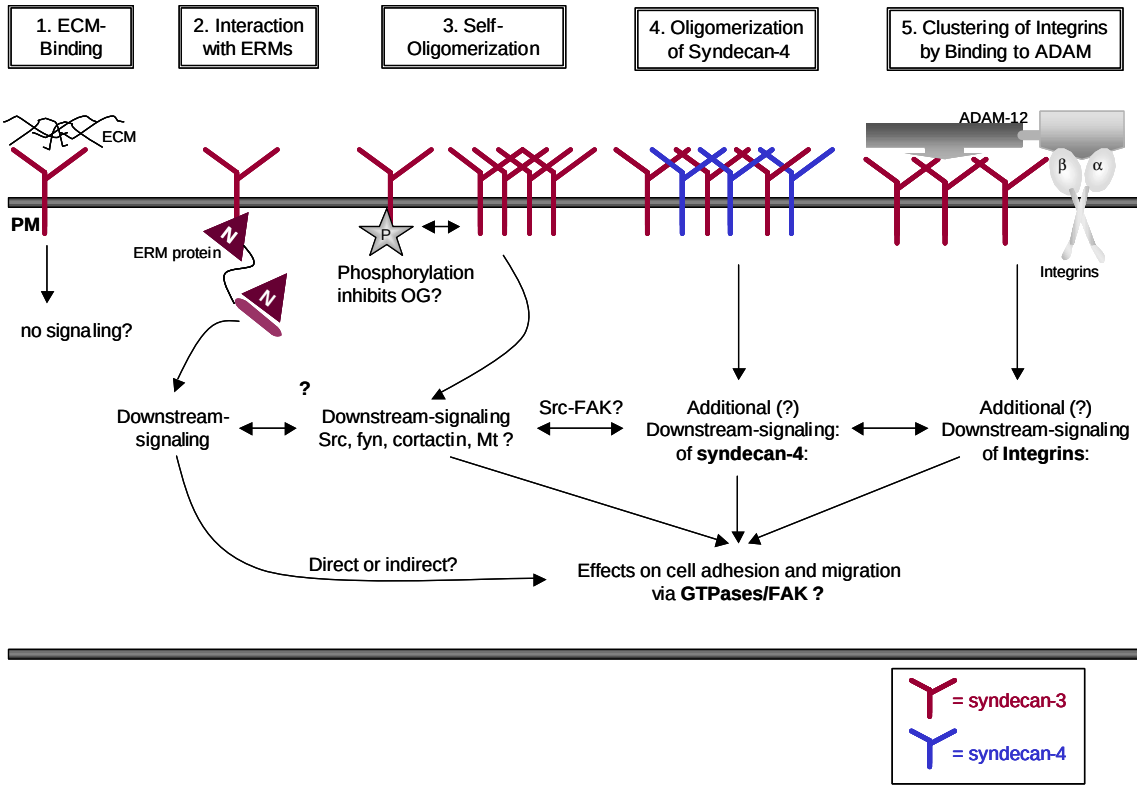

Fig. 4.11: ***Putative pathways implicated in increase of adhesion in DC 5 cells.*** **(1) increased binding due to sugar chains (higher cell surface net charge), (2) by interaction with ERM proteins, (3) by self-oligomerization, (4) by co-operating with syndecan-4 and/or integrins (5). PM = Plasma membrane, ECM = Extracellular matrix, OG = oligomerization, FAK = Focal adhesion kinase, Mt = Microtubule, ADAM = A disintegrin and metalloproteinase, ERM = Ezrin/Radixin/Moesin.**

4.3.3.1. Oligomerization of syndecan-3 or interactions via its transmembrane domain

Regarding the formation of FAs, the implication of syndecan-4 has been the most extensively described (***see 1.4.6.2***). However, as syndecan-4 $^{-/-}$ fibroblasts were able to form FAs, it has been suggested that another syndecan might substitute it in this function (Ishiguro et al., 2000). Indeed, syndecan-2 has also been found to have a role in SF formation (Munesue et al., 2002).
We therefore propose that an alternative mechanism for the stronger adhesion of DC 5 cells is by the contribution of syndecan-3 to the oligomerization of syndecan-4 although "trans-oligomerization" has not been analyzed. The oligomerization motif of syndecans has been described to lie in the TM regions and the ERKE sequence (Asundi and Carey, 1995), which are very similar among the syndecans. At a critical concentration, all syndecans oligomerize (Couchman and Woods, 1999), which depends neither on a ligand nor on the cytoplasmic domain (Asundi and Carey, 1995) but might be abolished if the latter is phosphorylated. The syndecan-3 induced oligomerization of syndecan-4 might then lead to the activation of PKC and finally to the formation of FA and SF as described before (***see 1.4.6.2***). Why should not the FL syndecan-3 contribute to this effect? For syndecan-4, oligomerization was inhibited by phosphorylation (Horowitz and Simons, 1998a). As it has been reported that syndecan-3 can be serine and tyrosine phosphorylated (Asundi and Carey, 1997; Prasthofer et al., 1995), the absence of the cytoplasmic tail in DC 5 might render it insensitive to this inhibition. Another example for the function of a cytoplasmic deleted syndecan was the induction of spreading by syndecan-1 even in the absence of the cytoplasmic domain (Lebakken and Rapraeger, 1996). These authors suggested an interaction of syndecan-1 with another membrane protein.

The "dominant negative" behavior of the DC 5 clone is comparable to the behavior of truncated syndecan-4. Here the deletion of the central V-region, which is specific for the syndecan-4 made it act as the "dominant negative" form by diminishing FA formation. Authors (Couchman and Woods, 1999; Longley et al., 1999) concluded that the cytoplasmatic region is necessary for FA formation and that truncated syndecan-4 oligomerizes with the wild-type form, therefore somehow abrogating signaling responses.

4.3.3.2. Cooperative action with integrins via ECM molecules (ADAMs/FN)

Another possibility is that syndecan-3 clusters integrins by binding to ADAM-12 (Iba et al., 2000). Authors showed that syndecans can serve as first attachment receptors when exposing a cryptic site of ADAM-12 to $ß_1$-integrin. In these experiments they demonstrated that the HS chains were necessary for syndecan function as well as an intact transmembrane and cytoplasmic domains. This finding argues against the hypothesis that the increased adhesion properties of DC 5 cells are related with ADAM binding, since cells of this clone express syndecan-3 without cytoplasmic domain. However, their experiments were performed with syndecan-1 chimers and, as described above, it seems that syndecan-1 and -3 cytoplasmic domains behave differently. A similar mechanism, as described for ADAM-12, might be also applied to other ECM molecules such as FN. In this context, it was shown that syndecan-4 and integrins bind cooperatively to two independent domains of FN in a Rho A-dependent manner (Saoncella et al., 1999). The binding of syndecan-3 was mapped to the HepII domain of FN, which binds to the HS chains of syndecan-4 and might therefore bind to all syndecans.

4.3.3.3. Implication of ERM proteins

Our results suggest that ERM proteins are implicated in the interaction of syndecan-3 with the actin cytoskeleton. DC 5 cells presented a lower level of ezrin in the TX-100 insoluble fraction, further indicating that the lack of the cytoplasmic domain reduces the proportion of ezrin associated with the cytoskeleton through syndecan-3. The mechanism is not clear, but it might have something to do with the connection between GTPases and ERM proteins.

Thus, it is known that Rho A activates dormant ERMs in two different ways, ***see also fig. 1.13***. Firstly, Rho A activates phosphatidyl-inositol 4-phosphate 5-kinase (PIP_4K), thereby augmenting PIP_2 concentration, which in turn activates ERM (Tsukita and Yonemura, 1999). Secondly, Rho A activates ROCK, which phosphorylates ERMs (Bretscher, 1999; Matsui et al., 1998; Tsukita and Yonemura, 1999). There is a positive feedback loop, since ERMs can bind the Rho A inhibitor RhoGDI. Rac can also activate ERMs (Mackay et al., 1997).
On the other hand, ERMs are necessary for Rho- and Rac- induced cytoskeletal effects (Hall, 1998; Mackay et al., 1997). Interestingly, distribution of ERM proteins to the cytoskeleton led to microvilli breakdown as an early event of apoptosis. Clone DC 5 may proliferate more slowly because of a higher apoptosis rate (Kondo et al., 1997).

Recently, a connection between ERMs and FAK has been established (Poullet et al., 2001). The authors report that ezrin can interact via its cryptic site with FAK, independently of src activity, and that over-expression of ezrin led to auto-phosphorylation of FAK. The fact that we found more ezrin in the TX-100 soluble fraction of cells from the DC 5 clone and at the same time more FAs and SFs than in the other clones may mean that the ezrin-FAK interaction also contributes to the phenotype observed in this clone.

4.3.3.4. Implication of src-FAK interactions

Src has been described extensively for its role in cell adhesion (Bjorge et al., 2000; Thomas and Brugge, 1997). Thus, once activated by partial dephosphorylation of its negative regulatory site (Y527), its kinase activity is transiently increased and Src is redistributed into new FA (Kaplan et al., 1995) where it binds to various proteins implicated in cell adhesion: such as paxilin via the src homology 3- (SH3)-domain (Weng et al., 1993). Src is thereby involved in the subcellular localization of many proteins. For its proper function it seems important that src itself is correctly delivered to its destination: This might be by binding to FAK after activation. (Schaller et al., 1999; Thomas et al., 1998). Src then phosphorylates other sites to create new binding sites for other proteins (Schlaepfer and Hunter, 1996). We found that in the S3 31 clone there was less interaction between src and FAK than in the CON MIX or the DC 5. The DC 5 clone also showed decreased src-FAK interaction but not to the same extent as S3 31. However, the role of src and FAK interaction needs to be further investigated.

We also studied the kinetic of localization of src in FAs by stimulating starved clones with FCS. We performed co-localization experiments of fixed cells at different time points with anti-Src, anti-FAK and anti-paxilin antibodies. Although some differences were observed between CON MIX, DC 5 and S3 31 cells, more work is required before conclusions can be drawn.

4.3.3.5. Implication of GTPases

As already mentioned, most of the changes in organization of the actin cytoskeleton are based on the activation of the small GTPases. The increase in Rho A activity observed in DC 5 cells is in agreement with their higher cell-substrate adhesion. The higher activity of cdc 42 was somehow surprising. It should be said that the interpretation of these results has to be taken with caution. Although several experiments were performed, only one valuable experiment could be obtained. This result is therefore specific for the exact conditions in which it was obtained. Abundant parameters influence the outcome of the pull-down experiments such as cell density, cell type, presence or absence of serum, etc. Besides, the kinetics for activation of the GTPases varies highly in each cell system. More experiments will have to be performed in order to establish more carefully and precisely the activity of each GTPase in the clones. One possibility would be to assess in each clone a kinetic of activation for each GTPase with the factors specific for each of them: PDGF for Rac 1, LPA for Rho A and bradykinin or S1P for cdc 42 (Kozma et al., 1995; Ridley, 2001; Ridley and Hall, 1992), ***see also tab. 1.2***. Injection of

dominant negative forms of the GTPases or their inhibitors into transiently or stably transfected cells can be used to reverse phenotypes.

Indeed, we performed the wound-healing experiments in the presence of the Rho A inhibitor C3-transferase in order to reverse the DC 5 phenotype. Under our experimental conditions, results were inconclusive and experiments need to be repeated.

As final remarks it should be said that of course it is not possible to discuss the results from the transient transfection experiments independently from those obtained with the stably transfected clones, since they were performed by analyzing the same protein.

Thus, why does the transient transfection of FL-syndecan-3 leads to the generation of filopodia while in stably transfected cells only slight phenotypic and functional effects are seen?

One could argue that the effects seen in the transient transfection experiments were artifacts due to over-expression of the protein. In order to eliminate these doubts, experiments were performed which compared syndecan-2 and syndecan-3 transfected cells behind an untransfected background. Labeling and therefore expression obtained after FL-transfection with syndecan-3 and syndecan-2 was comparable (Granes et al., 1999). In further experiments it was demonstrated that even the low syndecan-3 expresser showed significant changes in the organization of the cytoskeleton. This makes it clear that the filopodia-generating effect of syndecan-3 was no artifact.

Nevertheless, the amount of protein expression is clearly higher in transient than in stable transfectants. A possible hypothesis, which may link the observations made in both types of transfectants is that concentration-dependent oligomerization of syndecan-3 with itself or with syndecan-4 plays a key role in the observed effects. Thus, in transient transfected cells, the “critical” concentration for oligomerization may be reached independently of ligand binding, and downstream signaling is induced. In cells stably expressing syndecan-3, on the other hand, we would find a more “physiological” situation where syndecan-3 does not play any function when not binding to its specific ligand or where oligomerization is tightly controlled by kinases and phosphatases. On the other hand, when deleting the cytoplasmic domain, in transient transfection, oligomerization takes place but no down-stream signaling is induced. In the stable cell lines this cytoplasmic deleted construct does not lie under control by phosphorylation and oligomerize with syndecan-4 contributing to the formation of FAs.

In any case, whether oligomerization occurs or not and how, as well as the implications of the ERM proteins and the small GTPases in these processes remain to be established.

Conclusions

1: Human syndecan-3 shows a high homology with syndecan-3 cDNA and protein sequences from other species. In contrast, amino acids 7-23 lying in the putative signal peptide are strikingly different.

2: Human syndecan-3 mRNA is highly expressed in brain, spleen, colon and adrenal gland.

3: Transient expression of human syndecan-3 induces the generation of long filopodia-like structures, microspikes and varicosities in different cell lines.

4: Induction of filopodia-like structures depends on the presence of sugar chains since neither CHO 745 cells nor CHO K1 cells in the presence of heparin were able to generate filopodia-like structures upon syndecan-3 transfection.

5: The C1-region from human syndecan-3 cytoplasmic tail has been implicated in the filopodia-inducing effect. Deletion experiments demonstrated that PDZ-proteins are not direct partners for transducing signals from syndecan-3 towards the actin cytoskeleton.

6: Stable expression of full-length syndecan-3 in CHO K1 cell slightly changes their phenotypic and functional characteristics, while expression of cytoplasmic-deleted syndecan-3 decreases their proliferation and migration while increasing in cell-substrate adhesion.

7: The phenotypic and functional effects observed in the cytoplasmic-deleted transfectants are associated with molecular changes such as an increase of stress fibers and focal adhesions. We propose an implication of the small Rho GTPases activating members of the ERM family which function as cross-linker molecules between transmembrane proteins and the actin cytoskeleton.

Literature

A

Aktories,K. (1997). Bacterial toxins that target Rho proteins. J. Clin. Invest. 99, 827-9.

Alexander,C.M., Reichsman,F., Hinkes,M.T., Lincecum,J., Becker,K.A., Cumberledge,S., and Bernfield,M. (2000). Syndecan-1 is required for Wnt-1-induced mammary tumorigenesis in mice. Nat. Genet. Jul;25(3):329-32.

Allen,W.E., Jones,G.E., Pollard,J.W., and Ridley,A.J. (1997). Rho, Rac and Cdc42 regulate actin organization and cell adhesion in macrophages. J. Cell Sci. 110, 707-20.

Amieva,M.R., Litman,P., Huang,L., Ichimaru,E., and Furthmayr,H. (1999). Disruption of dynamic cell surface architecture of NIH3T3 fibroblasts by the N-terminal domains of moesin and ezrin: in vivo imaging with GFP fusion proteins. J. Cell Sci. 112, 111-125.

Angst,B.D., Marcozzi,C., and Magee,A.I. (2001). The cadherin superfamily: diversity in form and function. J. Cell Sci. *114*, 629-641.

Anttonen,A., Kajanti,M., Heikkila,P., Jalkanen,M., and Joensuu,H. (1999). Syndecan-1 expression has prognostic significance in head and neck carcinoma. Br. J. Cancer 79, 558-564.

Aplin,A.E., Howe,A.K., and Juliano,R.L. (1999). Cell adhesion molecules, signal transduction and cell growth. Curr. Opin. Cell Biol. 11, 737-44.

Asundi,V.K. and Carey,D.J. (1995). Self-association of N-syndecan (syndecan-3) core protein is mediated by a novel structural motif in the transmembrane domain and ectodomain flanking region. J. Biol. Chem. 270, 26404-26410.

Asundi,V.K. and Carey,D.J. (1997). Phosphorylation of recombinant N-syndecan (syndecan 3) core protein. Biochem. Biophys. Res. Commun. 240, 502-506.

Asundi,V.K., Keister,B.F., Stahl,R.C., and Carey,D.J. (1997). Developmental and cell-type-specific expression of cell surface heparan sulfate proteoglycans in the rat heart. Exp. Cell Res. 230, 145-153.

B

Baciu,P.C. and Goetinck,P.F. (1995). Protein kinase C regulates the recruitment of syndecan-4 into focal contacts. Mol. Biol. Cell 6, 1503-1513.

Baciu,P.C., Saoncella,S., Lee,S.H., Denhez,F., Leuthardt,D., and Goetinck,P.F. (2000). Syndesmos, a protein that interacts with the cytoplasmic domain of syndecan-4, mediates cell spreading and actin cytoskeletal organization. J. Cell Sci. Jan;113. Pt. 2:315-24.

Bansal,R. and Pfeiffer,S.E. (1994). Inhibition of protein and lipid sulfation in oligodendrocytes blocks biological responses to FGF-2 and retards cytoarchitectural maturation, but not developmental lineage progression. Dev. Biol. 162, 511-24.

Bar-Sagi,D. and Hall,A. (2000). Ras and Rho GTPases: a family reunion. Cell. Oct. 13;103(2):227-38.

Bernfield,M., Gotte,M., Park,P.W., Reizes,O., Fitzgerald,M.L., Lincecum,J., and Zako,M. (1999). Functions of cell surface heparan sulfate proteoglycans. Annu. Rev. Biochem. 68:729-77, 729-777.

Bernfield,M., Hinkes,M.T., and Gallo,R.L. (1993). Developmental expression of the syndecans: possible function and regulation. Dev. Suppl. *:205-12.*, 205-12.

Bernfield,M., Kokenyesi,R., Kato,M., Hinkes,M.T., Spring,J., Gallo,R.L., and Lose,E.J. (1992). Biology of the syndecans: a family of transmembrane heparan sulfate proteoglycans. Annu. Rev. Cell Biol. 8:365-93, 365-393.

Bjorge,J.D., Jakymiw,A., and Fujita,D.J. (2000). Selected glimpses into the activation and function of Src kinase. Oncogene 20;19, 5620-5635.

Blackhall,F.H., Merry,C.L., Davies,E.J., and Jayson,G.C. (2001). Heparan sulfate proteoglycans and cancer. Br. J. Cancer. Oct. 85, 1094-8.

Bobak,D.A. (1999). Clostridial toxins: molecular probes of Rho-dependent signaling and apoptosis. Mol. Cell Biochem. 193, 37-42.

Borman,L.S. and Branda,R.F. (1989). Nutritional folate deficiency in Chinese hamster ovary cells. I. Characterization of the pleiotropic response and its modulation by nucleic acid precursors. J. Cell Physiol 140, 335-343.

Bredt,D.S. (2000). Cell biology. Reeling CASK into the nucleus. Nature. Mar. 16;404(6775):241-2.

Bretscher,A. (1999). Regulation of cortical structure by the ezrin-radixin-moesin protein family. Curr. Opin. Cell Biol. 11, 109-116.

Bretscher,A., Chambers,D., Nguyen,R., and Reczek,D. (2000). ERM-Merlin and EBP50 protein families in plasma membrane organization and function. Annu. Rev. Cell Dev. Biol. *16:113-43.*, 113-143.

C

Calderwood,D.A., Shattil,S.J., and Ginsberg,M.H. (2000). Integrins and actin filaments: reciprocal regulation of cell adhesion and signaling. J. Biol. Chem. Jul. 28;275(30):22607-10.

Carey,D.J. (1996). N-syndecan: structure and function of a transmembrane heparan sulfate proteoglycan. Perspect. Dev. Neurobiol. 3, 331-346.

Carey,D.J. (1997). Syndecans: multifunctional cell-surface co-receptors. Biochem. J. 327, 1-16.

Carey,D.J., Bendt,K.M., and Stahl,R.C. (1996). The cytoplasmic domain of syndecan-1 is required for cytoskeleton association but not detergent insolubility. Identification of essential cytoplasmic domain residues. J. Biol. Chem. 271, 15253-15260.

Carey,D.J., Conner,K., Asundi,V.K., O'Mahony,D.J., Stahl,R.C., Showalter,L., Cizmeci-Smith,G., Hartman,J., and Rothblum,L.I. (1997). cDNA cloning, genomic organization, and in vivo expression of rat N-syndecan. J. Biol. Chem. 272, 2873-2879.

Carey,D.J., Evans,D.M., Stahl,R.C., Asundi,V.K., Conner,K.J., Garbes,P., and Cizmeci-Smith,G. (1992). Molecular cloning and characterization of N-syndecan, a novel transmembrane heparan sulfate proteoglycan. J. Cell Biol. 117, 191-201.

Carey,D.J., Stahl,R.C., Cizmeci-Smith,G., and Asundi,V.K. (1994a). Syndecan-1 expressed in Schwann cells causes morphological transformation and cytoskeletal reorganization and associates with actin during cell spreading. J. Cell Biol. 124, 161-170.

Carey,D.J., Stahl,R.C., Tucker,B., Bendt,K.A., and Cizmeci-Smith,G. (1994b). Aggregation-induced association of syndecan-1 with microfilaments mediated by the cytoplasmic domain. Exp. Cell Res. 214, 12-21.

Carlier,M.F., Ducruix,A., and Pantaloni,D. (1999). Signalling to actin: the Cdc42-N-WASP-Arp2/3 connection. Chem. Biol. 6, R235-R240.

Chernousov,M.A. and Carey,D.J. (1993). N-syndecan (syndecan 3) from neonatal rat brain binds basic fibroblast growth factor. J. Biol. Chem. 268, 16810-16814.

Chernousov,M.A., Stahl,R.C., and Carey,D.J. (1996). Schwann cells secrete a novel collagen-like adhesive protein that binds N-syndecan. J. Biol. Chem. 271, 13844-13853.

Chernousov,M.A., Stahl,R.C., and Carey,D.J. (2001). Schwann cell type V collagen inhibits axonal outgrowth and promotes Schwann cell migration via distinct adhesive activities of the collagen and noncollagen domains. J. Neurosci. Aug. 15;21(16):6125-35.

Cizmeci-Smith,G., Langan,E., Youkey,J., Showalter,L.J., and Carey,D.J. (1997). Syndecan-4 is a primary-response gene induced by basic fibroblast growth factor and arterial injury in vascular smooth muscle cells. Arterioscler. Thromb. Vasc. Biol. 17, 172-80.

Clasper,S., Vekemans,S., Fiore,M., Plebanski,M., Wordsworth,P., David,G., and Jackson,D.G. (1999). Inducible expression of the cell surface heparan sulfate proteoglycan syndecan-2 (fibroglycan) on human activated macrophages can regulate fibroblast growth factor action. J. Biol. Chem. 274, 24113-24123.

Cleveland,D.W., Fischer,S.G., Kirschner,M.W., and Laemmli,U.K. (1977). Peptide mapping by limited proteolysis in sodium dodecyl sulfate and analysis by gel electrophoresis. J. Biol. Chem. 252, 1102-1106.

Cohen,A.R., Woods,D.F., Marfatia,S.M., Walther,Z., Chishti,A.H., Anderson,J.M., and Wood,D.F.c.t.W.D. (1998). Human CASK/LIN-2 binds syndecan-2 and protein 4.1 and localizes to the basolateral membrane of epithelial cells. J. Cell Biol. 142, 129-138.

Coleman,M.L., Sahai,E.A., Yeo,M., Bosch,M., Dewar,A., and Olson,M.F. (2001). Membrane blebbing during apoptosis results from caspase-mediated activation of ROCK I. Nat. Cell Biol. Apr;3(4):339-45.

Conejo,J.R., Kleeff,J., Koliopanos,A., Matsuda,K., Zhu,Z.W., Goecke,H., Bicheng,N., Zimmermann,A., Korc,M., Friess,H., and Buchler,M.W. (2000). Syndecan-1 expression is up-regulated in pancreatic but not in other gastrointestinal cancers. Int. J. Cancer. Oct. 1;88(1):12-20.

Contreras,H.R., Fabre,M., Granes,F., Casaroli-Marano,R., Rocamora,N., Herreros,A.G., Reina,M., and Vilaro,S. (2001). Syndecan-2 expression in colorectal cancer-derived HT-29 M6 epithelial cells induces a migratory phenotype. Biochem. Biophys. Res. Commun. Aug. 31;286(4):742-51.

Cornelison,D.D., Filla,M.S., Stanley,H.M., Rapraeger,A.C., and Olwin,B.B. (2001). Syndecan-3 and syndecan-4 specifically mark skeletal muscle satellite cells and are implicated in satellite cell maintenance and muscle regeneration. Dev. Biol. 2001. Nov. 1;239(1):79-94. 239.

Coso,O.A., Chiariello,M., Yu,J.C., Teramoto,H., Crespo,P., Xu,N., Miki,T., and Gutkind,J.S. (1995). The small GTP-binding proteins Rac1 and Cdc42 regulate the activity of the JNK/SAPK signaling pathway. Cell 81, 1137-46.

Couchman,J.R. and Woods,A. (1996). Syndecans, signaling, and cell adhesion. J. Cell Biochem. 61, 578-584.

Couchman,J.R. and Woods,A. (1999). Syndecan-4 and integrins: combinatorial signaling in cell adhesion [comment]. J. Cell Sci. 112, 3415-3420.

Craven,S.E. and Bredt,D.S. (1998). PDZ proteins organize synaptic signaling pathways. Cell 93, 495-498.

D

David,G. (1993). Integral membrane heparan sulfate proteoglycans. FASEB J. 7, 1023-1030.

Delehedde,M., Lyon,M., Sergeant,N., Rahmoune,H., and Fernig,D.G. (2001). Proteoglycans: pericellular and cell surface multireceptors that integrate external stimuli in the mammary gland. J. Mammary. Gland. Biol. Neoplasia. Jul;6(3):253-73.

Denhez,F., Wilcox-Adelman,S.A., Baciu,P.C., Saoncella,S., Lee,S., French,B., Neveu,W., and Goetinck,P.F. (2002). Syndesmos, a syndecan-4 cytoplasmic domain interactor, binds to the focal adhesion adaptor proteins paxillin and hic-5. J. Biol. Chem. Apr. 5;277(14):12270-4.

Derksen,P.W., Keehnen,R.M., Evers,L.M., van Oers,M.H., Spaargaren,M., and Pals,S.T. (2002). Cell surface proteoglycan syndecan-1 mediates hepatocyte growth factor binding and promotes Met signaling in multiple myeloma. Blood. Feb. 15;99(4):1405-10.

Dhodapkar,M.V., Abe,E., Theus,A., Lacy,M., Langford,J.K., Barlogie,B., and Sanderson,R.D. (1998). Syndecan-1 is a multifunctional regulator of myeloma pathobiology: control of tumor cell survival, growth, and bone cell differentiation. Blood 91, 2679-88.

E

Echtermeyer,F., Baciu,P.C., Saoncella,S., Ge,Y., and Goetinck,P.F. (1999). Syndecan-4 core protein is sufficient for the assembly of focal adhesions and actin stress fibers. J. Cell Sci. 112, 3433-3441.

Echtermeyer,F., Streit,M., Wilcox-Adelman,S., Saoncella,S., Denhez,F., Detmar,M., and Goetinck,P. (2001). Delayed wound repair and impaired angiogenesis in mice lacking syndecan-4. J. Clin. Invest. Jan;107(2):R9-R14.

Elenius,K., Maatta,A., Salmivirta,M., and Jalkanen,M. (1992). Growth factors induce 3T3 cells to express bFGF-binding syndecan. J. Biol. Chem. 267, 6435-6441.

Elenius,K., Salmivirta,M., Inki,P., Mali,M., and Jalkanen,M. (1990). Binding of human syndecan to extracellular matrix proteins. J. Biol. Chem. 265, 17837-17843.

Elenius,K., Vainio,S., Laato,M., Salmivirta,M., Thesleff,I., and Jalkanen,M. (1991). Induced expression of syndecan in healing wounds. J. Cell Biol. 114, 585-595.

Erdman,R., Stahl,R.C., Rothblum,K., Chernousov,M.A., and Carey,D.J. (2002). Schwann cell adhesion to a novel heparan sulfate binding site in the N-terminal domain of alpha 4 type V collagen is mediated by syndecan-3. J. Biol. Chem. Mar. 1;277(9):7619-25.

Esko,J.D., Stewart,T.E., and Taylor,W.H. (1985). Animal cell mutants defective in glycosaminoglycan biosynthesis. Proc. Natl. Acad. Sci. U. S. A. 82, 3197-3201.

Ethell,I.M., Hagihara,K., Miura,Y., Irie,F., and Yamaguchi,Y. (2000). Synbindin, A novel syndecan-2-binding protein in neuronal dendritic spines [In Process Citation]. J. Cell Biol. Oct. 2;151(1):53-68.

Ethell,I.M., Irie,F., Kalo,M.S., Couchman,J.R., Pasquale,E.B., and Yamaguchi,Y. (2001). EphB/syndecan-2 signaling in dendritic spine morphogenesis. Neuron. Sep. 27;31(6):1001-13.

Ethell,I.M. and Yamaguchi,Y. (1999). Cell surface heparan sulfate proteoglycan syndecan-2 induces the maturation of dendritic spines in rat hippocampal neurons. J. Cell Biol. 144, 575-586.

F

Fages,C., Kaksonen,M., Kinnunen,T., Punnonen,E.L., and Rauvala,H. (1998). Regulation of mRNA localization by transmembrane signalling: local interaction of HB-GAM (heparin-binding growth-associated molecule) with the cell surface localizes beta-actin mRNA. J. Cell Sci. 111, 3073-3080.

Feyzi,E., Trybala,E., Bergstrom,T., Lindahl,U., and Spillmann,D. (1997). Structural requirement of heparan sulfate for interaction with herpes simplex virus type 1 virions and isolated glycoprotein C. J. Biol. Chem. 272, 24850-7.

Filla,M.S., Dam,P., and Rapraeger,A.C. (1998). The cell surface proteoglycan syndecan-1 mediates fibroblast growth factor-2 binding and activity. J. Cell Physiol. 174, 310-21.

Fitzgerald,M.L., Wang,Z., Park,P.W., Murphy,G., and Bernfield,M. (2000). Shedding of syndecan-1 and -4 ectodomains is regulated by multiple signaling pathways and mediated by a TIMP-3-sensitive metalloproteinase. J. Cell Biol. Feb. 21;148(4):811-24.

Fuentealba,L., Carey,D.J., and Brandan,E. (1999). Antisense inhibition of syndecan-3 expression during skeletal muscle differentiation accelerates myogenesis through a basic fibroblast growth factor-dependent mechanism. J. Biol. Chem. 274, 37876-37884.

Fukata,M., Nakagawa,M., Kuroda,S., and Kaibuchi,K. (1999). Cell adhesion and Rho small GTPases. J. Cell Sci. *112*, 4491-4500.

Fuki,I.V., Kuhn,K.M., Lomazov,I.R., Rothman,V.L., Tuszynski,G.P., Iozzo,R.V., Swenson,T.L., Fisher,E.A., and Williams,K.J. (1997). The syndecan family of proteoglycans. Novel receptors mediating internalization of atherogenic lipoproteins in vitro. J. Clin. Invest. 100, 1611-1622.

Fukuchi,K., Hart,M., and Li,L. (1998). Alzheimer's disease and heparan sulfate proteoglycan. Front Biosci. 3:d327-37., d327-d337.

G

Gahmberg,C.G. and Tolvanen,M. (1996). Why mammalian cell surface proteins are glycoproteins. Trends. Biochem. Sci. 21, 308-311.

Gallo,R., Kim,C., Kokenyesi,R., Adzick,N.S., and Bernfield,M. (1996). Syndecans-1 and -4 are induced during wound repair of neonatal but not fetal skin. J. Invest Dermatol. 107, 676-683.

Gao,Y., Li,M., Chen,W., and Simons,M. (2000). Synectin, syndecan-4 cytoplasmic domain binding PDZ protein, inhibits cell migration. J. Cell Physiol. Sep;184(3):373-9.

Gard,A.L. and Pfeiffer,S.E. (1993). Glial cell mitogens bFGF and PDGF differentially regulate development of O4+GalC- oligodendrocyte progenitors. Dev. Biol. 159, 618-30.

Giancotti,F.G. and Ruoslahti,E. (1999). Integrin signaling. Science 285, 1028-32.

Gould,S.E., Upholt,W.B., and Kosher,R.A. (1992). Syndecan 3: a member of the syndecan family of membrane- intercalated proteoglycans that is expressed in high amounts at the onset of chicken limb cartilage differentiation. Proc. Natl. Acad. Sci. U. S. A. 89, 3271-3275.

Gould,S.E., Upholt,W.B., and Kosher,R.A. (1995). Characterization of chicken syndecan-3 as a heparan sulfate proteoglycan and its expression during embryogenesis. Dev. Biol. 168, 438-451.

Granes,F., Garcia,R., Casaroli-Marano,R.P., Castel,S., Rocamora,N., Reina,M., Urena,J.M., and Vilaro,S. (1999). Syndecan-2 induces filopodia by active cdc42Hs. Exp. Cell Res. 248, 439-56.

Granes,F., Urena,J.M., Rocamora,N., and Vilaro,S. (2000). Ezrin links syndecan-2 to the cytoskeleton. J. Cell Sci. Apr;113. (Pt. 7):1267-76.

Grootjans,J.J., Reekmans,G., Ceulemans,H., and David,G. (2000). Syntenin-syndecan binding requires syndecan-synteny and the co- operation of both PDZ domains of syntenin. J. Biol. Chem. Jun. 30;275(26):19933-41.

Grootjans,J.J., Zimmermann,P., Reekmans,G., Smets,A., Degeest,G., Durr,J., and David,G. (1997). Syntenin, a PDZ protein that binds syndecan cytoplasmic domains. Proc. Natl. Acad. Sci. U. S. A. 94, 13683-13688.

H

Hall,A. (1998). Rho GTPases and the actin cytoskeleton. Science 279, 509-514.

Hayashi,K., Hayashi,M., Jalkanen,M., Firestone,J.H., Trelstad,R.L., and Bernfield,M. (1987). Immunocytochemistry of cell surface heparan sulfate proteoglycan in mouse tissues. A light and electron microscopic study. J. Histochem. Cytochem. 35, 1079-88.

Henkemeyer,M. and Frisen,J. (2001). Eph receptors tingle the spine. Neuron. Sep. 27;31(6):876-7.

Higgs,H.N. and Pollard,T.D. (2000). Activation by Cdc42 and PIP(2) of Wiskott-Aldrich syndrome protein (WASp) stimulates actin nucleation by Arp2/3 complex. J. Cell Biol. Sep. 18;150(6):1311-20.

Hilgard,P. and Stockert,R. (2000). Heparan sulfate proteoglycans initiate dengue virus infection of hepatocytes. Hepatology. Nov;32(5):1069-77.

Hinkes,M.T., Goldberger,O.A., Neumann,P.E., Kokenyesi,R., and Bernfield,M. (1993). Organization and promoter activity of the mouse syndecan-1 gene. J. Biol. Chem. 268, 11440-11448.

Horowitz,A. and Simons,M. (1998a). Phosphorylation of the cytoplasmic tail of syndecan-4 regulates activation of protein kinase Calpha. J. Biol. Chem. 273, 25548-25551.

Horowitz,A. and Simons,M. (1998b). Regulation of syndecan-4 phosphorylation in vivo. J. Biol. Chem. 273, 10914-10918.

Howe,A., Aplin,A.E., Alahari,S.K., and Juliano,R.L. (1998). Integrin signaling and cell growth control. Curr. Opin. Cell Biol. 10, 220-231.

Hsueh,Y.P. and Sheng,M. (1999). Regulated expression and subcellular localization of syndecan heparan sulfate proteoglycans and the syndecan-binding protein CASK/LIN-2 during rat brain development. J. Neurosci. 19, 7415-7425.

Hsueh,Y.P., Roberts,A.M., Volta,M., Sheng,M., and Roberts,R.G. (2001). Bipartite interaction between neurofibromatosis type I protein (neurofibromin) and syndecan transmembrane heparan sulfate proteoglycans. J. Neurosci. Jun. 1;21(11):3764-70.

Hsueh,Y.P., Wang,T.F., Yang,F.C., and Sheng,M. (2000). Nuclear translocation and transcription regulation by the membrane-associated guanylate kinase CASK/LIN-2. Nature. Mar. 16;404(6775):298-302.

Hsueh,Y.P., Yang,F.C., Kharazia,V., Naisbitt,S., Cohen,A.R., Weinberg,R.J., and Sheng,M. (1998). Direct interaction of CASK/LIN-2 and syndecan heparan sulfate proteoglycan and their overlapping distribution in neuronal synapses. J. Cell Biol. 142, 139-151.

Hu,S. and Reichardt,L.F. (1999). From membrane to cytoskeleton: enabling a connection. Neuron 22, 419-422.

Hynes,R.O. (1992). Integrins: versatility, modulation, and signaling in cell adhesion. Cell 69, 11-25.

I

Iba,K., Albrechtsen,R., Gilpin,B., Frohlich,C., Loechel,F., Zolkiewska,A., Ishiguro,K., Kojima,T., Liu,W., Langford,J.K., Sanderson,R.D., Brakebusch,C., Fassler,R., and Wewer,U.M. (2000). The cysteine-rich domain of human ADAM 12 supports cell adhesion through syndecans and triggers signaling events that lead to beta1 integrin-dependent cell spreading [see comments]. J. Cell Biol. May. 29;149(5):1143-56.

Inatani,M., Haruta,M., Honjo,M., Oohira,A., Kido,N., Takahashi,M., Honda,Y., and Tanihara,H. (2001). Upregulated expression of N-syndecan, a transmembrane heparan sulfate proteoglycan, in differentiated neural stem cells. Brain Res. Nov. 30;920(1-2):217-21.

Inki,P. and Jalkanen,M. (1996). The role of syndecan-1 in malignancies. Ann. Med. 28, 63-7.

Inki,P., Gomez,M., Quintanilla,M., Cano,A., and Jalkanen,M. (1992). Expression of syndecan in transformed mouse keratinocytes. Lab. Invest. 67, 225-33.

Inki,P., Larjava,H., Haapasalmi,K., Miettinen,H.M., Grenman,R., and Jalkanen,M. (1994). Expression of syndecan-1 is induced by differentiation and suppressed by malignant transformation of human keratinocytes. Eur. J. Cell Biol. 63, 43-51.

Ishiguro,K., Kadomatsu,K., Kojima,T., Muramatsu,H., Iwase,M., Yoshikai,Y., Yanada,M., Yamamoto,K., Matsushita,T., Nishimura,M., Kusugami,K., Saito,H., and Muramatsu,T. (2001a). Syndecan-4 deficiency leads to high mortality of lipopolysaccharide-injected mice. J. Biol. Chem. Dec. 14;276(50):47483-8.

Ishiguro,K., Kadomatsu,K., Kojima,T., Muramatsu,H., Matsuo,S., Kusugami,K., Saito,H., and Muramatsu,T. (2001b). Syndecan-4 deficiency increases susceptibility to kappa- carrageenan-induced renal damage. Lab. Invest. Apr;81(4):509-16.

Ishiguro,K., Kadomatsu,K., Kojima,T., Muramatsu,H., Tsuzuki,S., Nakamura,E., Kusugami,K., Saito,H., and Muramatsu,T. (2000). Syndecan-4 deficiency impairs focal adhesion formation only under restricted conditions. J. Biol. Chem. Feb. 25;275(8):5249-52.

J

Jaakkola,P. and Jalkanen,M. (1999). Transcriptional regulation of Syndecan-1 expression by growth factors. Prog. Nucleic. Acid. Res. Mol. Biol. 63:109-38, 109-138.

Jaakkola,P., Kontusaari,S., Kauppi,T., Maata,A., and Jalkanen,M. (1998). Wound reepithelialization activates a growth factor-responsive enhancer in migrating keratinocytes. FASEB J. 12, 959-69.

Jaakkola,P., Vihinen,T., Maatta,A., and Jalkanen,M. (1997). Activation of an enhancer on the syndecan-1 gene is restricted to fibroblast growth factor family members in mesenchymal cells. Mol. Cell Biol. 17, 3210-3219.

Jalkanen,M., Rapraeger,A., Saunders,S., and Bernfield,M. (1987). Cell surface proteoglycan of mouse mammary epithelial cells is shed by cleavage of its matrix-binding ectodomain from its membrane-associated domain. J. Cell Biol. 105, 3087-96.

Juliano,R.L. (2002). Signal transduction by cell adhesion receptors and the cytoskeleton: functions of integrins, cadherins, selectins, and immunoglobulin-superfamily members. Annu. Rev. Pharmacol. Toxicol. 42:283-323.

K

Kaibuchi,K., Kuroda,S., and Amano,M. (1999). Regulation of the cytoskeleton and cell adhesion by the Rho family GTPases in mammalian cells. Annu. Rev. Biochem. 68:459-86.

Kainulainen,V., Wang,H., Schick,C., and Bernfield,M. (1998). Syndecans, heparan sulfate proteoglycans, maintain the proteolytic balance of acute wound fluids. J. Biol. Chem. 273, 11563-9.

Kaplan,K.B., Swedlow,J.R., Morgan,D.O., and Varmus,H.E. (1995). c-Src enhances the spreading of src-/- fibroblasts on fibronectin by a kinase-independent mechanism. Genes Dev. 9, 1505-1517.

Kapus,A., Szaszi,K., Sun,J., Rizoli,S., and Rotstein,O.D. (1999). Cell shrinkage regulates Src kinases and induces tyrosine phosphorylation of cortactin, independent of the osmotic regulation of Na+/H+ exchangers. J. Biol. Chem. 19;274, 8093-8102.

Kato,M., Saunders,S., Nguyen,H., and Bernfield,M. (1995). Loss of cell surface syndecan-1 causes epithelia to transform into anchorage-independent mesenchyme-like cells. Mol. Biol. Cell 6, 559-576.

Kato,M., Wang,H., Kainulainen,V., Fitzgerald,M.L., Ledbetter,S., Ornitz,D.M., and Bernfield,M. (1998). Physiological degradation converts the soluble syndecan-1 ectodomain from an inhibitor to a potent activator of FGF-2. Nat. Med. 4, 691-7.

Kaverina,I., Krylyshkina,O., and Small,J.V. (2002). Regulation of substrate adhesion dynamics during cell motility. Int. J. Biochem. Cell Biol. 34, 746-761.

Kim,C.W., Goldberger,O.A., Gallo,R.L., and Bernfield,M. (1994). Members of the syndecan family of heparan sulfate proteoglycans are expressed in distinct cell-, tissue-, and development- specific patterns. Mol. Biol. Cell 5, 797-805.

Kinnunen,A., Kinnunen,T., Kaksonen,M., Nolo,R., Panula,P., and Rauvala,H. (1998a). N-syndecan and HB-GAM (heparin-binding growth-associated molecule) associate with early axonal tracts in the rat brain. Eur. J. Neurosci. 10, 635-48.

Kinnunen,A., Niemi,M., Kinnunen,T., Kaksonen,M., Nolo,R., and Rauvala,H. (1999). Heparan sulphate and HB-GAM (heparin-binding growth-associated molecule) in the development of the thalamocortical pathway of rat brain. Eur. J. Neurosci. 11, 491-502.

Kinnunen,T., Kaksonen,M., Saarinen,J., Kalkkinen,N., Peng,H.B., and Rauvala,H. (1998b). Cortactin-Src kinase signaling pathway is involved in N-syndecan- dependent neurite outgrowth. J. Biol. Chem. 273, 10702-10708.

Kinnunen,T., Raulo,E., Nolo,R., Maccarana,M., Lindahl,U., and Rauvala,H. (1996). Neurite outgrowth in brain neurons induced by heparin-binding growth-associated molecule (HB-GAM) depends on the specific interaction of HB-GAM with heparan sulfate at the cell surface. J. Biol. Chem. 271, 2243-2248.

Kolset,S.O. and Salmivirta,M. (1999). Cell surface heparan sulfate proteoglycans and lipoprotein metabolism. Cell Mol. Life Sci. 56, 857-70.

Kondo,T., Takeuchi,K., Doi,Y., Yonemura,S., Nagata,S., and Tsukita,S. (1997). ERM (ezrin/radixin/moesin)-based molecular mechanism of microvillar breakdown at an early stage of apoptosis. J. Cell Biol. 139, 749-758.

Kornberg,L., Earp,H.S., Parsons,J.T., Schaller,M., and Juliano,R.L. (1992). Cell adhesion or integrin clustering increases phosphorylation of a focal adhesion-associated tyrosine kinase. J. Biol. Chem. *267*, 23439-42.

Koyama,E., Leatherman,J.L., Shimazu,A., Nah,H.D., and Pacifici,M. (1996a). Syndecan-3, tenascin-C, and the development of cartilaginous skeletal elements and joints in chick limbs. Dev. Dyn. 203, 152-162.

Koyama,E., Shimazu,A., Leatherman,J.L., Golden,E.B., Nah,H.D., and Pacifici,M. (1996b). Expression of syndecan-3 and tenascin-C: possible involvement in periosteum development. J. Orthop. Res. 14, 403-412.

Kozma,R., Ahmed,S., Best,A., and Lim,L. (1995). The Ras-related protein Cdc42Hs and bradykinin promote formation of peripheral actin microspikes and filopodia in Swiss 3T3 fibroblasts. Mol. Cell Biol. 15, 1942-1952.

Kumar-Singh,S., Jacobs,W., Dhaene,K., Weyn,B., Bogers,J., Weyler,J., and Van Marck,E. (1998). Syndecan-1 expression in malignant mesothelioma: correlation with cell differentiation, WT1 expression, and clinical outcome. J. Pathol. 186, 300-305.

Kusano,Y., Oguri,K., Nagayasu,Y., Munesue,S., Ishihara,M., Saiki,I., Yonekura,H., Yamamoto,H., and Okayama,M. (2000). Participation of syndecan 2 in the induction of stress fiber formation in cooperation with integrin alpha5beta1: structural characteristics of heparan sulfate chains with avidity to COOH- terminal heparin-binding domain of fibronectin. Exp. Cell Res. May. 1;256(2):434-44.

L

Lamarche,N., Tapon,N., Stowers,L., Burbelo,P.D., Aspenstrom,P., Bridges,T., Chant,J., and Hall,A. (1996). Rac and Cdc42 induce actin polymerization and G1 cell cycle progression independently of p65PAK and the JNK/SAPK MAP kinase cascade. Cell 87, 519-29.

Lander,A.D. (1993). Proteoglycans in the nervous system. Curr. Opin. Neurobiol. 3, 716-723.

Lander,A.D. (1998). Proteoglycans: master regulators of molecular encounter? Matrix Biol. 17, 465-472.

Landry,R., Rioux,V., and Bensadoun,A. (2001). Characterization of syndecan-4 expression in 3T3-F442A mouse adipocytes: link between syndecan-4 induction and cell proliferation. Cell Growth Differ. Oct;12(10):497-504.

Larrain,J., Carey,D.J., and Brandan,E. (1998). Syndecan-1 expression inhibits myoblast differentiation through a basic fibroblast growth factor-dependent mechanism. J. Biol. Chem. 273, 32288-32296.

Lauri,S.E., Kaukinen,S., Kinnunen,T., Ylinen,A., Imai,S., Kaila,K., Taira,T., and Rauvala,H. (1999). Reg1ulatory role and molecular interactions of a cell-surface heparan sulfate proteoglycan (N-syndecan) in hippocampal long- term potentiation. J. Neurosci. 19, 1226-1235.

Lauri,S.E., Rauvala,H., Kaila,K., and Taira,T. (1998). Effect of heparin-binding growth-associated molecule (HB-GAM) on synaptic transmission and early LTP in rat hippocampal slices. Eur. J. Neurosci. 10, 188-194.

Lauri,S.E., Taira,T., Kaila,K., and Rauvala,H. (1996). Activity-induced enhancement of HB-GAM expression in rat hippocampal slices. Neuroreport. 7, 1670-1674.

Lebakken,C.S. and Rapraeger,A.C. (1996). Syndecan-1 mediates cell spreading in transfected human lymphoblastoid (Raji) cells. J. Cell Biol. 132, 1209-1221.

Lee,D., Oh,E.S., Woods,A., Couchman,J.R., and Lee,W. (1998). Solution structure of a syndecan-4 cytoplasmic domain and its interaction with phosphatidylinositol 4,5-bisphosphate. J. Biol. Chem. 273, 13022-13029.

Leppa,S., Mali,M., Miettinen,H.M., and Jalkanen,M. (1992). Syndecan expression regulates cell morphology and growth of mouse mammary epithelial tumor cells. Proc. Natl. Acad. Sci. U. S. A. 89, 932-936.

Lerm,M., Schmidt,G., and Aktories,K. (2000). Bacterial protein toxins targeting rho GTPases. FEMS Microbiol. Lett. Jul. 1;188(1):1-6.

Leverrier,Y. and Ridley,A.J. (2001). Apoptosis: caspases orchestrate the ROCK 'n' bleb. Nat. Cell Biol. Apr;3(4):E91-3.

Lindahl,U., Kusche-Gullberg,M., and Kjellen,L. (1998). Regulated diversity of heparan sulfate. J. Biol. Chem. 273, 24979-24982.

Longley,R.L., Woods,A., Fleetwood,A., Cowling,G.J., Gallagher,J.T., and Couchman,J.R. (1999). Control of morphology, cytoskeleton and migration by syndecan-4 [see comments]. J. Cell Sci. 112, 3421-3431.

Lookene,A., Savonen,R., and Olivecrona,G. (1997). Interaction of lipoproteins with heparan sulfate proteoglycans and with lipoprotein lipase. Studies by surface plasmon resonance technique. Biochemistry 36, 5267-75.

M

Maatta,A., Jaakkola,P., and Jalkanen,M. (1999). Extracellular matrix-dependent activation of syndecan-1 expression in keratinocyte growth factor-treated keratinocytes. J. Biol. Chem. 274, 9891-9898.

Mackay,D.J., Esch,F., Furthmayr,H., and Hall,A. (1997). Rho- and rac-dependent assembly of focal adhesion complexes and actin filaments in permeabilized fibroblasts: an essential role for ezrin/radixin/moesin proteins. J. Cell Biol. 138, 927-938.

Mali,M., Andtfolk,H., Miettinen,H.M., and Jalkanen,M. (1994). Suppression of tumor cell growth by syndecan-1 ectodomain. J. Biol. Chem. 269, 27795-27798.

Mali,M., Jaakkola,P., Arvilommi,A.M., and Jalkanen,M. (1990). Sequence of human syndecan indicates a novel gene family of integral membrane proteoglycans. J. Biol. Chem. 265, 6884-6889.

Mangeat,P., Roy,C., and Martin,M. (1999). ERM proteins in cell adhesion and membrane dynamics. Trends. Cell Biol. 9, 187-192.

Martinho,R.G., Castel,S., Urena,J., Fernandez-Borja,M., Makiya,R., Olivecrona,G., Reina,M., Alonso,A., and Vilaro,S. (1996). Ligand binding to heparan sulfate proteoglycans induces their aggregation and distribution along actin cytoskeleton. Mol. Biol. Cell 7, 1771-1788.

Matsui,T., Maeda,M., Doi,Y., Yonemura,S., Amano,M., Kaibuchi,K., Tsukita,S., and Tsukita,S. (1998). Rho-kinase phosphorylates COOH-terminal threonines of ezrin/radixin/moesin (ERM) proteins and regulates their head-to-tail association. J. Cell Biol. 140, 647-657.

Matsumoto,A., Ono,M., Fujimoto,Y., Gallo,R.L., Bernfield,M., and Kohgo,Y. (1997). Reduced expression of syndecan-1 in human hepatocellular carcinoma with high metastatic potential. Int. J. Cancer 74, 482-91.

McFall,A.J. and Rapraeger,A.C. (1997). Identification of an adhesion site within the syndecan-4 extracellular protein domain. J. Biol. Chem. 272, 12901-4.

McFall,A.J. and Rapraeger,A.C. (1998). Characterization of the high affinity cell-binding domain in the cell surface proteoglycan syndecan-4. J. Biol. Chem. 273, 28270-28276.

Mertens,G., Cassiman,J.J., Van den Berghe,H., Vermylen,J., and David,G. (1992). Cell surface heparan sulfate proteoglycans from human vascular endothelial cells. Core protein characterization and antithrombin III binding properties. J. Biol. Chem. 267, 20435-43.

Miki,H., Miura,K., and Takenawa,T. (1996). N-WASP, a novel actin-depolymerizing protein, regulates the cortical cytoskeletal rearrangement in a PIP2-dependent manner downstream of tyrosine kinases. EMBO J. 15, 5326-35.

Miki,H., Sasaki,T., Takai,Y., and Takenawa,T. (1998). Induction of filopodium formation by a WASP-related actin- depolymerizing protein N-WASP. Nature 391, 93-96.

Mills,J.C., Stone,N.L., Erhardt,J., and Pittman,R.N. (1998). Apoptotic membrane blebbing is regulated by myosin light chain phosphorylation. J. Cell Biol. 140, 627-636.

Minden,A., Lin,A., Claret,F.X., Abo,A., and Karin,M. (1995). Selective activation of the JNK signaling cascade and c-Jun transcriptional activity by the small GTPases Rac and Cdc42Hs. Cell 81, 1147-57.

Mitchison,T.J. and Cramer,L.P. (1996). Actin-based cell motility and cell locomotion. Cell 84, 371-379.

Modrowski,D., Basle,M., Lomri,A., and Marie,P.J. (2000). Syndecan-2 is involved in the mitogenic activity and signaling of granulocyte-macrophage colony-stimulating factor in osteoblasts. J. Biol. Chem. Mar. 31;275(13):9178-85.

Mueller,B.K. (1999). Growth cone guidance: first steps towards a deeper understanding. Annu. Rev. Neurosci. 22:351-88., 351-388.

Mullins,R.D. (2000). How WASP-family proteins and the Arp2/3 complex convert intracellular signals into cytoskeletal structures. Curr. Opin. Cell Biol. Feb;12(1):91-6.

Munesue,S., Kusano,Y., Oguri,K., Itano,N., Yoshitomi,Y., Nakanishi,H., Yamashina,I., and Okayama,M. (2002). The role of syndecan-2 in regulation of actin-cytoskeletal organization of Lewis lung carcinoma-derived metastatic clones. Biochem. J. Apr. 15;363(Pt. 2):201-9.

Murakami,M., Horowitz,A., Tang,S., Ware,J.A., and Simons,M. (2002). PKC-delta regulates PKC-alpha activity In a syndecan-4 dependent manner. J. Biol. Chem. *In preparation.*

N

Nakanishi,T., Kadomatsu,K., Okamoto,T., Ichihara-Tanaka,K., Kojima,T., Saito,H., Tomoda,Y., and Muramatsu,T. (1997). Expression of syndecan-1 and -3 during embryogenesis of the central nervous system in relation to binding with midkine. J. Biochem. (Tokyo) 121, 197-205.

Nielsen,H., Engelbrecht,J., Brunak,S., and von Heijne,G. (1997). Identification of prokaryotic and eukaryotic signal peptides and prediction of their cleavage sites. Protein Eng. 10, 1-6.

Nobes,C.D. and Hall,A. (1995). Rho, rac, and cdc42 GTPases regulate the assembly of multimolecular focal complexes associated with actin stress fibers, lamellipodia, and filopodia. Cell 81, 53-62.

Nobes,C.D. and Hall,A. (1999). Rho GTPases control polarity, protrusion, and adhesion during cell movement. J. Cell Biol. 144, 1235-1244.

Nobes,C.D., Hawkins,P., Stephens,L., and Hall,A. (1995). Activation of the small GTP-binding proteins rho and rac by growth factor receptors. J. Cell Sci. 108, 225-33.

Nolo,R., Kaksonen,M., Raulo,E., and Rauvala,H. (1995). Co-expression of heparin-binding growth-associated molecule (HB- GAM) and N-syndecan (syndecan-3) in developing rat brain. Neurosci. Lett. 191, 39-42.

O

Oh,E.S., Couchman,J.R., and Woods,A. (1997a). Serine phosphorylation of syndecan-2 proteoglycan cytoplasmic domain. Arch. Biochem. Biophys. 344, 67-74.

Oh,E.S., Woods,A., and Couchman,J.R. (1997b). Multimerization of the cytoplasmic domain of syndecan-4 is required for its ability to activate protein kinase C. J. Biol. Chem. 272, 11805-11811.

Oh,E.S., Woods,A., and Couchman,J.R. (1997c). Syndecan-4 proteoglycan regulates the distribution and activity of protein kinase C. J. Biol. Chem. 272, 8133-8136.

Oh,E.S., Woods,A., Lim,S.T., Theibert,A.W., and Couchman,J.R. (1998). Syndecan-4 proteoglycan cytoplasmic domain and phosphatidylinositol 4,5-bisphosphate coordinately regulate protein kinase C activity. J. Biol. Chem. 273, 10624-10629.

Olguin,H. and Brandan,E. (2001). Expression and localization of proteoglycans during limb myogenic activation. Dev. Dyn. May;221(1):106-15.

Olson,M.F., Ashworth,A., and Hall,A. (1995). An essential role for Rho, Rac, and Cdc42 GTPases in cell cycle progression through G1. Science 269, 1270-2.

Ott,V.L. and Rapraeger,A.C. (1998). Tyrosine phosphorylation of syndecan-1 and -4 cytoplasmic domains in adherent B82 fibroblasts. J. Biol. Chem. 273, 35291-35298.

P

Paglini,G., Kunda,P., Quiroga,S., Kosik,K., and Caceres,A. (1998). Suppression of radixin and moesin alters growth cone morphology, motility, and process formation in primary cultured neurons. J. Cell Biol. 19;143, 443-455.

Park,P.W., Pier,G.B., Hinkes,M.T., and Bernfield,M. (2001). Exploitation of syndecan-1 shedding by Pseudomonas aeruginosa enhances virulence. Nature. May. 3;411(6833):98-102.

Park,P.W., Pier,G.B., Preston,M.J., Goldberger,O., Fitzgerald,M.L., and Bernfield,M. (2000a). Syndecan-1 shedding is enhanced by LasA, a secreted virulence factor of Pseudomonas aeruginosa. J. Biol. Chem. Feb. 4;275(5):3057-64.

Park,P.W., Reizes,O., and Bernfield,M. (2000b). Cell surface heparan sulfate proteoglycans: selective regulators of ligand-receptor encounters. J. Biol. Chem. Sep. 29;275(39):29923-6.

Perrimon,N. and Bernfield,M. (2000). Specificities of heparan sulphate proteoglycans in developmental processes. Nature. Apr. 13;404(6779):725-8.

Pierce,A., Lyon,M., Hampson,I.N., Cowling,G.J., and Gallagher,J.T. (1992). Molecular cloning of the major cell surface heparan sulfate proteoglycan from rat liver. J. Biol. Chem. 267, 3894-3900.

Plow,E.F., Haas,T.A., Zhang,L., Loftus,J., and Smith,J.W. (2000). Ligand binding to integrins. J. Biol. Chem. Jul. 21;275(29):21785-8.

Poullet,P., Gautreau,A., Kadare,G., Girault,J.A., Louvard,D., and Arpin,M. (2001). Ezrin interacts with focal adhesion kinase and induces its activation independently of cell-matrix adhesion. J. Biol. Chem. Oct. 5;276(40):37686-91.

Prasthofer,T., Ek,B., Ekman,P., Owens,R., Hook,M., and Johansson,S. (1995). Protein kinase C phosphorylates two of the four known syndecan cytoplasmic domains in vitro. Biochem. Mol. Biol. Int. 36, 793-802.

R

Rapraeger,A.C. (1993). The coordinated regulation of heparan sulfate, syndecans and cell behavior. Curr. Opin. Cell Biol. 5, 844-853.

Rapraeger,A.C. (2000). Syndecan-regulated receptor signaling. J. Cell Biol. May. 29;149(5):995-8.

Rapraeger,A.C. (2001). Molecular interactions of syndecans during development. Semin. Cell Dev. Biol. Apr;12(2):107-16.

Raulo,E., Chernousov,M.A., Carey,D.J., Nolo,R., and Rauvala,H. (1994). Isolation of a neuronal cell surface receptor of heparin binding growth-associated molecule (HB-GAM). Identification as N-syndecan (syndecan-3). J. Biol. Chem. 269, 12999-13004.

Raulo,E., Julkunen,I., Merenmies,J., Pihlaskari,R., and Rauvala,H. (1992). Secretion and biological activities of heparin-binding growth- associated molecule. Neurite outgrowth-promoting and mitogenic actions of the recombinant and tissue-derived protein. J. Biol. Chem. 267, 11408-16.

Rauvala,H. and Peng,H.B. (1997). HB-GAM (heparin-binding growth-associated molecule) and heparin- type glycans in the development and plasticity of neuron-target contacts. Prog. Neurobiol. 52, 127-144.

Rauvala,H., Vanhala,A., Castren,E., Nolo,R., Raulo,E., Merenmies,J., and Panula,P. (1994). Expression of HB-GAM (heparin-binding growth-associated molecules) in the pathways of developing axonal processes in vivo and neurite outgrowth in vitro induced by HB-GAM. Brain Res. Dev. Brain Res. 79, 157-176.

Reiland,J., Ott,V.L., Lebakken,C.S., Yeaman,C., McCarthy,J., and Rapraeger,A.C. (1996). Pervanadate activation of intracellular kinases leads to tyrosine phosphorylation and shedding of syndecan-1. Biochem. J. 319, 39-47.

Reizes,O., Lincecum,J., Wang,Z., Goldberger,O., Huang,L., Kaksonen,M., Ahima,R., Hinkes,M.T., Barsh,G.S., Rauvala,H., and Bernfield,M. (2001). Transgenic expression of syndecan-1 uncovers a physiological control of feeding behavior by syndecan-3. Cell. Jul. 13;106(1):105-16.

Richardson,T.P., Trinkaus-Randall,V., and Nugent,M.A. (1999). Regulation of basic fibroblast growth factor binding and activity by cell density and heparan sulfate. J. Biol. Chem. 274, 13534-13540.

Ridley,A.J. (2001). Rho GTPases and cell migration. J. Cell Sci. Aug;114(Pt. 15):2713-22.

Ridley,A.J. and Hall,A. (1992). The small GTP-binding protein rho regulates the assembly of focal adhesions and actin stress fibers in response to growth factors. Cell 70, 389-99.

Rohatgi,R., Ma,L., Miki,H., Lopez,M., Kirchhausen,T., Takenawa,T., and Kirschner,M.W. (1999). The interaction between N-WASP and the Arp2/3 complex links Cdc42-dependent signals to actin assembly. Cell 97 , 221-31.

Rue,C.A. and Ryan,P. (2002). Characterization of pseudorabies virus glycoprotein C attachment to heparan sulfate proteoglycans. J. Gen. Virol. Feb;83(Pt. 2):301-9.

Ruoslahti,E. (1989). Proteoglycans in cell regulation. J. Biol. Chem. 264, 13369-13372.

Ruoslahti,E. and Yamaguchi,Y. (1991). Proteoglycans as modulators of growth factor activities. Cell 64, 867-869.

S

Salmivirta,M., Lidholt,K., and Lindahl,U. (1996). Heparan sulfate: a piece of information. FASEB J. 10, 1270-1279.

Sander,E.E., ten Klooster,J.P., van Delft,S., van der Kammen,R.A., and Collard,J.G. (1999). Rac downregulates Rho activity: reciprocal balance between both GTPases determines cellular morphology and migratory behavior. J. Cell Biol. 147, 1009-1022.

Sander,E.E., van Delft,S., ten Klooster,J.P., Reid,T., van der Kammen,R.A., Michiels,F., and Collard,J.G. (1998). Matrix-dependent Tiam1/Rac signaling in epithelial cells promotes either cell-cell adhesion or cell migration and is regulated by phosphatidylinositol 3-kinase. J. Cell Biol. 143, 1385-1398.

Sanderson,R.D., Sneed,T.B., Young,L.A., Sullivan,G.L., and Lander,A.D. (1992). Adhesion of B lymphoid (MPC-11) cells to type I collagen is mediated by integral membrane proteoglycan, syndecan. J. Immunol. 148, 3902-11.

Sanger,F., Nicklen,S., and Coulson,A.R. (1977). DNA sequencing with chain-terminating inhibitors. Proc. Natl. Acad. Sci. U. S. A 74, 5463-5467.

Saoncella,S., Echtermeyer,F., Denhez,F., Nowlen,J.K., Mosher,D.F., Robinson,S.D., Hynes,R.O., and Goetinck,P.F. (1999). Syndecan-4 signals cooperatively with integrins in a Rho- dependent manner in the assembly of focal adhesions and actin stress fibers. Proc. Natl. Acad. Sci. U. S. A. 96, 2805-2810.

Saphire,A.C., Bobardt,M.D., Zhang,Z., David,G., and Gallay,P.A. (2001). Syndecans serve as attachment receptors for human immunodeficiency virus type 1 on macrophages. J. Virol. Oct;75(19):9187-200.

Saunders,S., Jalkanen,M., O'Farrell,S., and Bernfield,M. (1989). Molecular cloning of syndecan, an integral membrane proteoglycan. J. Cell Biol. 108, 1547-1556.

Schaller,M.D., Hildebrand,J.D., and Parsons,J.T. (1999). Complex formation with focal adhesion kinase: A mechanism to regulate activity and subcellular localization of Src kinases. Mol. Biol. Cell 10, 3489-505.

Schlaepfer,D.D. and Hunter,T. (1996). Evidence for in vivo phosphorylation of the Grb2 SH2-domain binding site on focal adhesion kinase by Src-family protein- tyrosine kinases. Mol. Cell Biol. 16, 5623-33.

Schlessinger,J., Lax,I., and Lemmon,M. (1995). Regulation of growth factor activation by proteoglycans: what is the role of the low affinity receptors? Cell 83, 357-360.

Schubert,D., Schroeder,R., LaCorbiere,M., Saitoh,T., and Cole,G. (1988). Amyloid beta protein precursor is possibly a heparan sulfate proteoglycan core protein. Science 241, 223-226.

Schwartz,M.A. (2001). Integrin signaling revisited. Trends. Cell Biol. Dec;11(12):466-70.

Sebbagh,M., Renvoize,C., Hamelin,J., Riche,N., Bertoglio,J., and Breard,J. (2001). Caspase-3-mediated cleavage of ROCK I induces MLC phosphorylation and apoptotic membrane blebbing. Nat. Cell Biol. Apr;3(4):346-52.

Sebestyen,A., Totth,A., Mihalik,R., Szakacs,O., Paku,S., and Kopper,L. (2000). Syndecan-1-dependent homotypic cell adhesion in HT58 lymphoma cells. Tumour. Biol. *21*, 349-357.

Seghatoleslami,M.R. and Kosher,R.A. (1996). Inhibition of in vitro limb cartilage differentiation by syndecan-3 antibodies. Dev. Dyn. 207, 114-119.

Seidel,C., Sundan,A., Hjorth,M., Turesson,I., Dahl,I.M., Abildgaard,N., Waage,A., and Borset,M. (2000). Serum syndecan-1: a new independent prognostic marker in multiple myeloma. Blood. n. 15;95(2):388-92.

Seki,N., Ohira,M., Nagase,T., Ishikawa,K., Miyajima,N., Nakajima,D., Nomura,N., and Ohara,O. (1997). Characterization of cDNA clones in size-fractionated cDNA libraries from human brain. DNA Res. *4*, 345-349.

Selleck,S.B. (2000). Proteoglycans and pattern formation: sugar biochemistry meets developmental genetics. Trends. Genet. May;16(5):206-12.

Shimazu,A., Nah,H.D., Kirsch,T., Koyama,E., Leatherman,J.L., Golden,E.B., Kosher,R.A., and Pacifici,M. (1996). Syndecan-3 and the control of chondrocyte proliferation during endochondral ossification. Exp. Cell Res. 229, 126-136.

Small,J.V., Rottner,K., and Kaverina,I. (1999). Functional design in the actin cytoskeleton. Curr. Opin. Cell Biol. 11, 54-60.

Spring,J., Goldberger,O.A., Jenkins,N.A., Gilbert,D.J., Copeland,N.G., and Bernfield,M. (1994a). Mapping of the syndecan genes in the mouse: linkage with members of the myc gene family. Genomics *21*, 597-601.

Spring,J., Paine-Saunders,S.E., Hynes,R.O., and Bernfield,M. (1994b). Drosophila syndecan: conservation of a cell-surface heparan sulfate proteoglycan. Proc. Natl. Acad. Sci. U. S. A. 91, 3334-3338.

Stanley,M.J., Liebersbach,B.F., Liu,W., Anhalt,D.J., and Sanderson,R.D. (1995). Heparan sulfate-mediated cell aggregation. Syndecans-1 and -4 mediate intercellular adhesion following their transfection into human B lymphoid cells. J. Biol. Chem. *270*, 5077-5083.

Stanley,M.J., Stanley,M.W., Sanderson,R.D., and Zera,R. (1999). Syndecan-1 expression is induced in the stroma of infiltrating breast carcinoma. Am. J. Clin. Pathol. 112, 377-83.

Steinfeld,R., Van den Berghe,H., and David,G. (1996). Stimulation of fibroblast growth factor receptor-1 occupancy and signaling by cell surface-associated syndecans and glypican. J. Cell Biol. 133, 405-16.

Strauss,E. (2001). Cell biology. Fresh molecule whets appetite. Science. Jul. 13;293(5528):190.

Subramanian,S.V., Fitzgerald,M.L., and Bernfield,M. (1997). Regulated shedding of syndecan-1 and -4 ectodomains by thrombin and growth factor receptor activation. J. Biol. Chem. 272, 14713-14720.

Suetsugu,S., Miki,H., and Takenawa,T. (1998). The essential role of profilin in the assembly of actin for microspike formation. EMBO J. 17, 6516-6526.

T

Takagi,A., Kojima,T., Tsuzuki,S., Katsumi,A., Yamazaki,T., Sugiura,I., Hamaguchi,M., and Saito,H. (1996). Structural organization and promoter activity of the human ryudocan gene. J. Biochem. (Tokyo) 119, 979-84.

Takeichi,M. (1991). Cadherin cell adhesion receptors as a morphogenetic regulator. Science 251, 1451-1455.

Tapon,N. and Hall,A. (1997). Rho, Rac and Cdc42 GTPases regulate the organization of the actin cytoskeleton. Curr. Opin. Cell Biol. 9, 86-92.

Thomas,J.W., Ellis,B., Boerner,R.J., Knight,W.B., White,G.C., and Schaller,M.D. (1998). SH2- and SH3-mediated interactions between focal adhesion kinase and Src. J. Biol. Chem. 273, 577-583.

Thomas,S.M. and Brugge,J.S. (1997). Cellular functions regulated by Src family kinases. Annu. Rev. Cell Dev. Biol. 13:513-609., 513-609.

Timpson,P., Jones,G.E., Frame,M.C., and Brunton,V.G. (2001). Coordination of cell polarization and migration by the Rho family GTPases requires Src tyrosine kinase activity. Curr. Biol. Nov. 27;11(23):1836-46.

Tsuda,M., Kamimura,K., Nakato,H., Archer,M., Staatz,W., Fox,B., Humphrey,M., Olson,S., Futch,T., Kaluza,V., Siegfried,E., Stam,L., and Selleck,S.B. (1999). The cell-surface proteoglycan Dally regulates Wingless signalling in Drosophila. Nature 400, 276-80.

Tsujimoto,Y. and Suzuki,Y. (1979). Structural analysis of the fibroin gene at the 5' end and its surrounding regions. Cell 16, 425-436.

Tsukita,S. and Yonemura,S. (1997). ERM (ezrin/radixin/moesin) family: from cytoskeleton to signal transduction. Curr. Opin. Cell Biol. 9, 70-75.

Tsukita,S. and Yonemura,S. (1999). Cortical actin organization: lessons from ERM (ezrin/radixin/moesin) proteins. J. Biol. Chem. 274, 34507-10.

Tsuzuki,S., Kojima,T., Katsumi,A., Yamazaki,T., Sugiura,I., and Saito,H. (1997). Molecular cloning, genomic organization, promoter activity, and tissue-specific expression of the mouse ryudocan gene. J. Biochem. (Tokyo) 122, 17-24.

U/V

Utani,A., Nomizu,M., Matsuura,H., Kato,K., Kobayashi,T., Takeda,U., Aota,S., Nielsen,P.K., and Shinkai,H. (2001). A unique sequence of the laminin alpha 3 G domain binds to heparin and promotes cell adhesion through syndecan-2 and -4. J. Biol. Chem. Aug. 3;276(31):28779-88.

Vaheri,A., Carpen,O., Heiska,L., Helander,T.S., Jaaskelainen,J., Majander-Nordenswan,P., Sainio,M., Timonen,T., and Turunen,O. (1997). The ezrin protein family: membrane-cytoskeleton interactions and disease associations. Curr. Opin. Cell Biol. 9, 659-666.

Vainio,S., Lehtonen,E., Jalkanen,M., Bernfield,M., and Saxen,L. (1989). Epithelial-mesenchymal interactions regulate the stage-specific expression of a cell surface proteoglycan, syndecan, in the developing kidney. Dev. Biol. 134, 382-91.

van Horssen,J., Otte-Holler,I., David,G., Maat-Schieman,M.L., van den Heuvel,L.P., Wesseling,P., de Waal,R.M., and Verbeek,M.M. (2001). Heparan sulfate proteoglycan expression in cerebrovascular amyloid beta deposits in Alzheimer's disease and hereditary cerebral hemorrhage with amyloidosis (Dutch) brains. Acta Neuropathol. (Berl). Dec;102(6):604-14.

Vasioukhin,V., Bauer,C., Yin,M., and Fuchs,E. (2000). Directed actin polymerization is the driving force for epithelial cell-cell adhesion. Cell. Jan. 21;100(2):209-19.

Veugelers,M., Vermeesch,J., Watanabe,K., Yamaguchi,Y., Marynen,P., and David,G. (1998). GPC4, the gene for human K-glypican, flanks GPC3 on xq26: deletion of the GPC3-GPC4 gene cluster in one family with Simpson- Golabi-Behmel syndrome. Genomics 53, 1-11.

Vihinen,T., Auvinen,P., Alanen-Kurki,L., and Jalkanen,M. (1993). Structural organization and genomic sequence of mouse syndecan-1 gene. J. Biol. Chem. 268, 17261-17269.

Vihinen,T., Maatta,A., Jaakkola,P., Auvinen,P., and Jalkanen,M. (1996). Functional characterization of mouse syndecan-1 promoter. J. Biol. Chem. 271, 12532-41.

Volk,R., Schwartz,J.J., Li,J., Rosenberg,R.D., and Simons,M. (1999). The role of syndecan cytoplasmic domain in basic fibroblast growth factor-dependent signal transduction. J. Biol. Chem. 274, 24417-24.

W

Weaver,A.M., Karginov,A.V., Kinley,A.W., Weed,S.A., Li,Y., Parsons,J.T., and Cooper,J.A. (2001). Cortactin promotes and stabilizes Arp2/3-induced actin filament network formation. Curr. Biol. Mar. 6;11(5):370-4.

Weng,Z., Taylor,J.A., Turner,C.E., Brugge,J.S., and Seidel-Dugan,C. (1993). Detection of Src homology 3-binding proteins, including paxillin, in normal and v-Src-transformed Balb/c 3T3 cells. J. Biol. Chem. 268, 14956-63.

Williams,K.J. and Fuki,I.V. (1997). Cell-surface heparan sulfate proteoglycans: dynamic molecules mediating ligand catabolism. Curr. Opin. Lipidol. 8, 253-62.

Wood,W. and Martin,P. (2002). Structures in focus-filopodia. Int. J. Biochem. Cell Biol. 34, 726-730.

Woods,A. and Couchman,J.R. (1992). Protein kinase C involvement in focal adhesion formation. J. Cell Sci. 101, 277-90.

Woods,A. and Couchman,J.R. (1994). Syndecan 4 heparan sulfate proteoglycan is a selectively enriched and widespread focal adhesion component. Mol. Biol. Cell 5, 183-192.

Woods,A. and Couchman,J.R. (1998). Syndecans: synergistic activators of cell adhesion. Trends. Cell Biol. 8, 189-192.

Woods,A., Longley,R.L., Tumova,S., and Couchman,J.R. (2000). Syndecan-4 binding to the high affinity heparin-binding domain of fibronectin drives focal adhesion formation in fibroblasts. Arch. Biochem. Biophys. Feb. 1;374(1):66-72.

Woods,A., McCarthy,J.B., Furcht,L.T., and Couchman,J.R. (1993). A synthetic peptide from the COOH-terminal heparin-binding domain of fibronectin promotes focal adhesion formation. Mol. Biol. Cell 4, 605-13.

Y/Z

Yanagishita,M. and Hascall,V.C. (1992). Cell surface heparan sulfate proteoglycans. J. Biol. Chem. 267, 9451-9454.

Zak,I., Lewandowska,E., and Gnyp,W. (2000). Selectin glycoprotein ligands. Acta Biochim. Pol. *47*, 393-412.

Zhang,Z., Coomans,C., and David,G. (2001). Membrane heparan sulfate proteoglycan-supported FGF2-FGFR1 signaling: evidence in support of the "cooperative end structures" model. J. Biol. Chem. Nov. 9;276(45):41921-9.

Zhou,C., Yang,Y., and Jong,A.Y. (1990). Mini-prep in ten minutes. Biotechniques 8, 172-173.

Zimmermann,P. and David,G. (1999). The syndecans, tuners of transmembrane signaling. FASEB J. 13 Suppl:S91-S100.

Zimmermann,P., Tomatis,D., Rosas,M., Grootjans,J., Leenaerts,I., Degeest,G., Reekmans,G., Coomans,C., and David,G. (2001). Characterization of syntenin, a syndecan-binding PDZ protein, as a component of cell adhesion sites and microfilaments. Mol. Biol. Cell. Feb;12(2):339-50.

Zioncheck,T.F., Richardson,L., Liu,J., Chang,L., King,K.L., Bennett,G.L., Fugedi,P., Chamow,S.M., Schwall,R.H., and Stack,R.J. (1995). Sulfated oligosaccharides promote hepatocyte growth factor association and govern its mitogenic activity. J. Biol. Chem. 270, 16871-8.

b2-AdrR	β2-Adrenalin-Receptor
AD	Alzheimer's Disease
ADAM	A Disintegrin And Metalloproteinase
AGRP	Agouti-Related Protein
Amp	Ampicilin
AP	Alkaline Phosphatase
ARF	ADP Ribosylation Factor
ARP 2/3	Actin-Related Protein 2/3
ATCC	American Type Culture Collection
bFGF	basic Fibroblast Growth Factor
bp	base pair
BSA	Bovine Serum Albumin
CAM	Cell Adhesion Molecule
CAMK	Ca^{2+}-Calmodulin Dependent Protein Kinase
CAS	Crk-Associated Substrate
CASK	Ca^{2+}-Calmodulin-Dependent Serine Protein Kinase
CBD	Cell Binding Domain
CFTR	Cystic Fibrosis Transmembrane Conductance Regulator
CHO	Chinese Hamster Ovary
CIA	Chloroform:Isoamylacohol
CLSM	Confocal Laser Scanning Microscopy
CNS	Central Nervous System
CS	Chondroitin Sulfate
DAG	Diacylglycerol
dally	*division abnormally delayed*
dATP	2'-Deoxyadenosine-5'-Triphosphate
dCTP	2'-Deoxycytidine-5'-Triphosphate
ddNTPs	dideoxynucleosintriphosphate
DEAE	Diethylaminoethyl
DGTP	2'-Deoxyguanosine-5'-Triphosphate
DIC	Differential Interference Contrast
DMEM	Dulbecco's Modified Eagle Medium
DNA	Deoxyribonuclein Acid
dNTP	deoxynucleosintriphosphate
DPP	Decapentaplegic
DRGs	Dorsal Root Ganglions
DS	Dermatan Sulfalte
ds	double-strand
DTT	Dithiothreitol
DTTP	2'-Deoxythymidine-5'-Triphosphate
E3KARP	NHE3 Kinase A Regulatory Protein
EBP 50	(ERM)-binding phosphoprotein-50
ECL	Enhanced Chemiluminisence
ECM	Extracellular Matrix
EDTA	Ethylenediaminetetraacetic Acid
EGF	Epidermal Growth Factor
EphB2	Ephrin B2
ERK	Extracellular Signal-Regulated Kinase
ERM	Ezrin/Radixin/Moesin
FA	Focal Adhesion
FACS	Fluorescence Activated Cell Sorting
FAK	Focal Adhesion Kinase
FC	Focal Contact
FCS	Fetal Calf Serum
FGFR	Fibroblast Growth Factor Receptor
FIRE	FGF-Inducible Response Element
FL	Full-Length
FN	Fibronectin

g	gravity
GAG	Glycosaminoglycan
GalNAc	N-Acetylgalactosamine
GAP	GTPases Accelerating Protein
GCG	Genetics Computer Group
GDI	Guanine Nucleotide Dissociation Inhibitor
GEF	Guanine Nucleotide Exchange Factor
GFP	Green Fluorescent Protein
GlcA	Glucuronic Acid
GlcNAc	N-Acetylglucosamine
GPI	Glycosyl Phosphotidylinositol
GST	Glutathion-S-Transferase
GUK	Guanylate Kinase
HB-GAM	Heparin-Binding Growth-Associated Molecule
HEPES	N-[2-Hydroxyethyl]piperazine-N´-[2-ethanesulfonic acid]
HepII	Heparin-Binding (domain) II (of FN)
HFB	Human Fetal Brain
HGF	Hepatocyte Growth Factor
HIV	Human Immunodeficiency Virus
HL	Hepatic Lipase
HME	Hereditary Multiple Exostoses
HRP	Horse Radish Peroxidase
HS	Heparan Sulfate
HSPG	Heparan Sulfate Proteoglycan
HSV	Herpex Simplex Virus
IC	Immunocytochemistry
ICAM	Intercellular Adhesion Molecule
Ido A	Iduronic Acid
Ig	Immunoglobulin
IP	Immunoprecipitation
IPTG	Isopropyl-β-D-thiogalactopyranoside
JNK	C-Jun NH_2-Terminal Kinase
Kan	Kanamycin
KGF	Keratinocyte Growth Factor
KS	Keratan Sulfate
LB	Luria Broth
LPA	Lysophosphatidic Acid
LPL	Lipoprotein Lipase
LPS	Lipopolysaccharide
LSC	Laser Scanning Cytometer
LTP	Long Term Potentiation
MAGUK	Membrane-Associated Guanylate Kinase
MAP	Mitogen-Activated Protein Kinase
MC-3/4R	Melanocortin 3/4 Receptor
MCS	Multi-Cloning-Site
MEK-1	Mitogen-Activated Protein Kinase Kinase
MLCK	Myosin Light Chain Kinase
MP	Metalloproteinase
MSH	Melanocyte Stimulating Hormone
NDST	N-Deacetylase/N-Sulfotransferase
NF	Neurofibromatosis
NHE-3	Na+/H+ exchanger 3
N-WASP	Neural Wiskott-Aldrich Syndrome Protein
OD	Optical Density
OG	Oligosaccharide
OPA buffer	One-For-All Buffer
ORF	Open Reading Frame
OST	O-Sulfotransferase

PAK	p21-activated kinase
Pax	Paxilin
PB	Phosphate Buffer
PBS	Phosphate Buffered Saline
PCR	Polymerase Chain Reaction
PDGF	Platelet-Derived Growth Factor
PDZ	PSD-95/Discs-large/ZO-1
PfU	Plaque Forming Unit
PG	Proteoglycan
PI	Protease Inhibitors
PIP_2	Phosphatidyl-Inositol Phosphate 2
PIP4K	Phosphatidyl-Inositol 4-Phosphate 5-Kinase
PIPES	Piperazine-N,N´-bis[2-ethanesulfonic acid]
PKA	Protein Kinase A
PKC	Protein Kinase C
PM	Plasma Membrane
PMA	Phorbol Myristate Acetate
PMSF	Phenylmethylsulfonylfluoride
PNS	Peripheral Nervous System
PSD-95	Postsynaptic Density-95
PTK	Protein Tyrosine Kinase
Rab	Ras from brain
Rho	Ras Homologue
RhoGDI	Rho GDP Dissociation Inhibitor
RNA	Ribonuclein Acid
ROCK	Rho-Associated Kinase
Rpm	Rounds Per Minute
RT	Room Temperature
S1P	Sphingosine-1 phosphate
SAPK	Stress Activated Protein Kinase
SDS	Sodium Dodecyl Sulfate
SEM	Scanning Electron Microscopy
SF	Stress Fiber
SGBS	Simpson-Golabi-Behmel-Syndrome
SH3	Src Homology 3
SMase	Sphingomyelinase
SN	Supernatant
SOL	Solution
SRS	Sequence Retrieval System
ss	single-strand
Tal	Talin
TBS	Tris-Buffered-Saline
TEM	Transmisson Electron Microscopy
Tet	Tetracyclin
TGF	Transforming Growth Factor
TIMP	Tissue Inhibitor Of Metalloproteinase
TIU	Trypsin Inhibiting Units
T_m	Annealing Temperature
TM	Transmembrane
Tris (Trizma)	Tris (hidroxymethyl)aminotethane
U	Unit
UTR	Untranslated Region
Vin	Vinculin
WASP	Wiskott-Aldrich Syndrome Protein
WB	Western blot
Wg	Wingless

INTRODUCTION

MATERIALS AND METHODS

RESULTS

DISCUSSION

INTRODUCTION

MATERIALS AND METHODS

DISCUSSION

Construct	Use	Vector	Origin Insert	Ligation conditions	Analysis	Comments
Ce5 ***see fig. 3.4***	FL-S3 in PGEM3z				EcoRI/HindIII/SmaI/PstI digest Seq: 39b,39b$_3$,42f,46a,tini-1	
FL-S3 in Prk5	FL-S3 in eukaryotic expression vector	Prk5-1 EcoRI/HindIII	***Ce5*** EcoRI/HindIII	50 ng Vec/ 48 ng Ins 1 h RT; 17 ng for transf. Sel.: Amp	EcoRI/HindIII digest	
FL-S3 in pcDNA$_3$	Vector for the production of stable cell lines	PcDNA3 XhoI/Klenow/ EcoRI	***Ce5*** HinIII/Klenow/EcoRI	100 ng Vec/182 ng Ins o/n 15°C; 50 ng for transf. Sel.: Amp	Eco47III digest Seq: sp6,t7,39b$_2$,42c,46a	
DEFYA, DV, DC in pcDNA3 ***see fig. 3.20***	C-term-del. S3 in stable eukaryotic expression vector				Check by SmaI digest Seq:42d, sp6	
GFPS3	FL-S3 with GFP-tag in N-terminal	EGFP-C2 SmaI/EcoRI	***Ce5*** HindIII/Klenow/EcoRI	50 ng Vec/95 ng Ins o/n 15°C; 17 ng for transf. Sel.: Kan	EcoRI/SmaI digest Seq: 39b,39b$_2$,39b$_3$,42c,42d, 46a,tini-1,Eco-syn3,Syn3-NS-BamHI,sp6	
S3GFP	FL-S3 with GFP-tag in C-terminal	EGFP-N3 EcoRI/BamHI	PCR on ***Ce5*** with Eco-syn3/ Syn3-NS-BamHI	5 ng Vec/4,9 ng Ins 2 h RT; 2,5 ng for transf. Sel.: Kan	EcoRI/ BamHI digest Seq: 39b,39b$_2$,39b$_3$,42c,42d, 46a,tini-1,Eco-syn3,Syn3-NS-BamHI,sp6	Seq. Revealed errors in 5´-region of S3 New cloning: *see S3 GFPnew*
S3GFPnew	FL-S3 with GFP tag in C-terminal (II)	EGFP-N3 EcoRI/BamHI	***Clone #40*** EcoRI/SacI **and** ***S3GFP*** SacI/BamHI	50 ng Vec/ E-S 32 ng/ S-B 63 ng 3 h at 15°C and 1,5 h at RT 25 ng for transf. Sel.: Kan	EcoRI/SacI digest Seq: 39b,39b$_2$,39b$_3$,42c,42d, 46a,tini-1,Syn3-NS-BamHI	
S3pGEX #7	S3-FL-GST-fusion protein production (bact.)	pGEX XhoI/Klenow/ EcoRI	***Ce5*** HindIII/Klenow /EcoRI	100 ng Vec/ 182 ng Ins o/n 15ºC Sel.: Amp	EcoRI/SacI digest Seq: 39b$_2$, 42a, 46a,tini-1	Low yield of fusion protein
S3 ecto in pGEX6.1 #3	S3-ectodomain-GST fusion protein production (bact.)	pGEX EcoRI/SmaI	***S3pgex6.1*** Fragment of 1165 bp from EcoRI/PvuII digest	50 ng Vec/ 67 ng 40 ng for transf.; o/n 15°C Sel.: Amp	SacI/EcoRI digest Seq: 42c,46a,39b$_2$	Low yield of fusion protein
S3pGEX little, #2 and #3	S3-ectodomain-GST fusion protein production (bact.) (II)	pGEX SmaI, De-phos.	***Ce5*** EagI/Klenow/PvuII 1046 bp	100 ng Vec/384 ng Ins o/n 15°C; 83 ng for transf. Sel. Amp.	SacI/PstI digest Seq: 39b,42d,46a	Purified protein was used for antibody-production in rabbits

***Primers are underlined.**

“Kann man schreiben, ohne eine Rolle zu spielen?”
“Can one write without playing a role?”
“¿Se puede escribir sin interpretar un papel?”
Max Frisch (1954)